

**This dissertation has been
microfilmed exactly as received** 65-13,877

**AVENI, Anthony Francis, 1938-
THE EFFECT OF LINE EMISSION UPON
THE B-V COLORS OF T TAURI OBJECTS.**

**University of Arizona, Ph.D., 1965
Astronomy**

University Microfilms, Inc., Ann Arbor, Michigan

COPYRIGHT BY
ANTHONY FRANCIS AVENI
1966

THE EFFECT OF LINE EMISSION
UPON THE B-V COLORS OF T TAURI OBJECTS

by

Anthony F. Aveni

A Thesis Submitted to the Faculty of the
DEPARTMENT OF ASTRONOMY
In Partial Fulfillment of the Requirements
For the Degree of
DOCTOR OF PHILOSOPHY
In the Graduate College
THE UNIVERSITY OF ARIZONA

1965

THE UNIVERSITY OF ARIZONA

GRADUATE COLLEGE

I hereby recommend that this dissertation prepared under my direction by Anthony F. Aveni entitled "The Effect of Line Emission Upon the B-V Colors of T Tauri Objects" be accepted as fulfilling the dissertation requirement of the degree of Doctor of Philosophy

A. F. Aveni
Dissertation Director

June 10, 1965
Date

After inspection of the dissertation, the following members of the Final Examination Committee concur in its approval and recommend its acceptance:*

J. B. Wenzel Ronald L. But
Richard H. Duley _____
Stanley Richardson _____
Walter S. Slichter _____
Paul J. Veyron _____

*This approval and acceptance is contingent on the candidate's adequate performance and defense of this dissertation at the final oral examination. The inclusion of this sheet bound into the library copy of the dissertation is evidence of satisfactory performance at the final examination.

STATEMENT BY AUTHOR

This thesis has been submitted in partial fulfillment of requirements for an advanced degree at The University of Arizona and is deposited in the University Library to be made available to borrowers under rules of the Library.

Brief quotations from this thesis are allowable without special permission, provided that accurate acknowledgment of source is made. Requests for permission for extended quotation from or reproduction of this manuscript in whole or in part may be granted by the head of the major department or the Dean of the Graduate College when in his judgment the proposed use of the material is in the interests of scholarship. In all other instances, however, permission must be obtained from the author.

SIGNED: Anthony F. Ceveni

Table of Contents

	<u>Page</u>
Chapter I. Introduction	1
Definition and properties of T Tauri Variables	1
Problems associated with line emission . . .	5
Previous attempts to evaluate the continuum	
color effects of line emission	6
Chapter II Method of Investigation	9
The observational format	9
Correction for defocussing effect produced	
by multi-layered filters	11
Correction for non-neutrality of Wratten	
filters	12
Choice of appropriate slit width	13
Conversion of relative densities to logarithms	
of relative intensity	14
Reciprocity failure	16
Effect of chart readability errors upon the	
determination of continuum flux	32
Correction for differential extinction	
between standard star and program star .	35
Correction for plate and instrumental	
sensitivity	35
Correction for interstellar reddening . . .	41
Determination of B-V Color from reduced	
continuum	42
Determination of B-V Color of continuum with	
the addition of emission lines	43

Chapter III Presentation of Relevant Data	45
History of the program stars T Tau, RW Aur, AS 205, AS 209, DI Cep	45
Standard stars used as a test of the method .	48
Explanation of step wedge calibration tables used to obtain photographic characteristic curves	49
Explanation of continuum analysis tables used to obtain logarithms of relative intensity vs. wavelength for all stars	49
Explanation of line analysis tables used to evaluate the totality of line contributions to the continuum flux	52
Explanation of data summary sheets used to express the magnitude of the line emission effect in program T Tauri objects	54
The step wedge calibration tables	58
The continuum analysis tables	73
The line analysis tables	119
The data summary sheets for program T Tauri objects	157
Chapter IV The Nature of the Emission Lines in T Tauri Spectra	173
Variation of relative emission line intensity over the cycle of plates	173
Microdensitometer tracings of spectra	201
Fluorescent phenomena	212

Comparison of T Tauri and solar chromospheric spectra	215
Chapter V Results Regarding the Continuum and the Effect of Line Emission	217
Critique of Smak's photometric method of approximating the line emission effect	217
Further tests of the method	222
Definition of the emission line parameter,	226
Summary of the effects of emission lines upon the observed B-V color - comparison with photometric observations	226
Resulting shift in theoretical HR diagram and two color diagram	231
Continua of program stars and standards compared graphically	237
The problem of space reddening	242
Continuum spectral types of program stars	243
Chapter VI Summary and Final Discussion	245
Appendix	256
Useful Tables	257
The Reduction Procedure - Illustrative Examples	263
References	266

List of Tables

1.	Intensity Losses in Filter Stack
2.	Densities of Filters in Step Wedge
3.	Effects of Readability Error Upon the Continuum.
4.	Code's Standard Stars Used for Plate Calibration
5.	Monochromatic Magnitudes $m(1/\lambda)$
6.	Log Relative Intensity vs Wavelength for Standard Stars. . .
7.	Non-Variabile Program Stars
8.	Step Wedge Calibration
9.	Continuum Analysis
10.	Line Analysis.
11.	Data Summary Sheet for T Tauri Objects
12.	Intensity Variations in T Tauri Emission Lines
13a.	FeI Emission Lines Present in T Tauri Stars (By Ion and Multiplet)
13b.	FeII Emission Lines Present in T Tauri Stars (By Ion and Multiplet)
14.	Occurrence of Members of FeI (43).
15.	Occurrence of Members of FeI (41) (42)
16.	Density vs λ of Smak's Filter.
17.	B-V Line Analysis.
18.	Computed and Observed Colors of Standard Stars
19.	Summary of the Effect of Line Emission Upon B-V Color.
20.	Spectral Types of T Tauri Variables.

List of Tables (cont.)

	<u>Page</u>
A1. Calibrated Density vs Wavelength of Wratten Filters	258
A2. Extinction Curve for Kitt Peak	259
A3. The Kitt Peak Differential Atmospheric Extinction Correction ($\log k'(\lambda)$)	260
A4. Photometric Sensitivity Correction	261

List of Figures

	<u>Page</u>
1. Observing Format	10
2. Chart Reading (C) vs Density (d)	15
3. Relative Log Intensity ($\log I$) vs Density (d)	17
4. Instrumental Sensitivity Correction ($\log S'(\lambda)$)	40
5a. Partial Energy Level Diagram of FeI Showing Observed Transitions	199
5b. Partial Energy Level Diagram of FeII Showing Observed Transitions	200
6. Microdensitometer Tracings of the Blue Region of T Tauri Spectrum.	201
7. Microdensitometer Tracings of the Blue Region of RW Aurigae Spectrum	209
8. Transmission vs Wavelength for the B Filter	
9. Standard Star Continua	225
10. Line Emission Parameter (δ) vs Continuum Color ($(B-V)_c$) . .	230
11. Shift of Position in the $\log L/L_\odot$, $\log Te$ Diagram after Correction for Emission.	234
12. Shift of Position in the U-B, B-V Diagram after Correction for Emission.	235
13. Variable Star Continua (T Tauri)	237
14. Variable Star Continua (RW Aurigae).	239

Abstract

An exact method has been developed to determine the influence of line emission upon the UBV colors of the T Tauri objects T Tau and RW Aur. Calibrated spectra of these objects were obtained using the Steward Observatory 36-inch telescope and nebular spectrograph. These spectra were corrected for various extraneous effects and two colors were computed from microdensitometer traces of each spectrum: 1) the continuum color devoid of emission lines, and 2) the color including emission lines. The latter color can then be directly compared to the observed photometric color. Comparison of the observed B-V colors with the computed B-V shows good agreement, indicating that the photographic corrections were properly assessed. The difference of the colors, obtained for the continuum, $(B-V)_c$, and the continuum plus line emission, $(B-V)_{cl}$, referred to as the line emission parameter, shows apparent variations between $0^m.07$ and $0^m.14$ for T Tau and between $0^m.06$ and $0^m.15$ for RW Aur, with some apparent dependence upon continuum color. The line emission parameter shifts the position of both stars to the right in the $\log L/L_\odot$, $\log Te$ diagram; this can be interpreted as a correction to the contraction age of up to 20%.

This method of computing colors for emission is demonstrated to be more accurate than that of Smak (1964) who uses photometry only. The method employed in the present study is, however, quite laborious due to the problems introduced by the non-linearities of the photographic process.

Since unresolved line emission is almost certain to be present in

x

the spectra, the emission line correction is to be regarded only as a lower limit. The B region, for example, covers a portion of the spectrum where many metals lines occur, so a contribution of these lines would make the corrected B-V color determined in this study still too blue.

The previous spectral type assigned to both stars is G5Ve, though estimates have ranged from G0 to G8. From the intensity distribution of the continuum the types G0-K0 are assigned to T Tau, F7-G0 to RW Aur.

y

-
on

ss.
n

I. Introduction

T Tauri stars are objects of low luminosity having emission spectra consisting principally of lines due to FeI, FeII, TiI, TiII, CaII H and K, as well as the Balmer Series of hydrogen lines. The emission spectrum overlies a weak late-type Fraunhofer spectrum. All T Tauri objects exhibit irregular variations in brightness as well as in spectrum. The association of these objects with galactic nebulosity has been definitely established. Herbig (1958) has suggested an empirical procedure in establishing the conditions for membership in the T Tauri class of variables. He offers the following spectroscopic criteria:

- (1) The presence of hydrogen lines and the H and K lines of CaII in emission.
- (2) The presence of the fluorescent emission lines FeI 4063, 4132.
- (3) The presence (though not always) of the emission lines SII 4068, 4076.

Since the classic paper of Joy (1945), in which these peculiar objects were first described, the T Tauri stars have been a center of attention for those who are concerned with the earliest stages of stellar evolution. The intimate association of these objects with nebulosity suggests that these stars recently formed out of the gaseous nebulae with which they are associated. One can also interpret them as

older field stars which happen to be currently undergoing passage through a cloud. At the present time, evidence overwhelmingly favors the former hypothesis although the accretion idea was popular not too long ago (Greenstein (1948), (1950), Herbig (1948), Struve and Rudkjbing (1949), Struve (1950)). Herbig (1957) argues that one cannot explain away all the attributes of the group by assuming a normal star not associated genetically with the cloud in which it is embedded. The underlying F-K type absorption spectrum is characterized by diffuse lines. This is not the case for the MK standards in this spectral range. The T Tauri objects are found to be brighter than the main sequence stars of the same spectral type. Perhaps the strongest argument against the "accident" hypothesis concerns the absence of any evidence, spectroscopic or otherwise, that these passing stars are accreting any of the surrounding medium. If anything, radial velocity measurements of the lines of the emission spectrum relative to the absorption spectrum indicate ejection, rather than accretion of material. Kuhi (1964) has successfully fitted T Tauri CaII H and K line profiles to those computed from a spherically symmetric radially expanding envelope. Statistical arguments based upon data regarding the frequency of occurrence of emission stars in the Taurus dark clouds (Joy (1945), (1949); Haro et al (1953)) have resulted in the conclusion that the random collision of field stars with clouds can account for but one-tenth the number of T Tauri stars present in the clouds. In some places, one observes a clumping of emission objects near brighter early type stars, a quite unrealistic type of behavior for randomly scattered field stars.

As is often the case when the underlying physical process required to explain a particular phenomenon is not understood, one must resort to empirical means in order to treat the subject. Thus a classification scheme of the entire dwarf variable star group has been set up by Joy (1960). He divides all dwarf variables into three groups.

Group I: Rapid Irregular Variables

Group II: UV Ceti Flare Stars

Group III: SS Cygni Variables

His first group is broken down into four subgroups on the basis of range of spectral types and number of emission lines present. The T Tauri class is essentially one of the subgroups. Thirty-one members are listed in the spectral range G5-M2, nearly all located in the Taurus-Auriga cloud complex. All four subgroups contain a total of 114 members. Herbig (1962) has presented the most complete list of T Tauri and related objects. His table includes 126 members and near-members of the class. Many of the stars in Herbig's table are included in the other subgroups of Joy's Group I, though he makes no attempt to draw the line between T Tauri objects and non-T Tauri objects in his table. Of the stars in Herbig's table only eight exhibit what he calls the advanced T Tauri spectrum, characterized by strong H, CaII, and many lines due to other metals in emission. Twenty-three others exhibit a less advanced version of the type spectrum, the bright lines appearing somewhat fainter. On the other hand, twenty-nine of the stars he lists show either emission at H α only or emission at H α in addition to very weak emission in the photographic region. To these he attaches the name T Tauri-like stars,

emission. Twenty-three others exhibit a less advanced version of the type spectrum, the bright lines appearing somewhat fainter. On the other hand, twenty-nine of the stars he lists show either emission at H α only or emission at H α in addition to very weak emission in the photographic region. To these he attaches the name T Tauri-like stars, which is designed also to include some of the earlier type emission stars.

Still another property exhibited by most of the T Tauri variables which have been investigated in some detail is the abnormal intensity of ultraviolet continuous emission. One of the few detailed investigations has been that of Bohm (1958). He has mapped the energy distribution in the continuous spectrum of the ultraviolet stars LH α 22 and VY Ori, neither of which, curiously enough, is listed in Herbig's catalog of T Tauri and T Tauri-like stars. For $3800\text{\AA} < \lambda < 5000\text{\AA}$ the continua appear the same as that of a K dwarf but a steep increase in continuum intensity sets in below 3800\AA , much too steep to be accounted for in terms of hot-spot black body emission on portions of the surfaces of these stars. Bohm believes the only explanation for the rise to be due to unseparated Balmer series members and the Balmer continuum.

At least two different continua are present in the spectra of T Tauri stars. The first appears most strongly at the peak of intensity of the emission lines and veils the Fraunhofer spectrum in the photographic region. It has been postulated that one is merely witnessing a large number of unresolved emission lines. The amount of energy actually added to the spectrum by the so-called blue continuum is not known. The second, or ultraviolet continuum, appears to contribute significant amounts of

energy to the spectrum of many of the faint T Tauri stars in the Orion region, though for unknown reasons it appears weak or absent in the nearer stars. The peaks of intensity occur at about 3700 \AA .

A recent wave of interest in T Tauri stars has resulted from the observation that these stars may all show lines of LiI in absorption which indicate an overabundance of that element with respect to the Sun by a factor of 100. LiI λ 6707 was noted in the spectra of T Tau and RY Tau by Hunger (1957). Bonsack and Greenstein (1960) and Bonsack (1961) secured observations of twelve other T Tauri stars with the 200-inch telescop; the Li line was present in all their spectra. These authors favor surface nuclear reactions as a mode of production of Li.

The basic observational problem involved in the interpretation of the evolutionary configuration of the T Tauri objects is associated with the fact that numerous emission lines are superimposed upon the underlying continuous spectrum. Magnitudes measured in various passbands, such as the UBV or uvby systems, include the emission lines. Thus, the determination of the wavelength distribution of the continuous emission from the evolving stellar body requires an evaluation of the effect of the emission lines. The author is proposing in this paper a program for the determination of the effect of these emission lines upon the measured B and V magnitudes. This program is, therefore, intended to determine the energy distribution in the continuum after correction for the presence of emission. The spectral types of the T Tauri class are generally regarded to be in the range G0-K5. One should therefore find that the corrected continua agree with the absolute energy distribution curves for main sequence

stars as published by Code (1960).

In preparation for this program, the author had obtained plates from the Mount Wilson Observatory through the assistance of Dr. A. H. Joy. These include some of the objects for which he has published spectra. A preliminary study fo these plates indicated that significant corrections to the measured colors for the presence of emission are found for nearly all objects. This study has moreover indicated that when one corrects RW Aur for the presence of the emission lines the resulting continuum does not appear to be that for a normal main-sequence star. The reason for this discrepancy is not currently known, however, the extension of this study to a wider spectral region and to other objects should permit a deeper insight to be obtained into this problem. It must be admitted that the study of these older spectrograms, in which the calibration is to some extent open to uncertainties, must be accorded low weight even though the effect seems to be too large to explain in this manner.

The emission line problem has been investigated in the past by Varsavsky (1960) and more recently by Smak (1964). Varsavsky compared his measurements of the B-V color of several T Tauri variables with Joy's (1949) spectral types for these stars. He found that for a given effective temperature as determined from spectral type, the B-V color is up to $0^{\text{m}}.8$ bluer than that for main sequence stars of the same spectral type. Varsavsky proposed that at least part of the discrepancy between the T_{eff} vs B-V relationship for late type main sequence stars and T Tau variables is due to the influence of emission lines upon the continuous spectra of the latter. It should be pointed out that the spectra of these stars are

very difficult to classify owing to the multitude of emission lines which overlie the diffuse absorption features. Furthermore, there is no evidence to support the hypothesis that the spectral types of these variables remain constant in time. Kuhi (private communication) has noted marked changes in the spectra of several T Tauri stars. Varsavsky found that the largest discrepancies generally occurred for those stars having the strongest emission line spectrum. The strongest emission lines observed in T Tauri spectra are those of the Balmer series and CaII, H and K. Of these, the B filter is highly transparent to H γ and H δ and less transparent to the remaining lines. Observations with the V filter, however, are affected only slightly by the presence of H α and H β (The V filter transparency is 10% at H β and 5% at H α) and not at all by the remaining lines.

Smak (1964) has devised his own photometric system containing an "emission free" color index, $B-V$; the B filter combination is transparent between H γ and H β while V is the V magnitude of the UBV system. He has evaluated the emission line effect by comparing the color indices B-V and $B-V$ for twenty-six T Tauri type stars in the Taurus dark cloud. T Tauri stars are found to deviate from the standard B-V vs $B-V$ relationship for normal main sequence stars by up to $0^m.5$. Smak's method provides an immediate answer to the question whether an emission line influence exists. An exact evaluation of the effect, however, is not possible, since many FeI and FeII lines exist in the range in which the B filter is transparent. This is especially true in the spectra of such advanced T Tauri stars as RW Aur. Ideally, one wishes to determine the difference between the B-V

color of the continuum devoid of all emission lines, and the observed B-V color. In this paper an attempt will be made to compute the true continuum color as well as the $B - V$ color for one or two cases in order to determine the extent to which Smak's method can provide for this difference.

II. Method of Investigation

The observations for this program consist of spectra widened to 60\AA taken on 103a-E and 103a-F plates of the program stars T Tau and RW Aur together with those of standard late type dwarfs. Miscellaneous observations of a few other T Tauri stars are also included. These were arranged on the spectroscopic plate as indicated in Fig. 1. At least one of the standard stars for each plate has had its spectrum recorded through a step wedge consisting of an assortment of neutral density filters. Preliminary spectroscopic observations were taken on 1963 Oct. 10 - 18 with the f/0.8 nebular spectrograph attached to the 36-inch telescope at the University of Arizona's Kitt Peak Observing Station. Low dispersion ($250\text{\AA}/\text{mm}$) permitted the exposures to be taken in periods of two or three hours for these $V = 11\text{-}12$ magnitude stars, yet was not so low as to result in appreciable blending of emission lines. Supplementary observations consist of UBV photometric measurements made with the 16-inch photometric telescope of the Kitt Peak National Observatory and the 21-inch telescope of the University of Arizona's Lunar and Planetary Laboratory Catalina Observing Station. Both the spectroscopic and photometric observations were made simultaneously where possible.

The preliminary spectroscopic observations utilized a step wedge composed of multiple stacks (up to five layers) of a neutral filter of density 0.30. A more nearly exact set of observations was obtained during the period 1965 Jan. 1 - Feb. 19 with a step wedge consisting of

GO V

13974



AO V

4 Aur

Fig. I. Observing Format

RW Aur

single layers of filters of different density. The alteration in the step wedge was necessary because of the defocussing effect produced by the passage of light through a stack of filters as well as to the excessive transmission and reflection losses caused by stacking. Though the defocussing effect is obvious when one carefully examines the plates, the approximate magnitude of the effect is apparent only when one compares the intensity of transmitted light, I , through a stack of filters as observed by the Jarrell Ash microdensitometer, with the transmitted intensity, I' , assuming no light loss. This has been done in the visible region and the results are summarized in Table 1, where the ratio I/I' is listed for a stack of n filters with $0 < n < 5$.

Table 1 Intensity Losses in Filter Stack

<u>Number of Filters</u>	<u>I/I'</u>
0	1.000
1	1.000
2	0.955
3	0.871
4	0.794
5	0.675

One must either take this correction into account or, as has been done in the observations of 1964 July 26 - 28 and 1965 Jan. 1 - Feb. 19, employ single thickness. The densities of Wratten neutral filters used in the step wedge for the 1964-5 observations are quoted in Table 2.

Table 2. Densities of Filters in Step Wedge

.000
.300
.600
1.000
1.200
1.600

When difficulties were encountered in the initial reductions, the author was motivated to test the neutrality of all filters and combinations of filters employed in the observations. The density vs wavelength tabulations exhibited in Table A1 have been determined with the densitometer of the Kitt Peak Observatory. Such tabulations necessitate the introduction of a correction factor, quite appreciable in the violet region, into the program. Departures from quoted densities of up to 30% in the region around H and K are not uncommon. The table lists the quoted Wratten density and the corresponding transmission at the top of each column. Where multiple layers of a given filter have been employed, the transmissivity has been determined by placing multiple layers of the sample in the densitometer. Thus a triple layer of density 0.3 filter ($d = 3 \times 0.3$) is found to vary in density in a manner different from that of a single layer of $d = 0.9$ filter. The density of the former cannot be determined by successively compounding the contributions of three separate filters of density 0.3 for reasons mentioned in the last paragraph. The author has also noted periodic fluctuations resembling interference patterns in the transmission of some samples, amounting to approximately 1% in amplitude and 50\AA in wavelength.

Ten or a dozen such patterns were found on at least six tracings of different filters. Evidently the microscopic structure of these filters is producing an interference pattern. Fortunately the size of this disturbance is small enough relative to other incongruities which will be mentioned shortly, so that no correction for it is warranted.

Trailing of the image for the purpose of widening the spectra is simpler in the hour angle coordinate. Since the objects were observed as near to the zenith as possible, atmospheric refraction of the image takes place in a direction nearly normal to the slit. This necessitates widening the slit appreciably in order to eliminate light losses from the red and violet portions of the spectra. Thus it is not enough to widen the slit to include the entire visible seeing disk. A slit width of ten times that necessary to contain the normal image under good seeing conditions was employed in order to eliminate this source of error. In the f/5 36-inch telescope a slit width of 0.33mm is sufficient to subtend a 15" image. Since the focal ratio of the camera in the nebular spectrograph is 0.8 the width of an iron comparison line will be approximately 6 \AA on the plate, instrumental broadening neglected.

A standard method with some new variations has been employed to obtain relative intensity as a function of wavelength from the tracings of the spectra. Tracings were taken with the Jarrell Ash microdensitometer and Bristol recorder of Colgate University both along the direction of dispersion and, in the case of the stars taken through the step wedge, normal to the direction of dispersion. The stellar continua were sketched in upon each tracing and values of $C(\lambda)$, recorder chart readings for the continua as a function of wavelength, were tabulated at 200 \AA intervals

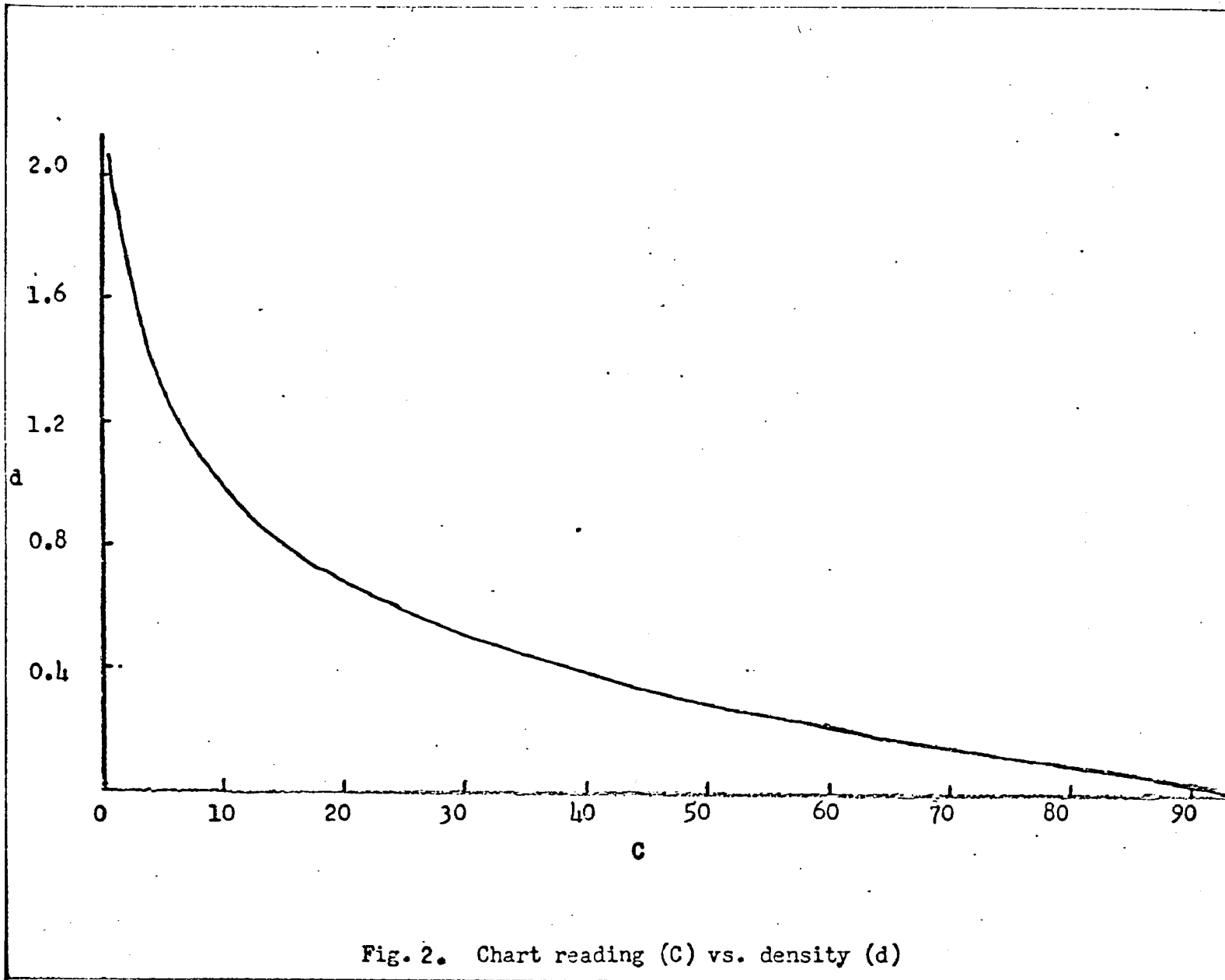
in the range 3600 - 6800 \AA . The detailed nature of the variable star microdensitometer tracings will be discussed at a later time. The tracings of the blue region for all variable star spectra are exhibited in Fig's. 6 and 7.

Chart readings (which are on a logarithmic scale) may be converted into intensity readings in the following manner: Let the difference between the chart readings for 100% transmission and for no transmission be defined as $\Delta = x-y$, where x is the chart reading corresponding to transmission through an infinitely dense neutral filter and y is that which corresponds to transmission through one of zero density; then one may set up a scale of recorder readings, C , corresponding to plate densities, d , according to the expression

$$C = \frac{\Delta}{\text{antilog } d} + y$$

Fig. 2 illustrates the C vs d curve for all plates. A single curve has been made possible for all plates by letting $C = 0$ for zero transmission and $C = 94$ for full transmission on each plate.

In order to obtain the change of relative intensity with apparent density on the photographic plate, one must have some knowledge of the characteristic curve of the plate. This data is obtainable from the microdensitometer tracings of the stellar spectrum normal to the direction of dispersion taken through the step wedge. The steps in density of successive spectra on the plate are given directly by the readings, C , converted to densities through use of Fig. 2. The actual diminution in $\log I$ between successively fainter spectra is known from the quantities



listed in the Appendix in Table A1. Ideally there is found to exist an infinity of $d=f(\log I)$ relationships. In the reduction program, characteristic curves have been determined at 500\AA intervals in the range $3500\text{\AA} < \lambda < 6500\text{\AA}$. These are shown in Fig's. 3. Values of $\log I$ on intermediate characteristic curves have been obtained by interpolation; thus, each continuum chart reading is readily converted to a $\log I$ reading through Fig. 2 and one of the appropriate Fig's. 3. The familiar systematic increase of slope with wavelength is apparent in each of these plots.

It is well known that if marked changes are made in intensity and time, e.g. one-tenth or one-hundredth of the intensity acting for ten or a hundred times as long, the density produced may be markedly different even though the product of intensity and time remains constant. For the density produced on photographic materials, therefore, there is a failure in the true reciprocity of time and intensity. The reciprocity failure of a material can simply be determined by exposing various portions of a strip of material to a constant intensity with exposure time increased by the same ratio. Repeating the experiment using only half the intensity but twice the exposure of the corresponding one in the previous experiment, one finds little change in the densities of corresponding steps. But by giving the strip $1/10$, $1/100$, $1/1000$ etc., of the intensity a progressively larger change in the density of a particular step is noted, although the exposure of any step, measured as $I \times t$, remains constant. Before conducting a series of such experiments, which can become quite complicated, one should determine whether they are even

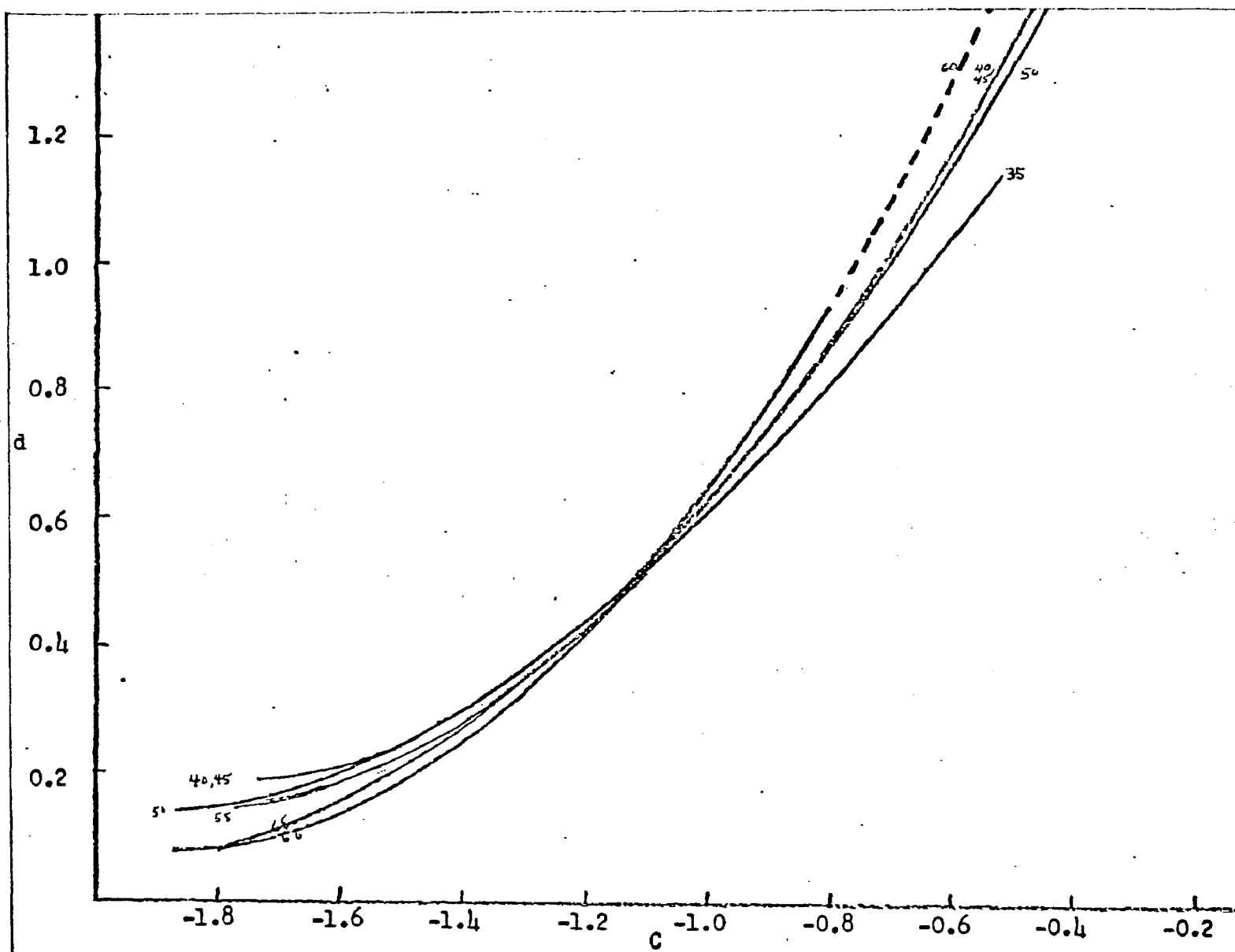


Fig. 3a. Relative log intensity ($\log I$) vs. density (d). Plate No. 23

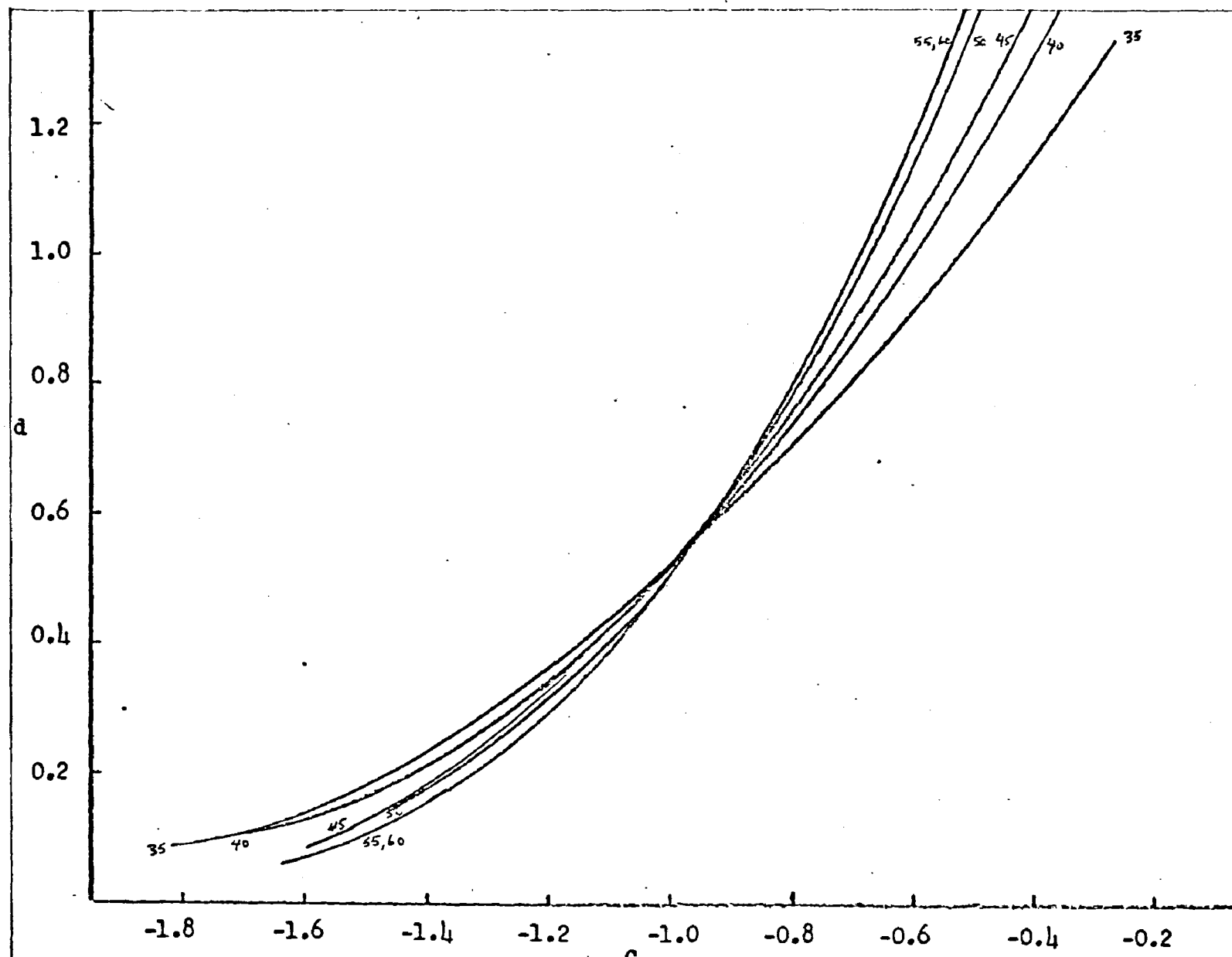
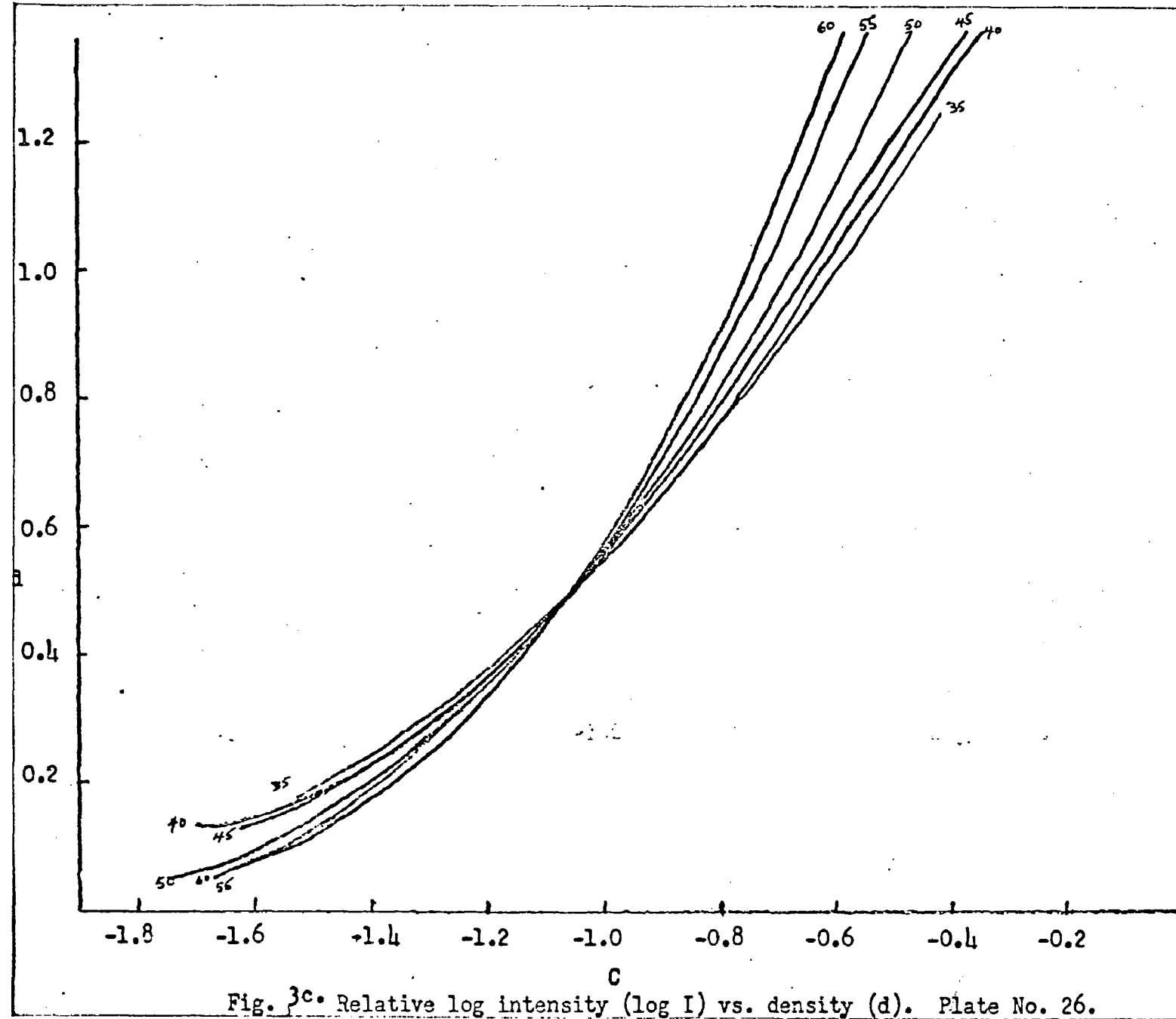
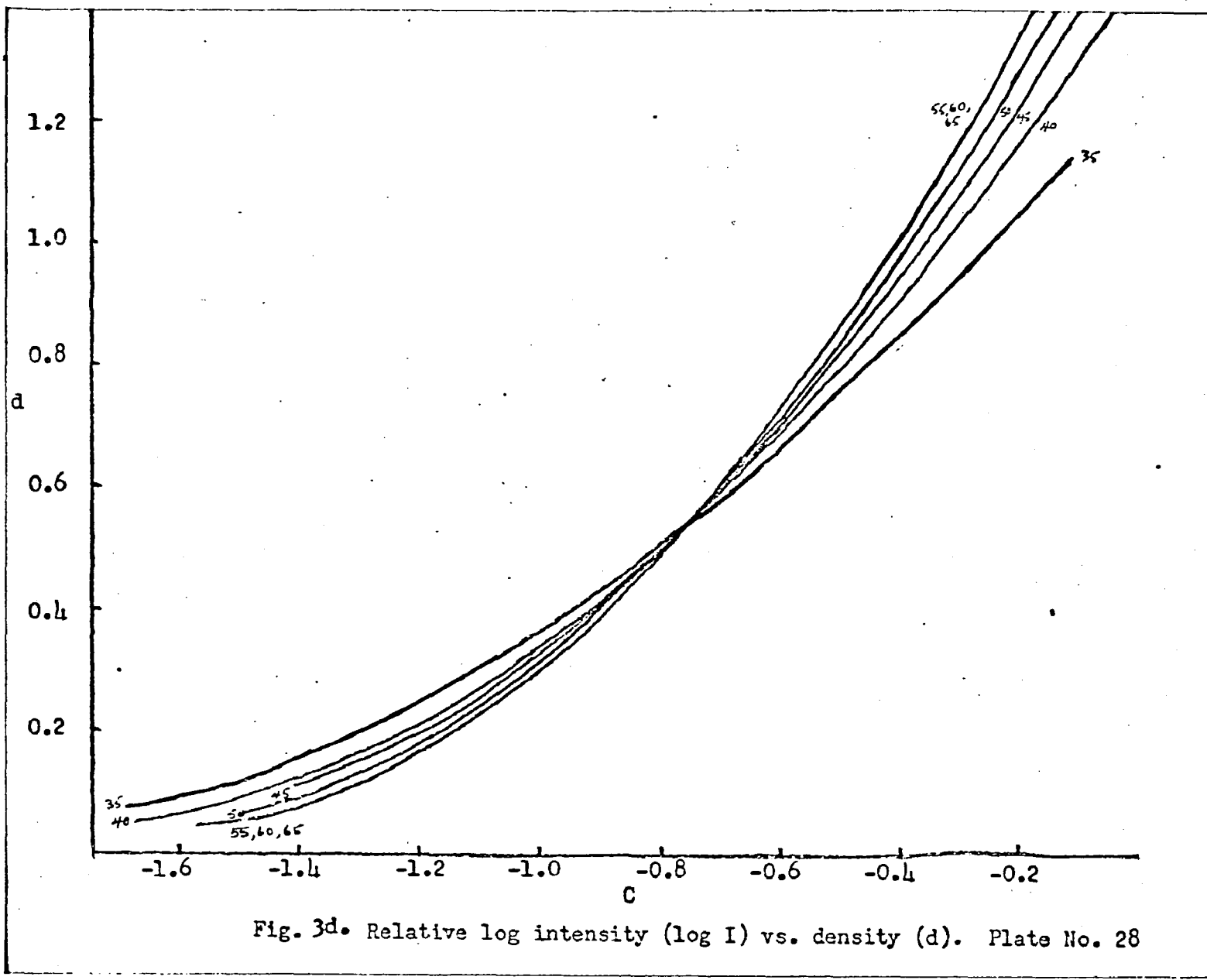


Fig. 3b. Relative log intensity (log I) vs. density (d). Plate No. 25





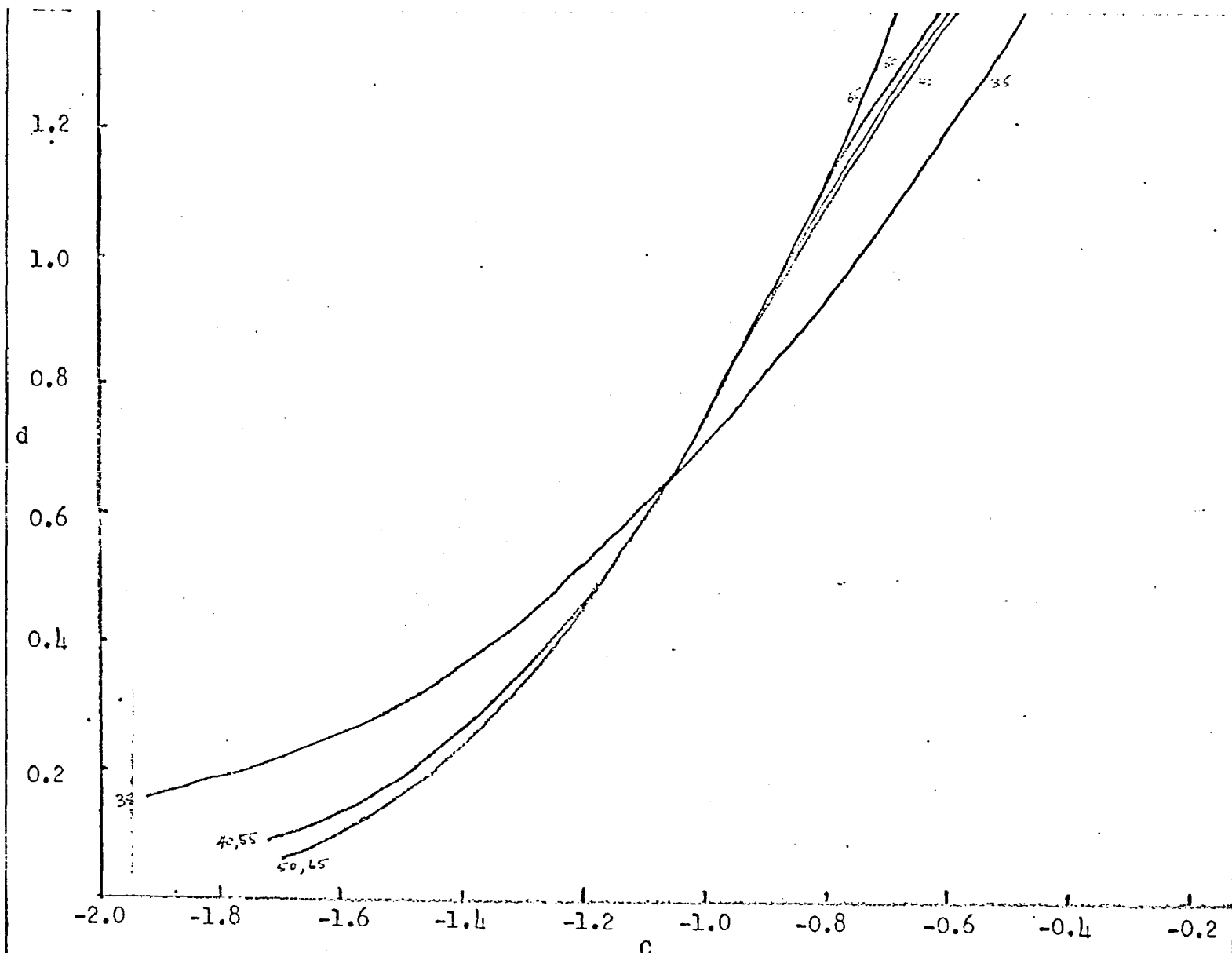
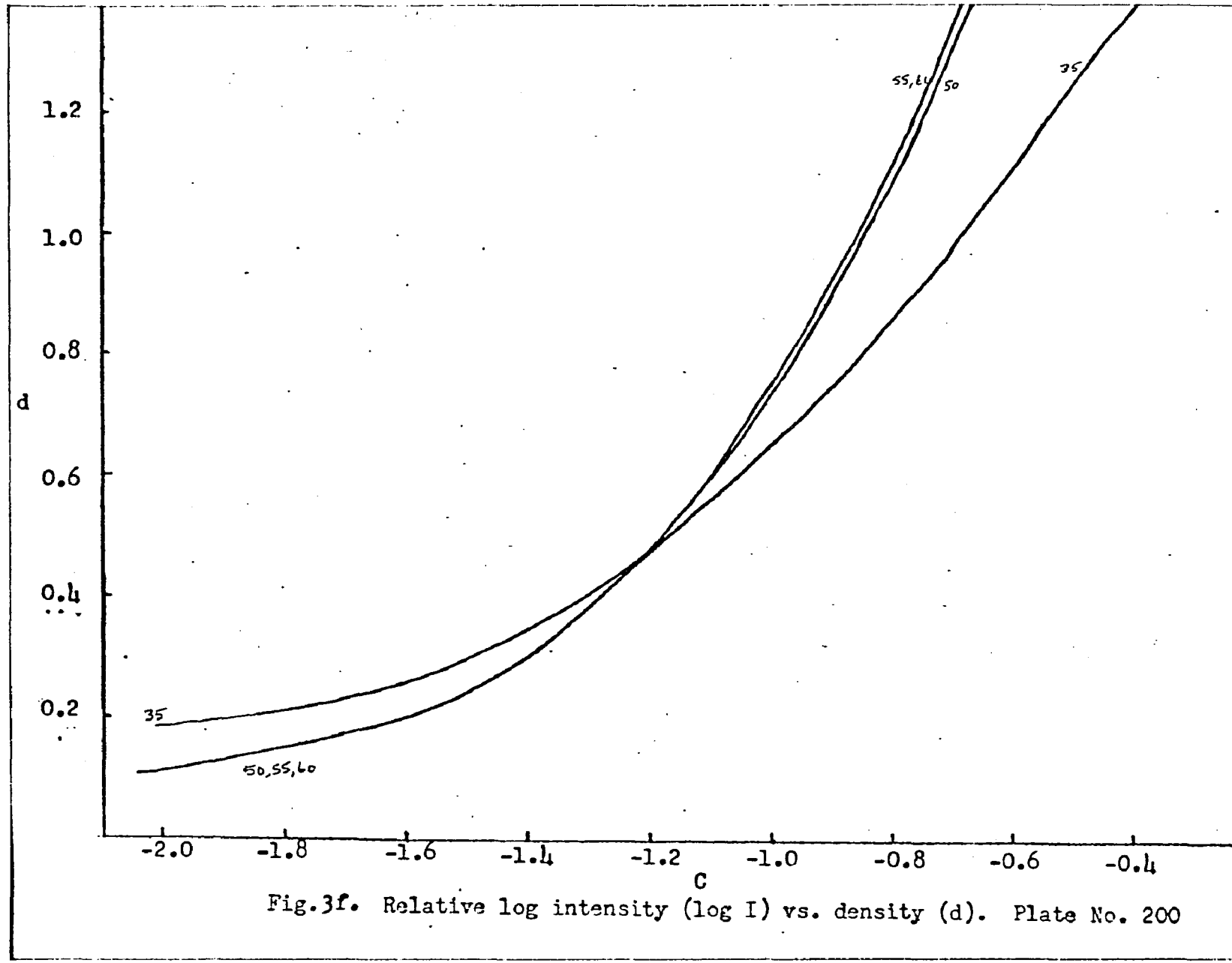


Fig. 3e. Relative log intensity (log I) vs. density (d). Plate No. 199



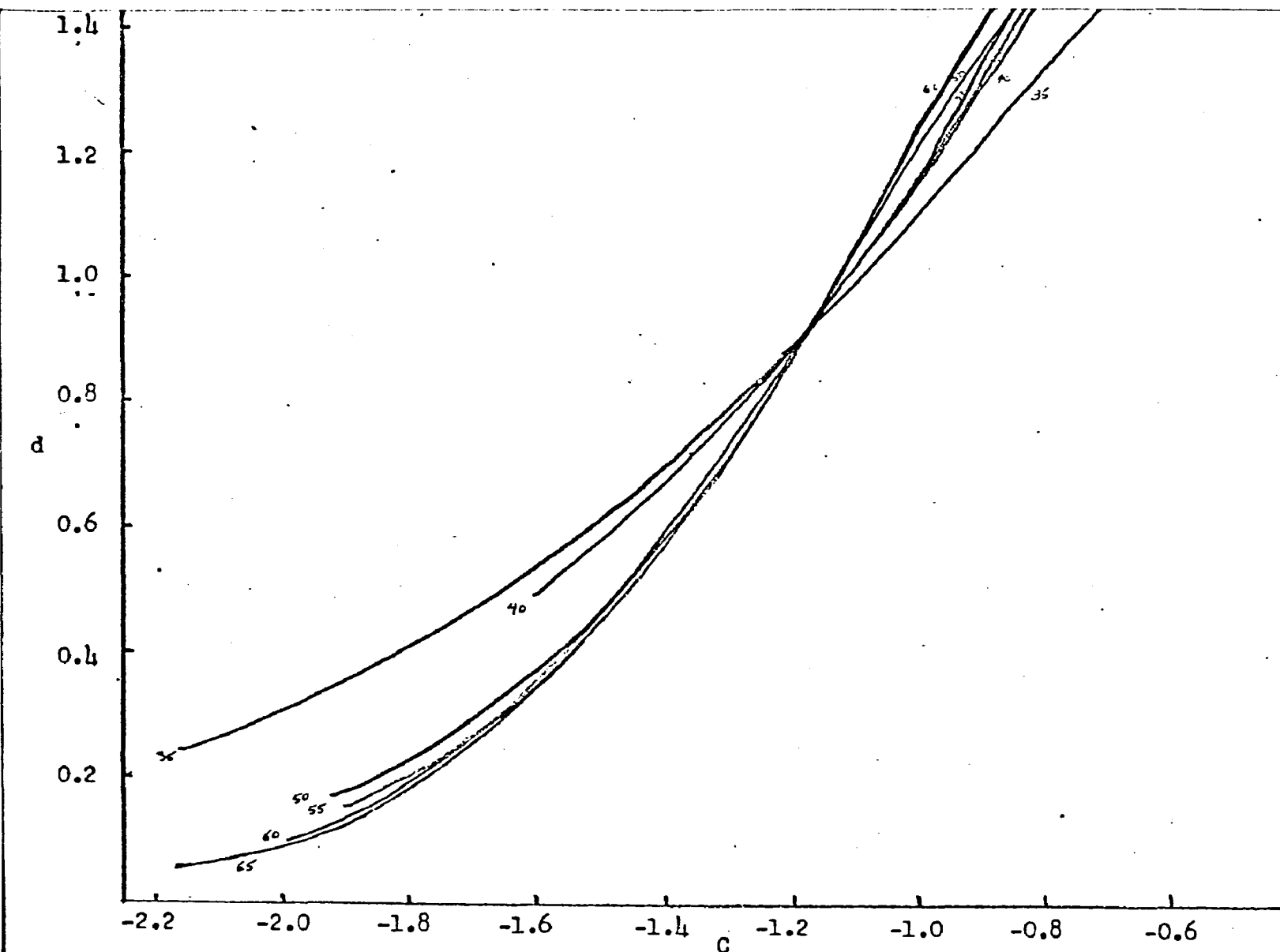
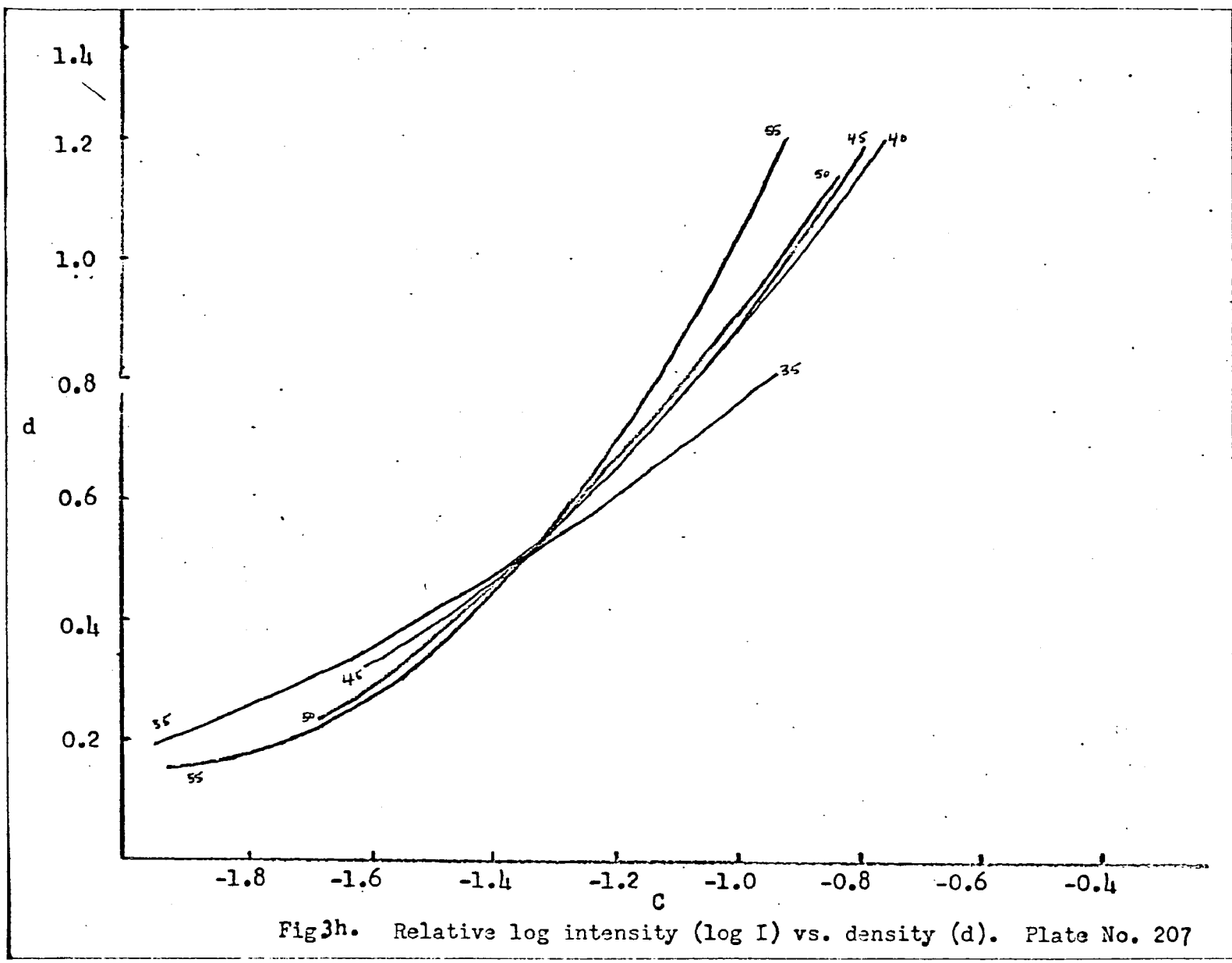
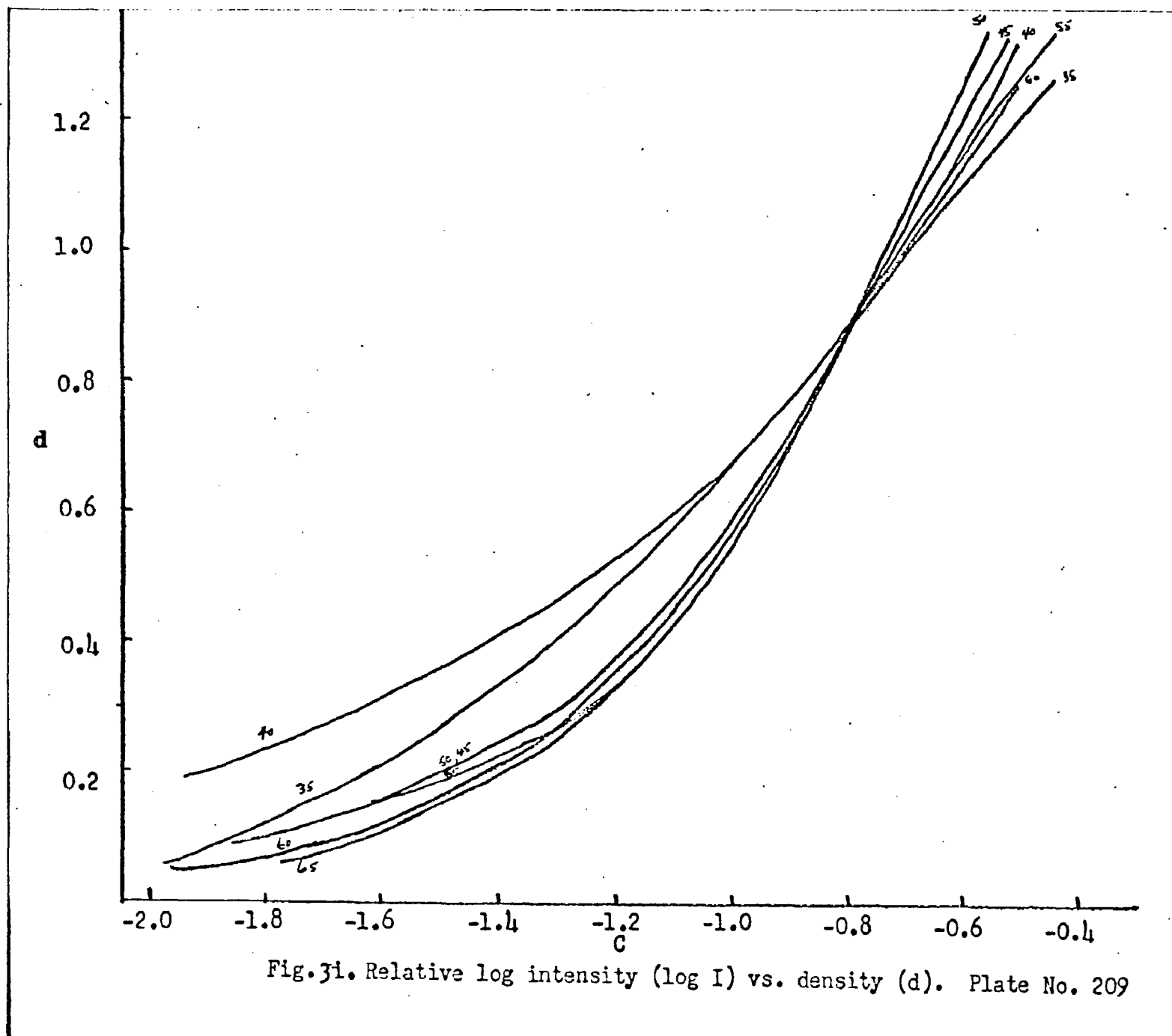
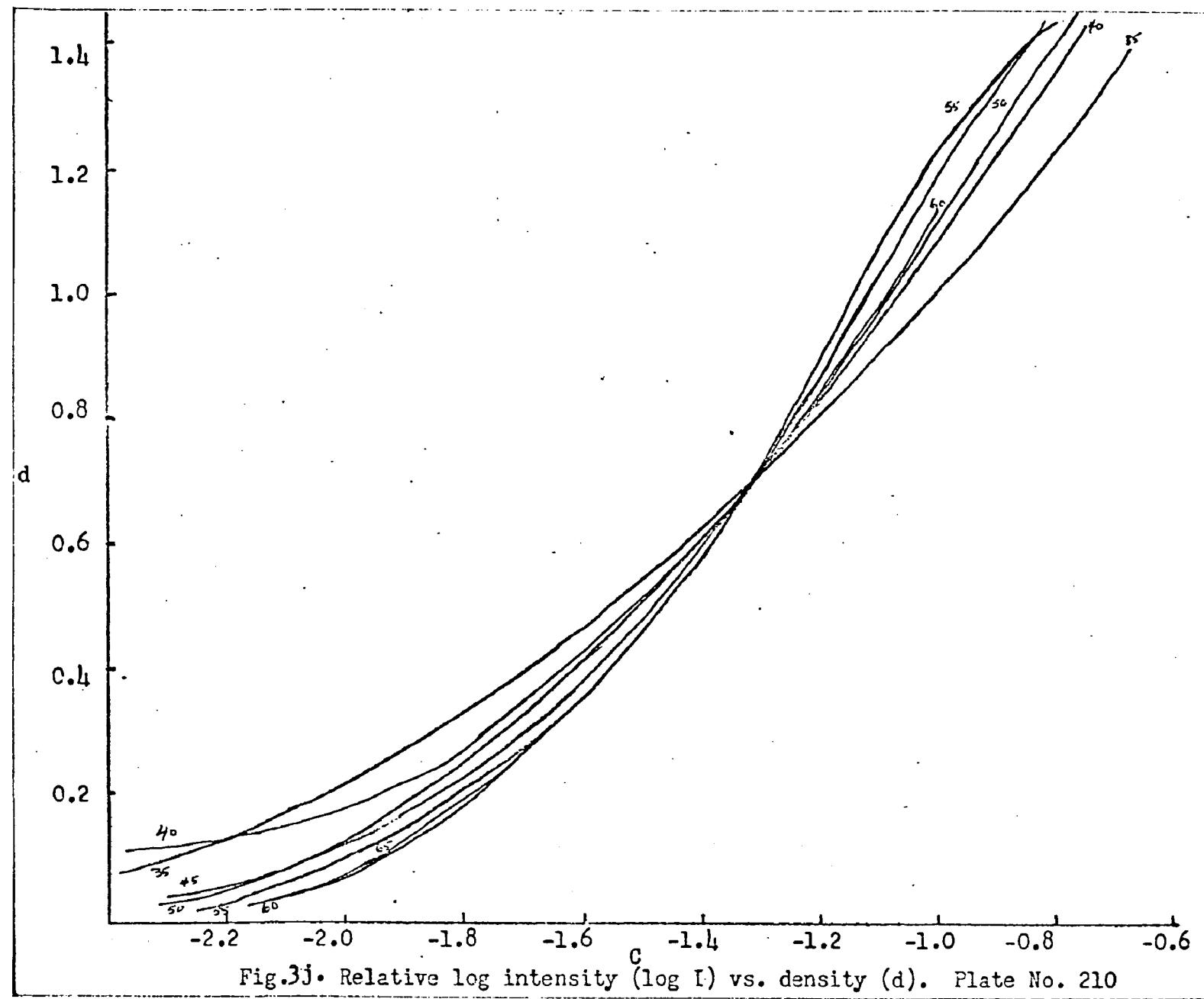


Fig. 3g. Relative log intensity (log I) vs. density (d). Plate No. 205







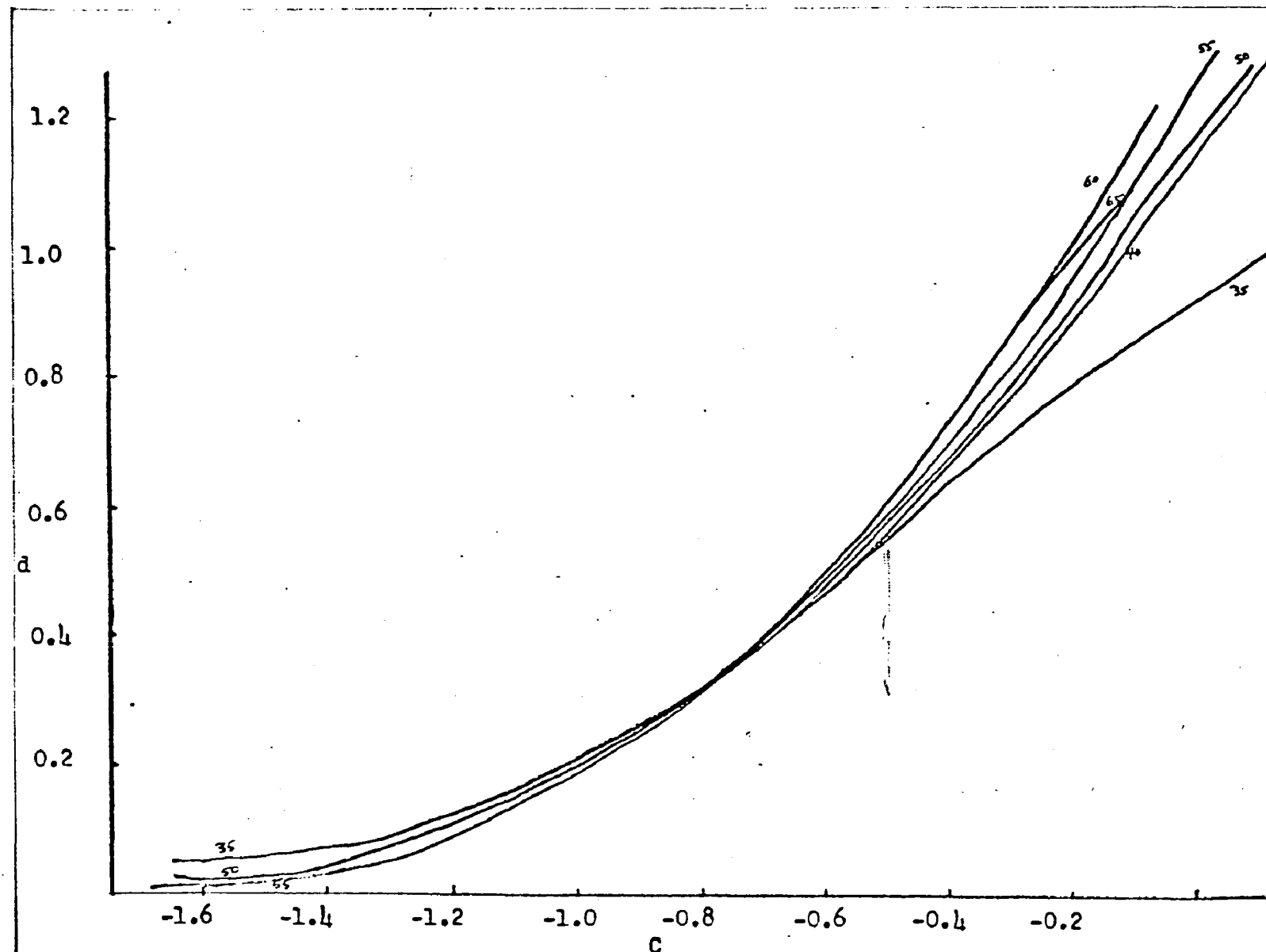
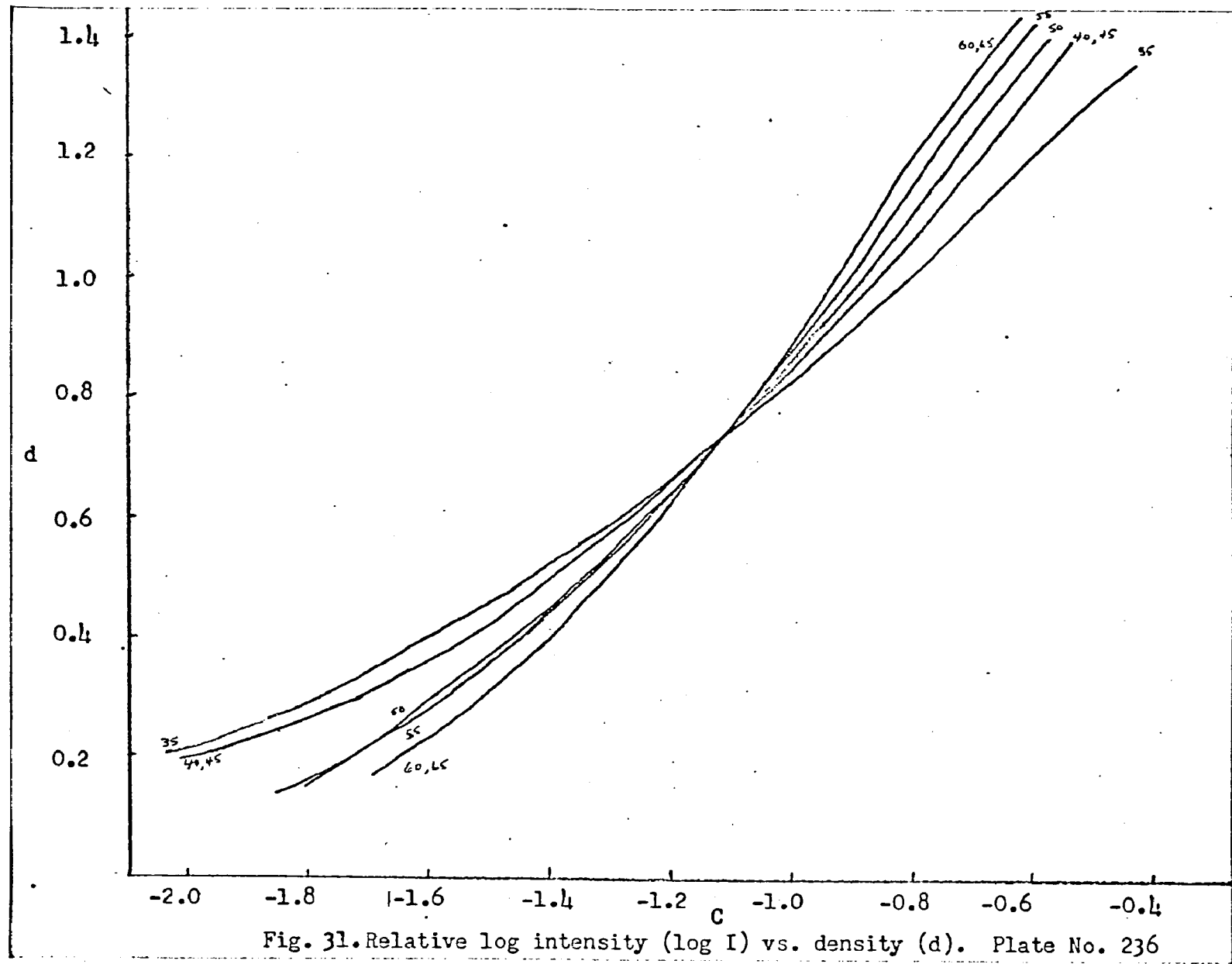


Fig. 3k. Relative log intensity ($\log I$) vs. density (d). Plate No. 232



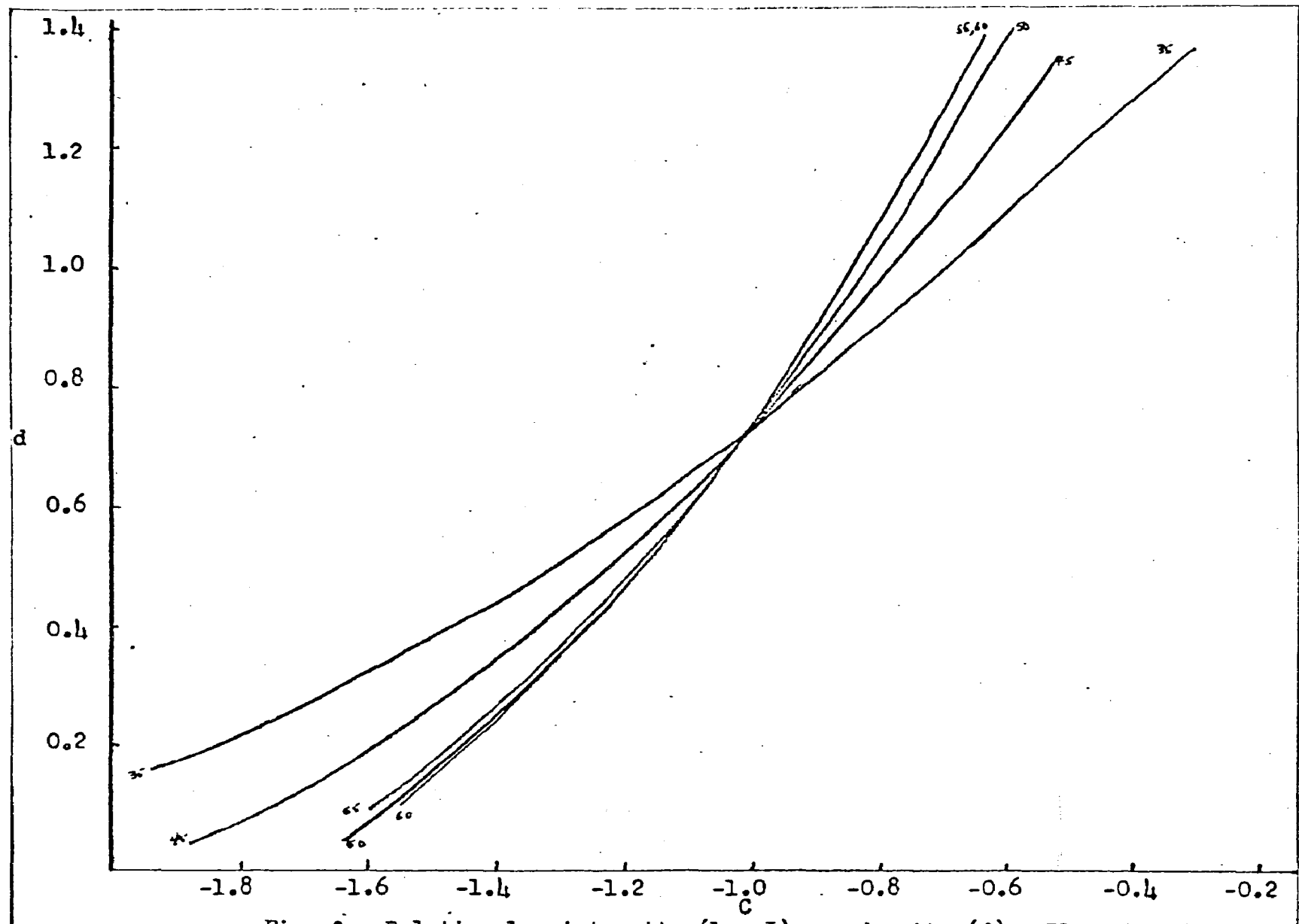
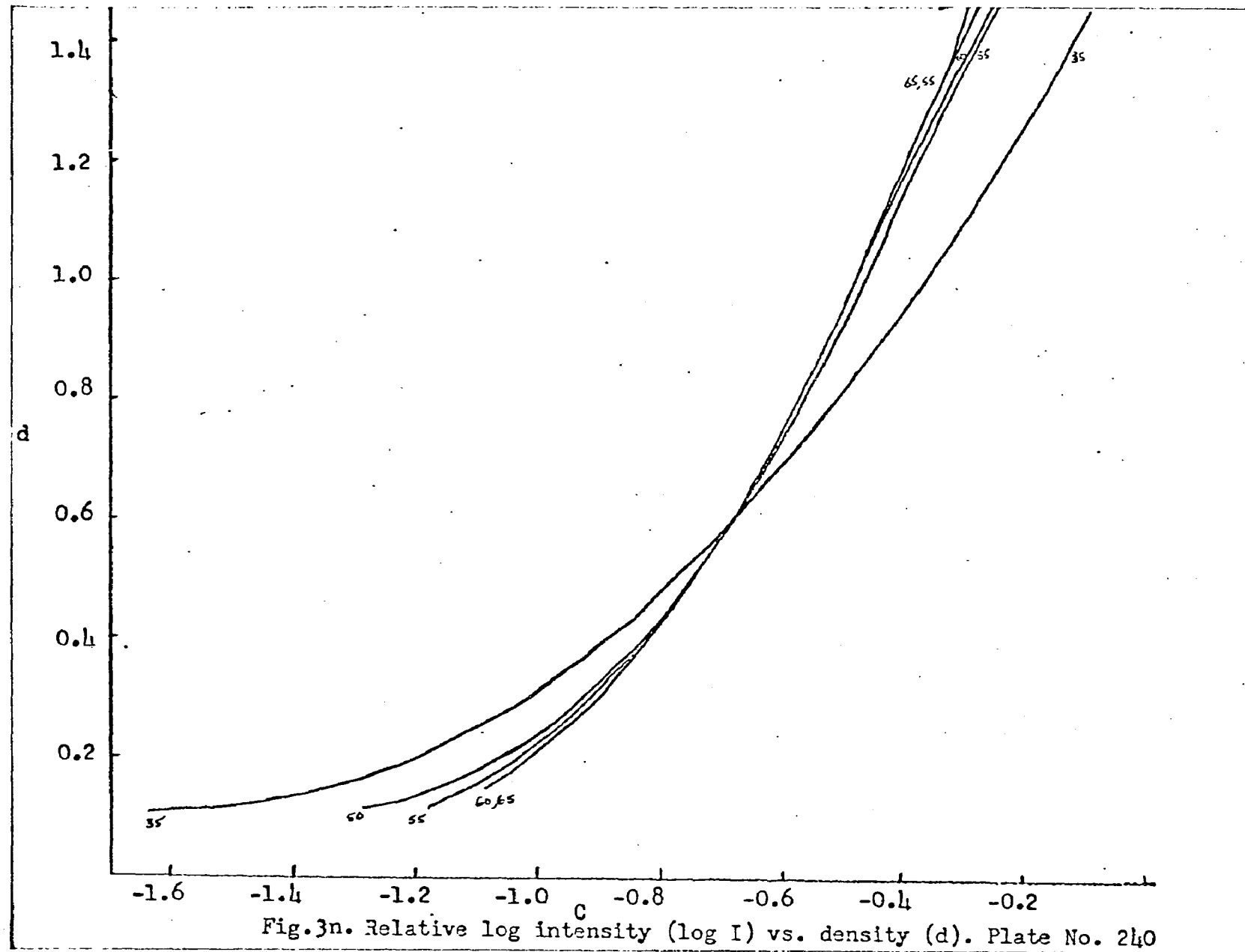
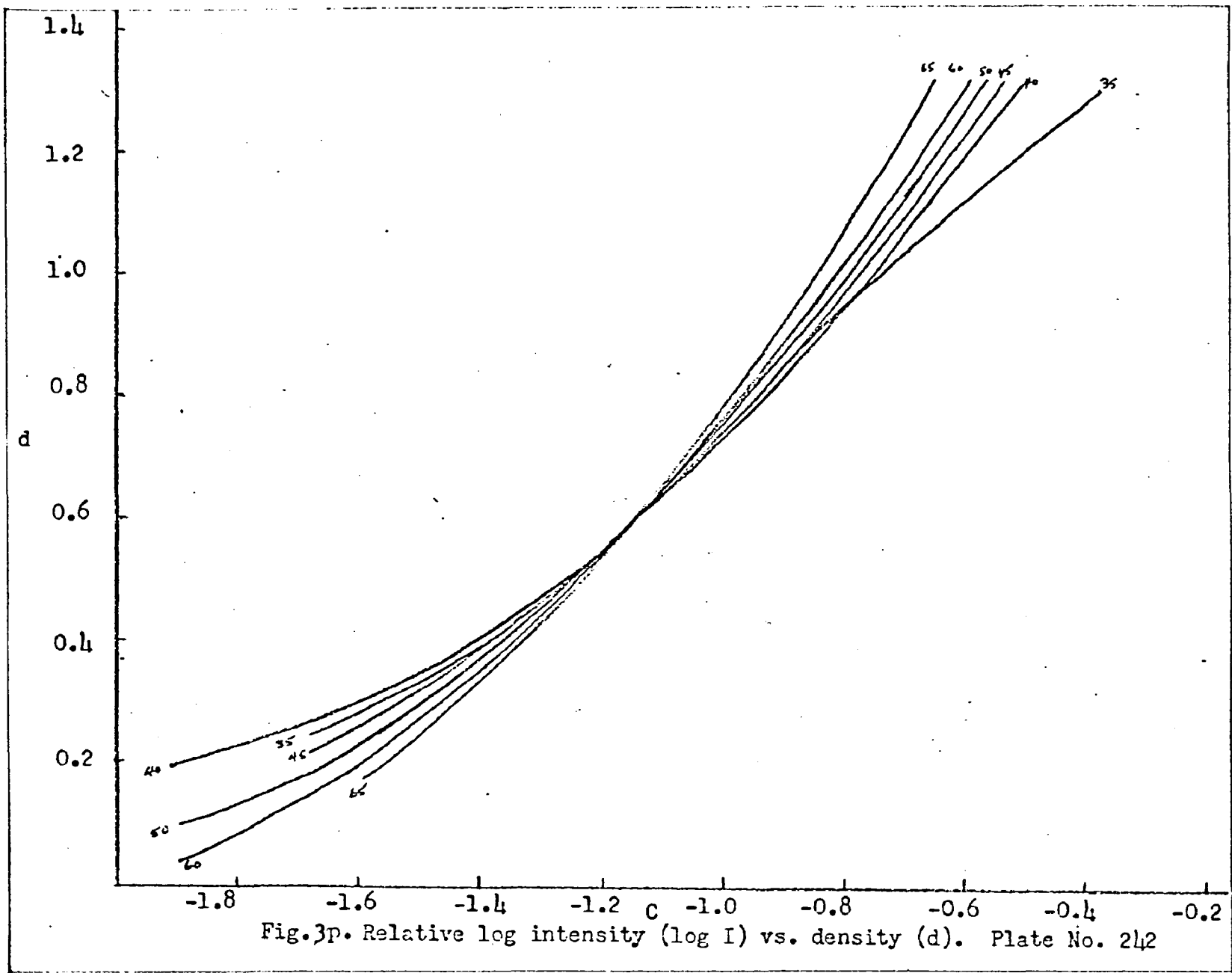


Fig. 3m. Relative log intensity ($\log I$) vs. density (d). Plate No. 237





necessary. Since the ratio of the longest to the shortest exposure times used in the program is only 18 it might be predicted that the error incurred by not correcting for the reciprocity failure would be insignificant. As the results displayed in the derived and actual standard star continua (Chapter V) will attest, such a set of experiments is indeed not necessary. Without the inclusion of a correction for this effect in the program, true standard star continua are predictable with great accuracy. Other effects in photographic materials (e.g. low intensity failure and intermittency effect) produce errors of too small a magnitude to be discussed relative to such major problems as strip chart readability errors and variation in the shape of the characteristic curve with wavelength.

It is important to know the magnitude of the error resulting in the determination of $\log I$ from readability errors, ΔC . As one approaches the fog level of the plate, random noise is more readily detectable; however, in this region of chart readings the corresponding density varies very slowly. An approximate determination of the size of the errors $\Delta \log I$ is revealed in the data of Table 3. The table exhibits for Steward Observatory Plate No. 28, values of the average readability error as a function of chart reading, the resulting errors Δd obtained from Fig. 2, and $\Delta \log I$ obtained from a pair of extreme characteristic curves fitted to the step wedge data at $\lambda = 4500$. These errors seem to imply that one should stay away from the top portions of the S-shaped characteristic curves. Although errors ΔC are small here, the steepest portion of the $f(C,d)$ curve is utilized. A large error Δd , is the result. This problem is easily remedied by refraining

from overexposing any spectrum. But underexposure is also a serious problem since the values of $\log I$ for portions of the spectrum near the fog level of the plate are subjected to large errors as a direct consequence of large errors ΔC . Along the so-called unity-gamma, or straight portion of the characteristic curve, a compromise is reached whereby the errors, $\Delta \log I$, are minimized. Quality control is of vital importance in the program and has been exercised to the utmost.

Table 3 Effects of Readability Error Upon the Continuum

(Plate No. 28)

<u>C</u>	<u>ΔC</u>	<u>Δd</u>	<u>$\Delta \log I$</u>
05.0	00.1	.010	.008
10.0	00.2	.006	.006
20.0	00.3	.006	.006
30.0	00.4	.005	.007
40.0	00.5	.005	.008
50.0	00.7	.006	.009
60.0	00.9	.006	.010
70.0	01.1	.006	.013
80.0	01.5	.009	.030

In the variable star spectra, however, one encounters the problem of having to slightly overexpose the blue continuum region and associated emission lines to record the visible region of the spectrum around $\lambda 5200$ wherein F plates are least sensitive. This problem cannot be remedied by choosing plates of more uniform sensitivity since a wavelength base is necessary which covers the region from H and K to $H\alpha$; a photographic plate has yet to be devised which is of more uniform sensitivity over so long a range of wavelength than is the F plate.

All correction factors considered thus far are of secondary importance when compared to those which we now consider. Let $I(\lambda)$ represent the true monochromatic intensity emitted by a star and $I_o(\lambda)$ that observed on the photographic plate. These quantities are related by the expression

$$I(\lambda) = a(\lambda)k(\lambda)s(\lambda)I_o(\lambda)$$

where

$a(\lambda)$ =the correction factor for the interstellar medium

(the inverse transmission coefficient of the interstellar medium).

$k(\lambda)$ =the correction factor for the terrestrial atmosphere

(the inverse transmission coefficient of the terrestrial atmosphere).

$s(\lambda)$ =the instrumental correction factor

(the inverse transmission coefficient of plate and optics).

Each of these corrections must be applied to the readings $I_o(\lambda)$ obtained with the microdensitometer in order to obtain the quantities $I(\lambda)$. Such computations are straightforward but lengthy. Employing logarithmic notation, however, has greatly reduced the time required to complete a plate.

Since calibration spectra were taken by observing the light of a standard star, rather than that of a tungsten lamp, the functions $s(\lambda)$ and $k(\lambda)$ are not separately obtainable, but must be treated as a product which can be broken up into two other factors: a) the transmission coefficient of the instruments and n air masses, where n is a function of the zenith distance of the calibration star at the middle of the exposure

and b) the transmission coefficient of the number of differential air masses between calibration and program star. This correction can, of course, exceed 100%. From this point on, the following symbols will be used with regard to the correction factors: $k'(\lambda)$ will be defined as the correction mentioned in b) above and $s'(\lambda)$ that mentioned in a); thus $s(\lambda)k(\lambda) = s'(\lambda)k'(\lambda)$.

A. The differential extinction correction $k'(\lambda)$

This correction plays a relatively minor role in altering the appearance of the function $I_o(\lambda)$. Meinel (1963) has determined the extinction in magnitudes as a function of wavelength in the region $3600 < \lambda < 6400$ for the atmosphere above Kitt Peak during 1960 March - June (Table A2). His extinction curve may be converted into a conveniently useful table (Table A3) giving $\log k'(\lambda)$ at 200\AA intervals for 15 equally spaced values of $\Delta \sec z$, the algebraic difference between the air mass of standard (step wedge) and program star, between 0.1 and 1.5. These terms must be added to the values of $\log I_o(\lambda)$ of a given program star for the case in which the program star air mass exceeds the standard star air mass and subtracted when the situation is reversed.

B. The Instrumental Correction Factor $s'(\lambda)$

Where one has usually employed a tungsten lamp as a source of determining this correction factor, the author has chosen to employ one or more of Code's (1960) standard stars whose continua are known. The principal reasons for this choice are that a) one encounters great difficulty determining the temperature and temperature variation of a built-in light source and b) practically all of the atmospheric extinction problem

is eliminated by using a "standard" source outside the atmosphere. The following of Code's (1960) standard stars (Table 4) have been utilized in the program for the purpose of calibrating $s'(\lambda)$:

Table 4. Code's Standard Stars Used for Plate Calibration

Name	<u>α</u>	<u>δ</u>	<u>V</u>	<u>B-V</u>	<u>Sp.</u>
π^3 Ori	04:47.1	+06:53	3.16	+0.46	F6V
4 Aur*	04:55.9	+37:49	5.0		AOV
γ Gem*	06:34.8	+16:27	1.95		AOIV
ρ Gem	07:25.9	+31:53	4.16	+0.31	F0V
η UMa	13:45.6	+49:34	1.91	-0.23	B3V
α CrB*	15:33.1	+26.53	2.3		AOV
α Lyr	18:35.6	+38:45	0.03	0.00	AOV
16 Cyg A	19:40.5	+50:24	5.96	+0.64	G2V
δ Cyg	19:43.4	+45:00	3.00		B9.5III

*Not a Code standard.

Use of the continuum of α Lyr as given by Code for other AOIV-V stars results in no appreciable error in B-V for the remaining stars on the plate.

True monochromatic magnitudes $m(l/\lambda)$ are defined by Code in wave number notation:

$$m(l/\lambda) = -2.5 \log \frac{F(l/\lambda)}{F(1.80)}$$

where $F(l/\lambda)$ is the area under the I vs $\frac{1}{\lambda}$ curve in a pass band centered at wavelength λ , and $F(1.80)$ is that centered at $1.80 \mu^{-1}$. The width of the latter pass band is given as 10\AA . Code has chosen pass band centers which are least affected by line absorption. Since the spectrograph

integrates light over equal wavelength and not wave number intervals, one is required to convert Code's monochromatic magnitudes, which are quoted in Table 5, into a more useful form. Since wave number intervals are related to wavelength intervals by

$$d\tilde{\nu} = \frac{d\lambda}{\lambda^2}$$

we have $\frac{d\tilde{\nu}}{d\tilde{\nu}}(1.80) = \frac{d\lambda}{\lambda^2} \times \frac{\lambda^2}{d\lambda} = 10\text{\AA} \times (1.80\mu^{-1})^2 \frac{\lambda^2}{d\lambda}$

But since $\frac{d\tilde{\nu}}{d\tilde{\nu}}(1.80) = 1$, the passband width at wavelength λ in units of μ^{-1} may be found by the relationship

$$d\lambda = \frac{3.21}{(\mu^{-1})^2} \times 10\text{\AA} \quad (1)$$

Table 5

Monochromatic Magnitudes m(1/\lambda)

Name	Sp/ $\lambda(\text{\AA})$	3650	3860	4040	4190	4590	5060	5810	6050	6670
η UMa	B3V	+0.05	-0.29	-0.37	-0.33	-0.28	-0.12	+0.08	+.21	+.29
δ Cyg	B9.5III	+0.86	-0.14	-0.19	-0.16	-0.12	-0.06	+.06	+.14	+.24
α Lyr	A0V	+1.04	-0.07	-0.19	-0.16	-0.14	-0.06	+.06	+.12	+.22
ρ Gem	F0V	+1.26	+0.56	+0.36	+0.28	+0.14	+.09	+.03	+.03	+.04
π^3 Ori	F6V	+1.22	+0.79	+0.50	+0.42	+0.22	+.11	-0.03	-0.02	-0.03
16 Cyg A	G2.5V	+1.52	+1.40	+0.88	+0.76	+0.39	+.19	-0.05	-0.07	-0.15
61 Cyg A	K5V	+3.13	+2.90	+2.03	+1.73	+0.73	+.53	-0.20	-0.25	-0.44

Code's monochromatic magnitudes were converted to relative intensities in passbands of equal wavelength, normalized to unity at $1.80\mu^{-1}$ for all stars used in the program. The choice of $1.80\mu^{-1}$, which corresponds to 5560\AA , as the normalization point, is particularly unsatisfactory for the spectra in this program since E and F plates are insensitive in this region.

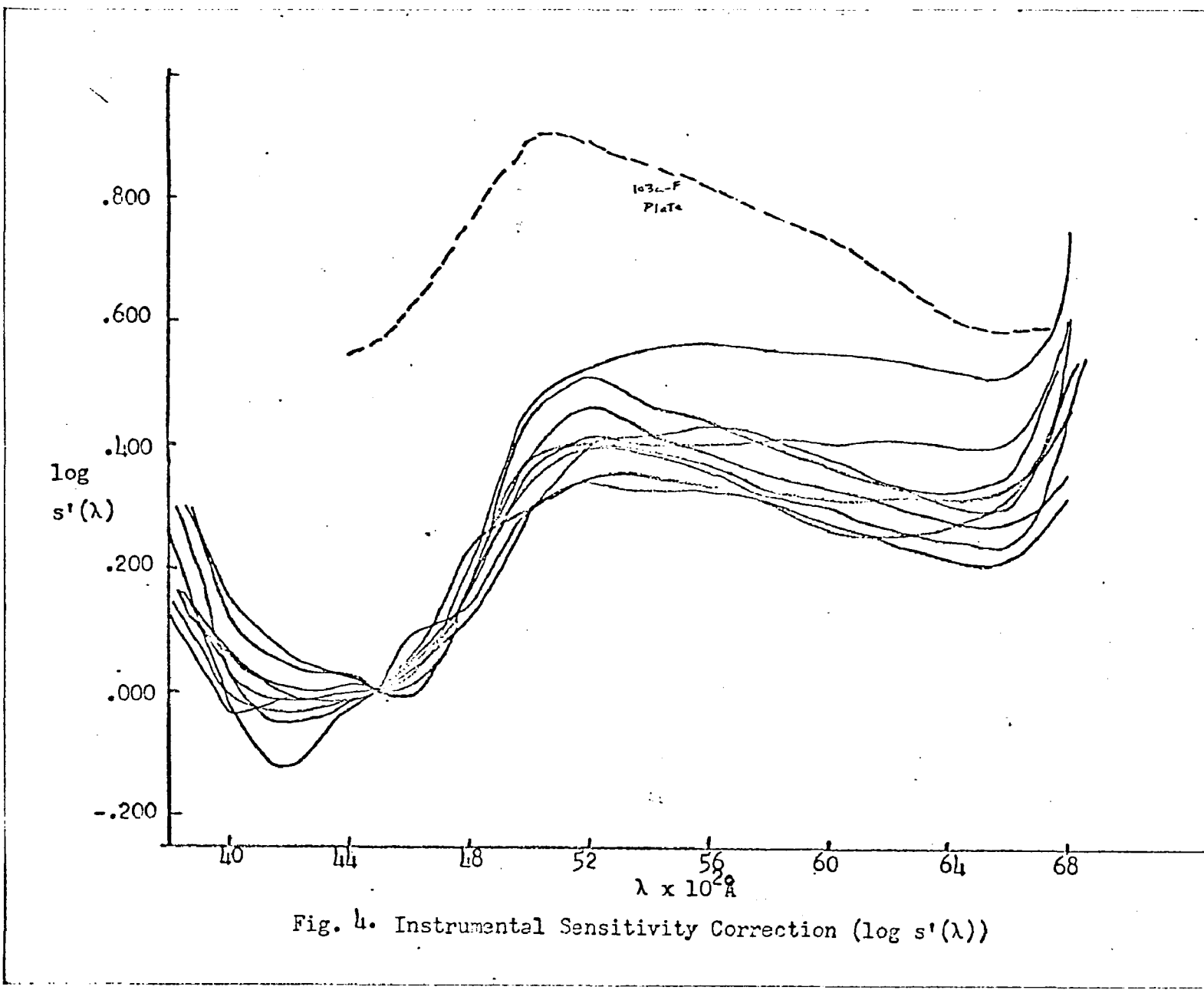
A new normalization point was chosen which lies in a much more transparent region at $\lambda 4500$. This necessitates a renormalization of Code's data. Thus, Table 6 gives the run of $\log I(\lambda) - \log I(4500\text{\AA})$ with λ for each of Code's stars which has been employed in the program. The instrumental sensitivity correction as a function of wavelength is given for each plate by the logarithm of the ratio of intensity according to Code to that determined from the plate. Fig. 4 illustrates the behavior of this function for all plates considered.

The instrumental correction is unique enough for each plate so that any thought of employing a single correction $s'(\lambda)$ for all plates should be forgotten. Primarily this difference exists because standard star spectra have been observed at different zenith distances; we might expect a smaller spread in these correction curves if they were obtained with a standard lamp located inside the spectrograph. This, as previously mentioned, requires rather definite knowledge about the temperature of the filament of that lamp and its dependence upon local conditions. On the other hand Code's standard star continua are found to be of sufficient accuracy to warrant their use in this program. Utilizing any one of Code's standards in the step wedge, one is able to predict the color of any other of his standards. This kind of test has been employed upon each plate in this program and its results will be discussed later.

The relative sensitivity of the 103a-F spectroscopic plate as given in the Kodak Reference Handbook is depicted by the dotted curve in Fig. 4; this curve has been raised above the others for ease in distinguishing it from them. The spectrograph and telescope optics appear to transmit

Table 6Log Relative Intensity vs Wavelength for Standard Stars

<u>$\lambda(\text{\AA})$</u>	<u>α Lyr</u>	<u>η UMa</u>	<u>δ Cyg</u>	<u>16 Cyg A</u>	<u>61 Cyg A</u>	<u>ρ Gem</u>	<u>π^3 Ori</u>
3600	-.410	.057	-.404	-.232	-.644	-.292	-.223
3800	.067	.114	.072	-.250	-.726	-.039	-.113
4000	.111	.146	.118	-.120	-.421	.009	-.009
4200	.072	.072	.070	-.054	-.259	.013	-.001
4400	.024	.022	.022	-.018	-.065	.006	.000
4500	.000	.000	.000	.000	.000	.000	.000
4600	-.025	-.025	-.022	.014	.060	-.008	-.001
4800	-.071	-.086	-.064	.014	.059	-.033	-.014
5000	-.121	-.149	-.116	.008	.048	-.064	-.035
5200	-.169	-.211	-.163	.002	.071	-.086	-.054
5400	-.210	-.257	-.203	.003	.130	-.103	-.068
5600	-.249	-.314	-.247	.000	.191	-.122	-.082
5800	-.306	-.374	-.299	-.034	.217	-.170	-.107
6000	-.356	-.446	-.355	-.043	.208	-.201	-.138
6200	-.403	-.495	-.404	-.054	.204	-.231	-.166
6400	-.445	-.535	-.450	-.071	.200	-.257	-.189
6600	-.471	-.561	-.483	-.084	.198	-.285	-.203
6800	-.499	-.583	-.502	-.121	.188	-.311	-.210



almost neutrally over a large portion of the wavelength region under investigation; however, in the region shortward of $\lambda 4000$, a great rise in $s'(\lambda)$ results because of low transmission of the optics. A similar but less exaggerated deviation of $s'(\lambda)$ from the sensitivity of the 103a-F plate occurs at the opposite end of the spectrum. This observation agrees with other independent tests which have been made of the optics of the Steward Reflector.

C. The Interstellar Reddening Correction

This term need not be taken into account in the computation of B-V color since such a correction is not included in the photometric reductions with which the spectroscopic observations are to be contrasted; however, it is of primary importance in deducing the nature of the true relative continuum to make some mention of interstellar reddening. The values $E_{B-V}=0.30$ for the mean reddening in T Tauri stars has been estimated by Herbig (1952), Kholopov (1958), and Varsavsky (1960). There is no reason to believe this does not vary considerably from star to star. Indeed the comma-shaped nebula around T Tauri may produce a large reddening effect. Final disagreement between the shapes of T Tauri and dwarf G star continua can serve as a means of determining interstellar reddening. One will nevertheless encounter difficulty in the determination of the space reddening of these objects since a) ultraviolet and blue emission continua are known to be present in these stars; these lead to distortions of the smooth underlying black body continuum; and b) it has not even been determined whether the T Tauri continua should correspond to those of MK standards of the same spectral class. Since these stars lie above the main

sequence this is a valid objection. Hence, the attitude will be taken that the reddening due to interstellar material is completely unknown and is to be treated as output rather than input data in the program.

D. Determination of B-V Color

If the intensities, $I(\lambda)$, corrected for all other effects, are separately multiplied by $Q_B(\lambda)$ and $Q_V(\lambda)$, the spectral responses of the B and V filters plus photometer, one will obtain two intensity curves which depict the character of the radiation as the photometer sees it when viewing in each of the two pass bands. Let the following intensity distributions thus be defined:

$$\begin{aligned} I_B(\lambda) &= Q_B(\lambda)I(\lambda) \\ I_V(\lambda) &= Q_V(\lambda)I(\lambda) \end{aligned} \quad (2)$$

The ratio of areas under the curves is proportional to the B-V color. The quantities $Q_B(\lambda)$ and $Q_V(\lambda)$ were taken from Allen (1963); their logarithms are tabulated in Table A4.

Determination of the area $\int_0^\infty Q_{B,V}(\lambda)I(\lambda)d\lambda = A_{B,V}$ under a given curve was accomplished by using a polar planimeter accurate to 0.5%. The B-V color is defined as (Allen (1963))

$$(B-V)_c = 2.5 \log \frac{A_{cV}}{A_{cB}} + 0.71 \quad (3)$$

where the subscript, c, indicates that only continuous emission has been considered in the color determination. Values of $(B-V)_c$ are recorded on each data sheet, the contents of which will be explained shortly.

E. The Effects of Line Emission

An entirely separate set of computations must be employed for the variable program stars in order to determine the color (B-V)_{cl} which includes the emission lines. Tables 12 list all emission lines which have been observed in the T Tauri type spectra over the entire range of plates. Those lines identified by Joy (1949) have been so indicated. A detailed discussion of line emission is deferred to Chapter IV. Under consideration here is the determination of the additional flux supplied by these lines.

Each line profile, approximated as rectangular, has a peak of true intensity and an associated adjacent continuum intensity, both which may be determined by exactly the same method used to find any of the values $I_{B,V}(\lambda)$. The flux contributed by a given profile to the B, V, or, indeed, both magnitudes is computed directly from its area

$$A_{B,V} = \frac{I_{B,V}(\lambda_1) - I_{B,V}(\lambda_c)}{\Delta\lambda} \quad (4)$$

where

$I_{B,V}(\lambda_1)$ is the true photometric intensity maximum in the line profile,

$I_{B,V}(\lambda_c)$ is the true photometric intensity of the continuum adjacent to the line,

$\Delta\lambda$ is the measured line width at its base. Various slit widths were employed and found not to affect the line width on the plate. An operational evaluation of the effect of line emission upon B-V color

is accomplished by defining the new color $(B-V)_{cl}$ composed of both continuous and line emission fluxes. In terms of the notation previously employed this color can be expressed as

$$(B-V)_{cl} = 2.5 \log \frac{A_{cV} + A_{LB,V}}{A_{cB} + A_{LB}} + 0.71 \quad (5)$$

where $A_{LB,V}$ is the sum of the individual line contributions to the area under the photometric intensity curve. Thus, one can speak of the color difference $\delta = (B-V)_{cl} - (B-V)_c$ as an index of the emission line effect.

III. Presentation of Relevant Data

This chapter contains a brief description of A) the T Tauri objects under investigation and B) the organization of observations made upon those objects. The final section C) consists of tabulations of the observational data.

A. T. Tauri Objects Studied

Observational limitations are placed upon this program which immediately exclude all but a handful of T Tauri stars from the program. Owing to their relative brightness and line emission activity the stars T Tau and RW Aur have been selected for examination.

T Tauri (= HD 41619 = BD+19°706) has been known to vary in brightness since its discovery in 1852 by Hind. The star is located half a minute of arc from the faint nebulous patch known as Hind's variable nebula (NGC 1555). In the course of a few weeks T Tau has been known to vary erratically between V = 9.0 and V = 12.8. Joy's (1945) classification of the absorption spectrum is dG5e but the overwhelming presence of line emission makes the classification task difficult; estimates have ranged from dG2e to dG8e between the years 1915 - 1947. Joy claims the CaII (H and K) emission lines appear "with an intensity unsurpassed by any star of the T Tauri group," but these lines appear still stronger today in spectra of RW Aur (See Fig. 1). He found, contrary to what is observed today, that the other metallic bright lines are not prominent

features of the spectrum. Adams and Pease's (1915) description of the first slit spectrogram taken of this object reveals further differences. Fifteen emission lines were useable for radial velocity determinations at that time. Less than a year later the emission spectrum was described as very weak. Owing to the low dispersion used almost no significance is attached to the published radial velocity measurements of this object. The strengthening of emission features appears to coincide with greatest brilliancy.

RW Aurigae (= HD 50130) was investigated by Ceraski (1906) who discovered the variability of this object; the total range in visual magnitude is 3.0 ($V = 9.0 - 12.0$). Zinner's light curve (1913) shows that fluctuations of a full magnitude or more in a 24-hour span are not uncommon. This observed fact has a very important bearing upon the investigation at hand.

The object behaved in a less erratic manner when investigated by Encke (1907), fluctuating smoothly between the 9th and 10th visual magnitudes during the first two months of 1907. The classification dG5e has been obtained from low dispersion spectra, but numerous bright lines, notably H and K, reveal only a glimpse of the underlying wide absorption features. On higher dispersion spectra, reversals are exhibited in the CaII H and K, $H\beta$, $H\gamma$, $H\delta$, and $H\epsilon$ emission features; the red component of the latter blends strongly with CaII H. Again radial velocity measurements leave much to be desired because of the lack of sharpness of both emission and absorption features. Sufficient numbers of spectra have not been acquired so that one can compare the strength of metallic emission

lines with the visual brightness of the star. Obscured areas are found nearby but not in the immediate vicinity of RW Aur.

Other T Tauri objects included in this study are AS 205, AS 209, and DI Cep. The first two of these are located in the Ophiuchus dark cloud, the latter in still a different region of the Milky Way. Only a handful of spectra of each has been secured. DI Cep is known (Joy (1945)) to fluctuate between $V = 11.9$ and $V = 13.5$ and is designated as a dK3e star. Strong H and K plus Balmer Series emission in addition to presence of the brightest T Tauri lines constitute all that is peculiar about the spectrum of this star. AS 205 and AS 209 have almost no history. Both classification type and V magnitude range are unknown. Their spectra exhibit faint H and K plus hydrogen emission. Owing to the short access time of these stars in northern latitudes, an extensive set of observations of them is hard to come by. Single observations of these objects were obtained for two reasons:

- 1) To determine roughly the magnitude of the line emission effect as well as whether and by how much that effect differs from what is found for the winter sky objects;
- 2) To launch a much wider investigation of T Tauri variables among different associations. This investigation will utilize the methods of reduction outlined in this paper to explore variations in the properties of known T Tauri variables in the Bootes, Cepheus, Ophiuchus, and Taurus regions of the Milky Way.

Table 7 contains a list of all objects, other than T Tauri variables and calibration stars, which have been investigated in this program. These are the so-called "test objects." At least one of these has been utilized per plate and the B-V color computed from its spectrum. Such colors are then compared with the measured photometric color. Agreement between the two signifies that the various correction factors computed for the plate can be applied to the program star with some certainty. Where possible, stars have been used whose detailed continuum structure is given in Code's Table. Comparison of derived and computed continua provides a more stringent test of the method.

Table 7 Non-Variable Program Stars

Name	<u>α</u>	<u>δ</u>	<u>V</u>	<u>B-V</u>	Sp
13974	02:14.2	+34:03	4.87	+0.61	G0V
K Cet	03:17.5	+03:14	4.82	+0.68	G5V
ε Eri	03:31.3	-09:35	3.73	+0.89	K2V
η ³ Cri	04:47.9	+06:55	3.19	+0.45	F6V
ρ Gem	07:26.9	+31:52	4.16	+0.32	F0V
θ Com	13:09.5	+28:08	4.28	+0.57	G0V
μ Her A	17:44.5	+27:45	3.42	+0.75	G5IV
16 Cyg A	19:40.5	+50:24	5.96	+0.64	G2V
η Cep	20:44.3	+61:39	3.43	+0.92	K0IV
61 Cyg A	21:04.7	+38:30	5.19	+1.19	K5V

B. Explanation of Tables

1. Table 8. Step Wedge Calibration (One table per plate)

The Wratten gelatin filter density as quoted from the Eastman Kodak Co. is written horizontally vs the wavelength, in hundreds of angstroms, at which cross-dispersion tracings were made. The figures comprising the table are the corresponding observed densities, d , on the plate. Since the true filter density is wavelength dependent, one must consult Table Al in order to obtain the true steps in $\log I$ and thus plot curves of d vs $\log I$ which will convert observed opacities into logarithms of relative intensity.

At the top are given the Steward Observatory plate number, (Kitt Peak Station record), emulsion type, and observation date.

2. Table 9. Continuum Analysis (One table per star)

At the top are given the Steward Observatory plate number, type of emulsion, date of observation, name of object, 1964 equatorial system coordinates of the object, air mass at which the object was observed, differential air mass between program and calibration star, MK spectral classification, observed B-V color according to Johnson and Harris (1954), Johnson (1955), or Johnson (unpublished), and computed B-V color.

At least one star per plate (labeled calibration star) is a Code standard whose continuum is known. For the calibration objects the columns in the continuum analysis table have the following meaning and origin:

Column 1 ($\lambda (\text{\AA}) \times 10^2$): The wavelength in hundreds of angstroms at which the continuum was studied.

Column 2 (C): The corresponding Bristol Recorder Chart reading (scale 0-94).

Column 3 (d): The apparent density corresponding to the reading in the previous column and determined from Fig. 2. The numbers in this and the remaining columns are in thousands of relative logarithmic units.

Column 4 (logI): The logarithm of relative intensity corresponding to the reading in the previous column and determined from the characteristic curve of the plate (Fig. 3).

Column 5 (logI(V.T.)): If the calibration star spectrum employed for the purposes of determining plate sensitivity is not the one of highest apparent density in the step wedge (i.e. a spectrum which has been taken through a "neutral" filter) the values in the previous column must be corrected for the effects of variable transmission (V.T.) by the "neutral" filter. This is easily done by utilizing the quantities in Table A1. If this correction is not required the components of column 4 are repeated in column 5.

Column 6 ($\log I(NORM)$): The quantity in column 5, normalized to $\log I = .000$ at $\lambda 4500$.

Column 7 ($\log S'$): The instrumental sensitivity correction obtained at a given wavelength by subtracting from the logarithm of true normalized intensity (Table 6), the corresponding observed quantity in column 6.

For all other stars on a plate the columns in the continuum analysis table have the following meaning and origin:

Columns 1, 2, 3, and 4: Exactly the same meaning as the columns so numbered for the calibration star. All logarithmic units have been multiplied by 1000.

Column 5 ($\log I(EXT.)$): The quantity in column 4 corrected for the effects of differential atmospheric extinction between the given program star, whose continuum is to be determined, and the calibration star for the plate in question, whose spectrum has been used to obtain the instrumental sensitivity correction. The figures in Table A3 corresponding to the appropriate $\Delta \sec z$ are added to or subtracted from those in column 4.

Column 6 ($\log I(EXT.NORM)$): The quantity in column 5 normalized to $\log I = .000$ at $\lambda 4500$.

Column 7 ($\log I(INST)$): The quantity in column 6 corrected for the effects instrument and plate sensitivity obtained by direct addition of that column with column 7 in the calibration star table.

Column 8 ($\log I$ (B PHTM)): The quantity in column 7 plus the corresponding quantity in the $\log Q_B$ column of Table A4. Thus the relative intensity is converted into that which is observed through the B filter and photometer.

Column 9 ($\log I$ (V PHTM)): The quantity in column 7 plus the corresponding quantity in the $\log Q_V$ column of Table A4. Thus the relative intensity is converted into that which is observed through the V filter.

Column 10 (I (B PHTM)): The antilogarithm of the quantity in column 8, or the intensity as viewed with the B filter and photometer.

Column 11 (I (V PHTM)): The antilogarithm of the quantity in column 9, or the intensity as viewed with the V filter and photometer.

3. Table 10. Line Analysis (One table per emission star)

The nature of the data at the top of the table has already been discussed. The vertical columns have the following meaning and origin:

Column 1 (λ^0): The observed wavelength of the center of the emission line whose contribution to the continuum flux is to be determined.

Column 2 (C_1): The Bristol Recorder reading (scale 0-94) of the peak of intensity of the line.

Column 3 (C_c): The Bristol Recorder reading (scale 0-94) of the continuum adjacent to the line.

Column 4 (d_1): The observed density of the peak of emission determined from the quantity in column 2 using Fig. 2.

Column 5 (d_c): The observed density of the adjacent continuum determined from the quantity in column 3 using Fig. 2.

Column 6 ($\log I_1$): The logarithm of relative intensity corresponding to the reading in column 4 and determined from the characteristic curves of the plate (Fig. 3).

Column 7 ($\log I_c$): The logarithm of relative intensity corresponding to the reading in column 5 and determined from the characteristic curves of the plate (Fig. 3).

Column 8 ($\Delta \log I$): The difference column 6 minus column 7.

Column 9 ($\log I_{CB} + \Delta \log I$): The sum of the logarithm of relative continuum intensity in the B filter pass band and the quantity in column 8. The former quantity is read, at the wavelength of the line under consideration, from a plot of $\log I$ (B PHTM) vs λ for the emission star (See Continuum Analysis Table, column 8).

Column 10 ($\log I_{cV} + \Delta \log I$): The sum of the logarithm of relative continuum intensity in the V filter pass band and the quantity in column 8. The former quantity is read, at the wavelength of the line under consideration, from a plot of $\log I$ (V PHTM) vs λ for the emission star (See Continuum Analysis Table, column 9).

Column 11 ($I_{lB} - I_{cB}$): The difference in intensity between line and continuum as viewed in the B filter pass band, obtained by subtracting from the antilogarithm of the quantity in column 9, the corresponding continuum intensity as viewed in the B filter pass band.

Column 12 ($I_{lV} - I_{cV}$): The difference in intensity between line and continuum as viewed in the V filter pass band, obtained by subtracting from the antilogarithm of the quantity in column 10, the corresponding continuum intensity as viewed in the V filter pass band.

Column 13 (Width Å): The width in angstroms of the (nearly) rectangular line profile as measured directly from the microdensitometer tracing.

Column 14 (A_B): The area contributed by the line to the I_B VS λ plot, obtained by taking the product of columns 11 and 13. This quantity has the dimensions angstroms x relative intensity units.

Column 15 (A_V): The area contributed by the line to the I_V vs λ plot, obtained by taking the product of columns 12 and 13. This quantity has the dimensions angstroms x relative intensity units.

4. Table 11. Data Summary Sheet for T Tauri Object (One table per emission star).

The quantities displayed in this table have the following meaning and origin:

1. (Plate No.): Steward Observatory Plate Number.
2. (Object): Name of emission star observed.
3. (A_{CV}): The area (angstroms x relative intensity units) under the intensity vs wavelength curve of the continuum as viewed with the V filter plus photometer. The derivation of this quantity has been discussed.
4. (A_{CB}): The area (angstroms x relative intensity units) under the intensity vs wavelength curve of the continuum as viewed with the B filter plus photometer. The derivation of this quantity has been discussed.
5. (A_{IV}): The total area contributed by all lines to the intensity, wavelength plot in the V pass band; the sum of all components of column 15 of the line analysis table.
6. (No. of lines contributing to V): The total number of lines and blends of lines which have been added to obtain the quantity, 5.

7. (A_{LB}) : The total area contributed by all lines to the intensity, wavelength plot in the B pass band; the sum of all components of column 14 of the line analysis table.
8. (No. of lines contributing to B): The total number of lines and blends of lines which have been added to obtain the quantity 7.
9. (A_{cV}/A_{cB}) : The ratio of quantities 3 and 4 of this table. This is also tabulated at the bottom of each emission star continuum analysis table and is used to compute the continuum color.
10. $((B-V)_c)$: The continuum color of the object, also reproduced on each emission star continuum analysis table.
11. $((A_{cV} + A_{lV})/(A_{cB} + A_{LB}))$: The ratio of the sum of quantities 3 and 5 to that of quantities 4 and 7 of this table, to be used in computing the color of the object when the presence of emission lines is considered.
12. $((B-V)_{cl})$: The color of the object derived from both continuum and line flux contributions, computed from quantity 11 of this table by the expression defined in the text (equation (5)).
13. (A_{lV}/A_{cV}) : The ratio of quantities 5 and 3 of this table; the line to continuous emission ratio in the V pass band. This is an approximate index of line contribution to measured fluxes in the V pass band.

14. (A_{LB}/A_{CB}): The ratio of quantities 7 and 4 of this table; the line to continuous emission ratio in the B pass band. This is an approximate index of line contribution to measured fluxes in the B pass band.

Table 8. Step Wedge Calibration

Plate No: 23		Emulsion: 103a-E			Date: 1963 Oct. 13		
Wratten Density $\lambda(\text{\AA}) \times 10^2$	4x0.3	3x0.3	2x0.3	0.3	0.0		
35	-	.061	.138	.366	.837		
40	.193	.421	.868	1.560	2.046		
45	.227	.491	.865	1.447	1.860		
50	-	.112	.251	.518	.871		
55	-	.070	.160	.361	.632		
60	-	.102	.225	.506	.836		
65	-	.166	.332	.681	1.088		

Table 8 Step Wedge Calibration

Plate No: 25		Emulsion: 103a-F			Date: 1963 Oct. 14		
Wratten Density	$\lambda(\text{\AA}) \times 10^2$	4x0.3	3x0.3	2x0.3	0.3	0.0	
35	-	.050	.160	.508	1.052		
40	.110	.305	.727	1.320	1.930		
45	.175	.463	.900	1.510	1.930		
50	.070	.130	.350	.738	1.320		
55	-	.108	.200	.530	1.030		
60	-	.058	.202	.478	.915		
65	-	-	-	-	-		

Table 8 Step Wedge Calibration

Plate No: 26		Emulsion: 103a-F			Date: 1963 Oct. 15		
Wratten Density $\lambda(\text{\AA}) \times 10^2$	4x0.3	3x0.3	2x0.3	0.3	0.0		
35	-	-	.097	.341	.852		
40	.132	.342	.751	1.320	1.760		
45	.221	.500	.938	1.421	1.960		
50	.059	.190	.408	.838	1.438		
55	-	.106	.318	.701	1.280		
60	-	.088	.284	.606	1.158		
65							

Table 8 Step Wedge Calibration

Plate No: 28		Emulsion: 103a-F			Date: 1903 Oct. 17		
Wratten Density $\lambda(\text{\AA}) \times 10^2$	4x0.3	3x0.3	2x0.3	0.3	0.0		
35	-	.023	.068	.255	.526		
40	.047	.195	.500	.913	1.450		
45	.112	.286	.607	1.050	1.550		
50	-	.082	.219	.515	.900		
55	-	.045	.133	.349	.700		
60	-	.052	.095	.313	.612		
65							

Table 8 Step Wedge Calibration

Plate No: 199		Emulsion: 103a-F			Date: 1964 June 17			
Wratten Density $\lambda(\text{\AA}) \times 10^2$		5x0.3	4x0.3	3x0.3	2x0.3	0.3	0.0	
35	-	.058	.250	.651	1.322	1.820		
40	.196	.657	1.378	1.960	2.500	2.670		
45	.322	.870	1.275	2.068	2.670	2.670		
50	.100	.341	.107	1.350	2.020	2.068		
55	.101	.282	.666	1.192	1.960	2.127		
60	.046	.215	.613	1.080	1.762	2.068		
65	-	.112	.441	.832	1.560	1.880		

Table 8 Step Wedge Calibration

Plate No: 200		Emulsion: 103a-F			Date: 1964 June 18			
Wratten Density $\lambda(\text{\AA}) \times 10^2$		5x0.3	4x0.3	3x0.3	2x0.3	0.3	0.0	
35	-	.073	.256	.600	1.232	1.443		
40	.196	.669	1.330	1.900	1.980	1.980		
45	.327	.869	1.500	1.880	1.900	1.980		
50	.193	.382	.913	1.458	1.780	1.882		
55	-	.378	.780	1.432	1.680	1.760		
60	-	.364	.710	1.290	1.660	1.740		
65	-	.326	.578	1.053	1.433	1.648		

Table 8 Step Wedge Calibration

Plate No: 205		Emulsion: 103a-F			Date: 1964 July 26		
Wratten Density $\lambda(\text{\AA}) \times 10^2$	1.6	1.2	1.0	0.6	0.3	0.0	
35	.112	.215	.510	1.120	1.640	2.020	
40	.135	.208	1.320	1.980	2.170	2.206	
45	.522	.935	1.445	2.020	2.206	2.206	
50	.182	.500	.900	1.505	2.020	2.170	
55	.106	.310	.630	1.285	1.240	2.143	
60	.042	.200	.480	1.000	1.500	1.990	
65	.015	.115	.285	.790	1.240	1.750	

Table 8 Step Wedge Calibration

Plate No: 207		Emulsion: 103a-F			Date: 1964 July 27		
Wratten Density $\lambda(\text{\AA}) \times 10^2$	1.6	1.2	1.0	0.6	0.3	0.0	
35	.018	.130	.326	.750	.912	1.765	
40	.063	.622	1.060	1.568	1.660	2.100	
45	.326	.729	1.152	1.649	1.720	2.130	
50	.079	.280	.540	1.006	1.126	2.220	
55	-	-	.166	.366	.790	2.100	
60							
65							

Table 8 Step Wedge Calibration

Plate No: 209		Emulsion: 103a-F			Date: 1964 July 27		
Wratten Density $\lambda(\text{\AA}) \times 10^2$	1.6	1.2	1.0	0.6	0.3	0.0	
35	-	.011	.193	.677	1.243	1.650	
40	.228	.540	.867	1.660	2.301	2.700	
45	.283	.634	1.090	1.760	2.220	3.000	
50	.122	.273	.523	1.153	1.740	2.097	
55	.100	.211	.360	.900	1.190	1.780	
60	.046	.142	.262	.717	1.163	1.508	
65	.008	.066	.182	.479	.957	1.289	

Table 8 Step Wedge Calibration

Plate No: 210		Emulsion: 103a-F			Date: 1964 July 28		
Wratten Density $\lambda(\text{\AA}) \times 10^2$	1.6	1.2	1.0	0.6	0.3	0.0	
35	.015	.028	.070	.338	.703	1.242	
40	.112	.309	.636	1.237	1.840	2.000	
45	.115	.404	.723	1.288	1.760	1.980	
50	-	.108	.260	.643	1.160	1.580	
55	-	.070	.195	.530	1.080	1.445	
60	-	-	.070	.330	.702	1.120	
65	-	-	.043	.272	.623	1.016	

Table 8 Step Wedge Calibration

Plate No: 232		Emulsion: 103a-F			Date: 1965 Jan. 1		
Wratten Density $\lambda(\text{\AA}) \times 10^2$	1.6	1.2	1.0	0.6	0.3	0.0	
35	-	-	.052	.192	.518	.904	
40	.052	.169	.429	.819	1.313	1.762	
45	.143	.337	.636	1.050	1.500	1.840	
50	.073	.139	.263	.547	1.017	1.373	
55	-	.079	.192	.451	.803	1.248	
60	.019	.071	.200	.468	.882	1.292	
65	-	.023	.122	.360	.712	1.092	

Table 8 Step Wedge Calibration

Plate No: 236		Emulsion: 103a-F			Date: 1965 Jan. 27		
Wratten Density $\lambda(\text{\AA}) \times 10^2$	1.6	1.2	1.0	0.6	0.3	0.0	
35	-	.198	.413	.860	1.338	1.740	
40	.241	.540	.970	1.441	1.985	2.070	
45	.531	.871	1.322	1.739	2.020	2.200	
50	.233	.560	.891	1.341	1.740	1.985	
55	.191	.441	.821	1.238	1.640	1.940	
60	-	.378	.724	1.200	1.620	1.840	
65	-	.227	.540	.931	1.420	1.740	

Table 8 Step Wedge Calibration

Plate No: 237		Emulsion: 103a-F			Date: 1965 Jan. 28		
Wratten Density $\lambda(\text{\AA}) \times 10^2$	1.6	1.2	1.0	0.6	0.3	0.0	
35	-	.061	.313	.740	1.202	1.640	
40	-	.191	.738	1.285	1.820	2.270	
45	.198	.367	.974	1.540	1.985	2.500	
50	-	.118	.489	.920	1.485	1.760	
55	-	.117	.392	.865	1.320	1.740	
60	-	.081	.378	.822	1.293	1.620	
65	-	.047	.262	.620	1.062	1.368	

Table 8 Step Wedge Calibration

Plate No: 240		Emulsion: 103a-F			Date: 1965 Jan. 29		
Wratten Density $\lambda(\text{\AA}) \times 10^2$	1.6	1.2	1.0	0.6	0.3	0.0	
35	-	-	.113	.300	.864	1.639	
40	-	-	.187	.446	1.162	1.900	
45	-	.037	.298	.680	1.293	2.000	
50	-	-	.109	.327	.810	1.520	
55	-	-	.086	.276	.739	1.368	
60	-	-	.079	.256	.680	1.320	
65	-	-	.012	.202	.585	1.242	

Table 8 Step Wedge Calibration

Plate No: 242		Emulsion: 103a-T			Date: 1965 Feb. 19		
Wratten Density $\lambda(\text{\AA}) \times 10^2$	1.6	1.2	1.0	0.6	0.3	0.0	
35	-	.022	.190	.421	.883	1.325	
40	.126	.270	.722	.951	1.442	1.740	
45	.203	.368	.802	1.095	1.443	1.740	
50	.002	.126	.371	.598	1.023	1.390	
55	-	-	.266	.567	.900	1.321	
60	-	.051	.268	.516	.880	1.277	
65	-	-	.144	.366	.748	1.152	

Table 9 Continuum Analysis

Plate No: 23		Emulsion: 103a-E			Date: 1963 Oct. 13			MK Sp: A0IV		
Object: γ Gem		$\alpha:$ 06:35.7			$\sec z:$ 1.079			$B-V:$ 0.00		
		$\delta:$ +16:26			$\Delta \sec z:$					
$\lambda(\text{\AA}) \times 10^2$	c	d	log I (FAT)	log I (INST) (NORM)	log I (INST) (EXT)	log I (INST) (PHTM)	log I (B) (PHTM)	log I (V) (PHTM)	I (B) (PHTM)	I (V) (PHTM)
36	69.5	130	-1900		-1080	670				
38	27.2	536	-1090		-270	203				
40	12.0	900	-792		028	083				
42	10.6	950	-758		062	010				
44	12.5	863	-806		014	010				
45	13.1	865	-820		000	000				
46	16.1	780	-881		-061	036				
48	30.7	482	-1151		-331	260				
50	61.9	182	-1648		-828	707				
52	73.4	106	-							
54	75.0	100	-1880		-1060	850				
56	73.9	102	-1780		-960	711				
58	72.3	112	-1703		-803	557				
60	70.0	123	-1652		-832	476				
62	61.9	182	-1512		-692	289				
64	58.0	210	-1466		-646	201				
66	85.3	040	-							
68	-									

Table 9 Continuum Analysis

Plate No: 23		Emulsion: 103a-E			Date: 1963 Oct. 13			MK Sp: G5V		
Object: K Cet		$\alpha:$ 03:17.5			$\Delta \text{sec z:}$ 1.367			$B-V:$ 0.68		
		$\delta:$ +03:14			$\Delta \text{sec z:}$.268			$(B-V)_C:$ 0.67		
$\lambda(\text{\AA}) \times 10^2$	c	d	$\log I$	$\log I$ (EXT) (NORM)	$\log I$ (EXT) (NORM)	$\log I$ (INST)	$\log I$ (B) (PHTM)	$\log I$ (V) (PHTM)	I (B) (PHTM)	I (V) (PHTM)
36	84.0	047	-				- ∞		000	
38	47.5	291	-1421	-1358	- 648	-445	-1299		050	
40	19.2	699	- 946	- 892	- 182	-099	- 126		748	
42	14.4	821	- 851	- 803	- 093	-083	- 087		819	
44	11.5	915	- 781	- 737	- 027	-017	- 063		665	
45	10.3	956	- 753	- 710	000	000				
46	10.9	936	- 767	- 726	- 016	020	- 114		769	
48	17.8	729	- 922	- 884	- 174	086	- 182	- ∞	650	000
50	46.9	301	-1370	-1336	- 626	081	- 363	- 363	434	434
52	72.3	112	-1770:	-1738	-1028	-				
54	62.3	179	-1565	-1535	- 825	025	-1130	016	074	1038
56	49.9	273	-1400	-1372	- 662	049	- ∞	010	000	1023
58	41.2	353	-1268	-1262	- 552	005		- 224		597
60	36.7	404	-1225	-1200	- 490	-014		- 412		388
62	24.6	583	-1060	-1036	- 326	-037		- 657		220
64	20.2	672	- 992	- 969	- 259	-058		-1058		088
66	32.5	458	-1158	-1146	- 436	-		-		-
68	-						- ∞		000	

Table 9 Continuum Analysis

Plate No: 23			Emulsion: 103a-E			Date: 1963 Oct. 13			MK Sp:		
Object: RW Aur			$\alpha: 05^{\text{h}} 05^{\text{m}} 4$			$\text{sec z: } 1.035$			$B-V:$		
			$\delta: +30^{\circ} 22.1$			$\Delta \text{sec z: } -.044$			$(B-V)_c: 0.67$		
$\lambda(\text{\AA}) \times 10^2$	c	d	log I	log I (EXT) (NORM)	log I (EXT) (INST)	log I (B) (PHTM)	log I (V) (PHTM)	I (B) (PHTM)	I (V) (PHTM)		
36	84.1	047	-			- ∞		000			
38	59.1	203	-1595	-1605	-510	-307	-1161		069		
40	38.1	384	-1280	-1288	-193	-110	-137		730		
42	30.0	493	-1143	-1150	-055	-045	-049		893		
44	26.9	540	-1095	-1102	-007	003	-043		885		
45	26.5	546	-1089	-1095	000	000					
46	29.0	505	-1129	-1135	-040	-004	-138		728		
48	47.3	292	-1400	-1435	-340	-080	-348	- ∞	449	000	
50	77.8	082	-			-	-				
52	83.8	048	-			-	-				
54	84.2	046	-			-	-				
56	79.7	073	-1852	-1856	-761	-050	- ∞	-147	000	713	
58	74.0	102	-1725	-1729	-634	-077		-306		494	
60	63.5	170	-1536	-1539	-444	032		-366		431	
62	47.2	297	-1344	-1347	-252	037		-583		261	
64	28.5	513	-1120	-1123	-028	173		-827		149	
66	67.0	145	-1589	-1592	-497			-			
68	-							- ∞	000		

Table 9 Continuum Analysis

Plate No: 25		Emulsion: 103a-F			Date: 1963 Oct. 1h		Calibration Star:		
Object: 4 Aur		α : 04:55.9			sec z: 1.058		MK Sp: AOV		
		δ : +37:49			Δ sec z:		B-V:		
$\lambda(\text{\AA}) \times 10^2$	c	d	log I (V.T.)	log I (NOR4)	log S'	log I (B PHTM)	log I (V PHTM)	I (B PHTM)	I (V PHTM)
35	62.5	178	-1500	-1320	-947	537			
38	14.5	820	-730	-601	-228	161			
40	04.5	1380	-362	-266	107	-004			
42	03.9	1440	-340	-269	104	-032			
44	04.3	1420	-375	-333	040	-016			
45	04.5	1385	-412	-373	000	000			
46	04.8	1342	-440	-404	-031	006			
48	10.3	955	-680	-652	-279	208			
50	21.3	648	-888	-874	-501	380			
52	29.5	500	-1007	-1002	-629	460			
54	29.5	500	-1006	-998	-625	415			
56	30.8	479	-1022	-1012	-639	390			
58	31.8	465	-1036	-1033	-660	354			
60	33.9	435	-1061	-1063	-690	334			
62	36.2	408	-1085	-1081	-708	305			
64	38.5	382	-1110	-1098	-725	280			
66	40.5	361	-1132	-1122	-749	278			
68	50.5	268	-1230	-1223	-850	351			

Table 9 Continuum Analysis

Plate No: 25			Emulsion: 103a-F			Date: 1963 Oct. 14			MK Sp: K2V		
Object: ε Eri			α: 03:31.3			sec z: 1.346			B-V: 0.89		
			δ: -09:34.8			Δsec z: .288			(B-V) _c : 0.88		
$\lambda(\text{\AA}) \times 10^2$	c	d	log I	log I (EXT) (NORM)	log I (INST)	log I (B) (PHOTM)	log I (V) (PHOTM)	I (B) (PHOTM)	I (V) (PHOTM)		
36	78.0	083	-1800	-1538	-1193	-656	-∞	000			
38	30.0	492	-1038	-844	-499	-338	-1192	064			
40	12.3	895	-680	-524	-179	-183	-210	617			
42	07.6	1115	-535	-411	-066	-099	-103	789			
44	05.9	1248	-470	-369	-024	-040	-086	820			
45	05.0	1330	-432	-345	000	000					
46	04.9	1340	-480	-398	-053	-017	-191	644			
48	06.6	1200	-550	-480	-135	073	-195	-∞	638	000	
50	12.4	888	-137	-683	-338	012	-402	-402	396	396	
52	15.2	803	-790	-749	-404	056	-622	024	239	1057	
54	12.0	900	-740	-699	-354	061	-1054	052	081	1205	
56	11.0	934	-724	-683	-338	052	-∞	045	000	902	
58	07.8	1098	-690	-660	-315	039		-190		646	
60	08.2	1081	-639	-614	-269	065		-333		465	
62	09.7	995	-692	-661	-316	-011		-631		234	
64	07.0	1160	-611	-574	-229	051		-949		113	
66	10.5	952	-716	-682	-337	-059		-1582		026	
68	27.9	522	-986	-957	-612	-261		-∞		000	

Table 9 Continuum Analysis

Plate No: 25		Emulsion: 103a-F			Date: 1963 Oct. 11			MK Sp:		
Object: T Tau		$\alpha: 04^{\text{h}}19.8$			$\text{sec z: } 1.016$			$B-V:$		
		$\delta: +19^{\circ}26.5$			$\Delta \text{sec z: } -0.012$			$(B-V)_c: 1.11$		
$\lambda(\text{\AA}) \times 10^2$	c	d	log I	log I (EXT)	log I (EXT) (NORM)	log I (INST)	log I (PHTM)	log I (PHTM)	I (PHTM)	I (PHTM)
36	-						- ∞		000	
38	85.0	041	-							
40	67.0	148	-1560	-1569	-450	-454	- 481		330	
42	53.2	247	-1325	-1333	-214	-246	- 250		562	
44	41.4	351	-1183	-1191	-072	-088	- 134		735	
45	36.0	412	-1112	-1119	000	000				
46	34.5	430	-1091	-1098	021	027	- 107		782	
48	46.8	300	-1225	-1232	-113	095	- 173	- ∞	671	000
50	67.0	148	-1470	-1476	-357	023	- 421	- 421	379	379
52	72.5	112	-1530	-1536	-417	043	- 635	011	232	1026
54	60.2	196	-1345	-1350	-231	084	-1071	075	085	1188
56	59.5	200	-1329	-1333	-214	176	- ∞	079	000	1199
58	58.4	207	-1315	-1319	-200	154		- 075		841
60	58.2	211	-1310	-1313	-194	140		- 258		552
62	58.8	203	-1322	-1325	-206	095		- 525		299
64	60.1	198	-1327	-1330	-211	069		- 931		117
66	61.8	182	-1358	-1361	-242	036		-1487		033
68	67.8	140	-1433	-1437	-318	033		- ∞		000

Table 9 Continuum Analysis

Plate No: 25		Emulsion: 103a-F			Date: 1963 Oct. 14			MK Sp:		
Object: RW Aur		$\alpha: 05^{\text{h}} 05^{\text{m}} .4$			$\text{sec z: } 1.004$			$B-V:$		
		$\delta: +30^{\circ} 22'$			$\Delta \text{sec z: } -0.054$			$(B-V)_c: 0.51$		
$\lambda(\text{\AA}) \times 10^2$	c	d	log I	log I (EXT) (NORM)	log I (EXT) (NORM)	log I (INST)	log I (B) (PHTM)	log I (V) (PHTM)	I (B) (PHTM)	I (V) (PHTM)
36	85.0	043	-				-\infty		000	
38	65.6	155	-1535	-1545	-431	-270	-1121		075	
40	15.5	312	-1239	-1248	-134	-138	-165		684	
42	39.0	375	-1158	-1166	-052	-084	-088		817	
44	35.5	415	-1110	-1118	-044	-020	-066		857	
45	35.5	415	-1107	-1114	000	000				
46	39.5	370	-1152	-1159	-045	-039	-173		671	
48	63.0	175	-1405	-1412	-298	-090	-358	-\infty	439	000
50	79.0	075	-1650	-1657	-543	-163	-507	-507	-311	-311
52	81.0	063	-1630	-1636	-522	-062	-740	-094	182	805
54	79.0	075	-1585	-1591	-477	-062	-1217	-071	061	849
56	81.5	061	-1630	-1636	-522	-132	-\infty	-229	000	590
58	78.0	082	-1560	-1565	-451	-197		-426		375
60	78.0	082	-1560	-1565	-451	-117		-515		306
62	76.0	093	-1535	-1540	-426	-121		-741		182
64	76.5	090	-1545	-1549	-435	-155		-1155		070
66	78.2	081	-1565	-1569	-455	-177		-1700		020
68	81.5	060	-1640	-1644	-530	-179		-\infty		000

Table 9 Continuum Analysis

Plate No: 26		Emulsion: 103a-F		Date: 1963 Oct. 15		Calibration Star:				
Object: α Lyr		α : 18:35.7		sec z: 1.414		MK Sp: A0V				
		δ : +38:45.7		Δ sec z:		B-V: 0.00				
$\lambda(\text{\AA}) \times 10^2$	c	d	log I	log I (V.T.)	log I (NORM)	log S'	log I (B) (PHTM)	log I (V) (PHTM)	I (B) (PHTM)	I (V) (PHTM)
36	60.4	193	-1490	-1310	-928	518				
38	15.4	798	-771	-642	-260	193				
40	05.2	1325	-383	-281	095	-016				
42	04.8	1340	-386	-315	067	005				
44	05.1	1321	-410	-368	014	010				
45	05.2	1319	-421	-382	000	000				
46	05.8	1247	-485	-449	-067	042				
48	08.2	1072	-610	-612	-230	159				
50	17.0	750	-852	-838	-456	335				
52	21.8	635	-945	-940	-558	389				
54	24.0	591	-984	-976	-594	384				
56	26.2	555	-1013	-1003	-621	372				
58	26.2	556	-1010	-1007	-625	319				
60	27.1	540	-1035	-1037	-655	299				
62	30.0	491	-1056	-1052	-670	267				
64	26.6	546	-1022	-1010	-628	183				
66	34.4	433	-1106	-1096	-714	243				
68	64.0	168	-1350	-1343	-961	462				

Table 9 Continuum Analysis

Plate No: 26		Emulsion: 103a-F			Date: 1963 Oct. 15			MK Sp: G5IV		
Object: μ Her A		$\alpha: 17:44.2$			$\delta: +27:44.6$			$\text{sec z: } 2.000$		
					$\Delta \text{sec z: } +.586$			$(B-V)_c: 0.74$		
$\lambda(\text{\AA}) \times 10^2$	c	d	log I	log I (EXT) (NORM)	log I (EXT) (NORM)	log I (INST)	log I (B) (PHTM)	log I (V) (PHTM)	I (B) (PHTM)	I (V) (PHTM)
36	-						- ∞		000	
38	73.1	108	-1730	-1475	-566	-373	-1227		060	
40	46.2	308	-1276	-1072	-163	-179	-206		622	
42	34.8	422	-1136	-998	-089	-084	-088		817	
44	27.6	530	-1038	-907	002	012	-034		925	
45	28.5	518	-1034	-909	000	000				
46	28.5	518	-1034	-916	-007	035	-099		796	
48	37.7	392	-1159	-1054	-115	014	-254	- ∞	557	000
50	57.1	219	-1371	-1287	-378	-043	-401	-401	397	397
52	62.6	179	-1420	-1350	-441	-052	-626	-084	237	824
54	58.9	203	-1360	-1292	-383	001	-1154	-008	070	982
56	54.2	240	-1332	-1267	-358	014	- ∞	-083	000	826
58	47.9	288	-1249	-1193	-284	035		-194		640
60	45.5	313	-1227	-1179	-270	029		-369		428
62	40.7	360	-1177	-1125	-216	051		-569		270
64	22.6	620	-968	-911	-002	181		-819		152
66	25.3	566	-1006	-953	-044	199		-1324		047
68	54.3	238	-1311	-1263	-354	108		- ∞	000	

Table 9 Continuum Analysis

Plate No: 26		Emulsion: 103a-F			Date: 1963 Oct. 15			MK Sp: KOIV		
Object: η Cep		$\alpha: 20:44.3$			$\sec z: 1.133$			$B-V: 0.92$		
		$\delta: +61:39$			$\Delta \sec z: -.281$			$(B-V)_c: 0.95$		
$\lambda(\text{\AA}) \times 10^2$	c	d	$\log I$	$\log I$ (EXT) (NORM)	$\log I$ (INST)	$\log I$ (B) (PTTM)	$\log I$ (V) (PTTM)	I (B) (PTTM)	I (V) (PTTM)	
36	75.0	100	-			- ∞		000		
38	29.6	498	-1055	-1247	-762	-569	-1123	038		
40	19.2	700	- 855	- 813	-328	-344	- 371	426		
42	08.1	1080	- 577	- 554	-069	-064	- 068	855		
44	06.4	1202	- 510	- 522	-037	-027	- 073	845		
45	05.8	1242	- 481	- 485	000	000				
46	05.3	1287	- 450	- 455	030	072	- 206	622		
48	06.3	1206	- 540	- 550	-065	094	- 362	- ∞	435	000
50	09.6	992	- 686	- 706	-221	114	- 330	- 330	468	468
52	09.0	1020	- 684	- 706	-221	168	- 110	136	776	1368
54	08.3	1060	- 681	- 693	-208	176	- 691	167	204	1169
56	07.8	1087	- 680	- 698	-213	159	-1426	056	038	1091
58	06.7	1194	- 638	- 661	-176	143	- ∞	- 086	000	820
60	06.9	1160	- 673	- 700	-215	084		- 314		485
62	07.0	1159	- 673	- 693	-208	059		- 561		275
64	05.8	1246	- 637	- 650	-155	018		- 982		104
66	06.9	1160	- 679	- 691	-206	037		-1486		032
68	19.5	690	- 921	- 934	-449	025		- ∞	000	

Table 9 Continuum Analysis

Plate No: 26			Emulsion: 103a-F			Date: 1963 Oct. 16			MK Sp:		
Object: RW Aur			$\alpha: 05:05.4$			$\sec z: 1.000$			$B-V:$		
			$\delta: +30:22.1$			$\Delta \sec z: -.471$			$(B-V)_c: 0.60$		
$\lambda(\text{\AA}) \times 10^2$	c	a	log I	log I (EXT) (NORM)	log I (EXT)	log I (INST)	log I (PHTM)	log I (V) (PHTM)	I (B) (PHTM)	I (V) (PHTM)	
36	80.0	070	-				- ∞		000		
38	62.4	180	-1515	-1599	-470	-277	-1011.1		072		
40	49.0	279	-1320	-1392	-263	-279	-306		494		
42	38.4	382	-1183	-1247	-118	-113	-117		764		
44	33.6	440	-1118	-1177	-048	-038	-064		824		
45	30.5	483	-1072	-1129	000	000					
46	40.6	360	-1211	-1265	-136	-094	-228		592		
48	62.6	179	-1461	-1502	-373	-214	-482	- ∞	330	000	
50	78.6	078	-1650	-1696	-567	-232	-676	-676	211	211	
52	78.1	079	-1625	-1668	-539	-150	-828	-182	149	658	
54	77.8	083	-1590	-1630	-501	-117	-1272	-126	053	748	
56	78.3	080	-1594	-1631	-502	-130	- ∞	-227	000	593	
58	77.0	088	-1571	-1606	-477	-158		-387		410	
60	77.4	085	-1576	-1609	-480	-181		-579		264	
62	72.3	122	-1500	-1532	-403	-136		-756		175	
64	58.8	204	-1357	-1387	-258	-075		-1075		084	
66	61.0	190	-1377	-1406	-277	-024		-1547		028	
68	76.0	095	-1555	-1582	-453	009		- ∞		000	

Table 9 Continuum Analysis

Plate No: 28		Emulsion: 103a-F			Date: 1963 Oct. 17			MK Sp: AOV		
Object: 4 Aur		$\alpha:$ 04:55.9			$\sec z: 1.466$			$B-V:$		
		$\delta: +37:49$			$\Delta \sec z:$					
$\lambda(\text{\AA}) \times 10^2$	c	d	$\log I$	$\log I$ (EXT)	$\log I$ (NORM)	$\log I$ (INST)	$\log I$ (B) PHTM	$\log I$ (V) PHTM	I (B) PHTM	I (V) PHTM
36	77.5	085	-1590	-1410	-1086	676				
38	25.5	568	-737	-608	-284	351				
40	09.4	995	-333	-237	087	024				
42	07.9	1095	-268	-197	127	-055				
44	08.4	1058	-310	-278	046	-022				
45	09.4	1000	-363	-324	000	000				
46	11.5	917	-431	-395	-071	046				
48	18.0	725	-580	-552	-228	157				
50	36.9	400	-906	-892	-568	447				
52	46.4	308	-1009	-1004	-680	511				
54	46.6	302	-1005	-997	-673	463				
56	48.3	283	-1027	-1017	-693	444				
58	49.0	278	-1030	-1027	-703	397				
60	50.2	271	-1039	-1041	-717	361				
62	52.2	253	-1062	-1058	-734	331				
64	54.4	237	-1086	-1074	-750	305				
66	56.5	223	-1106	-1096	-772	301				
68	64.0	168	-1191	-1184	-860	599				

Table 9 Continuum Analysis

Plate No: 28			Emulsion: 103a-F			Date: 1963 Oct. 17			MK Sp: G0V		
Object: HD 13974			$\alpha:$ 02:14.2			$\delta:$ +31:03			$\sec z: 1.035$		
						$\Delta \sec z: -1.431$			$(B-V)_c: 0.65$		
$\lambda(\text{\AA}) \times 10^2$	c.	d	log I	log I (EXT) (NORM)	log I (EXT) (NORM)	log I (INST)	log I (B) (PHOT)	log I (V) (PHOT)	I (B) (PHOT)	I (V) (PHOT)	
36	72.0	115	-1500	-1124	-982	-306	- ∞		000		
38	41.9	346	-1005	- 971	-529	-178	-1032		092		
40	17.1	751	- 542	- 529	-087	-063	- 090		813		
42	12.8	871	- 442	- 443	-001	-056	- 060		871		
44	11.4	918	- 420	- 445	-003	-025	- 071		649		
45	11.2	931	- 416	- 442	000	000					
46	11.7	912	- 433	- 459	-017	029	- 105		785		
48	17.2	750	- 569	- 599	-157	000	- 268	- ∞	540	000	
50	30.1	490	- 811	- 850	-408	039	- 405	- 405	393	393	
52	35.7	115	- 886	- 930	-488	023	- 655	- 009	221	980	
54	32.0	460	- 842	- 878	-436	027	-1128	018	075	1042	
56	31.2	475	- 825	- 856	-414	030	- ∞	- 067	000	857	
58	30.0	490	- 810	- 847	-405	-008		- 237		579	
60	28.5	511	- 785	- 825	-383	-022		- 420		380	
62	29.0	508	- 789	- 822	-380	-049		- 669		211	
64	30.0	491	- 806	- 829	-387	-082		-1082		083	
66	32.3	458	- 840	- 863	-421	-120		-1643		023	
68	-							- ∞			

Table 9 Continuum Analysis

Plate No: 28			Emulsion: 103a-F			Date: 1963 Oct. 17			MK Sp:		
Object: T Tau			$\alpha: 04^{\text{h}}19.8$			$\text{sec z: } 1.133$			$B-V:$		
			$\delta: +19^{\circ}26.5$			$\Delta \text{sec z: } -0.333$			$(B-V)_C: 1.27$		
$\lambda(\text{\AA}) \times 10^2$	c	d	log I	log I (EXT) (NORM)	log I (EXT) (NORM)	log I (INST)	log I (B) (PHOTM)	log I (V) (PHOTM)	I (B) (PHOTM)	I (V) (PHOTM)	
36	-						- ∞		000		
38	-										
40	81.6	043	-1690	-1750	-462	-418	- 391		406		
42	78.9	076	-1535	-1588	-300	-355	- 359		438		
44	67.0	146	-1319	-1368	-080	-102	- 148		711		
45	62.3	179	-1240	-1288	000	000					
46	62.3	179	-1235	-1281	008	054	- 080		832		
48	73.0	109	-1370	-1412	-124	033	- 235	- ∞	582	000	
50	88.5	023	-								
52	92.0	010	-								
54	86.7	035	-1600	-1633	-345	118	-1037	109	092	1285	
56	83.6	048	-1515	-1546	-258	116	- ∞	089	000	1227	
58	80.3	066	-1434	-1463	-175	222		- 007		984	
60	76.9	088	-1361	-1389	-101	260		- 138		728	
62	73.9	103	-1327	-1354	-066	265		- 355		442	
64	71.0	121	-1279	-1304	-016	289		- 711		195	
66	72.1	115	-1297	-1321	-033	268		-1255		056	
68	87.0	030	-					- ∞		000	

Table 9 Continuum Analysis

Plate No: 28		Emulsion: 103a-F			Date: 1963 Oct. 17			MK Sp:		
Object: RW Aur		$\alpha: 05^{\text{h}} 05^{\text{m}} 4$			$\text{sec z: } 1.022$			$B-V:$		
		$\delta: +30^{\circ} 22$			$\Delta \text{sec z: } -0.444$			$(B-V)_C: 0.70$		
$\lambda(\text{\AA}) \times 10^2$	c	d	log I	log I (EXT) (NORM)	log I (INST)	log I (B) (PHTM)	log I (V) (PHTM)	I (B) (PHTM)	I (V) (PHTM)	
36	89.0	022	-			- ∞		000		
38	64.1	166	-1360	-2153	-590	-239	-1093	081		
40	45.0	313	-1035	-1117	-254	-230	-257	553		
42	34.4	431	-887	-959	-096	-151	-155	700		
44	30.0	490	-809	-874	-009	-031	-077	838		
45	28.7	513	-800	-863	000	000				
46	38.2	386	-928	-986	-125	-079	-211	615		
48	54.8	233	-1120	-1177	-314	-157	-425	376	000	
50	75.8	093	-1397	-1448	-585	-138	-582	262	262	
52	76.7	078	-1430	-1478	-615	-104	-782	136	165	731
54	72.3	112	-1354	-1398	-535	-072	-1227	081	059	830
56	73.8	104	-1321	-1362	-499	-055	- ∞	-152	000	705
58	73.0	109	-1309	-1348	-485	-088		-317		482
60	71.7	118	-1290	-1327	-464	-103		-501		315
62	70.9	121	-1280	-1315	-452	-121		-741		182
64	60.4	193	-1151	-1184	-321	-016		-1016		096
66	63.5	170	-1187	-1219	-356	-055		-1578		027
68	83.7	049	-1520	-1550	-687	-088		- ∞		000

Table 9 Continuum Analysis

Plate No: 199		Emulsion: 103a-F		Date: 1964 June 17		Calibration Star:					
Object: α Cr B		α : 15:33.1		sec z: 1.010		MK Sp: A0V					
		δ : +26:50		Δ sec z:		B-V:					
$\lambda(\text{\AA}) \times 10^2$	c	d	log I	log I (V.T.)	log I (NORI)	log S'	log I (B) (PHTM)	log I (V) (PHTM)	I (B) (PHTM)	I (V) (PHTM)	
36	56.6	221	-1630:	-1268	-1145	735					
38	11.7	911	- 880:	- 597	- 484	417					
40	02.0	1747	- 350	- 138	- 015	126					
42	01.5	1860	- 250:	- 091	032	040					
44	01.3	1900	- 215:	- 118	005	019					
45	01.3	1900	- 220:	- 123	000	000					
46	01.3	1900	- 225:	- 139	- 016	-009					
48	02.6	1640	- 433	- 366	- 243	172					
50	05.2	1315	- 661	- 617	- 494	373					
52	06.1	1235	- 729	- 697	- 574	405					
54	06.8	1162	- 774	- 742	- 619	409					
56	08.0	1066	- 827	- 795	- 672	433					
58	09.3	1000	- 865	- 845	- 722	416					
60	09.2	1005	- 860	- 860	- 737	381					
62	13.6	846	- 949	- 928	- 804	401					
64	12.4	883	- 932	- 900	- 777	332					
66	15.6	792	- 980	- 948	- 825	354					
68	36.0	109	-1210	-1213	-1090	591					

Table 9 Continuum Analysis

Plate No: 199		Emulsion: 103a-F			Date: 1964 June 17			MK Sp: G0V		
Object: β Com		$\alpha:$ 13:10.1			$\sec z:$ 1.014			$B-V:$ 0.57		
		$\delta:$ +28:04			$\Delta \sec z:$ +.004			$(B-V)_c:$ 0.59		
$\lambda(\text{\AA}) \times 10^2$	c	d	log I	log I (FAT)	log I (EXT) (NORM)	log I (INST)	log I (B) (PHTM)	log I (V) (PHTM)	I (B) (PHTM)	I (V) (PHTM)
36	-						- ∞		000	
38	43.0	338	-1330	-1047	-317	-080	-934		116	
40	19.2	700	-1031	-819	-089	037	010		1023	
42	11.6	912	-961	-802	-072	-032	-036		921	
44	08.3	1060	-826	-718	-012	-031	015		1035	
45	08.2	1080	-827	-730	000	000				
46	07.8	1087	-815	-729	001	-008	-142		721	
48	15.8	781	-982	-915	-185	-013	-281	- ∞	512	000
50	27.3	531	-1150	-1106	-376	-003	-447	-447	357	357
52	31.2	477	-1190	-1158	-428	-023	-701	-055	199	881
54	30.5	483	-1182	-1150	-420	-011	-1166	-020	068	955
56	29.5	500	-1170	-1138	-498	025	- ∞	-07?		847
58	29.1	505	-1166	-1146	-416	000		-2?		590
60	27.2	538	-1143	-1137	-407	-026		-4?		377
62	34.0	437	-1220	-1198	-468	-067		-6?		201
64	32.8	450	-1206	-1174	-444	-112		-17?		077
66	44.2	326	-1314	-1282	-552	-198		-17?		019
68	72.5	111	-1602	-1575	-845	-254		- ∞		000

Table 9 Continuum Analysis

Plate No: 199		Emulsion: 103a-F			Date: 1961 June 17			MK Sp:		
Object: AS 205		$\alpha: 16:09.3$			$\sec z: 2.559$			$B-V:$		
		$\delta: +18:33$			$\Delta \sec z: +1.519$			$(B-V)_c: 1.48$		
$\lambda(\text{\AA}) \times 10^2$	c	d	log I	log I (EXT) (NORM)	log I (EXT) (INST)	log I (B) (PHTM)	log I (V) (PHTM)	I (B) (PHTM)	I (V) (PHTM)	
36	-					- ∞		000		
38	-									
40	78.0	082	-1820	-1550	-580	-454	-481	330		
42	60.9	192	-1494	-1254	-284	-244	-248	565		
44	35.1	420	-1232	-1010	-040	-021	-067	857		
45	30.6	482	-1183	-970	000	000				
46	27.2	539	-1142	-938	032	023	-134	735		
48	33.4	442	-1217	-1025	-055	117	-151	- ∞	706	000
50	53.4	243	-1397	-1223	-253	120	-324	-324	474	474
52	57.4	217	-1426	-1264	-294	111	-567	079	271	1200
54	40.7	360	-1280	-1130	-160	249	-906	240	124	1738
56	34.9	420	-1230	-1092	-122	311	- ∞	214	000	1637
58	25.5	566	-1122	-990	-020	386		157		1435
60	23.1	612	-1091	-965	005	386		-012		973
62	21.0	592	-1105	-985	-015	386		-234		583
64	15.9	781	-982	-868	102	434		-566		272
66	18.1	722	-1019	-911	059	413		-911		123
68	39.2	376	-1267	-1165	-195	396		- ∞		000

Table 9 Continuum Analysis

Plate No: 200		Emulsion: 103a-F			Date: 1964 June 18		Calibration Star:			
Object: ζ Cr B		$\alpha: 15^{\circ}33.1$			sec z: 1.006		MK Sp: AOV			
		$\delta: +26^{\circ}50'$			Δ sec z:		B-V:			
$\lambda(\text{\AA}) \times 10^2$	c	d	log I	log I (V.T.)	log I (NORM)	log S ¹	log I (B) PHTM	log I (V) PHTM	I (B) PHTM	I (V) PHTM
36	61.9	160	-							
38	19.6	688	- 990	- 571	-192	259				
40	03.8	1443	- 500	- 171	208	-097				
42	03.2	1558	- 440	- 179	200	-128				
44	02.9	1580	- 520	- 371	005	019				
45	03.0	1568	- 530	- 379	000	000				
46	03.0	1568	- 535	- 499	-120	095				
48	05.4	1288	- 685	- 581	-202	131				
50	10.4	954	- 872	- 802	-423	302				
52	13.6	848	- 932	- 882	-503	331				
54	15.1	802	- 962	- 912	-533	323				
56	17.5	739	-1007	- 957	-578	329				
58	18.1	723	-1018	- 990	-611	305				
60	17.5	739	-1006	-1000	-621	265				
62	22.0	631	-1078	-1016	-667	264				
64	18.0	722	-1018	- 964	-585	140				
66	23.3	602	-1100	- 946	-567	096				
68	34.1	131	-1211	-1198	-819	320				

Table 9 Continuum Analysis

Plate No: 200		Emulsion: 103a-F			Date: 1964 June 18			MK Sp:		
Object: AS 209		$\alpha: 16:47.0$			$\delta: -16:19.7$			$\Delta \text{sec z:} +1.373$		
$\lambda(\text{\AA}) \times 10^2$	c	d	log I	log I (EXT) (NORM)	log I (INST) (PHOTM)	log I (B) (PHOTM)	log I (V) (PHOTM)	I (B) (PHOTM)	I (V) (PHOTM)	
36	-					- ∞		000		
38	68.8	132	-							
40	60.3	195	-1750	-1498	-212	-309	- 336		461	
42	52.6	250	-1540	-1316	-030	-156	- 162		689	
44	51.2	262	-1515	-1302	-022	-003	- 049		893	
45	50.3	268	-1485	-1286	000	000				
46	52.4	250	-1525	-1335	-049	046	- 088		817	
48	58.5	208	-1570	-1591	-105	026	- 242	- ∞	573	000
50	68.1	140	-1840	-1678	-392	-090	- 534	- 534	292	292
52	71.9	115	-							
54	68.0	141	-1830	-1690	-404	-081	-1236	- 090	059	813
56	69.8	129	-			- ∞	-	000		-
58	65.1	159	-1752	-1629	-343	-038		- 267		541
60	62.1	182	-1654	-1537	-251	-074		- 384		413
62	62.1	182	-1654	-1542	-256	008		- 612		2111
64	58.8	204	-1581	-1475	-190	-050		-1050		089
66	58.8	204	-1581	-1480	-194	-098		-1621		024
68	-						- ∞		000	

Table 9 Continuum Analysis

Plate No: 205		Emulsion: 103a-F			Date: 1961 July 26			Calibration Star:		
Object: η UMa		α : 13:46.1			$\sec z$: 1.556			MK Sp: R3V		
		δ : 49:29.5			$\Delta \sec z$:			B-V:		
$\lambda(\text{\AA}) \times 10^2$	c	d	log I	log I (V.T.)	log I (NORM)	log S'	log I (B) (PHTM)	log I (V) (PHTM)	I (B) (PHTM)	I (V) (PHTM)
36	37.0	402	-1780	-1271	-540	597				
38	13.1	865	-1226	-839	-108	222				
40	05.0	1328	-896	-612	119	027				
42	04.2	1428	-831	-614	087	-016				
44	03.9	1448	-840	-704	027	-005				
45	03.9	1448	-848	-731	000	000				
46	04.1	1428	-850	-753	-022	-003				
48	06.7	1195	-985	-920	-189	103				
50	13.4	853	-1213	-1167	-436	287				
52	18.3	707	-1310	-1297	-548	337				
54	21.7	641	-1352	-1330	-599	342				
56	24.6	564	-1395	-1378	-647	333				
58	27.3	533	-1432	-1419	-688	311				
60	27.6	525	-1440	-1410	-709	263				
62	34.0	437	-1513	-1491	-760	265				
64	41.4	352	-1590	-1511	-813	278				
66	47.5	292	-1655	-1615	-884	323				
68	66.0	153	-1845	-1809	-1078	495				

Table 9 Continuum Analysis

Plate No: 205			Emulsion: 103a-F			Date: 1961 July 26			MK Sp: K5V		
Object: 61 Cyg A			$\alpha:$ 21:01.5			$\sec z:$ 1.167			$B-V:$ 1.19		
			$\delta:$ +38:34			$\Delta \sec z:$ -.389					
$\lambda(\text{\AA}) \times 10^2$	c	d	log I	log I (EAT)	log I (EXT) (NORM)	log I (LIST)	log I (B) (PHM)	log I (V) (PHM)	I (B) (PHM)	I (V) (PHM)	
36	78.0	082	-				- oo		000		
38	64.1	166	-2250	-2334	-928	-706	-1560		028		
40	23.0	612	-1177	-1549	-441	-414	-441		362		
42	16.5	767	-1300	-1364	-257	-253	-257		553		
44	09.1	1018	-1107	-1166	-059	-064	-110		776		
45	08.0	1080	-1060	-1107	000	000					
46	06.1	1238	-960	-1014	093	090	-044		904		
48	10.6	950	-1155	-1205	-099	004	-264	- oo	545	000	
50	22.4	622	-1381	-1427	-320	-033	-411	-411	388	388	
52	22.4	622	-1378	-1418	-311	026	-652	-006	223	986	
54	15.9	782	-1261	-1301	-194	148	-1007	139	098	1377	
56	16.1	778	-1261	-1298	-191	142	- oo	-045	000	1109	
58	12.6	880	-1200	-1235	-128	186		-043		906	
60	10.6	938	-1165	-1198	-091	172		-226		594	
62	10.8	938	-1167	-1199	-092	173		-447		357	
64	10.9	940	-1166	-1196	-089	189		-811		155	
66	12.4	883	-1197	-1226	-119	213		-1310		049	
68	23.8	593	-1386	-1413	-306	189		- oo		000	

Table 9 Continuum Analysis

Plate No: 207		Emulsion: 103a-F			Date: 1964 July 27			Calibration Star:		
Object: 16 Cyg A		$\alpha: 19^{\text{h}}40^{\text{m}}5^{\text{s}}$			$\text{sec z: } 1.079$			MK Sp: G2V		
		$\delta: +50^{\circ}24'$			$\Delta \text{sec z:}$			$B-V:$		
$\lambda(\text{\AA}) \times 10^2$	c	d	log I	log I (V.T.)	log I (NORM)	log S'	log I (B) (PHTM)	log I (V) (PHTM)	I (B) (PHTM)	I (V) (PHTM)
36	74.1	103	-							
38	37.3	392	-1510		-566	316				
40	16.0	780	-1069		-125	005				
42	11.9	900	-970		-026	-028				
44	09.7	992	-906		038	056				
45	10.5	950	-944		000	000				
46	10.9	932	-956		-012	026				
48	17.9	728	-1123		-179	193				
50	32.1	462	-1380		-436	444				
52	38.5	362	-1465		-521	523				
54	37.8	388	-1452		-508	521				
56	41.8	346	-1494		-550	550				
58	40.9	358	-1479		-535	501				
60	42.3	342	-1496		-552	509				
62	47.6	290	-1561		-617	563				
64	47.8	287	-1568		-624	553				
66	56.6	221	-1678		-734	650				
68	81.0	062	-							

Table 9 Continuum Analysis

Plate No: 207		Emulsion: 103a-F			Date: 1964 July 27			MK Sp: K5V		
Object: 61 Cyg A		$\alpha:$ 21:01.5			sec z: 1.269			B-V: 1.19		
		$\delta:$ +38:31			Δ sec z: +.190			$(B-V)_C:$ 1.21		
$\lambda(\text{\AA}) \times 10^2$	c	d	log I	log I (EXT)	log I (NORM)	log I (INST)	log I (B PHTM)	log I (V PHTM)	I (B PHTM)	I (V PHTM)
36	-						- ∞		000	
38	60.2	196	-1910	-1868	-1054	-738	-1592		026	
40	25.4	566	-1268	-1232	- 418	-413	- 440		363	
42	14.9	809	-1048	-1016	- 204	-232	- 236		581	
44	09.0	1020	- 887	- 858	- 126	-100	- 146		715	
45	07.8	1088	- 842	- 814	000	000				
46	07.5	1120	- 827	- 800	014	040	- 094		805	
48	12.7	680	-1000	- 974	- 160	033	- 235	- ∞	582	000
50	23.5	600	-1210	-1217	- 403	041	- 403	- 403	397	397
52	25.0	575	-1272	-1250	- 436	087	- 591	055	257	1135
54	20.7	663	-1208	-1188	- 374	137	-1083	128	083	1342
56	16.0	789	-1129	-1111	- 297	153	- ∞	056	000	1137
58	16.1	780	-1134	-1116	- 302	199		- 030		933
60	15.3	798	-1122	-1105	- 291	218		- 180		661
62	18.5	712	-1179	-1163	- 349	214		- 406		393
64	18.8	702	-1183	-1168	- 354	199		- 801		158
66	25.1	572	-1282	-1268	- 454	196		-1327		047
68	54.5	237	-1649	-1635	- 821	-	- ∞		000	

Table 9 Continuum Analysis

Plate No: 209		Emulsion: 103a-F		Date: 1964 July 27		Calibration Star:					
Object: η UMa		α: 13:16.1		sec z: 2.054		MK Sp: B3V					
		δ: +19:29.5		Δsec z:		B-V:					
$\lambda(\text{Å}) \times 10^2$	c	d	log I	log I (V.T.)	log I (NOM4)	log S'	log I (B) (PHM)	log I (V) (PHM)	I (B) (PHM)	I (V) (PHM)	
35	75.0	100	-1905	-1396	- 983	1040					
38	25.9	559	-1121	- 734	- 321	435					
40	09.0	1020	- 701	- 417	- 204	150					
42	06.5	1200	- 585	- 398	016	056					
44	05.6	1279	- 555	- 419	- 006	028					
45	05.0	1330	- 530	- 413	000	000					
46	06.2	1232	- 595	- 498	- 085	060					
48	12.4	882	- 801	- 736	- 323	227					
50	18.0	721	- 902	- 856	- 443	294					
52	29.3	500	-1065	-1034	- 621	410					
54	30.6	482	-1056	-1034	- 621	364					
56	35.4	418	-1115	-1098	- 685	371					
58	37.2	400	-1133	-1120	- 707	333					
60	40.9	358	-1177	-1177	- 764	318					
62	48.0	265	-1263	-1241	- 828	333					
64	50.4	267	-1312	-1266	- 853	318					
66	55.1	234	-1360	-1320	- 907	346					
68	64.9	161	-1495	-1459	-1046	463					

Table 9 Continuum Analysis

Plate No: 209			Emulsion: 103a-F			Date: 1964 July 27			MK Sp: G2V		
Object: 16 Cyg A			$\alpha: 19:40.5$			$\sec z: 1.064$			$B-V: 0.61$		
			$\delta: +50:21$			$\Delta \sec z: -1.000$			$(B-V)_c: .61$		
$\lambda(\text{\AA}) \times 10^2$	c	d	log I	log I (EXT) (NORM)	log I (EXT) (NORM)	log I (INST)	log I (B) PHOTM	log I (V) PHOTM	I (B) PHOTM	I (V) PHOTM	
36	63.0	173	-1680	-972	-1224	-221	-\infty		000		
38	26.2	521	-1190	-1100	-652	-217	-1071		085		
40	11.8	903	-781	-961	-213	-073	-101		792		
42	08.5	1058	-680	-860	-112	-054	-058		887		
44	07.0	1160	-625	-773	-025	003	-043		906		
45	06.4	1203	-605	-748	000	000					
46	07.0	1160	-635	-771	-023	037	-097		800		
48	12.9	867	-811	-938	-190	037	-231	-\infty	588	000	
50	24.0	592	-999	-1015	-267	027	-417	-417	383	383	
52	28.3	518	-1050	-1158	-410	000	-678	-032	210	929	
54	27.3	531	-1025	-1125	-377	-013	-1168	-022	068	951	
56	28.0	522	-1028	-1120	-372	-001	-\infty	-098	000	798	
58	28.1	521	-1029	-1117	-369	-036		-265		543	
60	28.6	506	-1039	-1123	-375	-057		-455		351	
62	29.9	493	-1056	-1136	-388	-055		-675		211	
64	30.0	492	-1065	-1141	-393	-075		-1075		084	
66	35.5	417	-1137	-1209	-461	-115		-1638		023	
68	46.4	305	-1263	-1331	-583	-120		-\infty	000		

Table 9 Continuum Analysis

Plate No: 209		Emulsion: 103a-F			Date: 1961 July 27		MK Sp:			
Object: DI Cep		$\alpha: 22:55.3$			sec z: 1.095		B-V:			
		$\delta: +58:27$			Δsec z: -.969		(B-V) _c : 0.60			
$\lambda(\text{\AA}) \times 10^2$	c	d	log I	log I (EXT) (NORM)	log I (INST)	log I (_{PHTM})	log I (_B) (_{PHTM})	log I (_V) (_{PHTM})	I (_B) (_{PHTM})	I (_V) (_{PHTM})
36	61.0	191	-1516	-1796	-889	-151	-∞		000	
38	40.0	366	-1356	-1566	-659	-221	-1078		083	
40	20.8	655	-1020	-1200	-293	-143	-170		676	
42	13.3	852	-820	-980	-072	-016	-020		955	
44	11.6	914	-773	-921	-014	014	-032		929	
45	11.0	932	-765	-907	000	000				
46	12.3	890	-795	-927	-020	040	-091		605	
48	20.2	678	-920	-1042	-135	092	-176	-∞	667	000
50	33.1	449	-1121	-1237	-330	-036	-408	-408	391	391
52	40.9	358	-1206	-1314	-407	003	-675	-029	211	935
54	41.2	353	-1195	-1295	-388	-021	-1179	-033	066	927
56	41.5	350	-1195	-1287	-380	-009	-∞	-106	000	783
58	41.0	357	-1170	-1258	-351	-018		-247		566
60	41.0	357	-1168	-1252	-345	-027		-425		376
62	40.9	358	-1185	-1265	-358	-025		-645		227
64	40.4	361	-1189	-1265	-358	-040		-1040		091
66	45.0	319	-1246	-1318	-411	-065		-1588		026
68	52.5	250	-1342	-1410	-503	-040		-∞		000

Table 9 Continuum Analysis

Plate No: 210		Emulsion: 103e-F		Date: 1961 July 27		Calibration Star:			
Object: 6 Cyg		$\alpha: 19:41:10$		$\delta: 45:00$		sec z: 1.167		MK Sp: A2.5III	
						$\Delta \text{sec z:}$		B-V:	
$\lambda(\text{\AA}) \times 10^2$	c	d	log I	log I (V.T.)	log I (NOR4)	log S'	log I (B) (PHTM)	log I (V) (PHTM)	I (B) (PHTM)
36	58.0	210	-1200	- 857	- 877	473			
38	12.2	895	- 345	- 088	- 108	036			
40	05.9	1250	- 090	099	079	-039			
42	05.0	1330	- 040	110	090	-020			
44	05.1	1325	- 055	061	044	-022			
45	05.4	1295	- 080	020	000	000			
46	06.0	1210	- 135	- 047	- 067	045			
48	09.1	1020	- 290	- 223	- 243	179			
50	18.0	725	- 505	- 455	- 475	359			
52	23.8	593	- 605	- 560	- 580	417			
54	25.8	558	- 630	- 583	- 605	402			
56	30.4	483	- 695	- 645	- 665	419			
58	33.1	448	- 730	- 690	- 710	411			
60	34.6	428	- 750	- 730	- 750	395			
62	43.3	338	- 830	- 800	- 820	416			
64	46.7	303	- 865	- 825	- 845	395			
66	52.0	258	- 915	- 875	- 895	412			
68	69.0	132	-1090	-1050	-1070	587			

Table 9 Continuum Analysis

Plate No: 210		Emulsion: 103a-F			Date: 1964 July 27			MK Sp: G2V		
Object: 16 Cyg A		$\alpha:$ 19:40.5			$\delta:$ +50:24			$(B-V)_C:$ 0.62		
$\lambda(\text{\AA}) \times 10^2$	C	d	log I	log I (EXT) (NORM)	log I (INST)	log I (B) (PHTM)	log I (V) (PHTM)	I (B) (PHTM)	I (V) (PHTM)	
36	55.0	230	-1180	-1186	-847	-347	- ∞	000		
38	28.0	525	-710	-715	-376	-340	-1194	064		
40	13.3	855	-390	-395	-056	-095	-122	755		
42	11.0	932	-330	-334	-005	-025	-029	935		
44	10.0	970	-305	-309	-030	-052	-098	798		
45	09.3	1005	-335	-339	000	000				
46	09.8	975	-310	-314	025	070	-064	863		
48	16.0	780	-460	-463	-124	055	-213	-00	612	000
50	27.4	532	-675	-678	-339	020	-424	-424	377	612
52	33.1	448	-735	-739	-399	018	-660	-014	219	968
54	35.6	418	-760	-763	-424	-022	-1177	-031	067	931
56	36.8	400	-770	-772	-433	-014	- ∞	-111	000	775
58	36.3	405	-765	-767	-428	-017		-246		568
60	37.3	392	-780	-782	-443	-048		-446		358
62	40.6	360	-810	-812	-473	-057		-677		210
64	41.0	356	-815	-817	-478	-083		-1083		083
66	46.0	310	-855	-857	-518	-106				
68	61.0	190	-990	-992	-653	-066	- ∞	000		

Table 9 Continuum Analysis

Plate No: 232		Emulsion: 103a-F			Date: 1965 Jan. 1			Calibration Star:			
Object: γ^3 Ori		$\alpha: 04:47.9$			$\delta: 06:55$			$\Delta \text{sec z:}$			
$\lambda(\text{\AA}) \times 10^2$	c	d	log I	log I (V.T.)	log I (NORI)	log S'	log I (B) (PHTM)	log I (V) (PHTM)	I (B) (PHTM)	I (V) (PHTM)	
36	93.0	003	-								
38	62.0	182	-1021	-634	-310	197					
40	35.3	416	-673	-389	-065	056					
42	26.4	550	-505	-318	006	-007					
44	22.9	613	-450	-314	010	-010					
45	22.6	621	-441	-324	000	000					
46	23.3	607	-457	-360	-036	035					
48	31.0	478	-604	-539	-215	201					
50	48.8	280	-858	-812	-489	454					
52	54.4	238	-928	-897	-573	519					
54	57.7	213	-970	-948	-624	556					
56	60.1	198	-991	-974	-650	568					
58	60.5	193	-1003	-990	-666	559					
60	60.0	199	-991	-991	-667	529					
62	64.9	160	-1061	-1039	-715	549					
64	66.7	118	-1081	-1035	-711	522					
66	72.5	111	-1160	-1120	-796	593					
68	84.7	043	-1325	-1289	-965	755					

Table 9 Continuum Analysis

Plate No: 232			Emulsion: 103a-F			Date: 1965 Jan. 1			MK Sp:		
Object: RW Aur			$\alpha: 05:05.4$			$\delta: +30:22.1$			$\sec z: 1.166$		
									$(B-V)_C: 0.13$		
$\lambda(\text{\AA}) \times 10^2$	C	d	log I	log I (EXT) (NORM)	log I (EXT) (NORM)	log I (INST)	log I (B) (PHOTM)	log I (V) (PHOTM)	I (B) (PHOTM)	I (V) (PHOTM)	
36	61.0	191	-1022	- 997	- 793		- ∞		000		
38	29.3	501	- 560	- 539	- 335	-138	- 992		101		
40	17.3	741	- 310	- 292	- 088	-032	- 059		873		
42	13.9	840	- 230	- 214	- 010	-017	- 021		953		
44	12.7	880	- 206	- 191	013	003	- 043		906		
45	12.9	870	- 218	- 204	000	000					
46	15.0	805	- 270	- 257	- 053	-018	- 152		705		
48	27.5	532	- 544	- 531	- 337	-136	- 404	- ∞	395	000	
50	43.9	327	- 790	- 778	- 568	-114	- 558	- 558	277	277	
52	49.5	296	- 833	- 822	- 618	-099	- 777	- 131	167	740	
54	46.9	300	- 824	- 814	- 610	-054	-1209	- 063	062	865	
56	50.8	263	- 875	- 866	- 662	-094	- ∞	- 191	000	644	
58	51.4	260	- 881	- 872	- 668	-109		- 338		459	
60	51.5	259	- 883	- 875	- 671	-142		- 540		289	
62	53.0	247	- 907	- 899	- 695	-146		- 766		171	
64	51.0	262	- 877	- 870	- 666	-144		-1114		072	
66	57.7	212	- 966	- 959	- 755	-162		-1685		021	
68	84.0	046	-1323	-1316	-1112	-357		- ∞		000	

Table 9 Continuum Analysis

Plate No: 232		Emulsion: 103a-F		Date: 1965 Jan. 1		MK Sp:				
Object: T Tau		$\alpha: 04^{\text{h}}19.6$		sec z: 1.071		B-V:				
		$\delta: +19^{\circ}26.5$		Asec z: -.296		$(B-V)_C = 0.99$				
$\lambda(\text{\AA}) \times 10^2$	c	d	log. I	log I (EXT) (NORM)	log I (EXT) (INST)	log I (B) (PHTM)	log I (V) (PHTM)	I (B) (PHTM)	I (V) (PHTM)	
36	-					- ∞		000		
38	91.0	011	-							
40	65.5	156	-1103	-1157	-397	-341	- 368	429		
42	50.6	266	- 890	- 938	-278	-285	- 289	511		
44	44.2	326	- 795	- 839	-079	-089	- 135	733		
45	38.5	382	- 717	- 760	000	000				
46	36.3	408	- 681	- 722	038	073	- 061	869		
48	50.5	266	- 881	- 919	-159	012	- 226	- ∞	594 000	
50	72.8	109	-1210	-1244	-484	-030	- 474	- 474	336 336	
52	77.1	088	-1252	-1281	-524	-005	- 683	- 037	208 918	
54	69.3	131	-1142	-1172	-412	144	-1011	135	098 1365	
56	71.9	116	-1175	-1203	-443	125	- ∞	028	000 1067	
58	65.3	158	-1080	-1106	-346	213		- 016		964
60	61.2	190	-1008	-1033	-273	256		- 142		721
62	68.4	139	-1101	-1125	-365	184		- 436		366
64	65.3	158	-1061	-1084	-324	198		- 802		158
66	67.9	140	-1100	-1122	-362	231		-1292		051
68	89.8	018	-1112	-1132	-672	083		- ∞		000

Table 9 Continuum Analysis

Plate No: 236		Emulsion: 103a-F		Date: 1965 Jan. 27			Calibration Star:		
Object: χ^2 Ori		$\alpha: 01:17.9$		$\delta: 06:55$			MK Sp: F0V		
				$\Delta\text{sec z:}$			B-V: 0.15		
$\lambda(\text{\AA}) \times 10^2$	c	d	log I	log I (V.T.)	log I (NORM)	log S ¹	log I (B) (PHTM)	log I (V) (PHTM)	I (B) (PHTM)
36	18.4	725	-1182		-906	683			
38	5.7	1237	- 694		-310	197			
40	2.5	1650	- 360		-084	075			
42	2.2	1710	- 297		-022	021			
44	2.1	1740	- 276		000	000			
45	2.1	1740	- 276		000	000			
46	2.1	1740	- 286		-010	009			
48	2.7	1612	- 421		-145	131			
50	4.6	1382	- 626		-350	315			
52	5.5	1281	- 720		-444	390			
54	8.3	1078	- 871		-601	533			
56	6.0	1241	- 780		-504	422			
58	6.1	1235	- 802		-526	419			
60	6.0	1211	- 806		-530	392			
62	7.1	1150	- 862		-586	420			
64	7.2	1145	- 866		-590	401			
66	10.0	971	- 980		-704	501			
68	21.2	648	-1217		-941	731			

Table 9 Continuum Analysis

Plate No: 236		Emulsion: 103e-F			Date: 1965 Jan. 27			MK Sp: FOV		
Object: ρ Gem		$\alpha: 07:26.9$			$\sec z: 1.316$			$B-V: 0.32$		
								$(B-V)_C: 0.29$		
$\lambda(\text{\AA}) \times 10^2$	c	d	log I	log I (EXT) (NORM)	log I (EXT) (INST)	log I (B) (PHOTM)	log I (V) (PHOTM)	I (B) (PHOTM)	I (V) (PHOTM)	
36	28.3	519	-1170	-1120	-1021	-338	- ∞	000		
38	6.3	1202	- 670	- 628	- 229	-032	- 886	130		
40	3.6	1191	- 497	- 461	- 062	013	014	1033		
42	2.7	1620	- 386	- 354	045	024	020	1047		
44	2.6	1582	- 427	- 398	001	001	- 045	902		
45	2.8	1582	- 427	- 399	000	000				
46	2.9	1560	- 445	- 418	- 019	-010	- 144	718		
48	4.4	1391	- 590	- 564	- 165	-034	- 302	- ∞	499	000
50	6.8	1161	- 797	- 774	- 375	-060	- 504	313	313	
52	7.8	1092	- 860	- 838	- 439	-069	- 747	- 101	179	793
54	7.5	1118	- 852	- 832	- 433	-100	-1255	- 109	056	778
56	10.5	950	- 983	- 965	- 566	-144	- ∞	- 241	000	574
58	10.6	948	- 990	- 972	- 573	-254		- 383	414	
60	11.8	901	-1024	-1007	- 608	-216		- 614		243
62	11.9	806	-1098	-1082	- 683	-263		- 883		131
64	14.1	831	-1080	-1065	- 666	-265		-1265		054
66	16.0	726	-1160	-1146	- 747	-246		-1779		017
68	37.8	388	-1162	-1148	-1049	-318		- ∞		000

Table 9 Continuum Analysis

Plate No: 236			Emulsion: 103a-F			Date: 1965 Jan. 27			MK So:		
Object: T Tau			$\alpha: 01:19.8$			$\sec z: 1.113$			B-V:		
			$\delta: +19:26.5$			$\wedge \sec z: +.010$			$(B-V)_c = 1.07$		
$\lambda(\text{\AA}) \times 10^2$	c	d	log I	log I (EXT) (NORM)	log I (EXT) (NORM)	log I (INST)	log I (B) (PHTM)	log I (V) (PHTM)	I (B) (PHTM)	I (V) (PHTM)	
36	91.3	011	-				.. ∞		000		
38	69.9	126	-						-		
40	32.8	450	-1534	-1534	-521	-446	-473		337		
42	18.4	716	-1186	-1186	-173	-152	-156		698		
44	14.9	806	-1093	-1093	-080	-060	-126		748		
45	12.4	883	-1013	-1013	000	000					
46	11.4	918	-983	-983	030	039	-095		804		
48	16.9	751	-1148	-1148	-135	-004	-272	- ∞	535	000	
50	33.9	438	-1471	-1471	-458	-143	-587	- 587	259	259	
52	34.9	422	-1487	-1487	-474	-084	-762	- 116	173	766	
54	28.7	512	-1380	-1380	-367	166	-989	157	103	1436	
56	29.8	196	-1385	-1385	-372	050	- ∞	- 047	000	897	
58	25.0	575	-1294	-1294	-281	138		- 091		811	
60	23.9	594	-1263	-1263	-250	142		- 256		555	
62	28.1	522	-1328	-1328	-315	105		- 515		306	
64	22.1	624	-1237	-1237	-224	177		- 823		150	
66	27.6	530	-1322	-1322	-309	192		-1332		047	
68	68.4	139	-1800	-1800	-867	-136:		- 02		000	

Table 9 .Continuum Analysis

Plate No: 236		Emulsion: 103e-F			Date: 1965 Jan. 27			MK Sp:		
Object: RW Aur		$\alpha: 05:05.1$			$\sec z: 1.912$			$B-V:$		
		$\delta: +30:22.1$			$\Delta \sec z: 3.802$			$(B-V)_C: 0.30$		
$\lambda(\text{\AA}) \times 10^2$	c	d	log I	log I (EXT) (NORM)	log I (EXT) (NORM)	log I (INST)	log I (B) (PHM)	log I (V) (PHM)	I (INST) (B)	I (INST) (V)
36	91.3	011	-				- ∞		000	
38	55.6	226	-2100:	-1932	-755	-558	-1412		039	
40	30.7	182	-1187	-1313	-166	-091	-118		762	
42	24.4	587	-1334	-1206	-029	-008	-012		973	
44	22.9	615	-1313	-1195	-018	--018	-061		863	
45	22.3	628	-1291	-1177	000	000				
46	26.1	556	-1371	-1262	-085	-076	-210		617	
48	43.0	338	-1630	-1528	-351	-220	-488	- ∞	325	000
50	63.9	167	-1910	-1817	-640	-325	-769	-769	170	170
52	70.0	126	-2000:	-1914	-737	-347	-1025	-379	094	418
54	63.3	172	-1880	-1800	-623	-090	-1245	-099	057	796
56	74.9	100	-1970:	-1896	-719	-297	- ∞	-394	000	404
58	76.4	091	-1920:	-1850	-673	-254		-483		329
60	74.8	101	-1910:	-1843	-666	-274		-672		213
62	78.9	078	-1930:	-1866	-689	-269		-889		129
64	71.6	102	-1860:	-1798	-621	-220		-1220		060
66	77.2	086	-1970:	-1912	-735	-234		-1757		018
68	85.2	020	-				- ∞		000	

Table 9 Continuum Analysis

Plate No: 237		Emulsion: 103a-F		Date: 1965 Jan. 28		Calibration Star:			
Object: γ^3 Ori		$\alpha: 01:47.9$		$\delta: +06:55$		sec z: 1.122		MK Sp: F8V	
						Δ sec z:		B-V: +0.45	
$\lambda(\text{\AA}) \times 10^2$	c	d	log I	log I (V.T.)	log I (PHTM)	log S ¹	log I (B) (PHTM)	log I (V) (PHTM)	I (B) (PHTM)
36	41.7	347	-1555		-1009	786			
38	14.1	638	-902		-356	243			
40	6.1	1237	-535		011	-020			
42	4.7	1369	-460		086	-087			
44	5.0	1330	-522		024	-024			
45	5.1	1322	-546		000	000			
46	4.0	1442	-482		-064	063			
48	13.8	811	-929		-383	369			
50	17.1	749	-991		-445	410			
52	23.4	603	-1110		-564	510			
54	19.6	685	-1046		-500	432			
56	23.4	601	-1126		-580	498			
58	23.0	613	-1105		-559	452			
60	25.1	574	-1126		-580	442			
62	29.2	505	-1178		-632	465			
64	29.0	506	-1176		-630	441			
66	38.3	382	-1279		-732	529			
68	30.2	489	-1679		-1133	923			

Table 9 Continuum Analysis

Plate No: 237		Emulsion: 103a-F			Date: 1965 Jan. 28			MK Sp: FOV	
Object: ρ Gem		$\alpha:$ 07:26.9			sec z: 1.167			B-V: 0.32	
		$\delta:$ +31:52			Δ sec z: +.015			$(B-V)_c:$ 0.29	
$\lambda(\text{\AA}) \times 10^2$	c	d	log I	log I (EXT) (NORM)	log I (EXT) (TEST)	log I (B) (PHOTM)	log I (V) (PHOTM)	I (B) (PHOTM)	I (V) (PHOTM)
36	44.4	322	-1590	-1578	-1053	-267	- ∞	000	
38	12.0	900	- 830	- 820	- 295	-052	- 906	124	
40	5.6	1280	- 498	- 489	036	016	- 011	975	
42	4.4	1388	- 423	- 415	110	023	019	1045	
44	4.6	1378	- 490	- 483	012	018	- 028	938	
45	4.9	1340	- 531	- 525	000	000			
46	5.1	1322	- 560	- 554	- 029	- 006	- 140	725	
48	7.9	1091	- 741	- 735	- 210	-041	- 309	- ∞	491 000
50	17.4	740	-1003	- 998	- 173	-063	- 507	311	311
52	22.3	628	-1044	-1039	- 514	-084	- 762	- 116	173 766
54	22.0	633	-1085	-1081	- 556	-124	-1279	- 133	053 736
56	25.2	575	-1129	-1125	- 600	-102	- ∞	- 199	000 632
58	27.8	524	-1169	-1165	- 640	-188		- 417	383
60	29.7	499	-1180	-1176	- 651	-209		- 607	247
62	34.4	432	-1237	-1234	- 709	-244		- 864	137
64	32.8	450	-1221	-1218	- 693	-252		-1252	056
66	40.5	361	-1298	-1295	- 770	-241		-1764	017
68	68.8	133	-1526	-1523	- 998	-315		- ∞	000

Table 9 Continuum Analysis

Plate No: 237		Emulsion: 103a-F			Date: 1965 Jan. 28			MK Sp:		
Object: T Tau		$\alpha: 04:19.8$			$\sec z: 1.252$			$B-V:$		
		$\delta: +19:26.5$			$\Delta \sec z: +.130$			$(B-V)_c: 1.20$		
$\lambda(\text{\AA}) \times 10^2$	c	d	log I	log I (EXT) (NORM)	log I (INST)	log I (B) (PHM)	log I (V) (PHM)	I (B) (PHM)	I (V) (PHM)	
36	-					- ∞		000		
38	77.0	087	-2100	-2072	-1000	-757	-1611	025		
40	44.1	325	-1429	-1105	- 333	-353	- 380	417		
42	30.5	483	-1280	-1259	- 187	-274	- 278	527		
44	26.0	558	-1185	-1165	- 093	-117	- 163	687		
45	21.9	638	-1091	-1072	000	000				
46	22.0	633	-1097	-1080	008	071	- 063	865		
48	29.1	506	-1214	-1197	- 125	214	- 021	- ∞	946	000
50	49.8	274	-1445	-1429	- 357	053	- 391	- 391	406	406
52	55.0	234	-1470	-1456	- 384	126	- 552	094	281	1242
54	47.3	292	-1393	-1380	- 308	124	- 1031	115	093	1303
56	46.0	309	-1361	-1349	- 277	221	- ∞	124	000	1331
58	38.9	378	-1290	-1278	- 206	246		017		1040
60	38.2	386	-1276	-1265	- 193	249		- 149		710
62	43.3	334	-1321	-1311	- 239	226		- 394		404
64	36.9	400	-1262	-1253	- 181	260		- 740		182
66	41.8	347	-1312	-1304	- 232	297		-1226		059
68	73.7	103	-1559	-1551	- 479	444		- ∞		000

Table 9 Continuum Analysis

Plate No: 240		Emulsion: 103e-F		Date: 1965 Jan. 28		Calibration Star:			
Object: γ^3 Ori		$\alpha: 04:17.9$		$\delta: +06:55$		sec z: 3.122		MK Sp: F6V	
$\lambda(\text{\AA}) \times 10^2$	c	d	log I (V.T.)	log I (HOKI)	log S:	log I (B) (PHM)	log I (V) (PHM)	I (B) (PHM)	I (V) (PHM)
36	48.0	285	- 990		-612	389			
38	23.3	612	- 677		-299	186			
40	6.9	1160	- 370		008	-017			
42	6.8	1165	- 350		026	-029			
44	7.6	1110	- 406		-028	-028			
45	7.7	1108	- 378		000	000			
46	8.6	1055	- 400		-022	021			
48	16.8	756	- 571		-193	179			
50	27.4	537	- 725		-347	312			
52	33.9	438	- 799		-421	367			
54	33.9	438	- 798		-420	352			
56	34.2	423	- 806		-428	346			
58	39.3	372	- 842		-464	357			
60	39.8	369	- 843		-465	317			
62	43.1	335	- 870		-492	326			
64	44.1	326	- 883		-505	316			
66	41.1	306	- 897		-519	316			
68	67.1	243	-1085		-707	497			

Table 9 Continuum Analysis

Plate No: 210			Emulsion: 1032-F			Date: 1965 Jan. 28			MK Sp: F0V		
Object: Q Gm			$\alpha:$ 07:26.9			sec z: 1.316			B-V: 0.32		
			$\delta:$ +31:52			Δ sec z: +.224			$(B-V)_C:$ 0.31		
$\lambda(\text{\AA}) \times 10^2$	c	d	log I	log I (EXT) (NORM)	log I (EXT) (NORM)	log I (INST)	log I (B) (PHM)	log I (V) (PHM)	I (B) (PHM)	I (V) (PHM)	
36	16.0	309	- 981	- 931	-659	-280	- ∞		000		
38	15.3	799	- 525	- 483	-221	-035	- 889		129		
40	6.4	1202	- 275	- 239	023	006	- 021		953		
42	5.6	1280	- 236	- 204	058	029	025		1060		
44	5.7	1272	- 251	- 221	041	003	- 043		906		
45	6.0	1212	- 290	- 262	000	000					
46	6.6	1198	- 328	- 301	-039	-018	- 152		705		
48	12.6	881	- 490	- 464	-202	-023	- 291	- ∞	512	000	
50	22.2	631	- 660	- 637	-637	-375	- 063	- 507	311	311	
52	27.0	540	- 722	- 700	-438	-071	- 749	- 103	178	789	
54	27.6	530	- 730	- 710	-448	-096	-1251	- 105	056	785	
56	30.1	490	- 756	- 738	-476	-130	- ∞	- 227	000	593	
58	31.5	470	- 770	- 752	-490	-133		- 362		435	
60	33.1	448	- 782	- 765	-503	-186		- 584		261	
62	39.6	370	- 842	- 826	-564	-238		- 858		139	
64	38.5	382	- 833	- 818	-556	-240		-1240		058	
66	45.4	318	- 884	- 870	-608	-292		-1815		016	
68	68.0	140	-1090	-1076	-812	-315		- ∞		000	

Table 9 Continuum Analysis

Plate No: 210			Emulsion: 103a-F			Date: 1965 Jan. 28			MK Sp:		
Object: T Tau			$\alpha: 01^{\text{h}}19.8$			$\delta: 19^{\circ}26.5$			$\text{sec } z: 1.058$		
						$\Delta \text{sec } z: +.061$			$(B-V)_c: 0.94$		
$\lambda(\text{\AA}) \times 10^2$	C	d	$\log I$	$\log I$ (EXT) (NORM)	$\log I$ (EXT) (NORM)	$\log I$ (INST)	$\log I$ (B)	$\log I$ (V)	I (B)	I (V)	
36	90.0	018	-				- ∞		000		
38	72.4	112	-1500	-1511	-834	-648	-1502		032		
40	47.4	291	-1005	-1015	-338	-355	-382		415		
42	34.4	129	-840	-849	-172	-201	-205		624		
44	27.5	530	-741	-749	-072	-100	-146		735		
45	22.9	615	-670	-677	000	000					
46	22.6	621	-655	-672	005	026	-108		780		
48	34.6	428	-816	-823	-046	133	-135	- ∞	733	000	
50	53.2	265	-960	-965	-289	023	-121	-421	379	379	
52	59.9	197	-1048	-1054	-377	-010	-688	-042	205	908	
54	51.6	260	-957	-963	-286	066	-1089	057	082	1140	
56	51.4	260	-950	-955	-278	068	-05	-029	000	935	
58	50.3	268	-938	-943	-266	091		-138		728	
60	48.7	283	-921	-926	-249	068		-330		437	
62	51.9	257	-943	-948	-271	055		-565		272	
64	45.6	320	-882	-886	-209	107		-893		128	
66	52.6	251	-947	-951	-274	012		-1481		032	
68	85.0	012	-				- ∞		00		

Table 9 Continuum Analysis

Plate No: 210		Emulsion: 103a-F			Date: 1965 Jan. 29			MK Sp:		
Object: RW Aur		$\alpha: 05^{\text{h}} 05^{\text{m}} 41^{\text{s}}$			$\sec z: 1.367$			$B-V:$		
		$\delta: +30^{\circ} 22' 11''$			$\Delta \sec z: +.215$			$(B-V)_C: 0.43$		
$\lambda(\text{\AA}) \times 10^2$	c	d	$\log I$	$\log I$ (B-V)	$\log I$ (EXT) (NOMA)	$\log I$ (LUST)	$\log I$ (PHEM)	$\log I$ (V) (PHEM)	I (B)	I (V) (PHEM)
36	79.1	078	-					- ∞		000
38	42.6	341	- 935	- 883	-327	-11.1	- 995		101	
40	23.6	600	- 679	- 634	-078	-095	- 122		755	
42	18.0	725	- 579	- 539	017	-012	- 016		964	
44	19.3	692	- 612	- 576	-020	-048	- 094		805	
45	18.2	723	- 591	- 556	000	000				
46	21.0	654	- 636	- 601	-015	-021	- 158		695	
48	35.5	115	- 812	- 780	-224	-015	- 313	- ∞	487	000
50	60.3	195	-1057	-1029	-473	-151	- 595	- 595	254	254
52	63.2	175	-1052	-1015	-459	-092	- 770	- 124	170	752
54	61.0	191	-1040	-1015	-459	-107	-1262	- 116	055	765
56	65.2	159	-1075	-1052	-496	-150	- ∞	- 217	000	566
58	64.1	166	-1057	-1035	-479	-122		- 351		446
60	62.6	179	-1031	-1010	-454	-137		- 535		292
62	69.3	130	-1112	-1092	-536	-210		- 830		148
64	66.6	147	-1077	-1058	-502	-186		-1186		065
66	71.8	118	-1125	-1107	-551	-235		-1758		018
68	-							- ∞		000

Table 9 Continuum Analysis

Plate No: 212	Emulsion: 103a-F			Date: 1966 Feb. 19			Calibration Star:		
Object: γ^3 Ori	$\alpha: 01:47.9$			$\delta: +06:55$			MK Sp: F0V		
				$\Delta\alpha: 1.133$			$B-V: 0.15$		
$\lambda(\text{\AA}) \times 10^2$	C	d	log I (V.T.)	log I (NORM)	log S ¹	log I (B) PHM	log I (V) PHM	I (B) PHM	I (V) PHM
36	67.1	215	-2100		-11.78	955			
38	22.8	416	-1316		-424	311			
40	17.1	757	-988		-066	057			
42	14.5	810	-946		-024	023			
44	11.1	818	-937		-015	-015			
45	13.6	850	-922		000	000			
46	11.6	819	-938		-016	015			
48	36.0	671	-1137		-215	201			
50	42.6	176	-1316		-424	369			
52	34.1	347	-1126		-504	450			
54	39.7	369	-1102		-480	412			
56	46.6	303	-1170		-548	466			
58	45.8	309	-1162		-540	433			
60	50.0	271	-1166		-544	406			
62	56.6	221	-1556		-634	468			
64	50.1	265	-1478		-556	367			
66	55.4	225	-1525		-603	400			
68	90.0	018	-						

Table 9 Continuous Analysis

Plate No: 242		Emulsion: 103a F			Date: 1965 Feb. 19			MK Sp:		
Object: ρ Gcm		$\alpha: 07^{\text{h}} 26^{\text{m}} 9^{\text{s}}$			$\sec z: 1.346$			$B-V: 0.32$		
		$\delta: +31^{\circ} 52'$			$\Delta \sec z: +.213$			$(B-V)_c: 0.29$		
$\lambda(\text{\AA}) \times 10^2$	c	d	log I	log I (EXT) (NORM)	log I (EXT) (NORM)	log I (INST)	log I (B) (PHOTM)	log I (V) (PHOTM)	I (B) (PHOTM)	I (V) (PHOTM)
36	80.1	070	-				- ∞		000	
38	33.1	448	-1310	-1298	-356	-055	-909		121	
40	18.6	711	-1033	-997	-055	.002	-025		944	
42	16.4	766	-985	-953	-011	.012	008		1019	
44	15.1	800	-950	-921	.021	.006	-010		912	
45	15.5	795	-970	-942	000	000				
46	17.1	751	-1008	-981	-039	-024	-158		695	
48	27.1	510	-1210	-1184	-212	-041	-309	- ∞	491	000
50	10.4	361	-1117	-1394	-452	-063	-517	-517	304	304
52	49.0	280	-1518	-1496	-575	-125	-803	-157	157	697
54	46.6	303	-1471	-1451	-519	-107	-1262	-116	055	766
56	53.3	243	-1560	-1542	-600	-134	- ∞	-231	000	588
58	52.7	250	-1540	-1522	-580	-147		-376		421
60	55.6	229	-1558	-1541	-599	-193		-591		256
62	61.6	181	-1615	-1599	-657	-189		-809		155
64	58.1	210	-1560	-1545	-603	-736		-1236		058
66	67.0	146	-1620	-1606	-654	-264		-1787		016
68	83.0	052	-				- ∞		000	

Table 9 Continuum Analysis

Plate No: 242			Emulsion: 103a-F			Date: 1965 Feb. 19			MK Sp:		
Object: T Tau			$\alpha:$ 04:19.8			sec z: 3.133			B-V:		
			$\delta:$ +12:26.5			Δ sec z: .000			(B-V) _c : 1.16		
$\lambda(\text{\AA}) \times 10^2$	C	d	log I	log I (EXT)	log I (EXT) (NORM)	log I (INST)	log I (B) (PHOT)	log I (V) (PHOT)	I (B) (PHOT)	I (V) (PHOT)	
36							-∞		000		
38	81.5	061	-				-				
40	64.1	163	-2210	-2240	-819	-752	-789		163		
42	49.0	279	-1620	-1620	-199	-176	-180		661		
44	42.4	340	-1170	-1170	-019	-051	-110		776		
45	39.6	370	-1121	-1121	000	000					
46	38.0	387	-1398	-1398	023	038	-096		802		
48	49.5	277	-1540	-1540	-119	082	-186	-∞	652	000	
50	69.2	131	-1800	-1800	-379	010	-434	-434	368	368	
52	71.1	120	-1810	-1810	-389	061	-627	029	236	1069	
54	69.3	130	-1755	-1755	-334	078	-1077	069	083	1172	
56	69.5	128	-1740	-1740	-319	147	-∞	050	000	1122	
58	67.5	142	-1710	-1710	-289	144		-085		822	
60	64.1	164	-1648	-1648	-227	179		-219		604	
62	68.1	140	-1680	-1680	-259	209		-411		388	
64	67.1	115	-1635	-1635	-211	153		-817		142	
66	70.4	122	-1640	-1640	-219	181		-1342		016	
68	-						-∞		000		

Table 10 Line Analysis

Plate No: 25			Emulsion: 1030-F				Date: 1963 Oct. 14			MK Sp:				
Object: T Tau			α: 0h 19.8				sec z:			B-V:				
			δ: 51° 26.5				Δsec z:							
$\lambda(\text{\AA})$	c_1	c_c	d_L	d_c	$\log I_L$	$\log I_c$	$\Delta \log I$	$\log I_{cB} + \Delta \log I$	$\log I_{cv} + \Delta \log I$	$I_{LB} - I_{cB}$	$I_{LV} - I_{cv}$	Width (\AA)	A_B	A_V
3933	62.6	82.4	179	055	-1470	-2050	580	-061		636		8	5.1	
3968	57.5	77.9	213	084	-1391	-1810	419	-128		461		8	3.7	
4033	56.8	66.0	219	152	-1386	-1530	144	-300		141		16	2.3	
4068	48.9	61.1	280	191	-1385	-1480	195	-201		228		18	4.1	
4080	49.8	60.3	273	193	-1298	-1447	149	-221		173		15	2.6	
4102	44.8	60.0	319	195	-1233	-1441	208	-149		269		45	12.1	
4133	55.0	59.1	233	207	-1358	-1410	052	-171		215		10	2.2	
4160	48.4	58.4	283	203	-1281	-1410	129	-157		179		10	1.8	
4208	50.0	58.0	272	211	-1290	-1385	095	-157		137		35	2.1	
4233	45.2	57.1	318	217	-1228	-1375	147	-051		211		18	4.3	
4258	44.7	56.9	322	218	-1217	-1372	155	-053		265		12	3.2	
4272	45.4	56.2	313	221	-1212	-1360	116	-084		196		12	2.4	
4294	47.7	55.7	290	226	-1257	-1350	093	-097		154		20	3.1	
4306	40.1	54.1	366	241	-1166	-1323	257	-025		287		10	2.9	
4340	31.1	53.4	472	243	-1015	-1322	277	110		608		20	12.2	
4376	34.6	50.0	429	272	-1093	-1280	187	039		383		12	4.6	
4390	40.1	44.0	366	327	-1161	-1210	049	-088		085		10	0.9	

Table 10 Line Analysis

Plate No: 25			Emulsion:			Date:			MK Sp:				
Object: T Cap (cont.)	$\alpha:$		$\delta:$		$\Delta \alpha, \delta:$		$\log I_{cB} + \Delta \log I$		$\log I_{cv} + \Delta \log I$		$E-V:$		
	c_1	c_c	d_1	d_c	$\log I_1$	$\log I_c$	$\Delta \log I$	I_{cB}	I_{cv}	I_{cv}	Width (\AA)	A_B	A_V
4415	37.6	42.3	392	342	-1135	-1189	054	-019		111	17	1.9	
4477	37.2	41.7	398	349	-1126	-1182	056	-071		103	17	1.8	
4490	30.5	40.6	485	360	-1034	-1167	133	019		276	30	8.3	
4515	30.4	38.8	486	376	-1036	-1150	114	005		220	15	3.3	
4558	30.4	38.8	487	377	-1034	-1148	111	006		234	30	7.0	
4584	33.1	39.0	449	377	-1071	-1146	077	-032		150	32	1.8	
4616	32.8	39.6	450	371	-1070	-1155	085	-027		168	15	2.5	
4634	34.8	39.8	422	367	-1100	-1160	060	-055		114	12	1.1	
4713	38.7	43.5	381	332	-1142	-1198	056	-079		101	9	0.9	
4731	40.9	45.9	357	310	-1170	-1224	054	-087		095	14	1.3	
4861	39.8	56.8	368	218	-1150	-1338	188	-034	-1006	325	036	15	4.9 0.5
5270	61.4	69.2	187	132	-1379	-1476	097	-673	135	042	21	0.9	5.7
5425	59.8	62.1	198	183	-1378	-1383	005	-1271	080	001	014	14	0.0 0.2
5810	40.2	58.5	366	206	-1136	-1316	180		092	419	15		6.3
6234	07.9	59.2	1090			150:			-442	105	13		1.4
6456						279:	275		-781	079	32		2.5
6516						225:	221		-1019	039	27		1.1

Table I Line Analysis

Table 10 Line Analysis

Plate No: 28				Emulsion: 103e/F				Date: 1963 Oct. 17				MK Sp:		
Object: T Tau				$\alpha: 04:19:6$				$\delta: +19:26.5$				$\Delta \text{sec. z:}$		
$\lambda(\text{\AA})$	c_L	c_c	d_L	d_c	$\log I_L$	$\log I_c$	$\Delta \log I$	$\log I_{cB} + \Delta \log I$	$\log I_{cv} + \Delta \log I$	$I_{LB} - I_{cB}$	$I_{LV} - I_{cv}$	Width	A_B	A_V
3833	77.5	94.0	086	000	-1512	-2120	608	063		869		8	7.0	
3968	71.4	88.2	119	026	-1109	-1900	491	057		772		8	6.2	
4033	76.4	84.0	093	016	-1181	-1680	199	-179		243		16	3.9	
4068	70.6	81.1	123	062	-1392	-1595	203	-170		252		18	4.0	
4080	71.0	80.8	115	063	-1420	-1590	170	-200		204		15	3.0	
4102	68.5	80.7	139	063	-1355	-1590	235	-134		307		15	13.8	
4133	72.0	79.9	115	071	-1413	-1552	139	-226		162		10	1.6	
4160	70.6	79.2	123	077	-1394	-1538	1114	-220		170		10	1.7	
4208	72.8	79.2	110	077	-1430	-1538	108	-219		124		15	1.9	
4233	69.2	78.9	128	078	-1365	-1538	173	-154		231		18	4.2	
4258	67.3	78.7	143	078	-1320	-1538	218	-074		333		32	4.0	
4272	71.4	78.6	118	079	-1408	-1537	129	-146		184		32	2.2	
4294	70.5	78.6	124	079	-1390	-1537	147	-103		229		20	4.6	
4306	65.1	78.5	160	079	-1306	-1537	231	-006		406		10	4.0	
4340	52.0	74.0	257	103	-1104	-1135	331	130		719		20	11.4	
4376	58.0	70.2	211	126	-1179	-1370	191	024		377		12	4.5	
4390	62.2	69.3	182	132	-1234	-1352	118	-037		218		12	2.6	

Table 10 Janc Analysis

Plate No:	20	Exposure:	Object: F Gru (cont.)	c:	δ :	Assig. Z:	Date:		M.K. Sp:					
							seq. n:	P-V:	log I _C	log I _C + $\Delta \log I$	log I _C - $\Delta \log I$	I _{IV} - I _{CB} I _{CV}	Width ($^{\circ}$)	A _B
4415	59.8	67.4	196	143	-1200	-1323	123	-016	237	17	4.6			
4427	59.5	66.9	201	147	-1196	-1323	127	-006	219	17	4.2			
4465	61.4	65.5	187	158	-1221	-1223	062	-056	117	12	1.1			
4490	54.8	65.2	234	152	-1110	-1282	112	039	306	30	2.2			
4515	54.9	62.3	234	179	-1117	-1240	053	005	196	15	2.9			
4558	51.7	61.4	259	187	-1101	-1222	121	039	167	30	5.0			
4561	56.8	61.6	219	167	-1089	-1222	133	052	297	12	3.6			
4616	56.1	62.1	222	162	-1161	-1232	071	-015	136	15	2.0			
4634	57.6	63.0	212	174	-1177	-1218	071	-056	132	12	1.6			
4700	62.3	65.9	180	155	-1236	-1291	053	-137	094	8	0.7			
4723	61.0	67.4	167	142	-1265	-1323	057	-092	099	9	0.9			
4731	66.7	66.6	149	138	-1305	-1333	026	-140	015	14	0.6			
4861	61.5	78.9	167	076	-1223	-1415	122	-165	-1052	168	021	16	2.5	0.3
5270	82.4	87.4	057	029	-1480	-1610	130	-454	187	095	398	21	2.0	8.4
5425	81.6	86.6	060	033	-1455	-1500	125	-1017	231	018	130	21	0.2	6.0
5810	66.7	78.5	148	078	-1230	-1380	150	-110	103	15		168	13	2.2
6231	59.9	72.1	197	115	-1113	-1295	152	-216						

Table 10 Line Analysis

Table 10 Line Analysis

Plate No: 232				Emulsion: 1035-F				Date: 1965 Jan. 1				MK Sp:		
Object: T Tau				$\alpha: 04^{\text{h}}19^{\text{m}}48^{\text{s}}$				$\delta: +19^{\circ}26'5$				R,V:		
$\lambda(\text{\AA})$	c_1	c_c	d_1	d_c	$\log I_1$	$\log I_c$	$\Delta \log I$	$\log I_{cB}$ + $\Delta \log I$	$\log I_{cv}$ + $\Delta \log I$	I_{1B} - I_{cB}	I_{1V} - I_{cv}	Width (\AA)	A_B	A_V
3933	50.1	76.0	270	093	- 865	-1291	426	- 127		467		12	5.6	
3963	45.2	73.0	319	109	- 808	-1241	433	- 011		615		15	9.2	
4033	56.7	58.8	221	204	- 761	-1000	232	- 332		302		15	1.6	
4068	45.3	56.2	323	223	- 814	- 951	137	- 210		167		16	2.7	
4080	48.8	54.0	279	240	- 870	- 933	063	- 274		072		10	0.7	
4102	44.0	53.4	327	243	- 796	- 928	132	- 199		065		20	1.3	
4133	50.3	52.2	267	251	- 890	- 907	017	- 302		019		15	0.3	
4160	48.7	51.5	282	260	- 856	- 890	034	- 271		010		18	0.7	
4233	48.4	51.2	282	261	- 856	- 890	031	- 223		015		20	0.9	
4258	42.3	51.0	311	262	- 772	- 890	118	- 231		080		20	1.6	
4272	47.1	51.0	295	262	- 838	- 890	052	- 171		076		18	1.4	
4294	46.6	53.0	298	262	- 831	- 890	059	- 147		085		12	1.0	
4306	39.6	50.2	370	272	- 733	- 870	137	- 057		237		15	3.6	
4340	28.0	19.3	522	277	- 546	- 810	264	093		564		30	16.9	
4376	35.1	48.3	420	282	- 670	- 846	176	027		354		15	5.3	
4390	37.3	17.5	394	291	- 700	- 837	137	- 005		267		12	3.2	
4415	36.7	44.0	403	326	- 690	- 794	104	- 020		203		25	5.1	

Table 10 Line Analysis

Plate No: 232			Emulsion:			Date:			B-V Sp:					
Object: T-Tau (cont.)			c:				sec z:				B-V:			
$\lambda(\text{\AA})$	c_1	c_c	d_1	d_c	$\log I_1$	$\log I_c$	$\Delta \log I$	$\frac{\log I_{cB}}{\Delta \log I}$	$\frac{\log I_{cv}}{\Delta \log I}$	$I_{LB} - I_{cB}$	$I_{LV} - I_{cv}$	Width ($^{\circ}$)	A_B	A_V
4466	38.9	42.3	388	310	- 708	- 771	053	- 042		123		15	1.8	
4490	33.1	40.4	441	361	- 645	- 741	029	007		206		20	4.2	
4515	33.0	38.0	450	386	- 633	- 722	079	005		169		15	2.5	
4558	33.4	36.4	442	406	- 646	- 686	040	- 027		082		32	2.7	
4616	34.2	35.2	422	420	- 670	- 673	003	- 065		005		30	0.2	
4631	36.0	37.6	410	392	- 677	- 703	026	- 051		051		22	1.1	
4700	40.4	42.3	361	311	- 743	- 768	025	- 103		045		12	0.5	
4723	40.2	41.1	358	321	- 745	- 797	052	- 087		093		17	1.6	
4731	42.9	46.5	339	304	- 771	- 820	049	- 110		082		20	1.6	
4861	34.4	58.5	431	207	- 650	- 1080	430	123	- 105	834	051	27	22.5	3.5
5227	70.9	78.2	120	080	- 1170	- 1290	120	- 609	128	059	325	20	1.2	6.5
5270	66.9	71.9	116	117	- 1111	- 1181	070	- 726	131	028	202	18	0.5	3.6
5425	64.5	69.0	162	132	- 1072	- 1140	068	- 1003	200	071	230	18	0.3	4.1
6234	50.2	69.3	270	131	- 862	- 1120	258	- 251		- 251	32		8.0	
6456	61.3	69.0	187	133	- 1012	- 1120	108	-	- 813		034	15		0.5
6516	66.8	69.5	147	130	- 1108	- 1121	013	-	- 1052		003	17		0.1
6563	07.8	69.0	1092	133	- 105	- 1119	104	-	- 509		200	25		8.5

Table 10 Line Analysis

Plate No: 236			Emulsion: 103e-F				Date: 1955 July 27				MK Sp:			
Object: T Tau			a: 01:19.8				sec z:				B-V:			
			δ: +19:26.5				Δsec z:							
$\lambda(\text{\AA})$	c_1	c_c	d_1	d_c	$\log I_1$	$\log I_c$	$\Delta \log I$	$\log I_{cB}$ + $\Delta \log I$	$\log I_{cv}$ + $\Delta \log I$	I_{cB}	I_{cv}	Width (\AA)	A_B	A_V
3734	46.8	75.1	300	099	-1868	-	300	-1098	-	010	-	17	0.7	
3836	58.2	67.3	210	112	-	-	215	-812	-	060	-	12	0.7	
3889	41.8	53.7	346	211	-1758	-	347	-423	-	203	-	9	1.9	
3933	26.8	48.9	541	280	-1410	-1880	470	-318	-	470	-	12	5.8	
3968	20.8	35.3	657	418	-1258	-1589	331	-209	-	329	-	22	3.9	
4026	26.2	27.0	554	510	-1381	-1404	020	-112	-	018	-	10	0.2	
4033	24.8	26.3	578	518	-1353	-1391	038	-380	-	035	-	16	0.6	
4068	18.1	23.1	722	611	-1182	-1312	130	-221	-	154	-	18	2.6	
4080	18.4	22.9	718	614	-1188	-1309	121	-209	-	150	-	15	2.2	
4102	16.1	21.6	780	641	-1114	-1275	161	-132	-	225	-	20	4.5	
4133	19.3	20.5	691	664	-1217	-1251	034	-224	-	044	-	9	0.4	
4160	18.9	20.1	701	677	-1205	-1243	037	-169	-	055	-	10	0.6	
4233	17.2	19.9	749	681	-1153	-1230	077	-074	-	136	-	18	2.4	
4258	16.7	18.5	760	712	-1141	-1194	053	-095	-	092	-	10	0.9	
4272	16.7	18.2	760	720	-1141	-1184	043	-101	-	076	-	10	0.8	
4294	16.0	18.2	780	720	-1118	-1184	066	-076	-	119	-	15	1.8	
4306	15.9	17.3	781	741	-1116	-1164	048	-094	-	083	-	10	0.8	

Table 10 Line A₁ 1974

Plate No: 236	Evaluation:	Date:	Age:						Ext. Sp.						
			c ₁	c _c	d ₁	d _c	log I _C	log I _C	Δ log I _C	log T _{CV}	T _{IP}	T _{CV}	(Å)	A _B	A _V
1310	08.6	17.1	1018	718	-901	-1153	21.9	212	-	565	-	25	21.1	-	-
1415	11.2	21.7	201	818	-296	-1001	035	-039	-	162	-	16	2.6	-	-
1427	11.6	21.3	913	825	-981	-1073	032	-031	-	172	-	15	2.6	-	-
1420	02.9	12.4	271	886	-929	-1011	082	-023	-	164	-	24	3.9	-	-
1515	08.7	12.2	1050	829	-856	-996	11.0	038	-	300	-	20	6.0	-	-
1558	02.8	11.6	974	911	-931	-926	057	-030	-	131	-	22	2.2	-	-
1584	10.6	11.5	950	917	-952	-987	035	-050	-	067	-	10	0.7	-	-
1616	10.2	11.7	967	911	-915	-933	018	-051	-	092	-	15	1.4	-	-
1631	13.3	15.0	851	803	-1012	-1097	018	-057	-	092	-	12	1.1	-	-
1861	11.2	20.1	931	676	-975	-1221	21.6	-324	-1578	205	011	20	4.1	0.2	-
1924	23.5	29.6	600	129	-1291	-1100	102	-51.5	-1016	063	202	30	1.9	0.6	-
5227	32.8	31.7	150	128	-1151	-1130	029	-751	-052	011	057	10	0.1	0.6	-
5270	26.6	29.8	545	195	-1343	-1100	057	-767	035	021	133	20	0.1	2.6	-
5810	21.0	25.1	578	571	-1288	-1299	011	-	081	-	021	12	-	0.3	-
6231	14.9	28.5	808	517	-1331	-1343	002	-	555	005	26	-	0.2	-	-
6563	02.6	25.8	1638	560	-196	-1296	000	-	921	-	101	30	3.0	-	-
6724	23.1	29.9	603	192	-1254	-1357	103	-	1987	-	002	21	0.0	-	-

Table 10 Line Analysis

Plate No: 237				Emulsion: 103e-F				Date: 1935 Aug. 28				HK Sp:		
Object: T Tauri				a: 01:19.8				Spec. z:				B-V:		
				δ: +19:26.5				Δsec. z:						
$\lambda(\text{\AA})$	c_1	c_c	d_1	d_c	$\log I_1$	$\log I_c$	$\Delta \log I$	$\log I_{cB}$ + $\Delta \log I$	$\log I_{cv}$ + $\Delta \log I$	I_{LB} - I_{cB}	I_{LV} - I_{cv}	Width (\AA)	A_B	A_V
3731	61.0	81.0	190	0.5	-1880	-	250	-1671	-	009	-	17	0.2	
3889	52.7	61.8	250	1.82	-1680	-1790	110	-1.86	-	073	-	10	0.7	
3933	38.8	57.1	379	2.19	-1442	-1691	249	-2.12	-	250	-	14	3.5	
3968	32.3	54.2	459	2.39	-1329	-1650	321	-3.07	-	409	-	14	5.7	
4026	35.3	39.0	478	378	-1373	-1422	0.9	-321	-	050	-	10	0.5	
4033	37.4	38.8	394	379	-1408	-1433	025	-344	-	025	-	16	0.4	
4038	29.3	37.2	502	396	-1260	-1401	11.1	-212	-	170	-	18	3.1	
4060	29.4	37.0	501	399	-1260	-1399	139	-208	-	169	-	15	2.5	
4102	25.5	34.0	565	435	-1190	-1342	152	-185	-	193	-	20	3.9	
4133	30.4	32.5	486	156	-1279	-1321	0.2	-279	-	149	-	12	1.8	
4160	27.5	32.5	530	456	-1229	-1321	092	-207	-	119	-	15	1.8	
4233	27.6	30.5	529	183	-1230	-1269	039	-222	-	052	-	18	0.9	
4258	27.5	30.0	530	190	-1229	-1265	036	-213	-	048	-	12	0.6	
4272	28.0	29.9	523	192	-1224	-1259	035	-205	-	049	-	10	0.5	
4294	27.0	29.9	516	192	-1200	-1259	059	-170	-	086	-	12	1.0	
4306	22.8	29.2	615	502	-1125	-1241	116	-104	-	185	-	10	1.9	
4310	15.4	29.0	796	501	-943	-1239	296	094	-	611	-	24	14.7	

Table 10. Time Analysis

Table 10. Line Analysis

Plate No: 237	Emission:	Object: P-Sen (contd.)	$\sigma:$	Acc. %:				Acc. %:				Acc. %:					
				C_1	C_c	d_1	d_c	$\log I_1$	$\log I_c$	$\Delta \log I$	$\Delta \log I_c$	$\log J_{cv}$	$\log J_{cv}$	I_{cv}	I_{cv}	$\log J_{bv}$	I_{bv}
14115	21.3	21.3	615	562	-1029	-1151	661	-	-098	-	-104	-	-	-	-	15	1.6
14127	21.1	21.3	652	568	-1081	-1143	662	-	-090	-	-108	-	-	-	-	18	1.9
14190	17.1	22.0	719	633	-	990	-	-1026	106	-	-013	-	-210	-	-	22	4.6
15115	16.2	21.9	778	635	-	965	-	-1026	131	025	-	-268	-	-	-	28	7.5
15558	17.5	22.0	739	634	-	1001	-	-1024	020	098	-	-192	-	-	-	18	3.5
15881	18.1	22.0	722	631	-	1014	-	-1024	000	008	-	-172	-	-	-	12	2.0
16116	18.1	22.0	722	634	-	1011	-	-1024	050	020	-	-177	-	-	-	20	3.5
16231	25.3	29.2	565	503	-	1155	-	-1226	071	015	-	-156	-	-	-	12	1.9
16251	19.0	35.0	700	421	-	1030	-	-1309	270	223	-	-168	-	-	-	20	15.5
52770	14.0	19.1	326	279	-	1373	-	-1121	018	-610	-	-152	-	-	-	20	2.7
58110	36.6	38.9	1.02	379	-	1271	-	-1291	020	-	028	-	018	-	11	-	0.7
62311	23.6	13.1	600	336	-	1105	-	-1321	216	-	-234	-	-228	-	26	-	5.9
6563	03.6	39.0	1190	378	-	596	-	-1297	701	-	-528	-	-238	-	30	-	7.1
6721	37.6	15.0	390	319	-	1285	-	-1352	067	-	-1933	-	-092	-	16	-	0

Table 10 Line Analysis

Plate No: 210				Emulsion: 1032-Y				Date: 1935 Jan. 29				MK Spec		
Object: T Tauri				$\alpha: 04^{\text{h}}19^{\text{m}}8^{\text{s}}$				$\delta: +19^{\circ}26.5$				B-V:		
$\lambda(\text{\AA})$	c_1	c_c	d_1	d_c	$\log I_1$	$\log I_c$	$\Delta \log I$	$\log I_{cB}$ + $\Delta \log I$	$\log I_{cv}$ + $\Delta \log I$	I_{1B} - I_{cB}	I_{cv} - I_{cV}	Width (\AA)	A_B	E_V
3731	61.5	80.1	186	069	-11.90	-	250	-18.47	-	005	-	17	0.1	-
3836	65.9	73.8	157	101	-12.55	-14.70	275	-8.03	-	061	-	16	1.0	-
3889	50.5	72.0	267	118	-10.33	-13.80	317	-3.31	-	254	-	20	5.1	-
3933	35.8	62.2	412	181	-8.55	-11.78	323	-7.97	-	333	-	12	4.0	-
3963	26.6	47.3	512	291	-7.58	-9.80	222	-2.28	-	237	-	31	3.3	-
4033	35.4	114.0	418	326	-8.42	-9.50	108	-2.35	-	128	-	12	1.5	-
4033	38.0	13.8	386	327	-8.78	-9.51	073	-2.01	-	085	-	12	1.0	-
4068	31.0	41.9	479	317	-7.87	-9.19	132	-1.72	-	176	-	15	2.6	-
4102	26.6	39.5	514	370	-7.26	-8.86	160	-1.13	-	238	-	24	5.7	-
4033	24.8	26.6	578	512	-6.96	-7.20	024	-2.21	-	032	-	10	0.3	-
4160	32.2	31.9	460	421	-8.00	-8.33	033	-1.89	-	047	-	15	0.7	-
4233	28.6	33.9	512	438	-7.53	-8.15	052	-1.33	-	098	-	18	1.8	-
4256	27.2	33.5	538	411	-7.31	-8.12	081	-1.04	-	134	-	15	2.0	-
4272	29.9	33.3	491	442	-7.71	-8.12	041	-1.39	-	066	-	10	0.7	-
4294	28.0	33.0	522	419	-7.43	-8.10	057	-1.06	-	111	-	15	1.7	-
4303	26.5	31.8	545	462	-7.25	-7.96	071	-0.98	-	120	-	10	1.2	-
4340	15.6	30.0	782	490	-5.50	-7.70	220	060	-	456	-	22	10.0	-

Table 10 Line Analysis

Object: P 500 (cont.)	Date:	PK Spec.										PK Spec.	
		sec. 5	sec. 6	sec. 7	sec. 8	sec. 9	sec. 10	sec. 11	sec. 12	sec. 13	sec. 14	B-V	M-B
1115 23.5 25.4	601	565	- 695	- 703	034	- 167		262	12	3.1			
1127 23.0 24.1	611	586	- 669	- 687	019	- 119	033		15	0.5			
1130 22.8 23.2	616	612	- 670	- 676	066	- 115	010		12	0.1			
1515 16.8 22.5	702	621	- 603	- 604	061	- 051		115		25	2.9		
1556 20.7 22.7	661	622	- 638	- 640	056	- 063	018		15	0.7			
1616 21.2 23.2	650	611	- 615	- 671	026	- 081	012		15	0.7			
1621 25.5 27.6	565	529	- 706	- 732	026	- 032	019		16	0.2			
1661 17.2 10.0	719	365	- 587	- 879	107	- 1250	001		15	0.7			
5227 55.2 57.1	231	219	- 992	- 1011	019	- 719	001	008	012	12	0.1		
5270 46.9 50.5	260	266	- 938	- 951	013	- 797	026	005	022	18	0.1		
5810 11.5 17.6	321	290	- 893	- 920	027	- 119	016	016	20	25	0.6		
6231 26.6 50.8	514	261	- 719	- 936	117	- 193	075		24	0.0			
6563 02.6 18.9	1115	280	- 301	- 918	615	- 504	265		25	0.6			
6721 52.2 57.7	256	213	- 213	- 987	016	- 2351	000		16	0.0			

Table 20 I_{V} , I_{B} , I_{R} , I_{C}

Plate No: 212	Emulsion: 1035, F	Peter, May 21, 1972						Peter, May 21, 1972		
		α: 0h 12m 0s	β: 18° 26' 5"	α: 0h 12m 0s	β: 18° 26' 5"	α: 0h 12m 0s	β: 18° 26' 5"	α: 0h 12m 0s	β: 18° 26' 5"	α: 0h 12m 0s
λ(Å)	c_1	c_c	a_1	$\log I_1$	$\log I_c$	$\log I_B$	$\log I_{\text{R}}$	I_{V}	I_{B}	I_{V}
37.3	66.3	92.0	150	0.05	-2.020	..	-2.617	0.03	1.2	0.0
38.6	68.4	85.0	136	0.12	-2.000	-	-1.217	0.15	1.5	0.2
39.3	45.6	81.1	310	0.16	-1.562	-	-1.001	-0.13	1.8	2.6
39.8	37.2	81.5	100	0.61	-1.146	..	-1.450	-1.60	2.0	3.5
40.3	50.8	58.5	263	2.07	-1.690	-1.651	1.61	-1.08	1.21	1.0
40.8	44.8	51.5	320	2.38	-1.545	-1.710	1.95	-2.20	2.08	1.8
41.3	39.6	57.1	367	2.62	-1.150	-1.650	2.10	-0.36	3.4	1.2
41.6	45.5	50.6	315	2.66	-1.538	-1.662	1.24	-0.99	2.03	8
41.7	41.6	50.0	350	2.71	-1.169	-1.625	1.57	-0.38	2.76	10
42.3	44.6	49.5	321	2.76	-1.520	-1.625	1.05	-0.63	1.85	12
42.3	47.2	49.3	352	2.77	-1.162	-1.625	1.63	0.02	3.14	8
42.9	47.2	46.6	352	2.03	-1.160	-1.553	0.93	-0.17	1.73	2.5
43.0	26.9	45.0	54.1	319	-1.212	-1.510	2.08	1.72	7.37	21
43.6	39.3	43.9	37.1	323	-1.131	-1.515	0.81	-0.31	1.63	8
44.5	36.4	42.3	103	342	-1.283	-1.60	0.77	-0.30	1.52	15
44.6	35.6	41.1	117	351	-1.365	-1.50	0.84	-0.17	1.62	8
44.9	32.6	39.6	45.6	369	-1.301	-1.23	1.19	0.20	2.57	7
										1.8

Table 10. Line List.

Plate No:	212	Position: 203°. P		Position: 203°. E. 26.5°		Position: 203°. S. E. 26.5°	
		α:	δ:	α:	δ:	α:	δ:
Object: T Tauri							
λ(A)	c ₁	c _c	d ₁	d _c	log I _c	log I _c	log I _c
3731	66.3	92.0	150	005	-2020	-	150: -1947
3836	65.4	85.0	136	042	-2000:	-	130: -1217
3933	115.6	81.1	310	046	-1562	-	100: -613
3968	37.2	81.5	100	031	-1406	-	150: -160
4033	50.6	58.5	263	207	-1620	-1051	161: -108
4051	111.8	54.5	320	238	-1515	-1710	195: -220
4133	39.6	51.1	367	262	-1450	-1160	161: -121
4160	115.5	50.6	315	263	-1538	-1612	124: -036
4176	41.6	50.0	350	271	-1468	-1625	157: -038
4203	11.6	49.5	321	276	-1520	-1625	105: -063
4233	41.3	49.3	352	277	-1462	-1625	163: -002
4291	11.3	46.6	352	303	-1460	-1553	093: -017
4310	26.9	45.0	541	319	-1212	-1510	298: -172
4376	39.3	43.9	371	323	-1131	-1515	081: -031
4415	36.1	42.3	403	342	-1383	-1160	077: -030
4456	35.6	41.1	417	351	-1365	-1150	084: -017
4490	32.6	39.6	456	369	-1301	-1123	119: -020

Table 10. *Line 2 - Nucleus*

Table 10 Line Index

Plate No:	23	Emulsion: 102c, F			Date: 1953 Oct. 13			P. V.		
		c: 05, 05, h	c: 05, 05, k	c: 05, 05, l	c: 05, 05, m	c: 05, 05, n	c: 05, 05, o	c: 05, 05, p	c: 05, 05, q	c: 05, 05, r
<i>Object: M1A</i>										
		5:30, 22, 1								
$\lambda(\text{\AA})$	c_1	c_c	a_1	a_c	$\log I_1$	$\log I_c$	$\Delta \log I$	$\log I_B$	$\log I_{\text{eq}}$	$\log I_V$
3933	12.5	12.7	885	31.0	-760	-1330	550	258	1301	16
3969	21.3	10.4	617	362	-982	-1312	330	113	740	11
4033	21.8	36.4	163	104	-1211	-1251	013	-073	630	21
4038	28.3	36.5	318	105	-2312	-1213	014	-027	129	11
4050	32.3	31.4	158	431	-2160	-1212	032	-014	661	22
4102	32.3	33.4	152	112	-1176	-1182	033	-036	661	11
4133	27.0	32.2	510	162	-1093	-1171	078	016	173	33
4160	28.9	31.1	508	178	-1123	-1154	031	-021	655	10
4176	27.1	30.5	532	135	-1101	-1150	016	-007	653	26
4204	26.8	23.8	512	193	-1055	-1110	015	-006	653	18
4233	26.0	29.4	558	501	-1076	-1131	015	-007	120	18
4272	23.3	28.9	606	509	-1030	-1123	023	016	215	10
4291	22.4	26.6	616	512	-1012	-1122	110	016	257	20
4306	25.0	26.5	578	513	-1056	-1120	014	016	112	20
4310	16.9	22.4	702	532	-913	-1103	060	010	131	26
4376	21.4	27.2	586	538	-1050	-1166	016	-007	656	36
4415	17.1	26.6	749	547	-902	-1086	184	126	162	28
										12.9

Plat. No: 23	Emulsion:				Date:	MK Spec.			
	c ₁	c ₂	a ₁	a ₂		R _V :	I _{CB}	I _{CV}	I _{IV}
Object: F ⁺ for (cont.)									
1455	24.5	26.2	583	554	-1021	1060	0.9	0.1	0.0
1459	23.6	26.3	600	550	-1035	1064	0.9	0.37	0.26
1515	21.3	26.7	611	516	-990	1060	0.9	0.1	0.0
1504	22.9	28.2	612	522	-1025	1112	0.7	0.6	267
4634	18.9	30.0	701	491	-942	1110	0.8	0.26	163
1700	36.9	36.0	461	367	-1232	1251	0.6	0.06	390
1731	39.4	42.4	371	312	-1277	1308	0.31	0.1	0.2
1817	46.2	47.5	308	291	-1351	1375	0.21	0.25	0.21
1861	27.1	53.5	54.0	24.3	-2096	-2111	345	0.25	-1.00
1924	55.2	63.5	232	170	-1461	-1701	163	-328	-911
5016	65.2	76.2	11.0	923	-1830	-	160;	-121	-261
5101	82.1	83.2	059	052	-	-	0.0;	-776	-261
5227	77.8	63.8	081	016	-	-	100;	-0.35	-927
5270	77.7	63.8	032	016	-	-	160;	0.61	-1601
5316	74.5	83.8	101	016	-	-	14.0;	0.68	-2111
5362	60.0	83.9	070	017	-	-	015;	-0.38	-166
5565	66.5	69.2	150	131	-1606	-1650	0.1	262	050

Table 30. *Tracheal*, *Tracheobronchial*

Table 10 Line Analysis

Plate No: 25				Emulsion:				Date:				M & E.M.		
Object: M31 And (cont.)				α :	δ :	sec Z:	Age Z:	sec Z:	Age Z:	sec Z:	Age Z:	M.V.	B-V:	
$\lambda(\text{\AA})$	c_1	c_c	d_1	d_c	$\log I_1$	$\log I_c$	$\Delta \log I$	$\log I_{CB}$ + $\Delta \log I$	$\log I_{CV}$ + $\Delta \log I$	I_{LB} - I_{CB}	I_{LY} - I_{CV}	Width (\AA)	I_B	A_V
4558	17.6	39.3	732	372	-817	-1110	323	380		793		16	14.3	
4581	21.8	40.5	655	362	-887	-1166	279	122		628		20	12.6	
4616	37.1	11.7	400	350	-1120	-1176	056	-124		092		10	0.9	
4631	33.6	42.4	441	341	-1026	-1185	097	-100		159		16	2.5	
4700	47.1	49.0	297	272	-1230	-1260	030	-226		039		10	0.4	
4731	50.9	52.6	263	251	-1271	-1291	017	-267		021		8	0.2	
4762	60.2	63.6	196	169	-1375	-1420	045	-302		049		10	0.5	
4817	52.9	65.5	197	157	-1374	-1440	036	-306	-1704	042	003	10	0.7	0.0
4861	39.2	67.7	377	112	-1138	-1166	228	-270	-056	276	036	32	8.6	1.2
4921	61.5	71.2	187	120	-1380	-1505	125	319	-720	120	048	14	1.7	0.7
5016	67.3	79.3	112	072	-1460	-1630	170	-353	-274	113	172	24	3.4	1.1
5017	79.1	80.8	075	063	-1505	-1615	030	-517	-357	020	029	10	0.2	0.3
5053	78.1	81.4	062	060	-1565	-1625	060	-500	-292	040	065	15	0.6	1.9
5101	81.2	83.0	061	052	-1630	-1650	020	-521	-232	011	026	10	0.1	0.3
5119	78.4	83.3	079	051	-1575	-1650	075	-552	-134	049	115	18	0.9	2.1
5168	74.9	83.6	101	049	-1520	-1650	130	-569	005	070	262	22	1.5	5.8
5227	76.4	83.9	092	048	-1513	-1655	112	-673	027	046	242	20	1.0	4.8

Table 20. Dimer Analysis

A ₀	Table 10 June 1974										Table 10 June 1974									
	Log ₁₀ N ₀																			
3933	27.8	55.1	725	231	733	-21405	572	063	896	218	218	218	218	218	218	218	218	218	218	218
3959	28.3	51.2	518	263	2033	-21343	310	-071	168	218	218	218	218	218	218	218	218	218	218	218
4033	32.1	45.8	371	310	21390	-21272	062	-279	218	218	218	218	218	218	218	218	218	218	218	218
4069	33.2	41.0	477	326	2111	-21353	212	011	139	218	218	218	218	218	218	218	218	218	218	218
4080	39.6	42.3	370	311	21198	-21232	036	-276	218	218	218	218	218	218	218	218	218	218	218	218
4133	33.0	40.5	418	361	2106	-21209	203	-063	183	218	218	218	218	218	218	218	218	218	218	218
4160	38.2	39.6	386	360	2179	-21201	022	-121	037	218	218	218	218	218	218	218	218	218	218	218
4176	27.2	39.3	538	371	2010	-21297	212	011	277	218	218	218	218	218	218	218	218	218	218	218
4200	34.6	38.3	628	382	2131	-21282	051	-059	096	218	218	218	218	218	218	218	218	218	218	218
4272	33.2	36.3	617	405	2110	-21253	013	-050	026	218	218	218	218	218	218	218	218	218	218	218
4233	29.6	37.6	658	390	2053	-21172	219	015	218	218	218	218	218	218	218	218	218	218	218	218
4289	34.6	38.3	628	382	2131	-21282	051	-059	096	218	218	218	218	218	218	218	218	218	218	218
4306	26.3	35.2	515	120	3012	-21138	126	038	275	218	218	218	218	218	218	218	218	218	218	218
4310	27.1	34.1	539	113	2027	-21281	207	025	232	218	218	218	218	218	218	218	218	218	218	218
4376	27.1	33.5	532	112	2023	-21219	096	011	206	218	218	218	218	218	218	218	218	218	218	218
4415	26.2	32.9	556	119	2002	-21208	206	011	223	218	218	218	218	218	218	218	218	218	218	218

Table 19. Ionic Analogies

Plate No.: 26	Position:	Depth:	ITC S _B :								
Object: H ₂ Amp (cont.)	g:	Sec. N:	P. M.								
	<i>G</i> :										
$\lambda(\text{A})$	C ₁	C _c	δ_1								
			a _c								
			log C ₁								
			log C _c								
			Δ log C ₁								
			Δ log C _c								
			log C _B								
			log C _V								
			log C _B + log C _V								
			I _{AB}								
			I _{AV}								
			T _{AV}								
			Weight								
			($\frac{\text{C}}{\text{A}}$)								
			A _B								
			t _V								
1.130	27.8	33.3	523	112	-1032	-1116	064	-051	156	15	2.3
1.1515	23.6	34.4	601	130	-939	-1125	166	011	326	32	10.4
1.1528	25.9	36.6	558	103	-1000	-1156	156	-032	281	16	5.1
1.1531	23.3	36.9	607	376	-961	-1167	226	011	456	20	6.3
1.1616	36.8	42.1	400	311	-1160	-1235	075	-162	108	10	1.1
1.1634	31.0	42.9	135	338	-1122	-1210	116	-116	170	16	2.7
1.1700	15.7	51.1	319	260	-1261	-1316	035	-252	100	10	1.0
1.1731	17.3	51.0	291	210	-1290	-1360	070	-313	072	8	0.6
1.1769	56.0	57.5	223	215	-1360	-1395	015	-446	072	10	0.7
1.1817	60.5	61.6	192	163	-1131	-1160	019	-412	-1951	038	0.0
1.1861	11.3	67.7	350	141	-1212	-1522	310	-220	-1611	308	013
1.1921	56.2	72.9	225	102	-1362	-1570	208	-361	-1090	158	036
501.8	67.0	76.8	115	078	-1493	-1650	157	-531	031	039	1.02
501.9	75.8	79.3	095	073	-1603	-1661	051	-659	-1682	024	0.37
505.3	77.6	79.5	032	072	-1633	-1662	029	-473	-695	022	0.13
507.0	74.1	79.8	103	071	-1579	-1663	089	-656	-216	038	1.13
510.1	76.0	79.7	094	071	-1602	-1657	055	-709	-285	024	0.61
										10	0.2
										0.2	0.6

Table 10 Line Analysis

$\lambda \text{ Å}$	Plate No: 26		Emulsion:		Date:		Exposure:		Acc. z:		Age z:		Acc. z:		Age z:	
	c ₁	c ₂	d ₁	d ₂	log I ₁	log I ₂	log I ₃	log I ₄	Δ log I ₁	Δ log I ₂	Δ log I ₃	Δ log I ₄	I _{1A} - I _{1B}	I _{2A} - I _{2B}	I _{3A} - I _{3B}	I _{4A} - I _{4B}
51.6	70.6	79.7	124	0.92	-151.0	-161.9	109	-703	-114	0.11	171	22	1.0	3.8		
52.0	64.3	77.5	123	0.92	-151.7	-163.1	116	-779	0.11	0.32	101	20	0.6	3.2		
53.0	70.7	77.7	121	0.92	-152.0	-163.0	0.60	-938	-0.22	0.06	111	20	0.1	3.5		
54.0	72.5	76.5	125	0.92	-152.5	-163.5	0.65	-1016	0.06	0.06	116	20	0.3	3.0		
54.5	68.0	74.5	103	1.01	-152.0	-163.0	0.60	-1016	0.06	0.06	116	20	0.3	3.0		
55.0	62.5	57.0	251	219	-129	-132	0.12	-2506	0.31	0.31	-76	20	0.7			
55.5	64.5	72.2	162	215	-129	-132	0.12	-2506	0.31	0.31	-76	20	0.6			
56.0	60.0	67.0	262	211	-127.6	-134.7	0.12	-1329	0.69	0.69	-176	20	0.3			
56.5	62.5	57.0	251	219	-129	-132	0.12	-2506	0.31	0.31	-76	20	0.6			
57.0	60.0	58.0	262	211	-127.6	-134.7	0.12	-1329	0.69	0.69	-176	20	0.3			
57.5	64.5	72.2	162	215	-129	-132	0.12	-2506	0.31	0.31	-76	20	0.6			
58.0	60.0	67.0	262	211	-127.6	-134.7	0.12	-1329	0.69	0.69	-176	20	0.3			
58.5	62.5	57.0	251	219	-129	-132	0.12	-2506	0.31	0.31	-76	20	0.6			
59.0	64.5	72.2	162	215	-129	-132	0.12	-2506	0.31	0.31	-76	20	0.6			
59.5	60.0	58.0	262	211	-127.6	-134.7	0.12	-1329	0.69	0.69	-176	20	0.3			
60.0	64.5	72.2	162	215	-129	-132	0.12	-2506	0.31	0.31	-76	20	0.6			
60.5	62.5	57.0	251	219	-129	-132	0.12	-2506	0.31	0.31	-76	20	0.6			
61.0	64.5	72.2	162	215	-129	-132	0.12	-2506	0.31	0.31	-76	20	0.6			
61.5	62.5	57.0	251	219	-129	-132	0.12	-2506	0.31	0.31	-76	20	0.6			
62.0	64.5	72.2	162	215	-129	-132	0.12	-2506	0.31	0.31	-76	20	0.6			
62.5	62.5	57.0	251	219	-129	-132	0.12	-2506	0.31	0.31	-76	20	0.6			
63.0	64.5	72.2	162	215	-129	-132	0.12	-2506	0.31	0.31	-76	20	0.6			
63.5	62.5	57.0	251	219	-129	-132	0.12	-2506	0.31	0.31	-76	20	0.6			
64.0	64.5	72.2	162	215	-129	-132	0.12	-2506	0.31	0.31	-76	20	0.6			
64.5	62.5	57.0	251	219	-129	-132	0.12	-2506	0.31	0.31	-76	20	0.6			
65.0	64.5	72.2	162	215	-129	-132	0.12	-2506	0.31	0.31	-76	20	0.6			
65.5	62.5	57.0	251	219	-129	-132	0.12	-2506	0.31	0.31	-76	20	0.6			
66.0	64.5	72.2	162	215	-129	-132	0.12	-2506	0.31	0.31	-76	20	0.6			
66.5	62.5	57.0	251	219	-129	-132	0.12	-2506	0.31	0.31	-76	20	0.6			
67.0	64.5	72.2	162	215	-129	-132	0.12	-2506	0.31	0.31	-76	20	0.6			
67.5	62.5	57.0	251	219	-129	-132	0.12	-2506	0.31	0.31	-76	20	0.6			
68.0	64.5	72.2	162	215	-129	-132	0.12	-2506	0.31	0.31	-76	20	0.6			
68.5	62.5	57.0	251	219	-129	-132	0.12	-2506	0.31	0.31	-76	20	0.6			
69.0	64.5	72.2	162	215	-129	-132	0.12	-2506	0.31	0.31	-76	20	0.6			
69.5	62.5	57.0	251	219	-129	-132	0.12	-2506	0.31	0.31	-76	20	0.6			
70.0	64.5	72.2	162	215	-129	-132	0.12	-2506	0.31	0.31	-76	20	0.6			
70.5	62.5	57.0	251	219	-129	-132	0.12	-2506	0.31	0.31	-76	20	0.6			
71.0	64.5	72.2	162	215	-129	-132	0.12	-2506	0.31	0.31	-76	20	0.6			
71.5	62.5	57.0	251	219	-129	-132	0.12	-2506	0.31	0.31	-76	20	0.6			
72.0	64.5	72.2	162	215	-129	-132	0.12	-2506	0.31	0.31	-76	20	0.6			
72.5	62.5	57.0	251	219	-129	-132	0.12	-2506	0.31	0.31	-76	20	0.6			
73.0	64.5	72.2	162	215	-129	-132	0.12	-2506	0.31	0.31	-76	20	0.6			
73.5	62.5	57.0	251	219	-129	-132	0.12	-2506	0.31	0.31	-76	20	0.6			
74.0	64.5	72.2	162	215	-129	-132	0.12	-2506	0.31	0.31	-76	20	0.6			
74.5	62.5	57.0	251	219	-129	-132	0.12	-2506	0.31	0.31	-76	20	0.6			
75.0	64.5	72.2	162	215	-129	-132	0.12	-2506	0.31	0.31	-76	20	0.6			
75.5	62.5	57.0	251	219	-129	-132	0.12	-2506	0.31	0.31	-76	20	0.6			
76.0	64.5	72.2	162	215	-129	-132	0.12	-2506	0.31	0.31	-76	20	0.6			
76.5	62.5	57.0	251	219	-129	-132	0.12	-2506	0.31	0.31	-76	20	0.6			
77.0	64.5	72.2	162	215	-129	-132	0.12	-2506	0.31	0.31	-76	20	0.6			
77.5	62.5	57.0	251	219	-129	-132	0.12	-2506	0.31	0.31	-76	20	0.6			
78.0	64.5	72.2	162	215	-129	-132	0.12	-2506	0.31	0.31	-76	20	0.6			
78.5	62.5	57.0	251	219	-129	-132	0.12	-2506	0.31	0.31	-76	20	0.6			
79.0	64.5	72.2	162	215	-129	-132	0.12	-2506	0.31	0.31	-76	20	0.6			
79.5	62.5	57.0	251	219	-129	-132	0.12	-2506	0.31	0.31	-76	20	0.6			
80.0	64.5	72.2	162	215	-129	-132	0.12	-2506	0.31	0.31	-76	20	0.6			
80.5	62.5	57.0	251	219	-129	-132	0.12	-2506	0.31	0.31	-76	20	0.6			
81.0	64.5	72.2	162	215	-129	-132	0.12	-2506	0.31	0.31	-76	20	0.6			
81.5	62.5	57.0	251	219	-129	-132	0.12	-2506	0.31	0.31	-76	20	0.6			
82.0	64.5	72.2	162	215	-129	-132	0.12	-2506	0.31	0.31	-76	20	0.6			
82.5	62.5	57.0	251	219	-129	-132	0.12	-2506	0.31	0.31	-76	20	0.6			
83.0	64.5	72.2	162	215	-129	-132	0.12	-2506	0.31	0.31	-76	20	0.6			
83.5	62.5	57.0	251	219	-129	-132	0.12	-2506	0.31	0.31	-76	20	0.6			
84.0	64.5	72.2	162	215	-129	-132	0.12	-2506	0.31	0.31	-76	20	0.6			
84.5	62.5	57.0	251	219	-129	-132	0.12	-2506	0.31	0.31	-76	20	0.6			
85.0	64.5	72.2	162	215	-129	-132	0.12	-2506	0.31	0.31	-76	20	0.6			
85.5	62.5	57.0	251	219	-129	-132	0.12	-2506	0.31	0.31	-76	20	0.6			
86.0	64.5	72.2	162	215	-129	-132	0.12	-2506	0.31	0.31	-76	20	0.6			
86.5	62.5	57.0	251	219	-129	-132	0.12	-2506	0.31	0.31	-76	20	0.6			
87.0	64.5	72.2	162	215	-129	-132	0.12	-2506	0.31	0.31	-76	20	0.6			
87.5	62.5	57.0	251	219	-129	-132	0.12	-2506	0.31	0.31	-76	20	0.6			
88.0	64.5	72.2	162	215	-129	-132	0.12	-2506	0.31	0.31	-76	20	0.6			
88.5	62.5	57.0	251	219	-129	-132	0.12	-2506	0.31	0.31	-76	20	0.6			
89.0	64.5	72.2	162	215	-129	-132	0.12	-2506	0.31	0.31	-76	20	0.6			
89.5	62.5	57.0	251	219	-129	-132	0.12	-2506	0.31	0.31	-76	20	0.6			
90.0	64.5	72.2	162	215	-129	-132	0.12	-2506	0.31</							

Table 10 Line for Yerkes

Plate No: 26	Exposition: 1963, F				Date: 1963 Oct., 17				MK Sp:	
	σ_1	c_c	δ_1	d_c	$\log I_A$	$\log I_c$	$\Delta \log I$	$\log I_B$	I_{IV}	I_{V}
Oudeck: 511 fm										
3933	11.0	46.7	933	305	- 380	- 1050	670	275	705	11.5
3956	21.4	11.8	61.6	320	- 611	- 1033	382	677	115	9.5
4033	37.6	15.0	391	318	- 936	- 1033	697	315	115	2.3
4063	28.0	11.6	525	346	- 116	- 923	217	- 033	391	11.5
4077	36.1	39.5	387	371	- 241	- 963	622	- 181	033	12
4102	36.7	36.0	465	369	- 820	- 940	620	- 172	029	1.6
4133	28.6	36.7	511	404	- 720	- 921	711	- 012	252	3.3
4160	34.2	35.4	424	417	- 898	- 907	609	- 156	011	10
4176	23.3	35.6	606	118	- 686	- 907	221	660	657	11.9
4200	32.4	36.0	158	110	- 856	- 911	655	- 026	095	10
4233	21.3	31.0	516	135	- 708	- 884	176	613	368	10
4272	32.1	31.3	462	123	- 813	- 880	037	- 072	68	10
4294	24.0	33.5	592	143	- 705	- 668	163	057	356	20
4305	25.9	33.1	578	143	- 720	- 668	148	018	321	20
4310	22.5	32.9	623	151	- 666	- 858	190	101	450	12.6
4376	25.3	30.5	568	183	- 728	- 825	997	022	211	36
4435	25.1	30.0	566	181	- 731	- 810	687	009	186	28

Table 10 Line Intensity

$\lambda(\text{\AA})$	Photo No: 26		Baseline: 102, F		Dif: 1633 GeV, M		Ext. Syst.	
	Objct: HII Ly α (cont.)	c ₁	c _c	a ₁	a _c	log τ_{I}	log τ_c	log $\tau_{\text{I}, \text{B}}$
Age: 7:								
1661	26.3	30.0	55.1	49.2	-7.7	-8.0	0.6	-0.26
1690	23.2	22.5	61.2	50.0	-6.9	-8.0	10.1	-0.15
1525	20.4	30.5	63.9	66.5	-6.3	-6.18	16.5	0.57
1558	23.1	31.5	61.2	47.0	-6.68	-8.31	11.3	-0.25
1581	23.3	36.0	60.8	41.0	-6.21	-9.03	11.2	-0.2
1616	31.2	32.4	43.4	37.2	-8.72	-9.15	9.9	-0.13
1631	21.5	10.1	53.0	35.9	-7.72	-9.83	19.1	-0.12
1703	13.7	15.4	33.2	31.4	-9.9	-10.20	0.21	-2.69
1731	18.7	12.8	28.2	27.2	-10.62	-11.12	0.69	-2.85
1789	50.5	55.4	26.6	22.9	-10.92	-11.12	0.17	-3.55
1617	51.1	51.7	26.0	21.3	-10.98	-11.75	0.77	-2.97
1634	30.0	63.7	19.1	17.1	-8.10	-12.18	1.26	-0.26
1624	54.0	70.6	21.0	12.3	-11.16	-13.31	2.15	-2.26
5018	52.9	77.7	19.7	8.3	-11.80	-11.20	21.0	-3.50
5041	74.1	79.2	103	97.5	-13.62	-11.50	0.81	-5.27
5053	73.9	80.3	102	97	-13.69	-11.28	0.59	-5.61
5070	77.0	80.3	98.8	95.7	-71.08	-31.28	0.20	-6.95

Table 10 Mean Analysis

Plate No: 28				Emulsion:				Ratio:				Extinction			
Object: PULW (cont.)				c:	Acc. No.			Acc. No.			Extinction	Extinction			
				d:	Acc. No.			Acc. No.			I _B	I _V	Width	A _B	A _V
$\lambda(\text{\AA})$	c _I	c _C	d _I	d _C	log I _I	log I _C	Δlog I	log I _B + Δlog I	log I _V + Δlog I	I _B / I _C	I _V / I _C	(\AA)	A _B	A _V	
5101	76.8	79.7	090	073	-1103	-1155	052	-614	-212	027	070	10	0.3	0.7	
5119	73.9	80.6	102	065	-1370	-1120	120	-568	-115	065	185	18	1.2	3.3	
5168	60.4	79.5	193	073	-1185	-1155	270	-277	109	244	595	22	5.4	13.1	
5227	66.4	76.3	139	079	-1205	-1135	150	-671	025	062	309	20	1.2	6.2	
5270	66.6	78.3	119	079	-1212	-1135	223	-673	111	085	518	32	2.7	16.6	
5316	60.2	74.6	197	101	-1180	-1365	185	-691	083	097	120	20	2.0	8.4	
5362	71.4	73.3	119	105	-1330	-1355	025	-1100	-061	001	019	18	0.1	0.8	
5865	62.3	75.0	179	100	-1208	-1371	163	-	-211	-	191	16	-	3.0	
6129	62.4	72.2	130	116	-1265	-1291	026	-	-613	-	011	17	-	0.2	
6170	60.1	72.3	140	113	-1212	-1300	058	-	-611	-	029	21	-	0.7	
6231	67.1	70.9	115	121	-1237	-1260	013	-	-731	-	019	25	-	0.5	
6130	49.3	59.2	276	203	-1033	-1136	103	-	-991	-	021	11	-	0.2	
6156	55.6	58.3	226	209	-1101	-1126	022	-	-1145	-	001	20	-	0.1	
6516	49.8	60.3	273	195	-1037	-1118	111	-	-1256	-	013	17	-	0.2	
6563	07.0	61.7	1158	186	-310	-1162	052	-	-701	-	172	21	-	3.6	

Table 10 Line Analysis

Plate No: 232				Exposure: 1030-F				Date: 1975 Jun. 1				MC Spc		
Object: R.L.A.W.				a: 05:05:41				sec. x:				B-V:		
				d: 430:22:3				ase. x:						
$\lambda(\text{\AA})$	c_L	c_c	δ_L	a_c	$\log T_L$	$\log T_c$	$\Delta \log I$	$\log T_{cB}$ + $\Delta \log I$	$\log T_{cv}$ + $\Delta \log I$	T_{cB} - T_{cB}	T_{cv} - T_{cv}	Width (\AA)	A_B	A_V
3933	07.7	18.9	2216	700	-250	-340	190	382		1620		17	27.7	
3968	14.8	17.8	807	727	-220	-330	110	029		239		15	3.5	
4033	15.7	16.7	805	779	-221	-252	028	-021		060		30	1.8	
4068	13.4	16.1	855	780	-160	-255	027	053		223		26	5.8	
4102	15.1	16.0	805	781	-229	-256	027	-009		060		20	1.2	
4133	12.8	15.3	868	798	-162	-210	071	039		101		34	5.6	
4160	13.4	14.8	853	808	-175	-231	056	039		129		18	2.3	
4176	11.7	11.4	912	822	-128	-222	094	069		232		25	5.8	
4208	12.6	13.8	883	811	-169	-205	036	014		063		30	2.5	
4233	11.5	13.3	915	853	-110	-200	060	038		111		30	4.2	
4310	11.3	13.0	916	867	-160	-194	034	002		077		26	2.2	
4376	11.6	13.0	911	867	-165	-194	029	-009		063		26	1.8	
4466	12.3	13.0	882	867	-174	-208	034	-031		070		25	1.8	
4490	12.3	13.0	889	867	-175	-213	038	-038		076		16	1.2	
4525	11.4	13.0	919	867	-173	-217	044	-043		086		26	2.3	
4558	11.7	13.5	912	851	-183	-232	049	-070		091		24	2.2	
4584	11.9	11.4	901	822	-193	-260	067	-070		122		34	4.2	

Table 10 Nine Am. Jour.

Table 10 Time Analysis

Plate No: 232	Position:	Date:	MK Sp.:						
			sec E.	sec N.	sec W.	sec S.	sec NE.	sec SW.	
Object: Jupiter (cont.)									
$\lambda(\text{A})$	c_1	c_c	a_1	a_c	$\log I_1$	$\log I_c$	$\Delta \log I$	$\log I_{\text{B}}$	I_{B}
16524	13.0	16.2	6.7	7.0	-23.6	-30.0	0.64	-12.0	104
17020	18.6	19.8	7.1	6.1	-36.3	-25.0	0.27	-23.1	035
17517	27.9	29.6	5.2	3	-55.1	-57.5	0.24	-46.6	021
18013	20.5	32.1	6.6	6.6	-11.8	-12.2	2.15	-21.1	224
18224	26.3	30.7	5.8	3.8	-55.9	-72.0	16.1	-31.6	627
19018	32.1	43.8	37.3	32.7	-7.32	-7.62	0.57	-53.6	036
19101	44.8	49.0	31.9	27.9	-8.01	-8.52	0.51	-62.1	-24.6
21119	47.5	49.8	29.2	27.3	-6.16	-6.60	0.24	-6.91	237
21165	37.0	50.0	39.2	27.1	-6.91	-6.63	1.72	-5.78	003
22227	45.1	50.2	31.1	27.0	-8.05	-8.62	0.57	-7.53	051
22270	43.3	48.7	33.2	28.2	-7.02	-8.16	0.54	-8.06	073
23216	36.5	40.0	40.5	28.7	-6.22	-8.10	0.58	-8.86	017
23262	13.0	16.6	33.7	30.2	-7.74	-8.20	0.16	-10.7	012
23276	50.2	53.3	27.0	21.3	-6.62	-9.12	0.50	-6.95	762
23279	50.1	53.7	27.1	24.2	-8.61	-9.18	0.57	-7.30	021
23276	50.8	51.2	26.2	24.0	-8.60	-9.17	0.37	-13.0	004
23263	08.8	55.3	103.3	23.1	-16.0	-9.32	7.72	-7.40	152

Table 10 Line Intensities

Plate No:	236	Exposition: 103° F		Date: 1932 Jan. 27		IR Sp.	
		Object: R.A. h	Dec: ° 05.4	Object: R.A. h	Dec: ° 30.29.1	Object: sec. z:	R.W. A
		$\lambda(\text{Å})$	c_1	c_c	\hat{a}_1	$\log I_c$	$\log I_{\text{cv}}$
						$\Delta \log I$	$\Delta \log I$
						$\log I_{\text{cv}}$	$\log I_{\text{cv}}$
						$+\Delta \log I$	(A)
						I_{cv}	A_{cv}
						I_{cv}	A_{cv}
3933	17.1	36.3	75.0	105	-1152	-1630	178
				117	-1120	-1512	169
						-032	292
3963	27.6	35.3	53.0	102	-1156	-1482	176
				184	-1156	-1482	026
						-050	051
4033	29.3	30.4	50.2	102	-1165	-1469	177
				196	-1165	-1469	017
						095	219
4068	26.6	29.7	56.6	102	-1170	-1411	178
				105	-1170	-1411	031
						-002	069
4090	27.5	29.1	53.1	102	-1170	-1384	179
				105	-1170	-1384	064
						014	152
4133	23.6	26.7	60.0	105	-1320	-1384	180
				102	-1320	-1384	077
						020	223
4176	20.8	24.2	65.6	102	-1251	-1311	181
				105	-1251	-1311	077
						020	223
4206	23.2	24.3	63.2	105	-1300	-1332	182
				102	-1300	-1332	032
						020	075
4233	23.2	24.2	61.2	102	-1300	-1310	183
				105	-1300	-1310	018
						003	040
4242	23.3	24.1	60.9	102	-1316	-1336	184
				105	-1316	-1336	020
						001	046
							075
4291	21.3	24.1	61.5	102	-1271	-1337	185
				105	-1271	-1337	065
						010	151
4310	19.0	23.8	70.0	105	-1206	-1333	186
				102	-1206	-1333	127
						077	310
4376	21.7	23.3	64.3	105	-1273	-1321	187
				102	-1273	-1321	042
						-007	102
4425	20.7	23.1	66.1	103	-1251	-1306	188
				102	-1251	-1306	057
						016	192
4465	21.3	22.5	64.5	102	-1272	-1301	189
				105	-1272	-1301	029
						-075	051
4490	17.1	22.5	71.2	102	-1153	-1301	190
				105	-1153	-1301	148
						020	302
4558	17.4	22.4	74.0	102	-1161	-1290	191
				105	-1161	-1290	129
						-053	228
							22
							5.0

Table 10 Line Analysis

Plate No: 236				Exposure:				Date:				MK Spec.		
Object: NGC 444 (cont.)				c _I	c _V	R _{CP}	R _V	log I _{cB}	log I _{cV}	T _{cB}	T _{cV}	Width	B-V	
$\lambda(\text{\AA})$	c _I	c _V	d _I	d _c	log I _I	log I _c	Δlog I	log I _{cB} + Δlog I	log I _{cV} + Δlog I	T _{cB}	T _{cV}	(\AA)	A _B	A _V
4524	21.6	23.6	611	600	-1265	-1322	057	-1111	-1111	088		20	1.8	
4616	26.1	28.0	547	521	-1381	-1413	032	-202	-202	041		8	0.1	
4631	23.8	28.8	594	509	-1320	-1427	117	-137	-137	173		14	2.1	
4700	33.0	33.8	1119	138	-1502	-1522	020	-320	-320	022		10	0.2	
4713	33.6	34.8	137	121	-1521	-1533	012	-349	-349	015		10	0.2	
4731	34.5	36.3	128	104	-1528	-1546	118	-362	-362	017		13	0.2	
4827	12.8	14.9	338	312	-1661	-1802	111	-375	-2513	117	003	8	0.9	0.0
4861	34.0	50.2	138	270	-2196	-2756	262	-310	-2562	222	012	30	6.7	0.1
4924	19.8	56.3	273	222	-1719	-1810	091	-563	-1083	052	016	12	0.6	0.2
5018	61.2	64.0	190	165	-1814	-1893	019	-775	-670	018	023	20	0.3	0.5
5070	66.8	69.5	135	130	-1950	-1970	020	-850	-633	006	011	12	0.1	0.1
5101	67.0	69.6	116	129	-1939	-1970	031	-876	-551	009	019	10	0.1	0.2
5119	67.2	69.8	115	127	-1939	-1972	034	-902	-521	009	022	9	0.1	0.2
5227	67.2	70.0	115	126	-1939	-1972	033	-1048	-270	007	039	20	0.1	0.7
5270	61.5	65.8	185	156	-1852	-1872	050	-1087	-108	009	071	22	0.2	1.6
5316	57.4	63.5	216	170	-1787	-1879	092	-1090	-1063	015	161	14	0.2	2.3
5362	60.8	62.2	191	181	-1641	-1861	020	-1188	-1090	003	035	16	0.1	0.6

Table 10 Line Analysis

Table 10. Lep. A. V. data.

Plate No: 240	Position: 1032.8				Position: 1032.82				Position: 1032.82			
	Obj. #:	Obj. h	Obj. m	Obj. s	log T _B	log T _C	Δ log T _B	Δ log T _C	log T _B	log T _C	Δ log T _B	Δ log T _C
3233	07.3	28.3	1151	519	-290	-725	165	179	292	20	-12.5	-
3268	13.5	25.4	150	567	-491	-707	213	206	172	15	6.2	-
4032	20.0	23.4	679	603	-616	-676	069	-020	124	16	2.2	-
4068	17.0	23.6	750	600	-562	-680	110	663	274	16	h.h.	-
4090	17.6	22.6	736	620	-573	-662	069	074	203	16	3.2	-
4133	16.7	20.1	760	676	-558	-612	061	032	110	22	3.1	-
4176	15.6	19.2	721	681	-532	-615	063	065	202	21	h.f.	-
4208	17.8	18.4	722	711	-500	-591	011	-055	026	15	0.4	-
4233	16.8	18.4	752	711	-562	-593	029	002	057	16	1.1	-
4272	16.2	19.0	721	700	-581	-650	019	-011	017	12	0.5	-
4291	17.6	19.0	735	700	-574	-600	026	-012	057	20	1.1	-
4310	15.7	19.0	769	700	-540	-600	069	-004	121	20	2.1	-
4376	16.6	19.1	761	699	-558	-601	013	-016	070	18	1.3	-
4415	16.6	19.2	761	697	-558	-603	015	-001	077	10	0.8	-
4466	15.5	19.3	792	695	-512	-603	061	-051	114	25	2.2	-
4490	14.2	19.5	832	692	-571	-600	062	-001	169	13	2.2	-
4558	16.8	20.1	756	679	-561	-621	060	-031	104	16	1.7	-

Table 20

Plate No.: 210	Panel Side	Defect	Defect Description	Defect Count	Defect Area (cm²)
100% S.A.	Front Side	Defect 1	Scratches	1	0.5

$\chi^2(\text{f})$	C_1	C_2	a_1	a_2	$\log_{10} I$	$\log_{10} I_{\text{ref}}$	$\Delta \log_{10} I$	$\Delta \log_{10} I_{\text{ref}}$	I_{ref}	I_{var}	A_B	A_A
1639	28.1	24.4	723	-582	-693	-692	0.72	0.73	279	37	3.0	2.0
1700	26.3	29.9	550	1941	-721	-751	0.73	0.73	662	20	1.2	0.3
1731	29.4	31.4	500	1770	-759	-780	0.21	0.26	10	10	0.3	0.0
1863	19.0	10.1	700	361	-634	-616	234	232	299	26	7.8	0.7
1924	41.9	16.7	317	282	-873	-911	0.68	0.50	0.33	22	0.7	0.2
2018	15.4	60.3	315	196	-306	-307	111	111	0.61	16	1.0	1.2
2227	58.2	63.8	210	376	-1021	-1012	0.55	0.57	0.73	15	0.4	1.1
2270	55.8	60.5	226	196	-1003	-1003	0.39	0.37	0.76	27	0.3	1.9
2326	51.4	59.5	260	200	-2030	-2030	0.71	0.71	0.22	36	0.3	2.5
2341	66.2	69.2	152	133	-301	-303	0.69	0.63	0.20	20	0.2	1.6
2352	53.1	59.5	216	200	-2030	-2030	0.51	0.51	0.23	36	0.2	1.0
2363	65.7	68.5	128	130	-301	-303	0.69	0.63	0.20	20	0.2	1.6

JOURNAL OF SCIENCE

Table 10 Line Analysis

Plate No: 209			Emulsion: 103a-F				Date: 1964 July 27				MK Spm			
Object: DI Cap			a: 22:55:3 δ: +58:27				sec z:				B-V:			
$\lambda(\text{\AA})$	c_1	c_c	d_1	d_c	$\log I_1$	$\log I_c$	$\Delta \log I$	$\log I_{cB} + \Delta \log I$	$\log I_{cv} + \Delta \log I$	$I_{IB} - I_{cB}$	$I_{IV} - I_{cv}$	Width (\AA)	A_B	A_V
3933	14.8	25.2	805	573	- 874	-1110	236	-053		370		16	6.5	
3968	08.4	21.0	1060	655	- 673	-1020	347	132		755		17	12.5	
4033	14.8	17.3	805	710	- 873	- 933	060	-058		113		15	1.7	
4133	12.8	13.5	870	851	- 819	- 834	015	-024		032		18	0.6	
4233	12.4	13.2	806	865	- 805	- 812	007	-017		015		20	0.3	
4258	12.8	13.2	872	865	- 807	- 812	005	-014		012		13	0.2	
4306	12.4	12.7	886	880	- 800	- 804	004	-016		008		20	0.2	
4340	10.0	12.3	970	868	- 745	- 725	050	027		115		22	2.5	
4376	10.5	12.2	952	900	- 755	- 783	028	000		062		10	0.6	
4415	10.3	11.4	953	917	- 755	- 780	020	-015		013		21	1.0	
4427	10.4	11.3	954	920	- 755	- 788	035	-005		072		18	1.3	
4490	10.6	11.2	950	931	- 757	- 772	015	-011		030		15	0.5	
4515	09.6	11.0	995	935	- 730	- 762	032	-019		107		27	2.9	
4558	09.1	11.0	1019	935	- 716	- 782	066	-013		136		20	2.7	
4634	12.3	13.2	888	865	- 796	- 809	013	-102		024		10	0.2	
4861	16.4	27.5	769	531	- 872	-1048	176	-071	-1569	283	009	25	7.1	0.2
4924	32.6	36.0	455	410	-1127	-1163	036	-286	-964	042	009	20	0.8	0.2

Table 10. Time from T₀

	$A_{T_x} : 0.98$		$A_{T_x} : 0.97$
	$(B-V)_C : 0.94$	$\frac{A_{T_x} + A_{O_x}}{A_{T_x} + A_{O_x}} : 1.290$	
	$T_x : 2.115$		$T_x : 2.119$
No. of lines contributing to B: 30			$A_{T_x} : 1.06$
No. of lines contributing to V: 6			$A_{T_x} : 0.98$
	$A_{O_x} : 1.767$		$A_{O_x} : 2.222$
Object: η Peg			Plate No: 25
Table II Data Summary Sheet for Tauri Object			

Table II Data Summary Sheet for T Tauri Object

Plate No: 28	Object: T Tau
A_{c_V} : 1.242	A_{c_B} : .735
A_{l_V} : .009	No. of lines contributing to V: 9
A_{l_B} : .124	No. of lines contributing to B: 32
A_{c_V}/A_{c_B} : 1.690	$(B-V)_c$: 1.28
$\frac{A_{c_V} + A_{l_V}}{A_{c_B} + A_{l_B}}$: 1.490	$(B-V)_{c_1}$: 1.11
A_{l_V}/A_{c_V} : .040	A_{l_B}/A_{c_B} : .190

Table II Data Summary Sheet for T Tauri Object

Plate No: 232	Object: T Tau
A_{C_V} : 2.187	A_{C_B} : .762
A_{L_V} : .032	No. of lines contributing to V: 8
A_{L_B} : .105	No. of lines contributing to B: 30
A_{C_V}/A_{C_B} : 1.558	$(B-V)_C$: 1.19
$\frac{A_{C_V} + A_{L_V}}{A_{C_B} + A_{L_B}}$: 1.107	$(B-V)_{C_L}$: 1.08
A_{L_V}/A_{C_V} : .028	A_{L_B}/A_{C_B} : .137

Table II Data Summary Sheet for T Tauri Object

Plate No: 236	Object: T Tau
A_{C_V} : 1.025	A_{C_B} : .736
A_{I_V} : .008	No. of lines contributing to V: 7
A_{I_B} : .072	No. of lines contributing to B: 30
A_{C_V}/A_{C_B} : 1.393	$(B-V)_C$: 1.07
$\frac{A_{C_V} + A_{I_V}}{A_{C_B} + A_{I_B}}$: 1.280	$(B-V)_{C_1}$: 0.98
A_{I_V}/A_{C_V} : .003	A_{I_B}/A_{C_B} : .096

Table II Data Summary Sheet for T Tauri Object

Plate No: 237	Object: T Tau
A_{C_V} : 1.637	A_{C_B} : .851
A_{L_V} : .019	No. of lines contributing to V: 5
A_{L_B} : .086	No. of lines contributing to B: 27
A_{C_V}/A_{C_B} : 1.569	$(B-V)_c$: 1.20
$\frac{A_{C_V} + A_{L_V}}{A_{C_B} + A_{L_B}}$: 1.447	$(B-V)_{c_1}$: 1.11
A_{L_V}/A_{C_V} : .014	A_{L_B}/A_{C_B} : .101

Table II Data Summary Sheet for T Tauri Object

Plate No: 240	Object: T Tau
A_{C_V} : .907	A_{C_B} : .796
A_{I_V} : .011	No. of lines contributing to V: 6
A_{I_B} : .064	No. of lines contributing to B: 27
A_{C_V}/A_{C_B} : 1.240	$(B-V)_C$: 0.94
$\frac{A_{C_V} + A_{I_V}}{A_{C_B} + A_{I_B}}$: 1.160	$(B-V)_{C_1}$: 0.87
A_{I_V}/A_{C_V} : .012	A_{I_B}/A_{C_B} : .080

Table II Data Summary Sheet for T Tauri Object

Plate No: 242	Object: T Tau
A_{CV} : 1.158	A_{C_B} : .769
A_{LV} : .034	No. of lines contributing to V: 6
A_{LB} : .067	No. of lines contributing to B: 23
A_{CV}/A_{C_B} : 1.506	$(B-V)_C$: 1.16
$\frac{A_{CV} + A_{LV}}{A_{CB} + A_{LB}}$: 1.393	$(B-V)_{C_1}$: 1.07
A_{LV}/A_{CV} : .029	A_{LB}/A_{CB} : .113

Table II Data Summary Sheet for T Tauri Object

Plate No: 23	Object: RW Aur
A_{c_V} : .765	A_{c_B} : .612
A_{I_V} : .640	No. of lines contributing to V: 15
A_{I_B} : .123	No. of lines contributing to E: 33
A_{c_V}/A_{c_B} : .964	$(B-V)_C$: 0.67
$\frac{A_{c_V} + A_{I_V}}{A_{c_B} + A_{I_B}}$: .879	$(B-V)_{C_1}$: 0.57
A_{I_V}/A_{c_V} : .050	A_{I_B}/A_{c_B} : .152

Table II Data Summary Sheet for T Tauri Object

Plate No: 25	Object: R1 Mar
A_{C_V} : .392	A_{C_B} : .824
A_{L_V} : .040	No. of lines contributing to V: 17
A_{L_B} : .192	No. of lines contributing to B: 56
A_{C_V}/A_{C_B} : .847	$(B-V)_C$: 0.51
$\frac{A_{C_V} + A_{L_V}}{A_{C_B} + A_{L_B}}$: .700	$(B-V)_{C_1}$: 0.36
A_{L_V}/A_{C_V} : .057	A_{L_B}/A_{C_B} : .233

Table II Date Summary Sheet for T Tauri Object

Plate No: 26	Object: RW Aur
A_{C_V} : .625	A_{C_B} : .692
A_{L_V} : .035	No. of lines contributing to V: 19
A_{L_B} : .132	No. of lines contributing to B: 39
A_{C_V}/A_{C_B} : .903	$(B-V)_c$: 0.60
$\frac{A_{C_V} + A_{L_V}}{A_{C_B} + A_{L_B}}$: .801	$(B-V)_{c_1}$: 0.47
A_{L_V}/A_{C_V} : .056	A_{L_B}/A_{C_B} : .192

Table II Data Summary Sheet for T Tauri Object

Plate No: 20	Object: PW Lyr
A_{C_V} : .716	A_{C_B} : .725
A_{L_V} : .069	No. of lines contributing to V: 21
A_{L_B} : .109	No. of lines contributing to B: 41
A_{C_V}/A_{C_B} : .996	$(B-V)_C$: 0.70
$\frac{A_{C_V} + A_{L_V}}{A_{C_B} + A_{L_B}}$: .662	$(B-V)_{C_1}$: 0.55
A_{L_V}/A_{C_V} : .100	A_{L_B}/A_{C_B} : .260

Table II Data Summary Sheet for T Tauri Object

Plate No: 232	Object: π Aur
A_{CV} : .704	A_{CB} : .509
A_{BV} : .032	No. of lines contributing to V: 11
A_{B_B} : .098	No. of lines contributing to B: 30
A_{CV}/A_{CB} : .774	$(B-V)_C$: 0.43
$\frac{A_{CV} + A_{BV}}{A_{CB} + A_{B_B}}$: .731	$(B-V)_{C_L}$: 0.37
A_{BV}/A_{CV} : .016	A_{B_B}/A_{CB} : .108

Table II Data Summary Sheet for T Tauri Object

Plate No: 236	Object: RW Aur
A_{C_V} : .525	A_{C_B} : .766
A_{L_V} : .014	No. of lines contributing to V: 12
A_{L_B} : .072	No. of lines contributing to B: 34
A_{C_V}/A_{C_B} : .685	$(B-V)_C$: 0.30
$\frac{A_{C_V} + A_{L_V}}{A_{C_B} + A_{L_B}}$: .638	$(B-V)_{C_L}$: 0.22
A_{L_V}/A_{C_V} : .027	A_{L_B}/A_{C_B} : .103

Table II Data Summary Sheet for T Tauri Object

Plate No: 240	Object: Zeta Aur
A_{C_V} : .062	A_{C_B} : .056
A_{I_V} : .014	No. of lines contributing to V: 10
A_{I_B} : .074	No. of lines contributing to B: 29
A_{C_V}/A_{C_B} : .773	$(B-V)_C$: 0.43
$\frac{A_{C_V} + A_{I_V}}{A_{C_B} + A_{I_B}}$: .727	$(B-V)_{C_1}$: 0.36
A_{I_V}/A_{C_V} : .021	A_{I_B}/A_{C_B} : .036

Table II Data Summary Sheet for T Tauri Object

Plate No: 200	Object: AS 209
A_{c_V} : .754	A_{c_B} : .807
A_{l_V} : .003	No. of lines contributing to V: 2
A_{l_B} : .054	No. of lines contributing to B: 6
A_{c_V}/A_{c_B} : .934	$(B-V)_c$: 0.63
$\frac{A_{c_V} + A_{l_V}}{A_{c_B} + A_{l_B}}$: .880	$(B-V)_{c_l}$: 0.57
A_{l_V}/A_{c_V} : .004	A_{l_B}/A_{c_B} : .066

Table II Data Summary Sheet for T Tauri Object

Plate No.: 209	Object: DM Cap
A_{C_V} : .657	A_{C_B} : .548
A_{L_V} : .004	No. of lines contributing to V: 3
A_{L_B} : .042	No. of lines contributing to B: 17
A_{C_V}/A_{C_B} : .901	$(B-V)_C$: 0.60
$\frac{A_{C_V} + A_{L_V}}{A_{C_B} + A_{L_B}}$: .669	$(B-V)_{C_1}$: 0.56
A_{L_V}/A_{C_V} : .004	A_{L_B}/A_{C_B} : .044

IV. The Nature of the Emission Lines in T Tauri Spectra

The FeI doublet in the comparison spectrum at $\lambda\lambda$ 3921.3, 3929.1 is barely resolvable on low dispersion plates with the slit set at 0.35 mm; the resolution $\Delta\lambda/\lambda$, at CaII K is approximately .002. Since the T Tauri star emission lines are quite diffuse and numerous, great difficulty will be encountered in attempting to resolve them. However, the identification process has been greatly aided by the author's access to some of Joy's original 1945 plates. The variable dispersion of Joy's widened spectra makes a $(B-V)_c$ analysis, as outlined in the previous chapter, entirely impossible; but, the relative high dispersion ($35\text{\AA}/\text{mm}$ at H γ) in the over-crowded emission region between H β and CaII H and K has been used to great advantage to identify lines and to decide about possible blends of lines. It must be fully understood that the identifications exhibited in the following tables (Tables 12 and 13) are subject to the usual uncertainties due to blending. Misidentifications are admittedly possible even though the best available spectral comparator at the Steward Observatory has been used. The following publications have been employed in the process of identifying T Tauri emission lines:

Allen (1963)

Corliss and Bozman (1962)

Crosswhite (1958)

Merrill (1958)

Moore (1952) (1959)

The lines have been arranged in Table 12 in order of observed wavelength. The data has been delineated in the most comprehensive manner by cross referencing emission features with individual stellar spectra. Thus all spectra (object and plate number) are listed horizontally across the top of the table. The extent of the presence of a given feature in a spectrum is designated by a number in the appropriate space in the table. The numbers are meant to convey, on an arbitrary scale allowing for variable plate quality, the following approximate information regarding the strength of an emission feature:

4 - very strong

3 - strong

2 - moderate

1 - weak

0 - complete absence

More accurate data regarding the relative strength of emission is obtainable from the line analysis tables (Table 10). Table 12 is intended to serve as a brief index of the line spectral variability of T Tauri stars. A large enough statistical sample of FeI and FeII lines exists to warrant separate listing by ion and multiplet number; this has been done in Table 13. Finally Fig's. 5 are partial energy level diagrams showing the observed FeI and FeII transitions. Some of the microdensitometer tracings of the blue regions are reproduced in Fig's. 6 and 7.

Table 12. Estimated Variations in Frequency Distribution $\hat{F}_n(x)$.

λ	$T_{\text{des}}(x)$	$10/23/3$	$1/11/63$	$10/17/63$	$10/57/63$	$1/11/65$	$1/13/65$	$1/10/65$	$1/10/65$
3724	H 3724, 4(3)	0	0	0	0	0	0	0	0
3825	H 3825, 4(2)	0	0	0	0	0	0	0	0
3902	H 3902, 0(2)	0	0	0	0	0	0	0	0
3953	G 3953, 7(1)	1	1	1	1	1	1	1	1
3959	$\left\{ \begin{array}{l} G 3959, 25/48, 7(1) \\ G 25/48, 7(1) \end{array} \right\}$	1	1	1	1	1	1	1	1
4023	$\left\{ \begin{array}{l} H 4023, 1025, 2 \\ H 1023, 8 \end{array} \right\}$	1	1	2	2	1	1	2	1
4059	$\left\{ \begin{array}{l} H 4059, 4(12) \\ P 4059, 7(12) \\ G 4059, 7(12) \end{array} \right\}$	3	3	3	3	3	2	3	3
4060	$\left\{ \begin{array}{l} G 4060, 1077, 7(1) \\ P 4060, 7(1) \end{array} \right\}$	1	0	1	1	0	1	3	2
4102	H 4102, 7(1)	1	1	1	1	1	0	0	1
4133	P 4133, 0(13)	3	3	3	3	3	2	3	2
4160	G 4160, 7(10)	1	0	1	1	2	3^{17}	3^{17}	2
4176	$\left\{ \begin{array}{l} G 4176, 1171, 8(10)^2 \\ G 1171, 8(10)^2 \\ G 1171, 8(10)^2 \end{array} \right\}$	2	3	3	3	3	3	3	3

Table 12. Intensity Variations in Tauri Region Lines (cont.)

L.	Ident.	10/13/63	10/14/63	10/17/63	10/17/63	1/1/65	1/21/65	Joy(1945)
		23	25	26	28	212	235	
		EM Ave	EM Ave	EM Ave	EM Ave	EM Ave	EM Ave	EM Ave
4206	{ FeI 4202.0(42) }	2	2	2	2	2	1	2
	{ SrII 4215.1(1) }							
4233	{ CaI 4226.7(2) }	2	3	3	3	2	1	3
	{ FeII 4233.2(27) }							
	FeII 4258.2(28) ¹⁹	0	0	0	0	0	0	1
4272	{ CrI 4271.8(1) }	3	3	2	2	0	1	2
	{ FeI 4271.8 }							
4294	{ FeI 4228.4(71) }	3	3 ⁶	3	3	0	2 ⁶	1
	{ CrI 4289.7 (1) ³ }							
4306	{ FeII 4303.2(27) }	2	3	3	3	0	2	2
	{ FeI 4307.9(42) }							
	TiIII 4301.9(41)							
4340	H 4340.5(1)	3	3	3	4	2	3	4
4351	FeII 4351.8(27)	0	0	0	0	0	0	0
4376	FeI 4375.9(2)	2 ⁸	2 ⁸	2	2	0	2 ⁸	2

Table 12. Determining weight sum in π^0 decay by iteration (cont.).

λ	Euler_∞	$10/3/63$	$10/11/63$	$10/17/63$	$10/23/63$	$10/29/63$	$10/35/63$
4390	$\{\text{PCT } h_{332}, 6(19)\}$ $\{\text{PCT } h_{333}, 6(21)\}$ $\{\text{PCT } h_{355}, 6(27)\}$	2 2	2 2	2 2	0 0	2 2	2 2
4415	$\{\text{PCT } h_{355}, 6(11)^2\}$ $\{\text{PCT } h_{375}, 6(27)\}$	3 3	3 3	2 2	0 0	2 2	2 2
4427	$\{\text{PCT } h_{427}, 3(9)\}$	0 0	0 0	0 0	0 0	0 0	0 0
4453	$\{\text{PCT } h_{453}, 7(9)\}$ $\{\text{PCT } h_{455}, 7(9)\}$ $\{\text{PCT } h_{465}, 7(9)\}$ $\{\text{PCT } h_{471}, 5(11)\}$	3 3	0 0	0 0	0 0	0 0	0 0
4480	$\{\text{PCT } h_{482}, 2(2)\}$ $\{\text{PCT } h_{494}, 6(9)\}$ $\{\text{PCT } h_{499}, 2(37)\}$ $\{\text{PCT } h_{514}, 2(37)\}$	2 2	3 3	3 3	3 3	3 3	3 3
4515	$\{\text{PCT } h_{515}, 3(38)\}$ $\{\text{PCT } h_{515}, 3(37)\}$ $\{\text{PCT } h_{520}, 2(37)\}$ $\{\text{PCT } h_{522}, 5(38)\}$?	4 4	3 3	2 2	0 0	0 0
4552	$\{\text{PCT } h_{512}, 5(38)\}$ $\{\text{PCT } h_{515}, 9(37)\}$ $\{\text{PCT } h_{563}, 2(50)\}$ $\{\text{PCT } h_{564}, 7(11)\}$	2 2	4 4	3 3	3 3	2 2	2 2

Table Ic. Intensity Variations in T-Tauri Radiation Lines (cont.)

<u>λ</u>	<u>Ident.</u>	<u>10/13/63 23</u>	<u>10/14/63 25</u>	<u>10/17/63 26</u>	<u>10/17/63 27</u>	<u>3/1/65 232</u>	<u>3/27/65 235</u>	<u>4/20/65 240</u>	<u>Dec. (1965)</u>
<u>R.I.</u>	<u>R.I. Apr.</u>	<u>R.I. Apr.</u>	<u>R.I. Apr.</u>	<u>R.I. Apr.</u>	<u>R.I. Apr.</u>	<u>R.I. Apr.</u>	<u>R.I. Apr.</u>	<u>R.I. Apr.</u>	<u>R.I. Apr.</u>
4594	FeII 4583.9(38) ¹²	0	2	3	3	3	2	0	3
4616	CrII 4618.8(44)	3	3	2	2	0	-	0	3
4635	{FeII 4622.2(37) ¹² CrII 4634.2(41)}	3	2	3	3	3	3	3	2
4703	FeII 4702.4(7)	1	2	1	1	2	1	2	0
4713	FeII 4713.2(26)	0	0	0	0	0	1	2	0
4731	FeI 4731.8(67)	1	1	2	1	0	1	2	1
4792	TiII 4791.8(29)	0	1	1	2	0	0	2	0
4817	TiII 4821.0(29)	1	2	2	2	1	2	2	0
4861	H 4861.3(1)	4	4	4	4	4	4	4	4
4924	FeII 4923.9(42)	2	2	3	3	3	3	3	4

Table 12 Intensity Variations in T Tauri Emission Lines (cont.)

λ	Ident.	10/13/63	10/14/63	10/17/63	10/17/63	1/1/65	1/27/65	1/29/65	Joy(1945)
		23 RJ Aur	25 EJ Aur	26 EJ Aur	28 RW Aur	232 RW Aur	236 EJ Aur	240 EW Aur	
5018	{FeII 5018.4(42)}	2	3	3	3	2	2	3	4
	{FeI 5012.1(16)}								
5041	{FeI 5041.8(36)}	0	1	1	1	0	0	0	0
	{FeII 5036.9(36)}								
5053	FeI 5051.6(16)	0	0	1	2	0	0	0	0
5070	CrI 5068.2(20)	0	0	1	1	0	1	0	0
5101	FeII 5100.7(35)	1	1	1	1	1	2	0	0
5119	FeII 5120.3(35)	0	1	0	1	1	2	1	0
5168	FeII 5169.0(42)	0	2	2	3	3	0	0	0
5227	FeII 5234.6(49)	1	2	2	3	2	2	2	2
5270	{FeII 5264.8(48)} ¹¹	1	2	2	2	2	2	2	2
	{FeII 5275.0(49)}								
5316	{FeII 5316.5(48)} ¹²	2	2	3	3	3	2	2	2
	{FeII 5316.8 (48)} ¹³								
5362	FeII 5362.2(48)	1	0	2	1	2	1	2	0
5810	FeII 5811.9(24)	0	0	0	0	0	0	0	0

Table 12 Intensity Variations in T Tauri Emission Lines (cont.)

<u>λ</u>	Ident.	10/13/63	10/14/63	10/17/63	10/17/63	1/1/65	1/27/65	1/29/65	Joy(1945)
		23 R ⁺ Aur	25 R ⁺ Aur	26 R ⁺ Aur	28 R ⁺ Aur	232 R ⁺ Aur	236 R ⁺ Aur	240 R ⁺ Aur	
5866	{FeII 5864.5(24)} {HeI 5875.6(11)}	1	2	1	2	0	0	0	1
6129	FeII 6129.7(46)	1	1	1	1	0	0	0	0
6150	FeII 6150.1(46)	1	0	0	0	0	0	0	0
6178	FeII 6178.1(46)	0	1	1	1	1	0	0	0
6234	{FeII 6222.3(34)} {FeII 6239.4(34)}	1	0	2	1	1	1	1	0
6430	FeII 6432.6(40)	2	2	0	3	0	2	0	0
6456	FeII 6456.4(74)	0	2	2	2	0	0	0	0
6516	FeII 6516.1(40)	2	2	2	3	2	0	0	0
6563	H 6562.8(1)	4	4	4	4	4	4	4	4
6724		0	0	0	0	0	0	0	0

Table 12 Intensity Variations in T Tauri Emission Lines (cont.)

<u>λ</u>	<u>Ident.</u>	10/14/63	10/17/63	1/1/65	1/27/65	1/28/65	1/29/65	Joy(1945)	2/19/65
		25 T Tau	28 T Tau	232 T Tau	236 T Tau	237 T Tau	240 T Tau		
3734	H 3734.4(3)	0	0	0	3	3	3	0	3
3836	H 3835.4(2)	0	0	0	3	0	2	0	3
3889	H 3889.0(2)	0	0	0	3	3	3	2	0
3933	CaII 3933.7(1)	h	h	4	h	h	h	4	h
3962	{CaII 3962.5(1) H 3970.1(1)}	h	h	h	h	1	h	h	h
4033	{HeI 4026.2 KnI 4030.8}	2	2	2	2 ¹⁸	2 ¹⁵	2 ¹⁸	0	2
4069	{FeI 4063.6(19) FeI 4071.7(13) [CII] 4069.6(1F)}	3	2	3	3	3	3	2	2
4090	{SrII 4077.7(1) [CII] 4076.2(1F)}	2	2	1	3	3	0	0	0
4102 ¹	H 4101.7(1)	3	3	1	3	3	3	4	0
4133	FeI 4132.0(13)	2	2	1	2	2	2	2	2
4140	TaIII 4143.7(105)	2	2	1	2	3	2	1	2
4176	{TaIII 4171.9 (105) ² FeII 4173.5(27) FeII 4178.9(29)}	0	0	0	0	0	0	2	2

Table 12 Intensity Variations in T Tauri Emission Lines (cont.)

λ	Ident.	10/14/63 25	10/17/63 28	1/1/65 232	1/27/65 236	1/28/65 237	1/29/65 240	Jcy(1965) T Tau	2/12/65 242
		T Tau	T Tau	T Tau	T Tau	T Tau	T Tau	T Tau	T Tau
4208	{FeI 4202.0(42) SrII 4215.5(1)}	2	2	0	0	0	0	0	2
4233	{CaI 4226.7(2) FeII 4233.2(27)}	3	3	2	2	2	2	3	2
	FeII 4253.2 ¹⁹ 28)	3	3	3	2	2	3	1	0
4272	{CrI 4271.3(1) FeI 4271.3(42)}	3	3	3	2	0	2	2	0
4294	{FeI 4282.4(7) CrI 4282.7 (1) TiIII 4294.1(20)}	3	3	3	2	2	2	1	2
4306	{FeII 4303.2(27) FeI 4307.9(42) TiIII 4301.2(41)}	3	3	3	2	3	2	2	0
4340	H 4340.5(1)	4	4	4	4	4	4	4	4
4351	FeII 4351.8(27)			0	0	0	0	1	0
4376	{FeI 4375.2(2) FeI 4383.5}	2	2	2	0	0	0	2	2
4390	{TiII 4395.0(19) FeI 4383.6(41) FeII 4385.4(27)}	2	2	2	0	0	0	2	0

Table 12 Intensity Variations in T Tauri Emission Lines (cont.)

λ	Ident.	10/14/63 25 T Tau	10/17/63 28 T Tau	1/1/65 232 T Tau	1/27/65 236 T Tau	1/28/65 237 T Tau	1/29/65 240 T Tau	Joy(1945) T Tau	2/19/65 242 T Tau
4415	{FeI 4415.1 (17) ⁹ } {FeII 4416.8 (27)}	2	3	3 ¹⁰	3	2	2	1	2
4427	FeI 4427.3 (2)	2	3	3	3	2	1	1	0
4466	{FeI 4461.7 (?) ₁₁ } {FeI 4465.6 (?) ₁₁ } {TiIII 4469.5 (31)} {HeI 4471.5 (1h)}	0	1	2	0	0	0	1	2
4490	{FeI 4492.2 (2)} {FeI 4494.6 (6 ^o)} {FeII 4489.2 (37)} {FeII 4491.4 (37)}	3	3	3	3	3	1	2	2
4515	{FeII 4508.3 (38)} {FeII 4515.3 (37)} {FeII 4520.2 (37)} {FeII 4522.6 (38)}	3	3	3	3	3	2	2	2
4558	{FeII 4549.5 (38)} {FeII 4555.9 (37)} {TiIII 4563.8 (50)} {CrII 4558.7 (14)}	2	2	2	2	3	2	1	0
4584	FeII 4583.9 (38) ¹²	3	2	0	2	3	0	3	2
4626	CrII 4618.8 (14)	3	2	1	2	3	2	3	0
4634	{FeII 4629.3 (37) ¹² } {CrII 4634.1 (14)}	2	2	1	2	3	2	2	2

Table 12 Intensity Variations in T Tauri Emission Lines (cont.)

λ	Ident.	10/11/63	10/17/63	1/1/65	1/27/65	1/28/65	1/29/65	Avg(1945)	2/19/65
		25 T Tau	28 T Tau	232 T Tau	236 T Tau	237 T Tau	240 T Tau		
4700	FeI 4700.4(67)	0	1	2	0	0	0	0	0
4713	FeII 4713.2(26)	2	1	2	0	0	0	1	0
4731	FeI 4731.8(67)	2	1	0	0	0	0	0	0
4789	TiIII 4794.8(29)	0	0	0	0	0	0	0	0
4817	TiIII 4821.0(29)	0	0	0	0	0	0	0	?
4861	H 4861.3(1)	4	4	4	4	4	4	3	1
4924	FeII 4923.9(12)	0	0	0	3	0	0	3	1
5018	{FeII 5018.4(12)}	0	0	0	0	0	0	3	0
	{FeI 5012.1(16)}								
5041	{FeI 5041.8(36)}	0	0	0	0	0	0	0	0
	{FeII 5036.9(36)}								
5053	FeI 5051.6(16)	0	0	0	0	0	0	0	0
5070	CrI 5068.2(20)	0	0	0	0	0	0	0	0
5101	FeII 5100.7(35)	0	0	0	0	0	0	0	0
5119	FeII 5120.3(35)	0	0	0	0	0	0	0	0
5168	FeII 5169.6(12)	0	0	0	0	0	0	0	0
5227	FeII 5234.6(12)	0	0	0	2	0	1	0	0

Table 12 Intensity Variations in T Tauri Emission Lines (cont.)

<u>λ</u>	<u>Ident.</u>	10/14/63 25 T Tau	10/17/63 28 T Tau	1/1/65 232 T Tau	1/27/65 236 T Tau	1/28/65 237 T Tau	1/29/65 240 T Tau	Joy(1945) T Tau	2/19/65 242 T Tau
5270	{FeII 5264.9(48) ¹⁴ FeII 5276.0(49)}	2	1	2	2	2	1	0	0
5316	{FeII 5316.6(49) ₁₅ FeII 5316.8(48) ₁₅ }	0	0	0	0	0	0	3	3
5362	FeII 5362.9(46)	0	0	0	0	0	0	0	0
5810	FeII 5811.6(24)	3	2	0	1	2	2	0	0
5865	{HeI 5870.5(24) HeI 5875.6(11)}	0	0	0	0	0	0	0	0
6129	FeII 6129.7(46)	0	0	0	0	0	0	0	0
6150	FeII 6150.1(46)	0	0	0	0	0	0	0	0
6178	FeII 6178.1(46)	0	0	0	0	0	0	0	0
6234	{FeII 6229.3(34) FeII 6239.4(34)}	3	3	3	4	4	4	0	4
6430	FeII 6432.6(46)	0	2	0	0	0	0	0	0
6456	FeII 6456.4(74)	0	2	2	0	0	0	0	0
6516	FeII 6516.1(49)	0	2	1	0	0	0	0	0
6563	H 6562.8(1)	4	1	1	1	1	1	4	4
6724		0	0	0	2	3	2	2	2

Table 12 Intensity Variations in T Tauri Emission Lines (cont.)

<u>λ</u>	<u>Ident.</u>	<u>6/27/64 209 DI CEF</u>	<u>6/17/64 199 AS205</u>	<u>6/18/64 200 AS209</u>
3734	H 3734.4(3)	0	0	0
3836	H 3835.4(2)	0	0	0
3889	H 3889.0(2)	0	0	0
3933	CaII 3933.7(1)	4	2	3
3968	{ CaII 3968.5(1) H 3970.1(1) }	4	2	3
4033	{ HeI 4026.2 MnI 4030.8 }	2	0	2
4063	{ FeI 4063.6(19) FeI 4071.7(13) [SII] 4063.6(1F) }	0	0	0
4080	{ SrII 4077.7(1) SII 4076.2(1F) }	0	0	0
4102 ¹	H 4101.7(1)	0	0	0
4133	FeI 4132.0(13)	1	0	3
4160	TiII 4163.7(105)	0	0	0

Table 12 Intensity Variations in T Tauri Emission Lines (cont.)

<u>λ</u>	<u>Ident.</u>	<u>6/27/64</u>	<u>6/17/64</u>	<u>6/18/64</u>
		<u>209</u> <u>DI Cep</u>	<u>199</u> <u>AS205</u>	<u>200</u> <u>AS209</u>
4176	{ TiIII 4171.9(105) ² FeII 4173.5(27) FeII 4178.9(28) }	0	0	.0
4208	{ FeI 4202.0(42) SrII 4215.5(1) }	0	0	0
4233	{ CaI 4226.7(2) FeII 4233.2(27) }	1	0	0
	FeII 4259.2(28) ¹⁹	0	0	0
4272	{ CrI 4274.8(1) FeI 4271.8(42) }	1	0	0
4294	{ FeI 4282.4(71) CrI 4289.7 (1) ³ TiIII 4294.1(20) }	0	0	0
4306	{ FeII 4303.2(27) FeI 4307.9(42) TiIII 4301.9(41) }	0	0	0
4340	H 4340.5(1)	2	0	3
4351	FeII 4351.8(27)	0	0	0
4376	{ FeI 4375.9(2) FeI 4383.5 }	2	0	0

Table 12 Intensity Variations in T Tauri Emission Lines (cont.)

<u>λ</u>	<u>Ident.</u>	<u>6/27/61; 209</u> <u>DI Cep</u>	<u>6/17/61; 199</u> <u>AS 205</u>	<u>6/18/61; 200</u> <u>AS 209</u>
4390	{TiII 4395.0(12) FeI 4383.6(h1) FeII 4385.4(27)}	0	0	0
4415	{FeI 4415.9(h1) ⁹ FeII 4416.8(27)}	2	0	0
4427	FeI 4427.3(3)	2	0	0
4466	{FeI 4461.7(2) FeI 4466.6(2) ¹¹ TiII 4469.5(27) FeI 4471.5(14)}	1	0	0
4490	{FeI 4482.2(2) FeI 4491.6(63) FeII 4489.2(37) FeII 4491.1(37)}	1	0	0
4515	{FeII 4503.3(38) FeII 4515.3(37) FeII 4520.2(37) FeII 4522.6(38)}	2	0	0
4558	{FeII 4542.5(38) FeII 4555.9(37) TiII 4553.8(50) Ceti 4552.7(h4)}	2	0	0

Table 1.2 Intensity Variations in T Tauri Emission Lines (cont.)

<u>λ</u>	<u>Ident.</u>	<u>6/27/64 200 DI Cep</u>	<u>6/17/64 199 AS 205</u>	<u>6/18/64 200 AS 202</u>
4584	FeII 4583.9(38) ^{1,2}	0	0	0
4616	CrII 4619.8(44)	0	0	0
4634	{FeII 4629.3(37) ^{1,2} CrII 4634.1(44)}	2	0	0
4700	FeI 4700.1(67)	0	0	0
4713	FeII 4713.2(26)	0	0	0
4731	FeI 4731.8(67)	0	0	0
4789	TiIII 4794.8(29)	0	0	0
4817	TiIII 4821.0(29)	0	0	0
4861	H 4861.3(1)	4	2	3
4924	FeII 4923.9(42)	2	0	0

Table 12 Intensity Variations in T Tauri Emission Lines (cont.)

<u>λ</u>	<u>Ident.</u>	<u>6/27/64 209 DI Cen</u>	<u>6/17/64 199 AS 205</u>	<u>6/18/64 200 AS 209</u>
5018	{ FeII 5012.4(42) FeI 5012.1(16) }	0	0	0
5041	{ FeI 5041.8(36) FeII 5036.9(36) }	0	0	0
5053	FeI 5051.6(16)	0	0	0
5070	CRI 5068.2(20)	0	0	0
5101	FeII 5100.7(35)	0	0	0
5119	FeII 5120.3(35)	0	0	0
5169	FeII 5169.0(42)	0	0	0
5227	FeII 5234.6(49)	0	0	0
5270	{ FeII 5244.8(48) ¹⁴ FeII 5276.8(49) }	0	0	0
5316	{ FeII 5316.6(49) ₁₅ FeII 5316.8(43) ¹⁵ }	0	0	0
5362	FeII 5362.9(43)	0	0	0
5810	FeII 5811.9(24)	0	0	0

Table 12 Intensity Variations in T Tauri Emission Lines (cont.)

<u>λ</u>	<u>Ident.</u>	6/27/64	6/17/64	6/13/64
		209 DI Cep	199 AS 205	200 AS 209
5866	{FeII 5864.5(24) HeI 5875.6(11)}	0	0	0
6129	FeII 6129.7(46)	0	0	0
6150	FeII 6150.1(46)	0	0	0
6178	FeII 6178.1(46)	0	0	0
6234	{FeII 6229.3(31) FeII 6232.4(34)}	0	0	0
6430	FeII 6432.6(10)	0	0	0
6456	FeII 6456.4(74)	0	0	0
6563	H 6562.8(1)	4	2	4
6724		0	0	0

Supplementary Notes to Table 12

1. Blended with an unidentified feature on plates 25 and 28 of T Tau.
2. $\lambda 4171.9$ is absent in Joy's spectra of these objects but has been found in other T Tau stars. $\lambda 4173.5$ is strong in RW Aur, moderate in T Tau.
3. FeI strong in both; CrI moderate in RW Aur, absent in T Tau (Joy (1945)).
4. $\lambda 4427.3$ absent in Joy's spectra of T Tau but present in RW Aur.
5. CrI present in RW Aur only in Joy's spectra.
6. Blended with $\lambda 4306$.
7. TiII moderate in RW Aur but absent in T Tau (Joy (1945)).
8. Blended with $\lambda 4390$.
9. FeI absent in Joy's 1945 spectra of T Tau.
10. Blended with $\lambda 4427$.
11. $\lambda 4466$ absent in Joy's 1945 spectra.
12. FeII is dominant in Joy's spectra.
13. Absent in Joy's spectra of RW Aur.
14. $\lambda 5264.8$ absent in Joy's 1945 spectra of T Tau and RW Aur.
15. $\lambda 5316.8$ absent in Joy's 1945 spectra of T Tau and RW Aur.
16. $\lambda 5875.6$ weak in Joy's 1945 spectra of RW Aur.
17. Blended with $\lambda 4176$.
18. Appears as two distinct features.
19. CrI 4254.3(1) should be strongest line in its multiplet but has not been observed in any of the program stars by either Joy or the author.

General Note:

Those lines which have been found to occur in T Tauri spectra but which were not identified by the author are listed below. It should be pointed out that low dispersion though advantageous for some purposes necessarily implies greater difficulty in the line identification problem.

TIII	4300.1 (41)	FeI	4250.8 (42)
"	4321.0 (41)	"	4325.8 (42)
"	4330.7 (41)	"	4404.8 (41)
"	4399.8 (51)	"	4435.2 (2)
"	4407.7 (51)	"	4528.6 (68)
"	4443.8 (19)	FeII	4122.6 (28)
"	4450.5 (19)	"	4666.8 (37)
"	4501.3 (31)	"	4541.5 (38)
"	4572.0 (82)	"	4576.3 (38)
CrI	4254.3 (1)	"	4620.5 (38)
CrII	4824.1 (30)	"	5197.6 (49)

Table 13a FeI Emission Lines Present in T Tauri Stars

(By Ion and Multiplet)

Laboratory Wavelength ^a	Mult.No.	Transition	EPVolts	Lab.Int.	Solar Chromos.	T Tau
4375.9	2	5 _{D₄} -7 _{F₅}	0.00-2.82	9		2
4427.3		5 _{D₃} -7 _{F₄}	0.05-2.84	10		0
4461.6		5 _{D₂} -7 _{F₃}	0.09-2.85	8	2	
4466.6		5 _{D₁} -7 _{F₃}	0.11-2.87	-		2
5012.1	16	5 _{F₅} -5 _{F₅}	0.86-3.32	12		3
5051.6		5 _{F₄} -5 _{F₄}	0.91-3.35	10		4
5041.3	36	3 _{F₄} -3 _{F₃}	1.48-3.93	10		1
4383.5	41	3 _{F₄} -5 _{G₅}	1.48-4.29	45	1	2
4415.1		3 _{F₂} -5 _{G₃}	1.60-4.40	20		3
4202.0	42	3 _{F₄} -3 _{G₄}	1.48-4.42	30	2	2
4271.6		3 _{F₄} -3 _{G₅}	1.48-4.37	35	2	3
4307.9		3 _{F₃} -3 _{G₄}	1.55-4.42	35		2
4063.6	43	3 _{F₃} -3 _{F₃}	1.55-4.59	45	3	3
4071.7		3 _{F₂} -3 _{F₂}	1.60-4.63	40	2	3
4132.0		3 _{F₂} -3 _{F₃}	1.60-4.59	25		2
4700.4	67	5 _{P₂} -3 _{D₁}	2.19-4.81			1
4731.8		5 _{F₃} -3 _{D₂}	2.17-4.77			1

Table 13a FeI Emission Lines Present in T Tauri Stars
 (By Ion and Multiplet)

<u>Laboratory Wavelength^o</u>	<u>Labt. No.</u>	<u>Transition</u>	<u>EPVolts</u>	<u>Lab. Int.</u>	<u>Solar Chromos.</u>	<u>T Tau</u>
4482.3	68	$5_{P_1} - 5_{D_2^o}$	2.21-4.97	6		3}
4494.5		$5_{P_2} - 5_{D_3^o}$	2.19-4.93	12		3}

Table 13b FeII Emission Lines Present in T-Tauri Stars
(By Ion and Multiplet)

Laboratory Wavelength ^a	Mult.No.	Transition	E[Volts]	Lab.Int.	Solar Chromos.	T Tau
5311.9	24	$4P_{3/2} - 6D_{3/2}^0$	2.69-4.82	-		0
5364.5		$4P_{3/2} - 6D_{5/2}^0$	2.69-4.80	-		1
4713.2	26	$4P_{1/2} - 6P_{3/2}^0$	2.77-5.39			0
4173.5	27	$4P_{5/2} - 4D_{5/2}^0$	2.57-5.53	3		1
4233.2		$4P_{5/2} - 4D_{7/2}^0$	2.57-5.49	11	3	2
4351.8		$4D_{3/2} - 4D_{5/2}^0$	2.69-5.53	9	1	0
4416.3		$4P_{1/2} - 4D_{3/2}^0$	2.77-5.56	7		3
4303.2		$4P_{3/2} - 4D_{3/2}^0$	2.69-5.56	8		3
4385.4		$4P_{1/2} - 4D_{1/2}^0$	2.77-5.58	7		2
4178.9	28	$4P_{5/2} - 4F_{7/2}^0$	2.60-5.50	10		2
4259.2		$4P_{3/2} - 4F_{3/2}^0$	2.69-5.59	3		1
6229.3	34	$4P_{7/2} - 6D_{5/2}^0$	2.82-4.80	-		1
6239.4		$4P_{9/2} - 6D_{7/2}^0$	2.79-4.77	-		1
5100.7	35	$4P_{9/2} - 6F_{7/2}^0$	2.79-5.21			1
5120.3		$4P_{7/2} - 6F_{5/2}^0$	2.82-5.23			1
5036.9	36	$4P_{7/2} - 6P_{7/2}^0$	2.82-5.27	2		1

Table 13b FeII Emission Lines Present in T Tauri Stars

(By Ion and Multiplet)

Laboratory Wavelength ^a	Mult.No.	Transition	EPVolts	Lab.Int.	Solar Chromos.	T Tau
4489.2	37	$4_F_{7/2} - 4_F^o_{5/2}$	2.82-5.57	4		2 }
4491.4		$4_F_{3/2} - 4_F^o_{3/2}$	2.84-5.59	5		2 }
4515.3		$4_F_{5/2} - 4_F^o_{5/2}$	2.83-5.57	7	3	3 }
4520.2		$4_F_{9/2} - 4_F^o_{7/2}$	2.79-5.52	7	1	3 }
4555.9		$4_F_{7/2} - 4_F^o_{7/2}$	2.82-5.52	8	1	2
4629.3		$4_F_{9/2} - 4_F^o_{9/2}$	2.79-5.46	7	1	2
4508.3	38	$4_F_{3/2} - 4_D^o_{1/2}$	2.84-5.58	8	1	3 }
4522.6		$4_F_{5/2} - 4_D^o_{3/2}$	2.83-5.56	9	1	3 }
4549.6		$4_F_{7/2} - 4_D^o_{5/2}$	2.82-5.53	10	2	2
4583.9		$4_F_{9/2} - 4_D^o_{7/2}$	2.79-5.49	11	2	2
6432.6	40	$6_S_{5/2} - 6_D^o_{5/2}$	2.88-4.80	8		0
6516.1		$6_S_{5/2} - 6_D^o_{7/2}$	2.88-4.77	20		1
4923.9	42	$6_S_{5/2} - 6_P^o_{3/2}$	2.88-5.39	12		2
5018.4		$6_S_{5/2} - 6_P^o_{5/2}$	2.88-5.34	12	3	1
5169.0		$6_S_{5/2} - 6_P^o_{7/2}$	2.88-5.27	12	3	0
4731.4	43	$6_S_{5/2} - 4_D^o_{7/2}$	2.88-5.49	3		1

Table 13b FeII Emission Lines Present in T Tauri Stars
(By Ion and Multiplet)

Laboratory Wavelength ^Å	Mult.No.	Transition	EPVolts	Lab.Int.	Solar Chromos.	T Tau
6129.7	46	$4G_{9/2} - 4F_{7/2}^o$	3.19-5.20	-		0
6150.1		$4G_{7/2} - 4F_{7/2}^o$	3.21-5.21	-		0
6178.1		$4G_{5/2} - 4F_{7/2}^o$	3.22-5.21			0
5254.8	48	$4G_{5/2} - 4D_{3/2}^o$	3.22-5.56	2		2
5316.8		$4G_{7/2} - 4D_{5/2}^o$	3.21-5.53	4		1
5362.9		$4G_{9/2} - 4D_{7/2}^o$	3.19-5.49	5		0
5234.6	49	$4G_{7/2} - 4F_{5/2}^o$	3.21-5.57	7	2	1
5276.0		$4G_{9/2} - 4F_{7/2}^o$	3.19-5.52	7		1
5316.6		$4G_{11/2} - 4F_{9/2}^o$	3.14-5.46	8		1
6456.4	74	$4D_{7/2} - 4P_{5/2}^o$	3.89-5.80	200		1

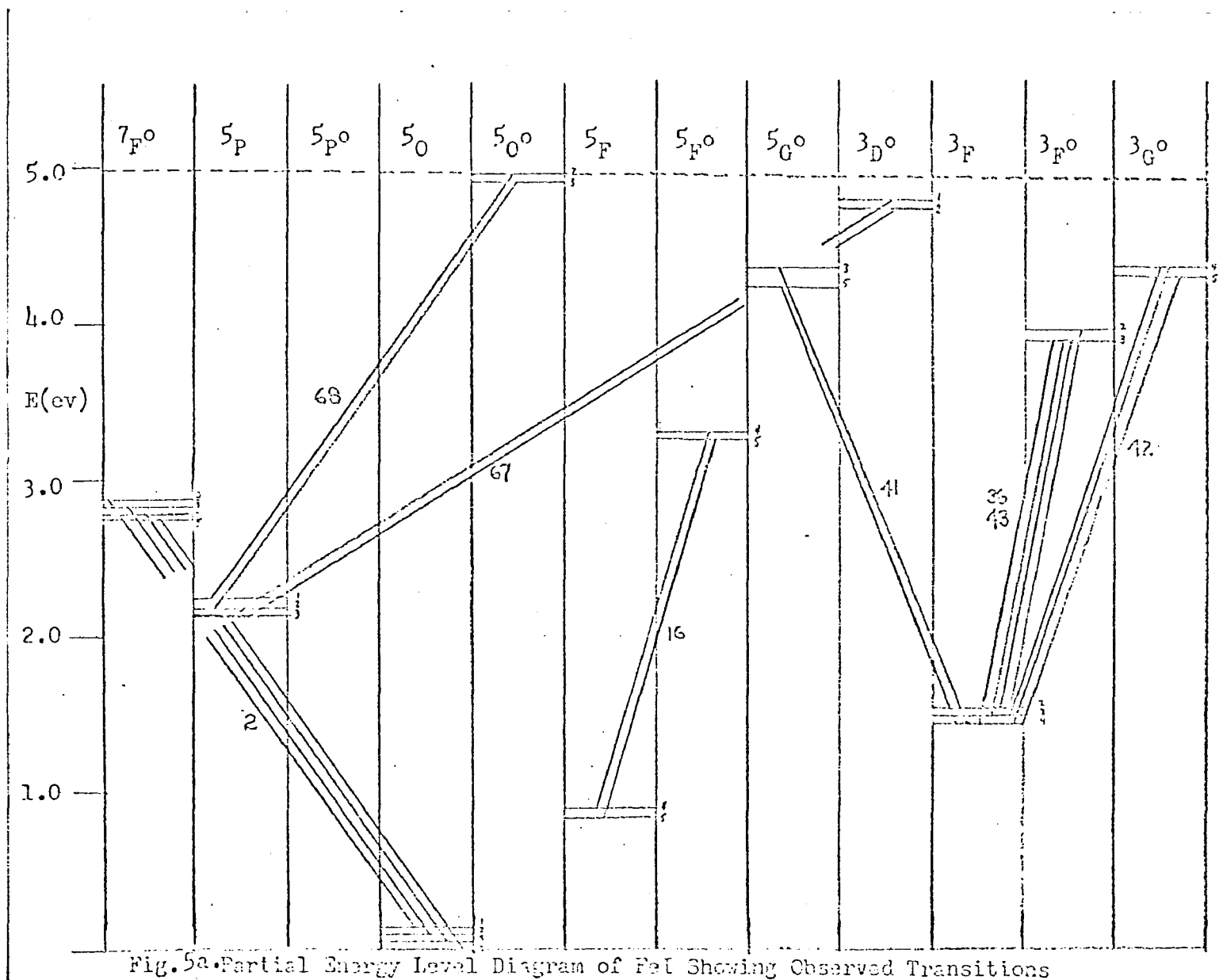


Fig. 5a. Partial Energy Level Diagram of FeI Showing Observed Transitions

Fig. 5b. Partial Energy Level Diagram of Bell Shoring Observed Transitions

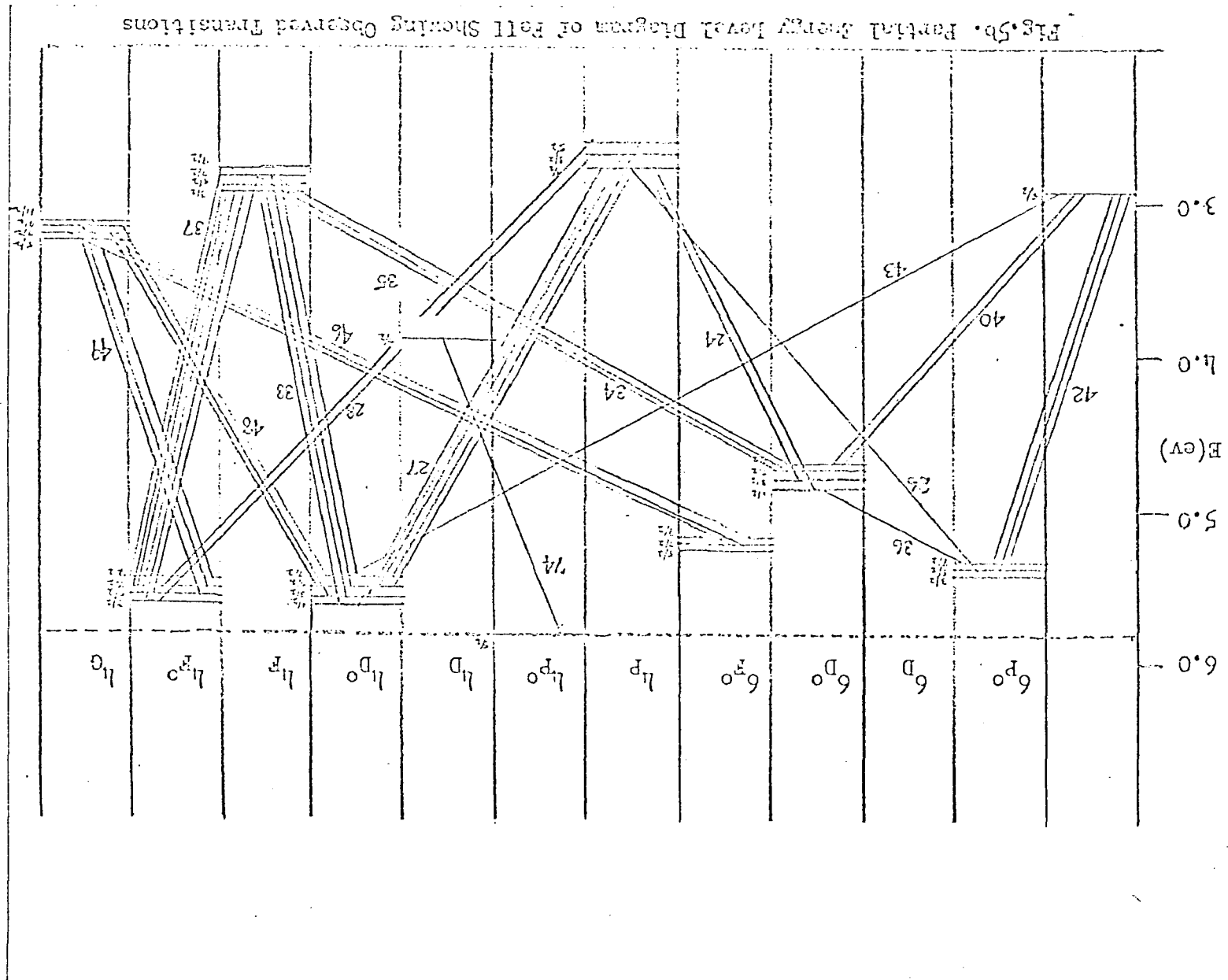
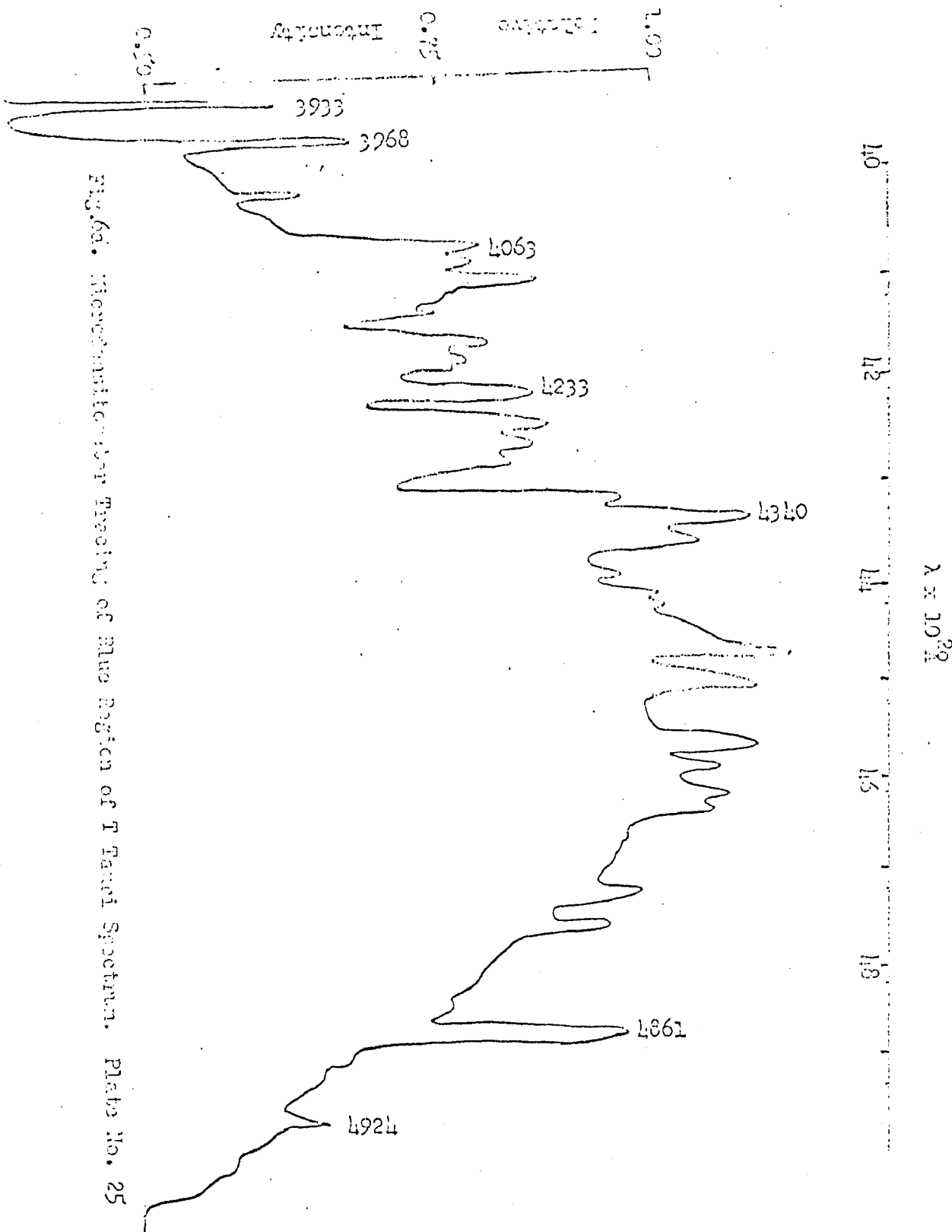
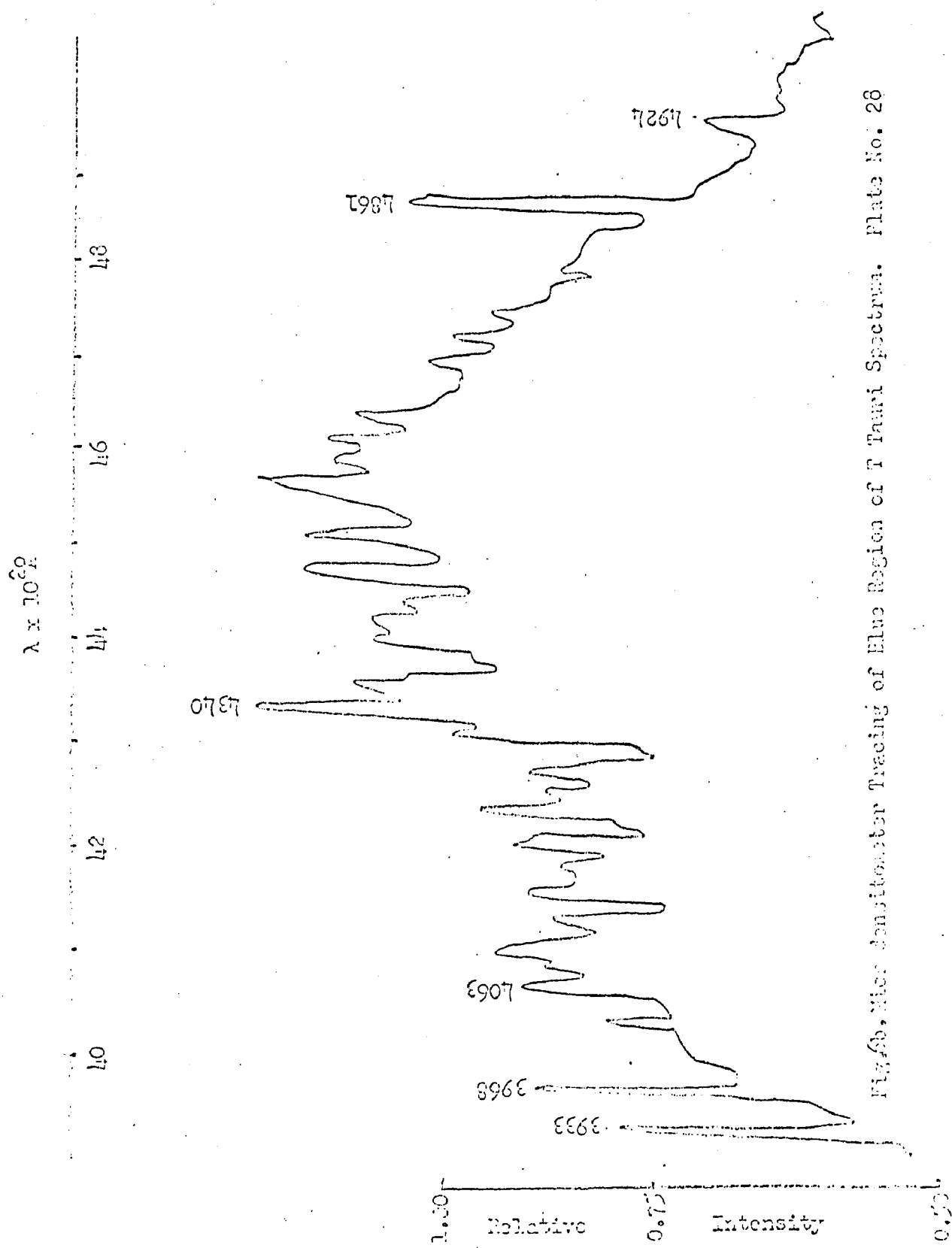
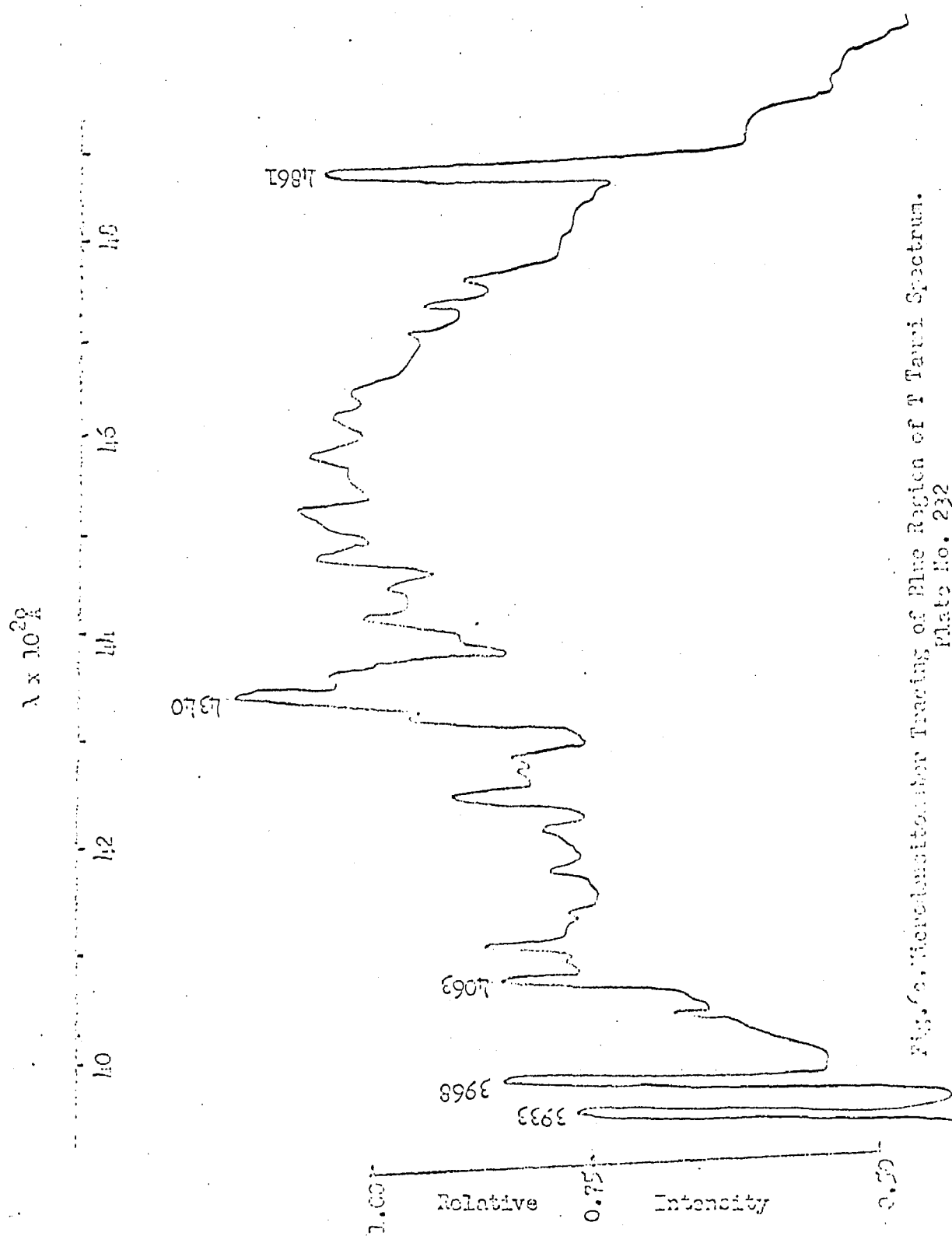


Fig. 6. Intensity-Var. Record of Blue Region of T-Tauet Spectrum. Plate No. 25







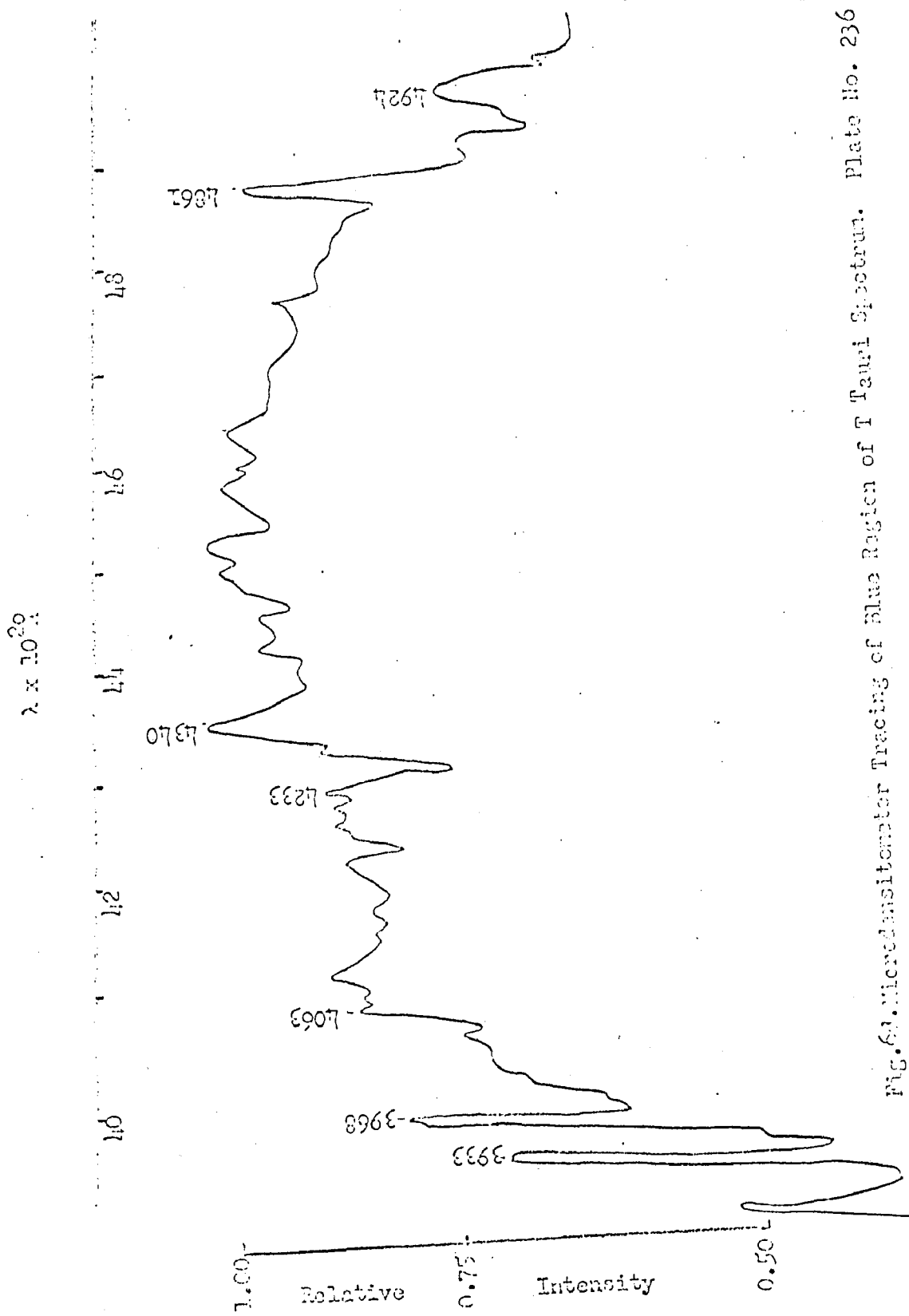


Fig. 61. Microdensitometer Tracing of Blue Region of T Tauri Spectrum. Plate No. 236

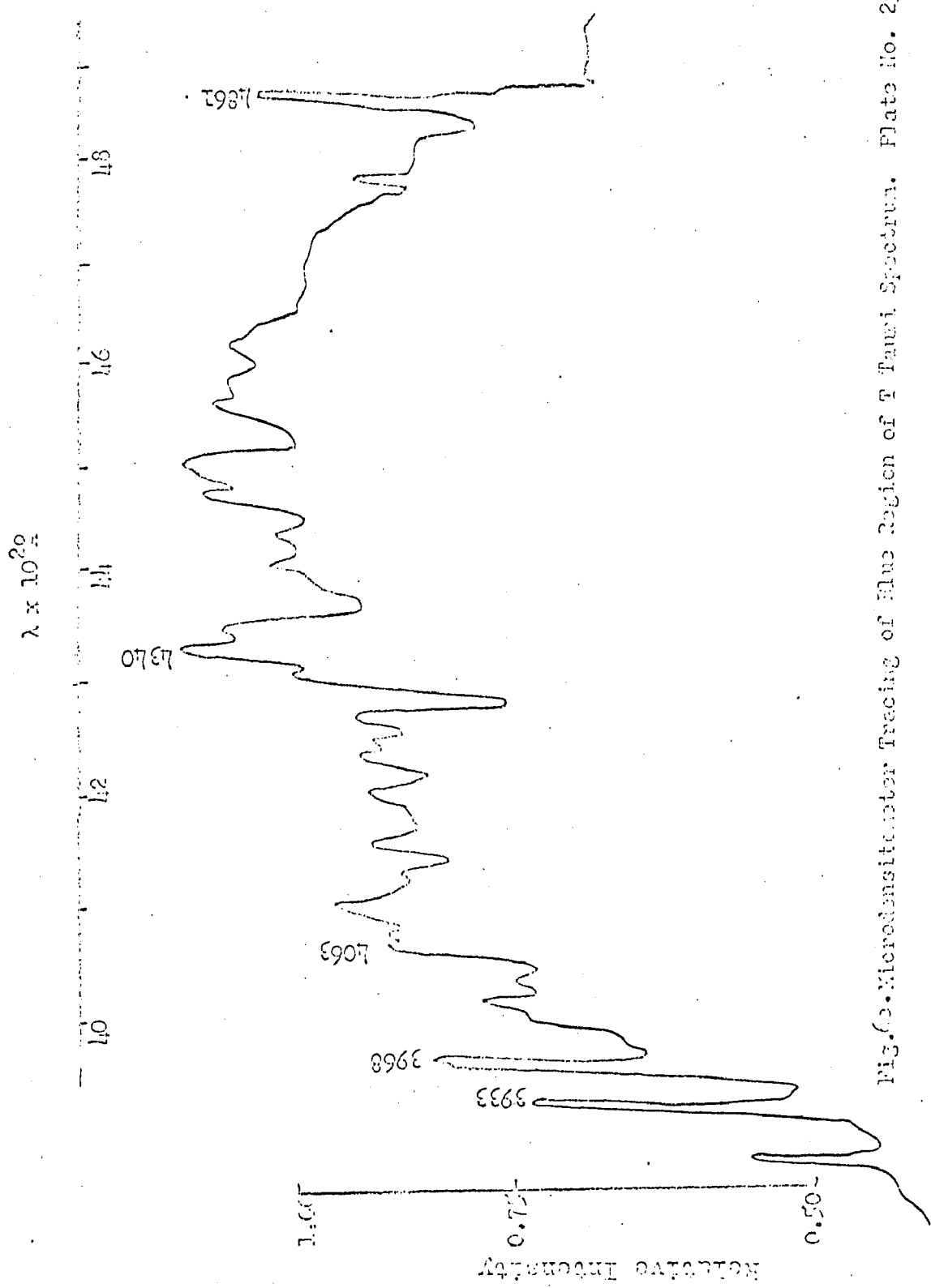


Fig. 6. Microdensitometer Tracing of Flux Region of T Tauri Spectrum. Plate No. 237

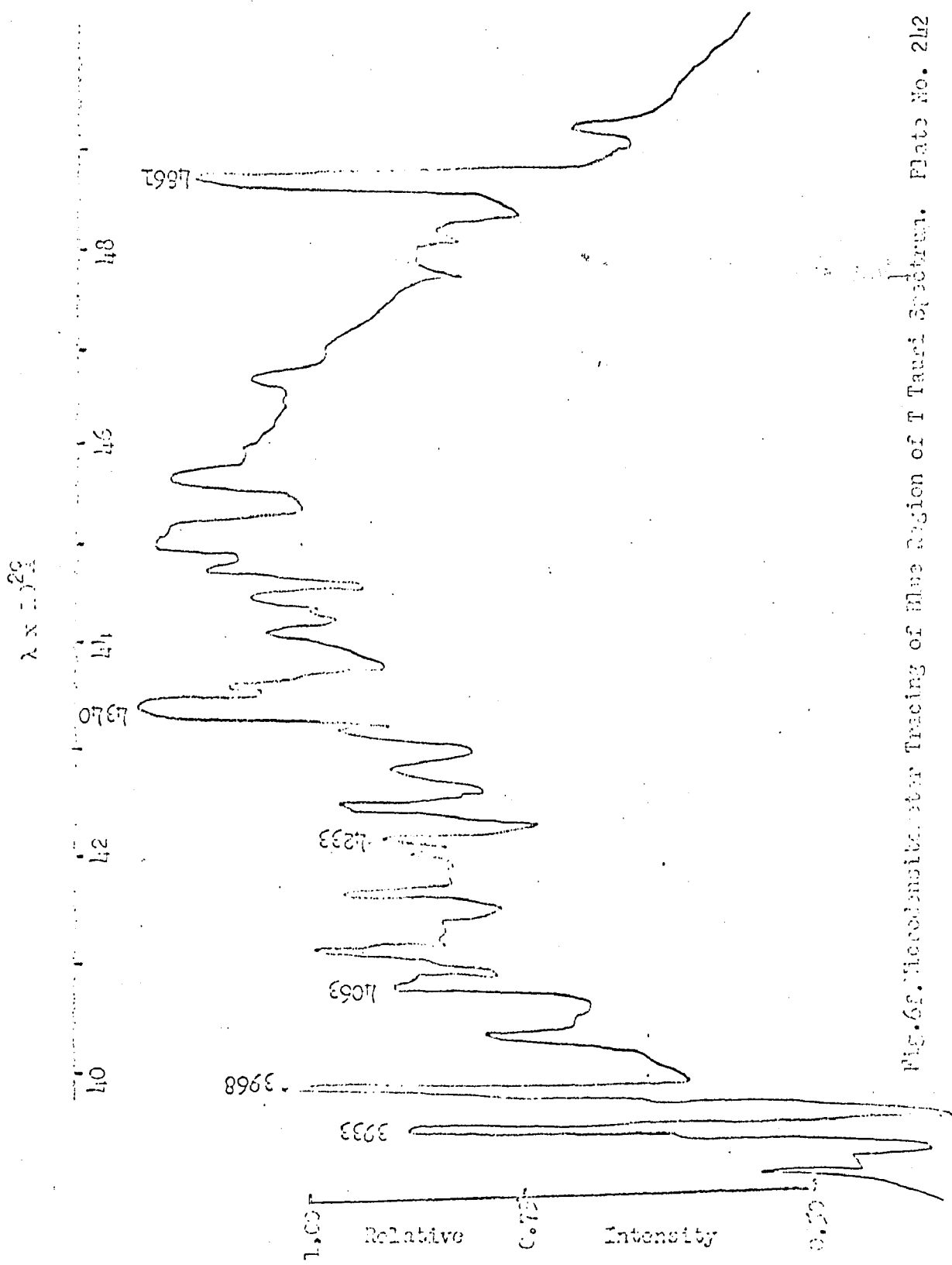


Fig. 62. Hand-drawn tracing of line region of $\text{T}_{\text{Th-232}}$. Plate No. 22

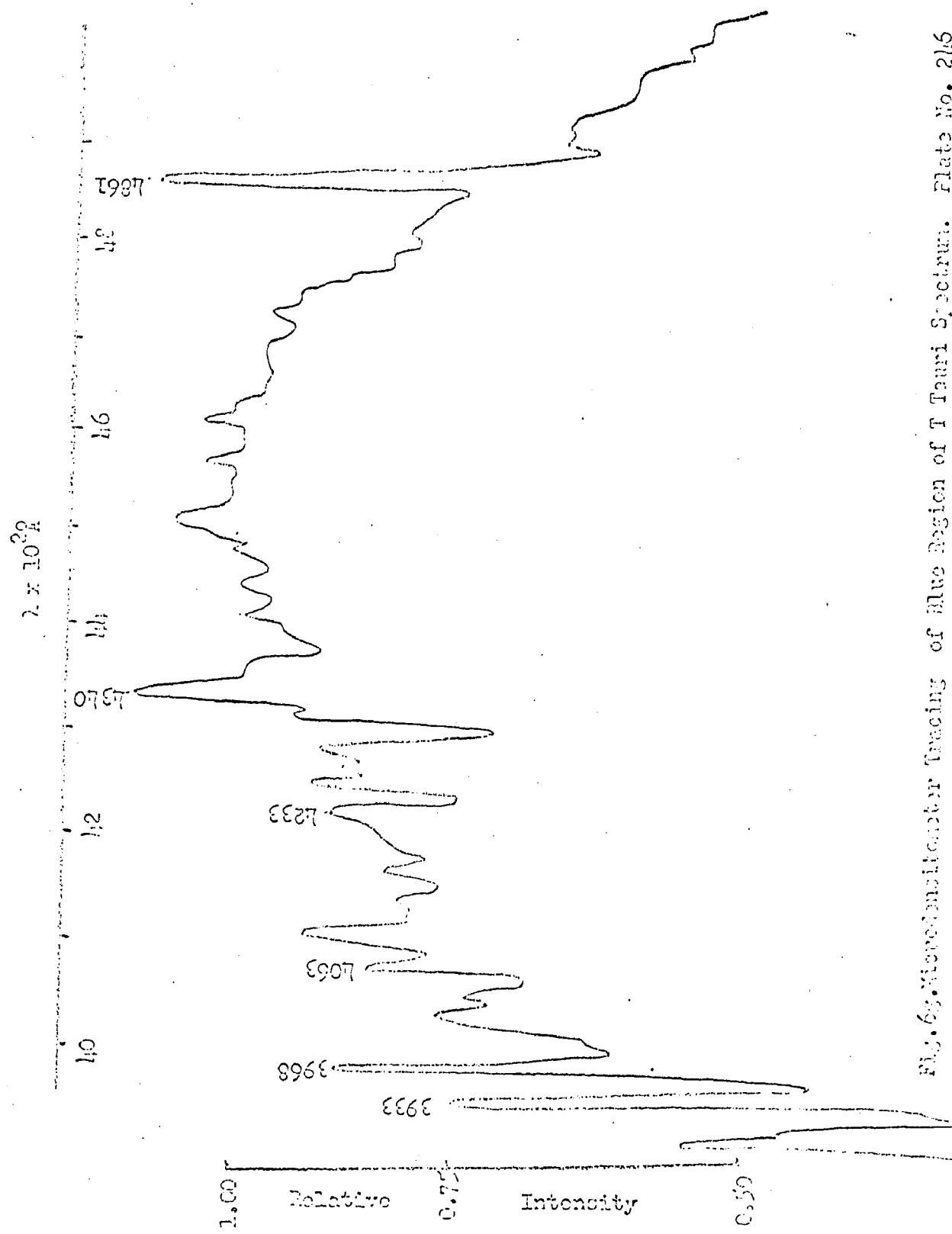


Fig. 6. Hand-drawn tracing of blue region of T Tauri Spectrum. Plate no. 216

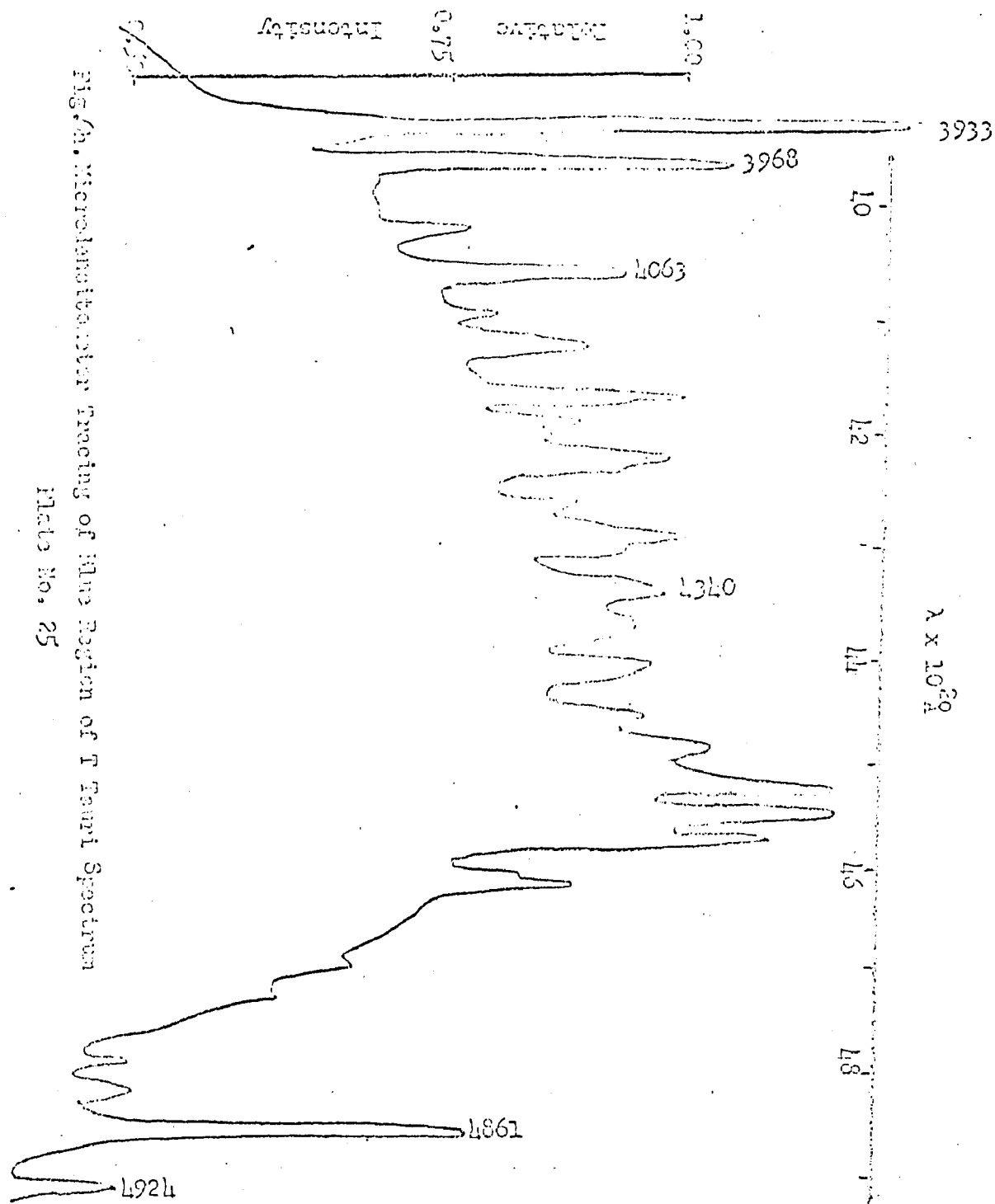


Fig. 9. Microheliograph Tracing of Blue Region of T-Tauri Spectrum
Plate No. 25

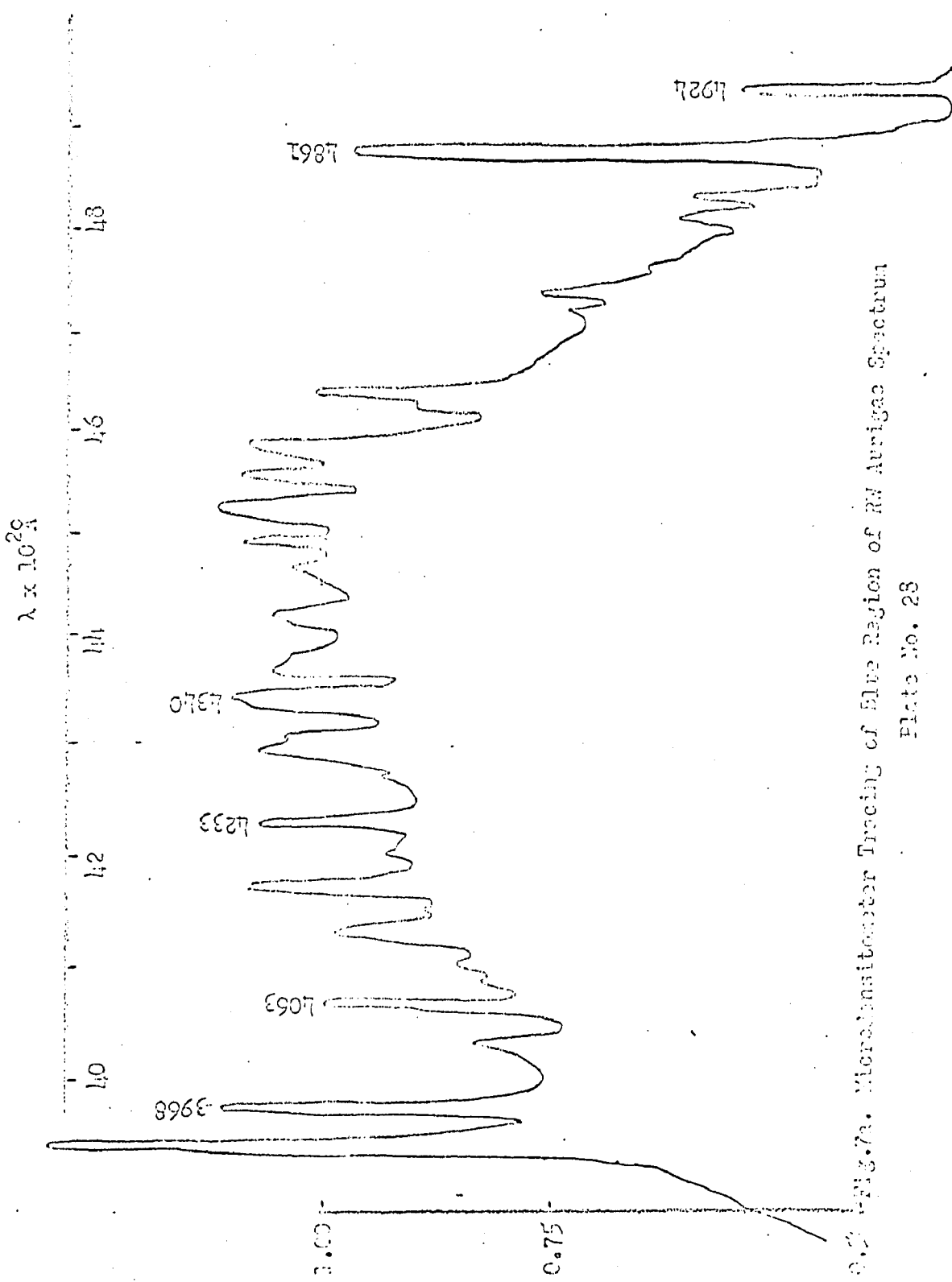


Fig. 73. Microtransitometer Tracing of Blue Region of Rb Auger Spectrum
Plate No. 28

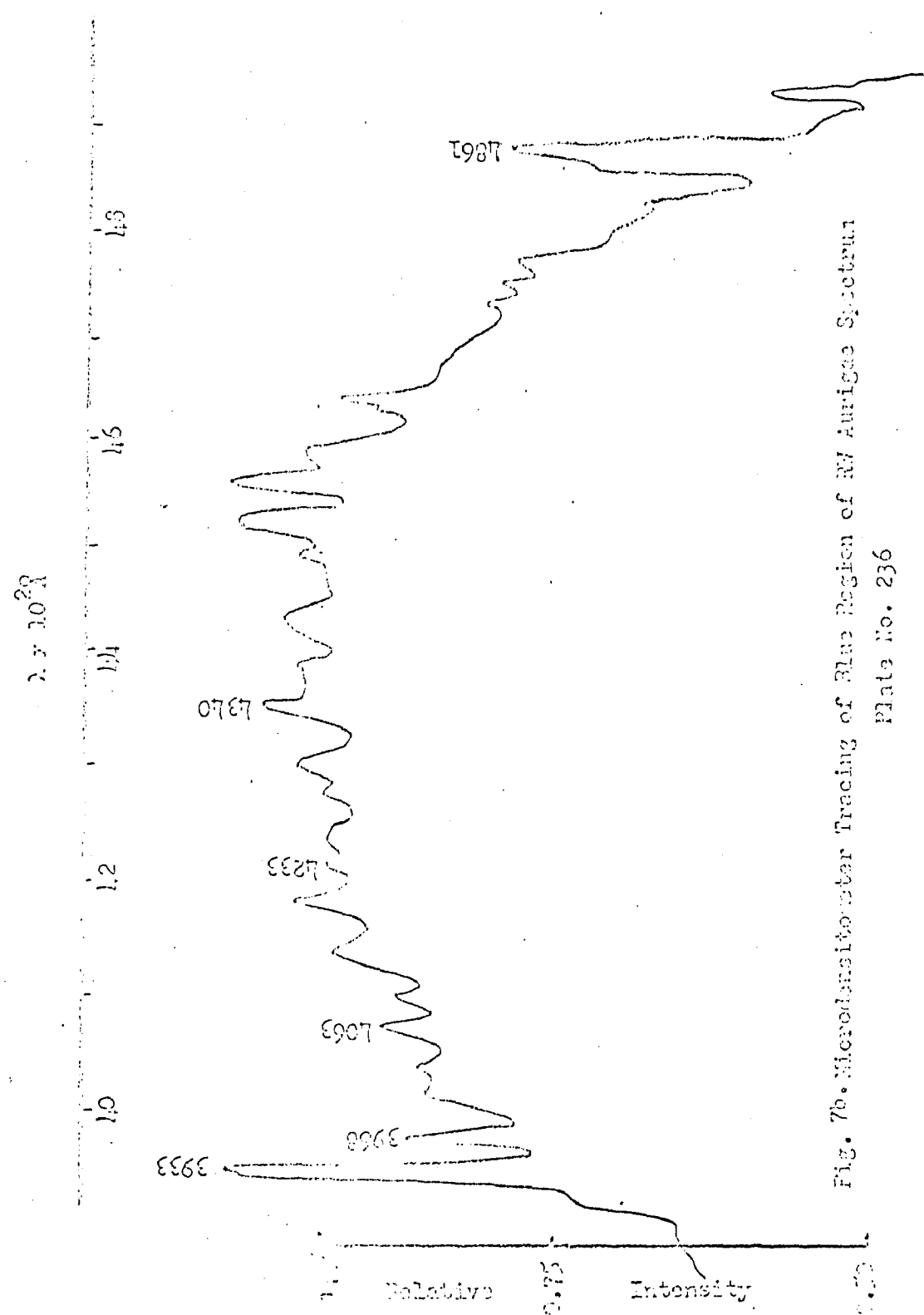


Fig. 7b. Microheliograph Tracing of Blue Region of X_γ Aurora Spectrum
Plate No. 236

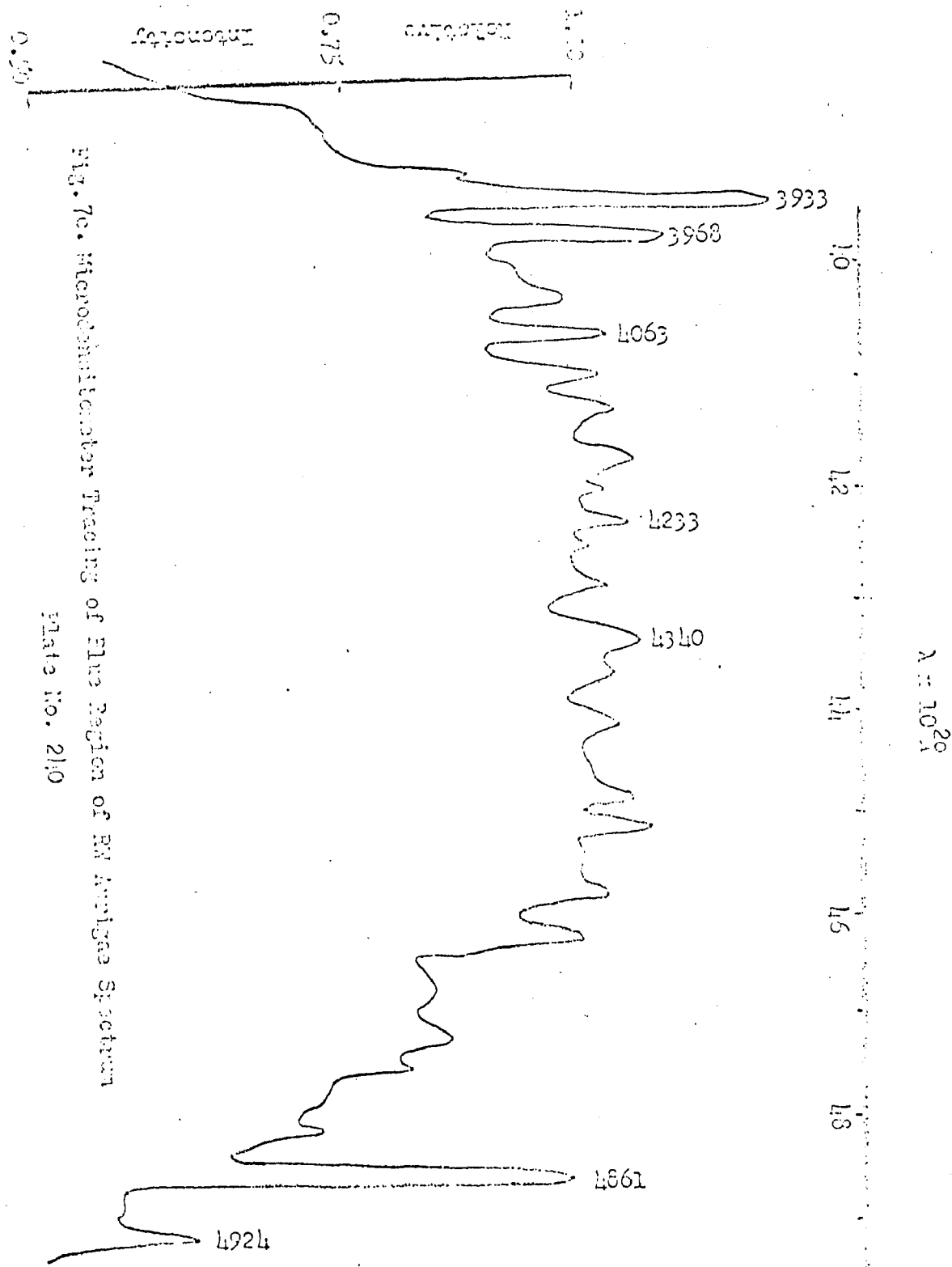


Fig. 7c. Microphotometer Tracing of Blue Region of Kautzsch Spectrum
Plate No. 210

Tables 12 and 13 reveal the following important informations:

- 1) The emission line effect is an ever changing phenomenon. This is well borne out by the resulting values of δ , the change in B-V due to the presence of lines, as will be seen in the next chapter. It is in accord with the observations of Joy and Kubi that not only does the intensity of the emission spectrum vary greatly from star to star but varies also in short periods within a given star. In particular, on plate 232 of EW Aur several features have diminished intensities; this plate was taken about 14 1/2 months after the lower numbered plates in the series.
- 2) Of the 56 diffuse emission features occurring in the spectra nearly all arise from low levels of excitation and are metallic, neutral and singly ionized iron contributing a majority.
- 3) Certain similarities obtain between T Tauri spectra and the spectrum of the solar chromosphere. Thomas and Athay (1961) give the most complete list of solar chromospheric spectra. Their list of identifications has been incorporated into Table 13.

$\lambda 4063$ and $\lambda 4132$ of FeI(43) appear strengthened relative to the other members of that multiplet; this was observed by Joy (1945). Herbig (1945) attributes the enhancement of these lines to population of the upper 3F level through the action of CaII 3968.5 upon $\lambda 3969.3$. The difference in wavelength is compensated by the great width of the calcium line in T Tauri spectra. Now although this phenomenon occurs among the T Tauri variables it is absent in the solar chromosphere. The sharper width of the chromospheric CaII line may offer a possible explanation.

Table 1h summarizes the situation regarding the forty-third multiplet of FeI; gf values are given by Allen (1963).

Table 1h
Occurrence of Members of FeI(43)

<u>Wavelength</u>	<u>Transition</u>	<u>gf</u>	<u>RV Aur</u>	<u>Presence In Solar Chromosphere</u>
4045.8	$3_{F_4} - 3_{F_4}^o$	3.0	Absent	Very Strong
4063.6	$3_{F_3} - 3_{F_3}^o$.86	Strong	Moderate
4132.6	$3_{F_2} - 3_{F_3}^o$.8	Moderate	Absent
3969.3	$3_{F_4} - 3_{F_3}^o$.8	Blended with Ca H	Absent
4071.7	$3_{F_2} - 3_{F_2}^o$		Strong (Blended with $\lambda 4063$)	Moderate

Next let us examine the relative strengths of the members of multiplets 41 and 42 of FeI. These contain lines arising from omission transitions beginning on the 5_G^o and 3_G^o levels, respectively; two of these appear to have anomalous intensities in the T Tauri stars. The line FeI $\lambda 4115.1$ (41) which appeared abnormally strong in the spectrum of RV Aur, though Joy found it to be blended with an FeII feature, is found not to occur in the chromosphere. The line resulting from the emission transition having the highest gf value in the multiplet, $\lambda 4383.5$, is the strongest chromospheric line in the multiplet and the strongest FeI line in the chromosphere. An identical situation exists with regard to the FeI $\lambda 4271.8$ line (42). This line is surpassed in intensity in the chromosphere by $\lambda 4325.8$, the line with the larger gf

value; $\lambda 4325.8$ is totally absent in the spectrum of EW Aur. Table 15 summarizes. Can the cause of the abnormal appearance of the lines in these multiplets in EW Aur be attributed indirectly to strong CaII and K or other emission? Since such emission is far weaker in the chromosphere and since the appearance of the lines of multiplets 41, 42, and 43 are different in the two sources, perhaps the answer is yes.

Table 15

Occurrence of Members of FeI (41) (42)

<u>Wavelength</u>	<u>Transition</u>	<u>λ^2</u>	<u>EW Aur</u>	<u>Presence In Solar Chromosphere</u>
4383.5(41)	$3_{F_4} - 5_{G_5}^o$	1.2	Moderate	Very Strong
4415.1(41)	$3_{F_2} - 5_{G_3}^o$	0.8	Moderate	Absent
4325.8(42)	$3_{F_2} - 3_{G_3}$.8	Absent	Very Strong
4271.8(42)	$3_{F_4} - 3_{G_5}$.5	Strong	Moderately Strong

Since the excitation potential of the upper level associated with each of the transitions is approximately 4.4 eV only lines longward of $\lambda 2818$ can be responsible for exciting atoms to the levels concerned. This eliminates the strong solar MgII doublet at $2795, 2797\text{\AA}$ as a possibility. The only possibility of the CaII K line as a source is the $3_{G_3} - 5_{G_3}^o$ transition which produces a line at 3929.1\AA ; but this is nearly 5\AA to the violet of Ca K. A thorough search of FeI multiplet tables reveals no known coincidental matching of FeI wavelengths with

that of a strong source of excitation which can lead to a supply of atoms in the 5C_3^o and 3C_5^o levels. Kuij (1964) has noted the presence of absorption features associated with strong emission, displaced to the violet with velocities as much as -230 km/sec, corresponding to 3 Å at CaII H and K.

It is difficult to decide whether the excitation conditions in the solar chromosphere exceed those in the region producing the T Tauri emission lines. Joy (1945) made a study of this question based upon line counts for various ions. Though remarkable similarities were found between the number and intensity of lines in both sources, Joy noted that some differences between the two sources were obvious (the deep reversals occurring in the H and K lines and the generally great width of emission features in the T Tau stars are not duplicated in the spectrum of the solar chromosphere). On the other hand, Herbig (1958) has concluded that the T Tauri spectra show a considerably higher degree of ionization and excitation than the solar chromosphere. This is seen by a) the predominance of ScII and TiII over FeII in the chromosphere and the opposite effect in the T Tauri stars, b) the prominence of the easily produced resonance lines of SrII and BaII in the chromosphere and their weakness in T Tauri spectra, and c) the strength of CrI lines in the chromosphere and their weakness in T Tauri spectra. One problem associated with comparing the two sources arises because of the great amount of self absorption in advanced T Tauri spectra. The reversals are particularly heavy in EW Aurigae and certainly remove a large fraction of energy from the emission lines. Even the

self absorption in the weaker lines (Herbig (1948)) is much greater than in the solar chromosphere. For this reason, only a lower limit to the flux subtracted by the emission lines can be determined. Table 13 reveals that only 5 of 19 FeI lines and 13 of 42 FeII lines found in the spectra of T Tau and RW Aur have been identified in the spectrum of the solar chromosphere; all have relatively large gf values. Only two FeII lines and 10 FeI lines appear in the chromosphere which have not been identified in T Tauri spectra but it should be pointed out that all but two of the 12 lines occur in the crowded 4000-4400 \AA region. They may actually be present in these spectra but have escaped detection simply because of their proximity to a vast number of very strong lines.

4) The appearance of spectra of the T Tauri summer sky objects are markedly different from those of RW Aur and T Tau itself. Only the very strongest lines in the spectra of the latter show up in DI Cep and AS 209.

V. Results Regarding the Continuum and the Effect of Line Emission

Smak (1960) uses a photometric method to evaluate the line emission effect. His filter (2mm. BG12 + 2mm. GG3 + 1mm. Corning 3387) is employed with the conventional wide band V filter to establish a color base that is relatively free of line emission. Although the H _{α} and H _{γ} contributions are greatly diminished, 21 emission features are still visible in the transparent region ($4300 < \lambda < 5100$) of the filter in low dispersion spectra of RW Aur. A typical line analysis was run on Steward Observatory Plate No. 26 of this object to determine to what extent Smak's color base is actually emission free. Table 16 lists the filter transmission and density as a function of λ . This is plotted in Fig. 8. The reduced data are presented in Tables 17.

Table 16 Density vs λ of 2mm BG12 + 2mm GG3 + 1mm Corn. 3387

(Smak's Filter)

λ (Å)	Transmission %	Density
4300	0	- ∞
4400	13	- .886
4500	27	- .568
4600	28	- .553
4700	22	- .658
4800	12	- .920
4900	5.5	- 1.260
5000	2	- 1.699
5100	0	- ∞

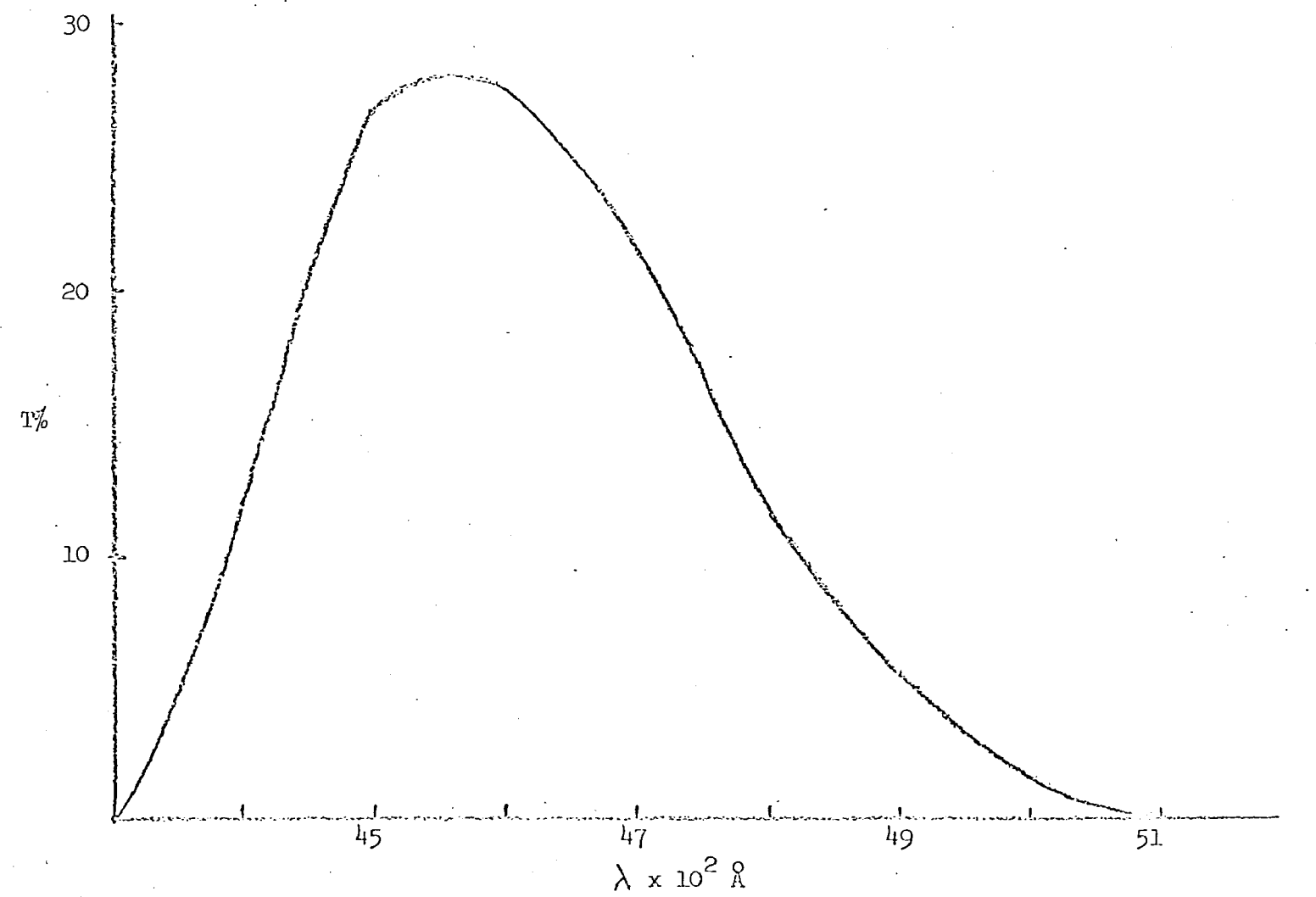


Fig. 8. Transmission vs. Wavelength for the V Filter.

B-V
Table 17a Line Analysis

Plate No: 28			Emulsion: 103a-F			Date: 1963 Oct. 17			MK Sp:					
Object: RV Aur			$\alpha: 05:05.4$			$\delta: +30:22.1$			$\Delta \text{sec z:}$			$B-V$		
$\lambda(\text{\AA})$	c_1	c_c	d_1	d_c	$\log I_1$	$\log I_c$	$\Delta \log I$	$\frac{\log I_{c_B} +}{\Delta \log I}$	$\frac{\log I_{c_V} +}{\Delta \log I}$	$I_{1B} - I_{c_B}$	$I_{1V} - I_{c_V}$	Width (\AA)	A_B	A_V
4306								-1491		009		0.2		
4340								-965		038		1.1		
4376								-727		038		1.4		
4415								-658		040		1.1		
4461								-556		038		1.1		
4490								-479		069		1.0		
4515								-383		143		4.6		
4558								-447		100		1.8		
4584								-502		072		1.4		
4616								-565		045		0.5		
4634								-475		119		1.9		
4700								-749		008		0.1		
4731								-773		022		0.2		
4789								-943		014		0.1		
4817								-1037		015		0.2		
4861								-830		094		3.0		
4924								-1308		019		0.3		

Table 17a Line Analysis

$B - V$ Analysis

Table 17b Data Summary Sheet for T Tauri Object

Plate No: 28	Object: RY Aur
A_{CV} : .718	A_{CB} : .098
A_{LV} : .069	No. of lines contributing to V: 21
A_{LB} : .020	No. of lines contributing to B: 18
A_{CV}/A_{CB} : 7.326	$(B-V)_C$: 1.62
$\frac{A_{CV} + A_{LV}}{A_{CB} + A_{LB}}$: 6.703	$(B-V)_{C_1}$: 1.53
A_{LV}/A_{CV} : .100	A_{LB}/A_{CB} : .210

In the region under consideration Smak's colors may be determined according to the expression

$$\text{B} - \text{V} = 2.5 \log \frac{\text{AcV}}{\text{AcB}} - 3.04$$

Thus the $\text{B} - \text{V}$ continuum color index of RW Aur is found to be +1.62, corresponding to $(\text{B}-\text{V})_c = +0.70$. Previous computations have revealed RW Aur to be bluened by $\delta_{\text{B}-\text{V}} = 0.15$ when the line contribution is added; the ratio of line to continuum flux is .26 in the B window, .10 in the V window. The same ratio in the B passband is found to be 0.21, fully two-thirds as large as that in the B passband which it is designed to replace. With the inclusion of emission features, $(\text{B}-\text{V})_{cl} = +1.53$. Thus Smak's continuum color index is altered by $\delta_{\text{B}-\text{V}} = 0.09$. The magnitude of the line emission effect is only slightly reduced when one employs the B filter. There is a great difficulty in choosing a filter less sensitive to emission than Smak's B filter. The enormous crowding of bright lines coupled with their apparent variation in intensity make such a choice impossible. The method employed in this work is admittedly less capable of providing as large masses of data as the photometric observations, but it has the distinct advantage that it treats each emission feature separately. There results a more exact evaluation of the nature of T Tauri continua.

The present method is testable in at least two ways. Table 18 reveals that the reduction procedure followed is sufficient to predict the observed photometric colors of UBV standards. Spectra of at least one

of these stars have been put on each plate for this reason. The probable error of a single determination of $(B-V)_c$ is $\pm .016$. Repeatability has been stressed particularly in the most recent plates. Derived and observed standard star continua are plotted in Fig. 9 for a few of the plates.

Errors due to readability of microdensitometer tracings have been found to play a primary role (Chapter II) but other errors of an intrinsic nature are also present. For late type stars it is very difficult to decide about the ultraviolet level of the continuum. There was at first a tendency to underestimate the true continuum flux since the gaps between spectral lines in this region, which serve to indicate the level of the continuum, are few and far between. Furthermore, the low F. plate sensitivity makes the situation even more confused. Even with the well-chosen filters of UBV photometry, the true continuum color of any star is never duplicated in photometric observations since absorption lines alter the shape of the spectral energy curve too.

A second test of the method turned out to be less fruitful, principally because of observational limitations. It was thought that simultaneous photometry would provide a highly accurate check of the spectroscopic observations of T Tauri stars. The difficulty associated with obtaining two instruments for the same night increased with time as Tucson and environs came to be realized as the promised land for obtaining astronomical observations; nevertheless, simultaneous photometry was made available for nearly three quarters of the spectroscopic

Table 18 Computed and Observed Colors of Standard Stars

<u>Object</u>	<u>Plate No.</u>	<u>Observed B-V</u>	<u>Computed (B-V)_c</u>	<u>(B-V)-(B-V)_c</u>
X Cet	23	+0.68	+0.67	+0.01
E Eri	25	+0.89	+0.88	+0.01
μ Her A	26	+0.75	+0.74	+0.01
η Cep	26	+0.92	+0.95	-0.03
13974	28	+0.61	+0.65	-0.04
β Com	199	+0.57	+0.59	-0.02
61 Cyg A	205	+1.19	+1.20	-0.01
61 Cyg A	207	+1.19	+1.21	-0.02
16 Cyg A	209	+0.64	+0.61	+0.03
16 Cyg A	210	+0.64	+0.61	+0.03
ρ Gem	236	+0.32	+0.29	+0.03
ρ Gem	237	+0.32	+0.29	+0.03
ρ Gem	240	+0.32	+0.31	+0.01
ρ Gem	242	+0.32	+0.29	+0.03

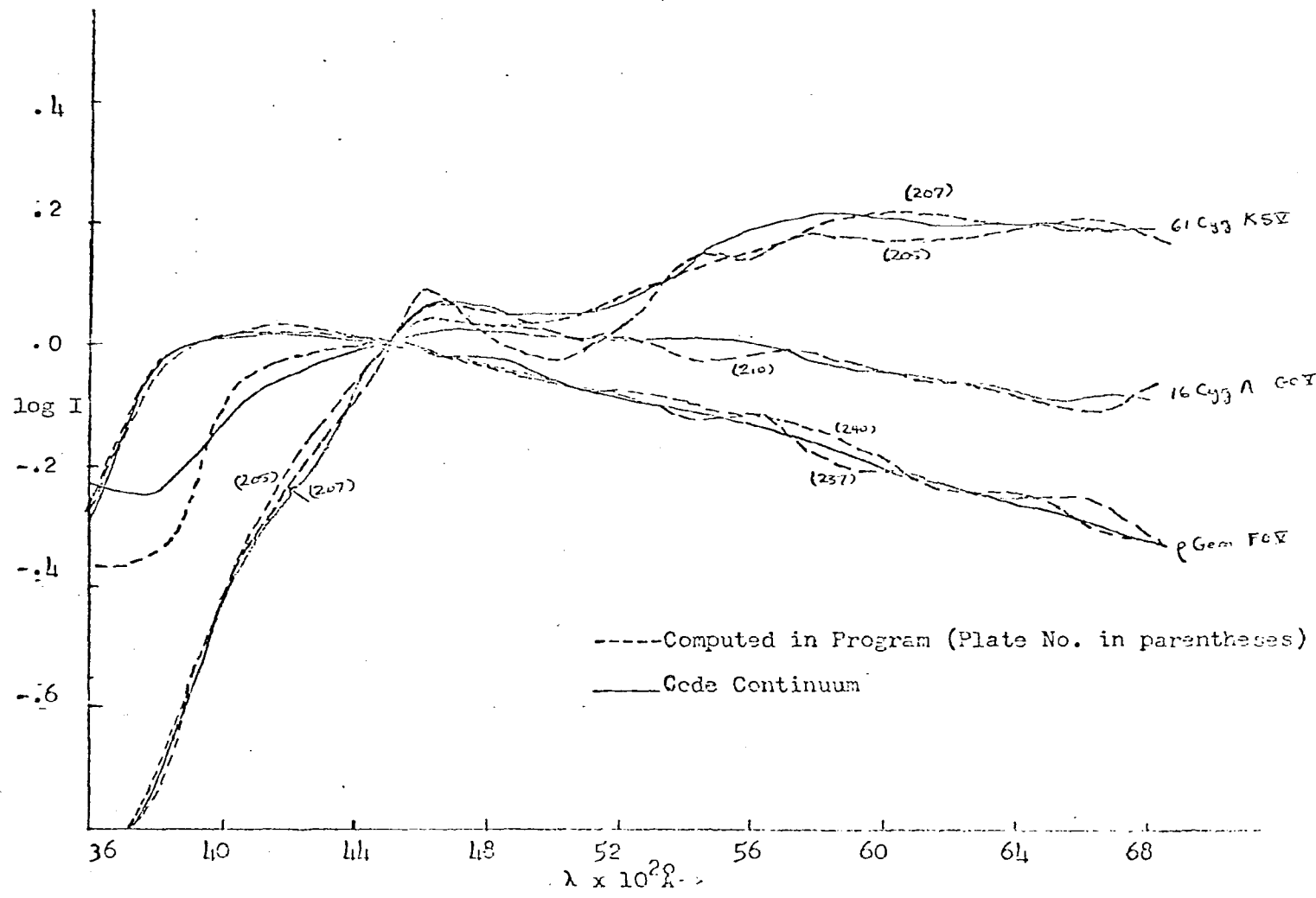


Fig. 9. Standard Star Continua

nights. One period of unusually poor transparency reduced this to about 331/3%. This test is only an approximate one owing to the extremely rapid color variations exhibited by certain active T Tauri stars. During a typical plate exposure (two or three hours) color variations of up to $0^m.1$ were observed. These data comprise part of Table 19 which displays the results initially sought in the investigation. The author is indebted to the Kitt Peak National Observatory for permitting him to use the 16 - inch photometric telescope in order to obtain several observing runs at the same time the Steward 36-inch instrument was being employed for spectroscopic purposes. Simultaneous photometry and spectroscopy would have been totally impossible without the cooperation of the staff of the National Observatory.

The colors $(B-V)_c$ and $(B-V)_{cl}$ as well as the parameter δ for every variable star spectrum are displayed in this Table. It is apparent that the range of observed photometric colors more closely approximates $(B-V)_{cl}$ than the line free color index as theory predicts. This test could lead to greater accuracy if the program utilized brighter T Tauri stars; these simply do not exist. Employing lower dispersion is a poorer possibility. Although this offers shorter exposure times, it magnifies the problem of detecting unresolved emission lines.

The most significant facts obtained from a study of the observational material follow:

- a) The emission lines in T Tauri variables profoundly influence the observed colors, causing the stars to appear bluer by as much as $\delta = 0^m.15$. This constitutes only a lower limit since there is reason to believe that unresolved emission lines have been included in the deter-

mination of continuum color; this subject will be dealt with below.

b) The effect of line emission upon color varies in some complicated manner. The limits for seven spectra of RW Aur give $0.06 < \delta < 0.15$; seven spectra of T Tau give $0.07 < \delta < 0.14$. Can these variations be correlated with changes in continuum color and/or light cycle? In order to decide the first question the line emission parameter δ has been plotted against the continuum color (Fig. 10). The range of probable error for both coordinates is indicated by spikes. It is difficult to estimate the error in the determination of δ . Even if unresolved emission lines are excluded, one has to contend with numerous cases of blending and overlapping line profiles. Here line widths can only be roughly estimated. When considering line intensities one finds it more difficult to confine the plate density observations to the straight line portions of the characteristic curves. Indeed, no realistic quantitative treatment of probable error is possible for the coordinate. A generous estimate of $\pm 2\%$ appended to the ratio of B and V continuum plus line fluxes gives $\Delta\delta = \pm .02$.

That δ and $(B-V)_c$ are related is suggested by the positions of plotted points in Fig. 10 even though they are scattered over a large range. The trend toward larger values of δ with redder continuum color for T Tau is particularly tempting. A straight line of slope $\Delta\delta/\Delta(B-V)_c = 1/5$ fits the observations well for that star. There is, then, at least a possibility that the emission lines are strongest when the continuum color is reddest. This may be connected with the fact that most of the lines are located in the blue region. When the blue continuum becomes

Table 19 Summary of the Effect of Line Emission Upon B-V Color

<u>Object</u>	<u>S.O.</u> <u>Plate No.</u>	<u>Date</u>	<u>(B-V)_c</u>	<u>(B-V)_{cl}</u>	<u>δ</u>	<u>Remarks Concerning Concurrent Photometry</u>
R Aur	23	1963 Oct. 13	+0.67	+0.57	0.10	
	25	1963 Oct. 14	0.51	0.36	0.15	
	26	1963 Oct. 15	0.60	0.47	0.13	
	28	1963 Oct. 17	0.70	0.55	0.15	0.50 < B-V < 0.60; 8.53 < V < 8.56
	232	1965 Jan. 1	0.43	0.37	0.06	
	236	1965 Jan. 27	0.30	0.22	0.08	
	240	1965 Jan. 29	0.43	0.36	0.07	
T Tau	25	1963 Oct. 14	1.11	0.99	0.12	1.00 < B-V < 1.05; 9.90 < V < 10.02
	28	1963 Oct. 17	1.28	1.14	0.14	1.14 < B-V < 1.17; 9.53 < V < 9.57
	232	1965 Jan. 1	1.19	1.08	0.11	
	236	1965 Jan. 27	1.07	0.98	0.09	
	237	1965 Jan. 28	1.20	1.11	0.09	B-V = 1.17* V = 10.39*
	240	1965 Jan. 29	0.94	0.87	0.07	
	242	1965 Feb. 19	1.16	1.07	0.09	

*One observation only.

Table 19 Summary of the Effect of Line Emission Upon B-V Color

<u>Object</u>	<u>S.O.</u> <u>Plate No.</u>	<u>Date</u>	<u>(B-V)_C</u>	<u>(B-V)_{cl}</u>	<u>δ</u>	<u>Remarks Concerning Concurrent Photometry</u>
DI Cep	209	1964 Jul. 27	0.60	0.56	0.01	
AS 205	199	1964 Jun. 17	1.43	1.48	0.00	
AS 209	200	1964 Jun. 18	0.63	0.57	0.06	

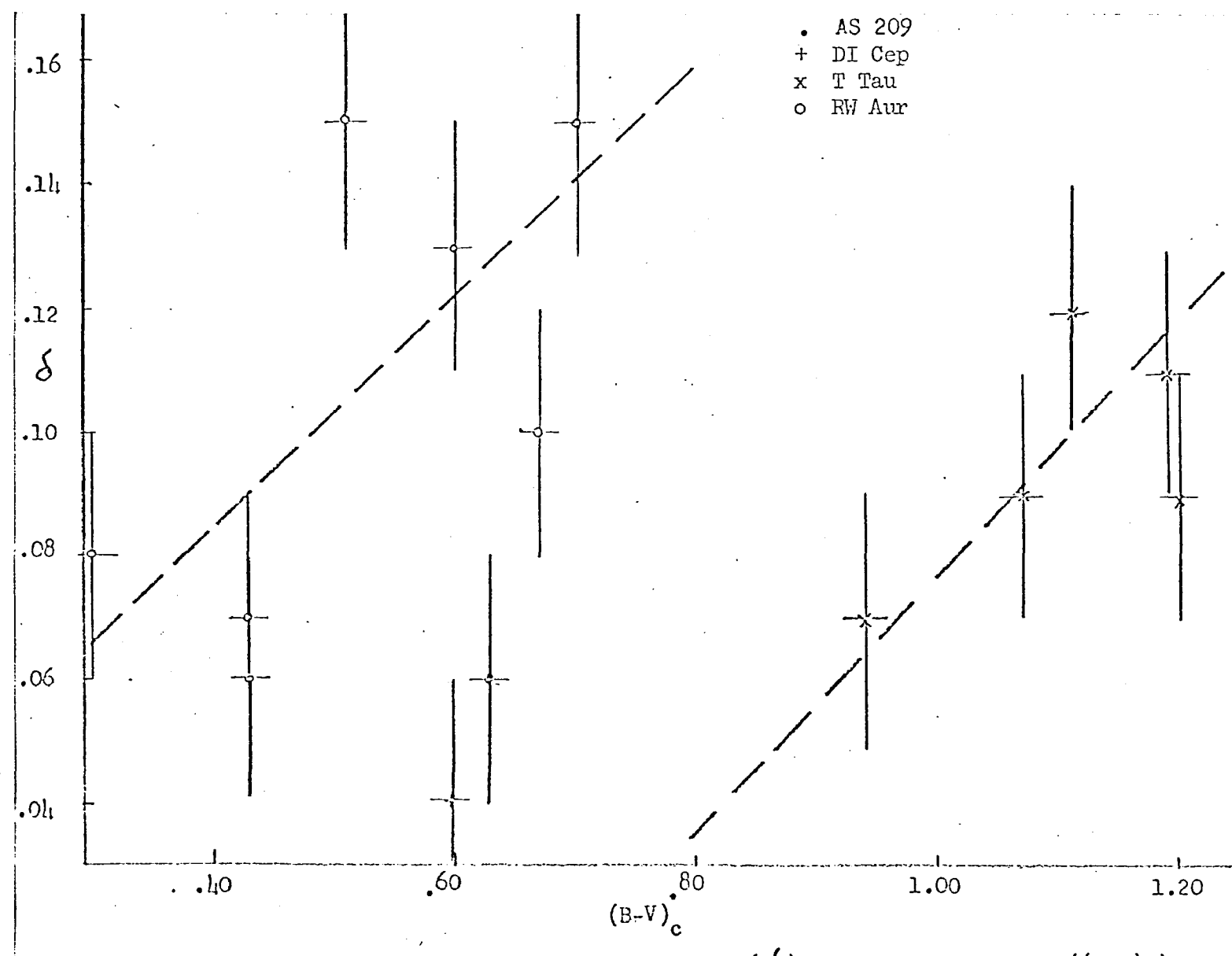


Fig. 9. Line Emission Parameter (δ) vs. Continuum Color $((B-V)_c)$

depressed relative to the red some of the lines which were burned out on previous spectrograms then show up against the less dense background. The summary tables reveal that a larger number of lines contribute to the bluening effect when (B-V) approaches large positive values. An alternative explanation would require one to devise a special physical process in the atmosphere of T Tauri stars which produces greater emission line fluxes at the same time the continuum flux diminishes in the blue. The explanation that the effect is extrinsic is much simpler.

The relation between light cycle and δ is much more difficult to establish quantitatively. The lack of available concurrent photometry is principally the cause of this. Herbig (1958) found that emission line activity is generally richer at light maximum. The observations displayed for T Tau in Table 19 seem to agree with this. Apparently T Tau and RW Aur were caught in periods of great activity during the 1963 Oct. observations. For each of them δ was quite large. The following year δ diminished, by nearly 0^m.1 for RW Aur and somewhat less for T Tau. It is not so surprising to find large fluctuations of up to 0^m.1 in V over the course of a three hour exposure. These stars have long been known to behave in this manner. These fluctuations are accompanied by equally large color fluctuations. The irregularity of the continuum is obvious in Fig's. 6 and 7. The emission lines depicted appear to rise and fall in an irregular manner from plate to plate like so many spicules on the limb of the sun. Fig's. 13 and 14 illustrate even more vividly the wavy appearance of the continuum.

What is the effect of the line emission correction upon the determination of T Tauri star positions in the color magnitude diagram?

This is perhaps the most important question that can be answered from this study. Since the removal of emission lines reddens the star, the star will shift to the right or toward younger apparent contraction age. For neither of the program variables is the "emission track" long enough to place them in the wholly convective fast evolutionary phase given by Hayashi et al (1962). The true position along the abscissa of the $\log L/L_\odot$ vs $\log T_e$ diagram was found by averaging the $(B-V)_c$ for each star (corrected for space reddening by employing results to be discussed later) and converting to $\log T_e$ using Arp's table. The same computation was made for the apparent colors, $(B-V)_{cl}$. The results are:

	<u>True $\log T_e$</u>	<u>Apparent $\log T_e$</u>	<u>$\Delta \log T_e$</u>
RW Aur	3.792	3.860	.068
T Tau	3.742	3.789	.047

Absolute magnitudes are very difficult to estimate for these objects. Using the bolometric magnitude of T Tau given by Kuhi (1964), the position on the ordinate in the HR plane is $\log L/L_\odot = 0.728$. With the correction for line emission, T Tau is placed at twice the previous distance from the main sequence. For RW Aur the shift will be even larger. To what error does this amount in the determination of the contraction age of these objects? Due to the inexactness associated with transforming between theoretical and observed color magnitude diagrams one can only obtain an approximate answer. An examination of the contraction tracks given by Henyey et al (1955), along which equal time intervals are marked, reveals that $\Delta t/t$ lies between 0.12 and 0.15. It is conceivable that an overestimate in age of 20% or more will result, if the emission line correction is neglected in advanced T Tauri stars.

Fig. 11 depicts the shift of position in the theoretical HR Diagram; the evolutionary track for stars of $1M_{\odot}$ and $2M_{\odot}$ according to Hayashi et al are shown for reference. The effect upon the variable star positions in the two color plot is shown in Fig. 12. The average of the photometric U-B observations obtained by the author was used to locate the position on the ordinate; the "emission track" in the diagram is given by the average of the computed δ values.

The results depicted in Fig. 12 should be observed with a word of caution. There is reason to believe that the U magnitude is affected by the presence of emission lines to a greater degree than the B or V magnitudes.

The number of lines in the spectra of FeI and FeII increases toward shorter wavelengths. These ions have already been found to produce most of the emission lines in T Tauri spectra. Strong ultraviolet continua ($\lambda 3800\text{\AA}$) which may be the result of blending of emission lines seem to be characteristic of T Tauri stars. This means that the actual shift in the two color diagram is not a horizontal line but one of rather large negative slope. Furthermore, there is no reason to believe that the emission track in the color magnitude diagram is a horizontal line. Better concurrent photometry will aid greatly in the determination of the slope of the emission track in the color magnitude diagram. The slope can be found only when the U magnitude correction is measured. This is not possible photographically. From the discussions at the beginning of Chapter IV, the photometric method seems to offer no better possibility.

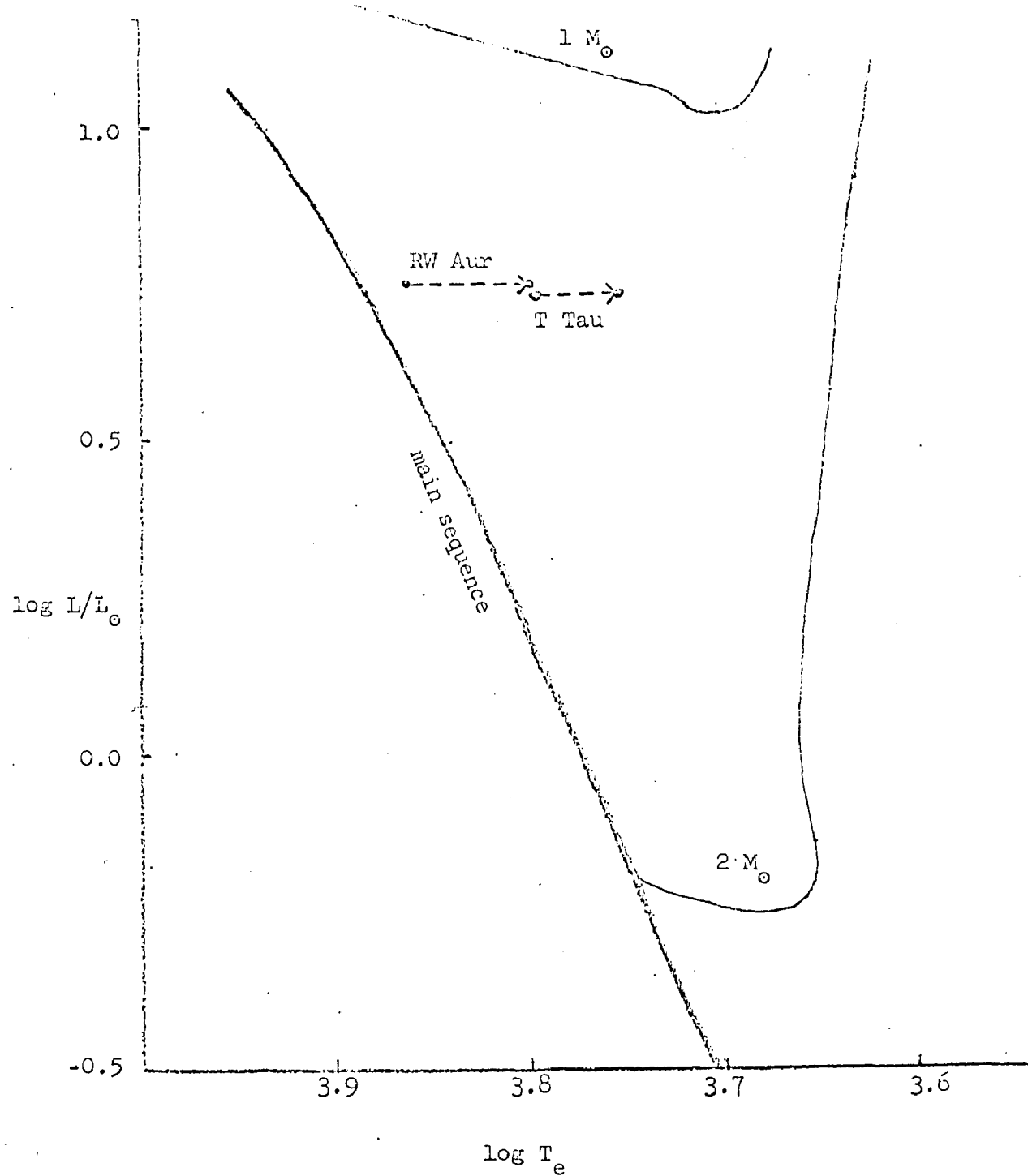


Fig. 11. Shift of Position in $\log L/L_\odot$, $\log T_e$ Diagram After Correction for Emission

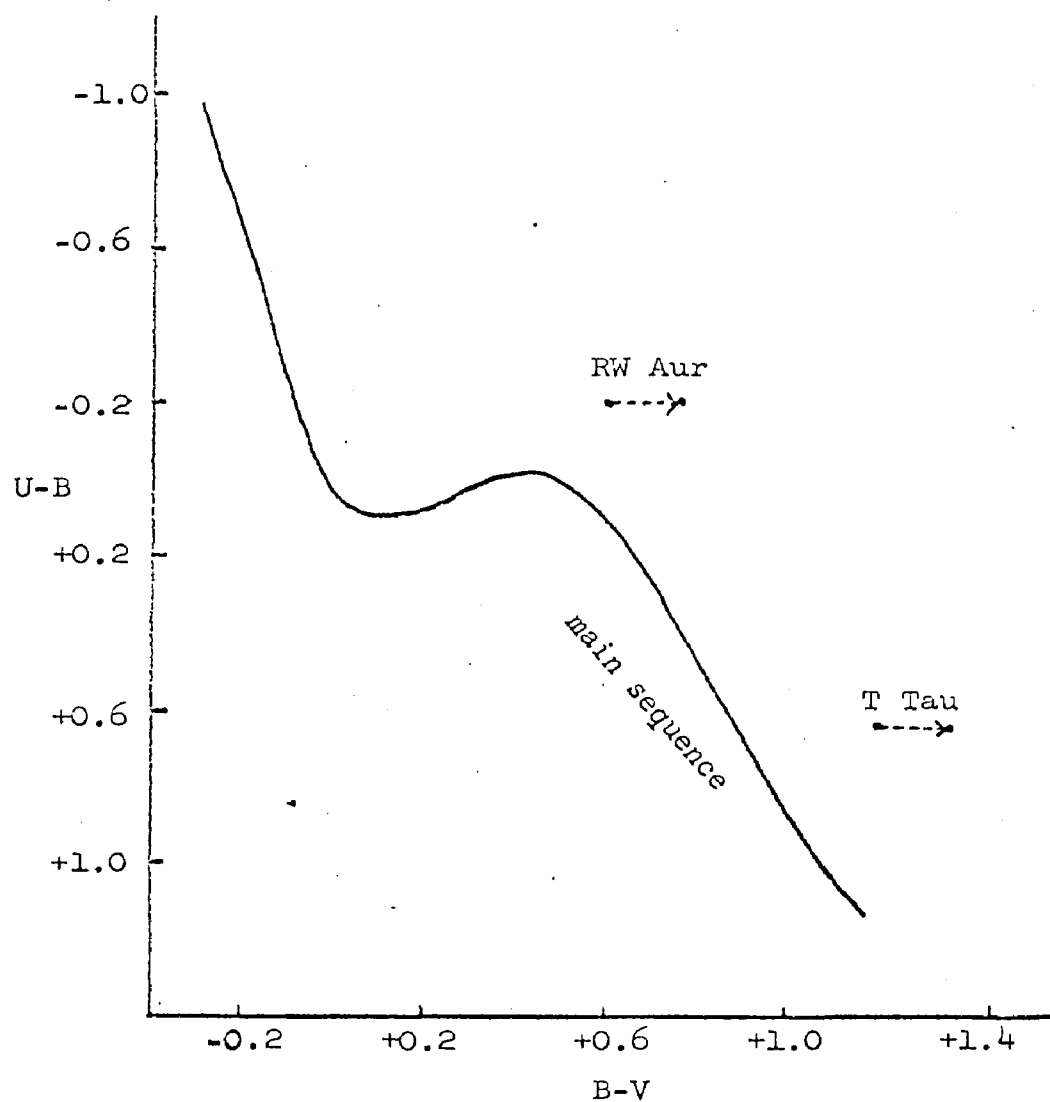
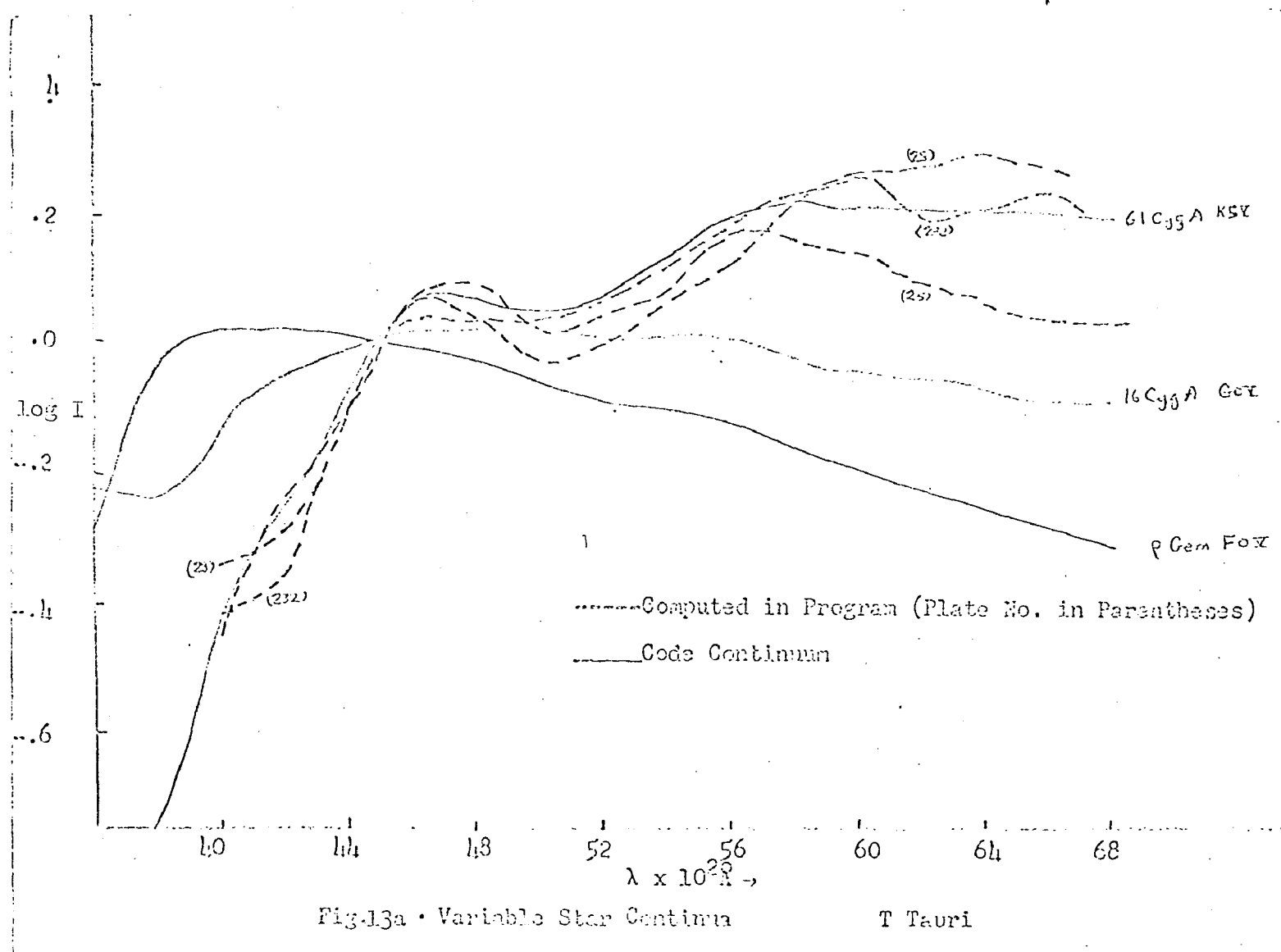


Fig. 12. Shift of Position in the $U-B$, $B-V$ Diagram After Correction for Emission.

The nature of the continua of RW Aur and T Tau is revealed in Fig's. 13 and 14 where the normalized log I are plotted against wavelength as dotted curves for program stars. Code's standard star continua are represented by solid curves. It should be stressed that the variable star continua are not corrected for space reddening. There are a number of important facts revealed by this series of plots. One immediately obvious conclusion is that the variable star curves behave in an irregular fashion, exhibiting a number of bumps and troughs. The most reasonable explanation for this phenomenon includes a combination of effects: unresolved emission in addition to masking of the underlying continuum by partial blending of lines. One very large hump occurs at approximately λ 5000 and is common to nearly all variable star spectra. Extreme crowding of emission lines occurs over this range. It is interesting to note that a similar hump appears in the same region in the continuum curves of the T Tauri stars LH α 22 and VY Ori (Bohm (1958)). Both these stars show an unusually strong ultraviolet continuum ($3600\text{\AA} < \lambda < 3800\text{\AA}$); the existence of this latter property is not detectable on plates of the T Tauri stars in the present program. Many T Tauri stars show conspicuous veiling in the photographic region (the "blue continuum") which Herbig (1958) attributes to extreme crowding of a great number of weak emission lines. The hypothesis is supported by the notable absence of all underlying absorption features and by the correlation of strong emission line activity with a brightening of the continuum. This feature appears most exaggerated on plates 25, 232, and 240 of T Tau and on 25, 26, and 28 of RW Aur. All three of these plates for RW Aur and two



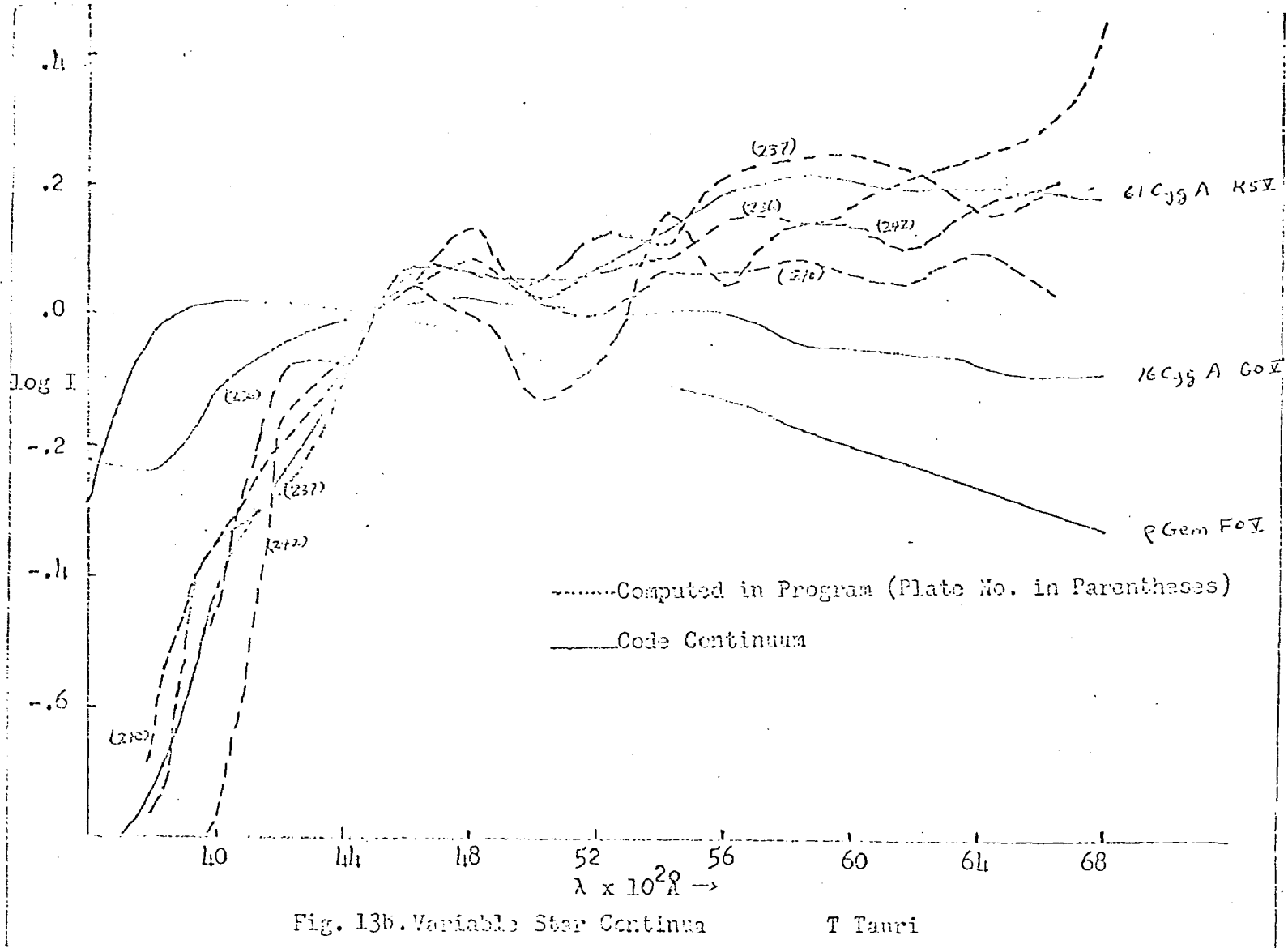
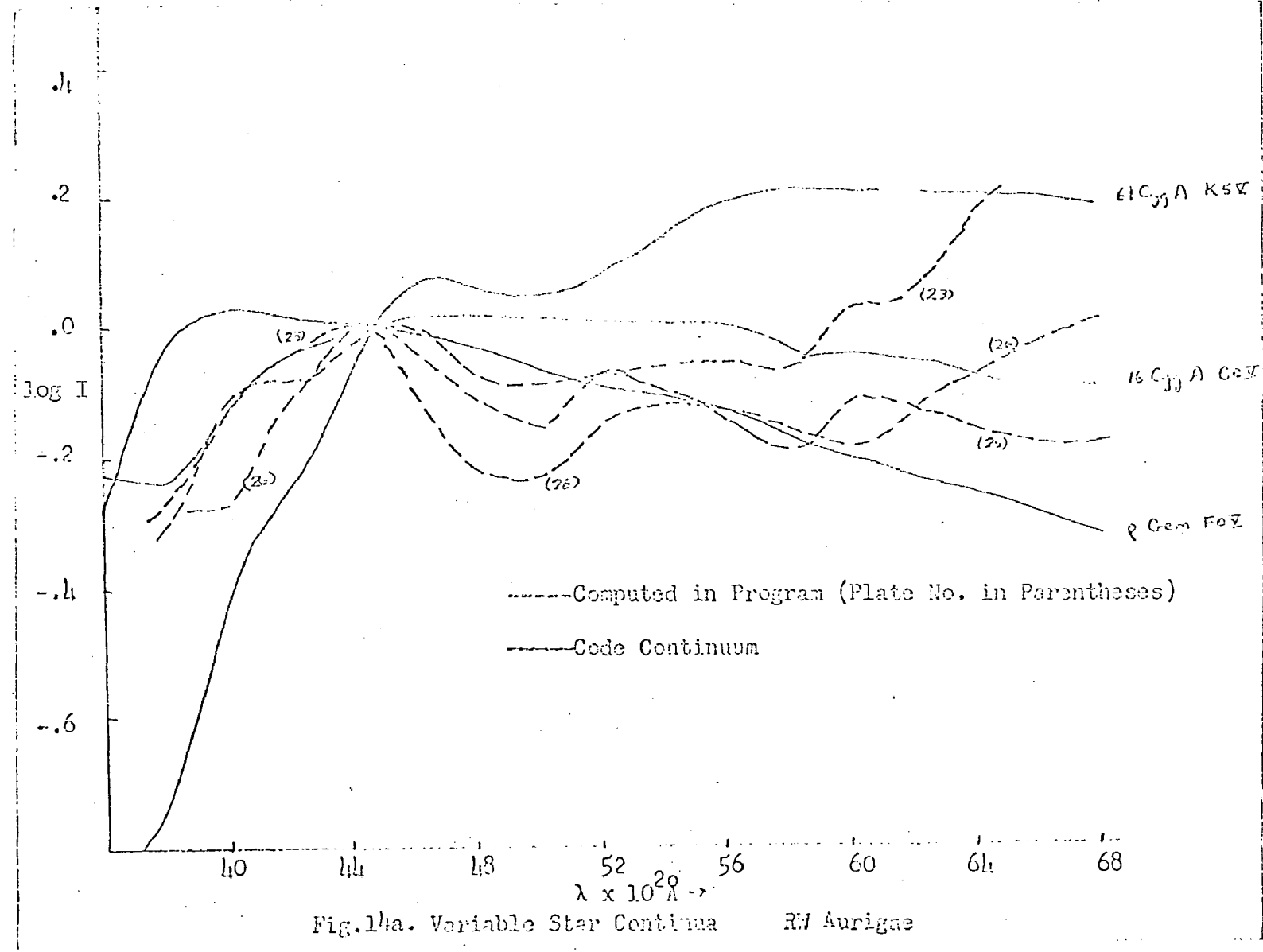


Fig. 13b. Variable Star Continua T Tauri



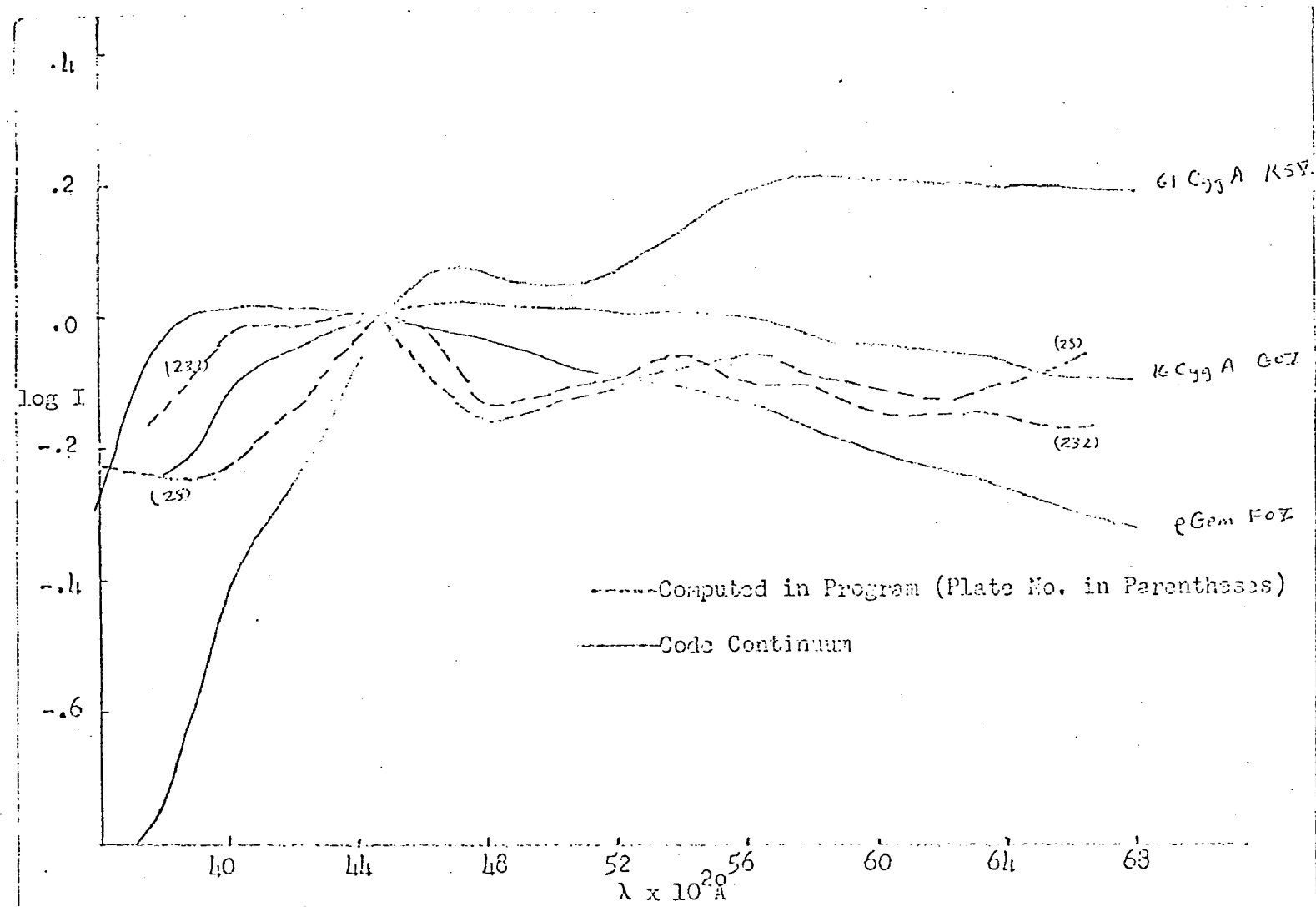


Fig. 14b. Variable Star Continua RW Aurigae

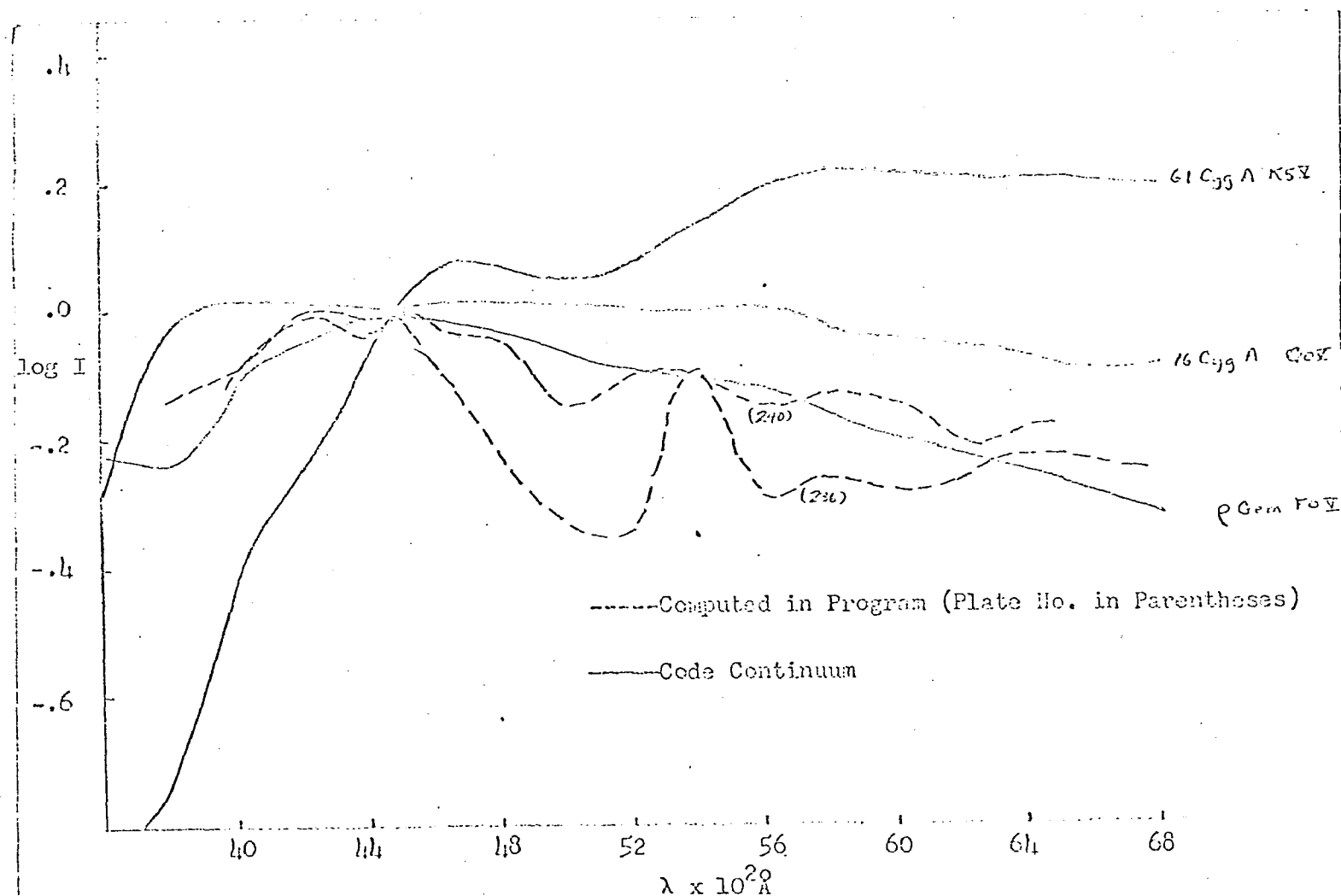


Fig. 14c. Variable Star Continua RW Aurigae

of the three for T Tau yield the largest values of δ ; this agrees with the suggestion of Herbig. If the blue continuum is due to unresolved emission, the corrections to the observed continuum colors should be even larger than previously believed. For example, if the continuum of T Tau on plate 25 is smoothed by eliminating this hump in the photographic region the emission track increases by $m^m .06$ to $\delta = 0^m .18$. Tracks as long as one quarter of a magnitude may exist in some cases.

In some spectra after line emission has been removed (T Tau 232, 236, 237, 240; RW Aur 23, 25, 240) one notes a very slight rise in intensity centered about $\lambda 6000$. No previous mention has been made of this in the literature but if it is due to unresolved emission, its effects upon $(B-V)_c$ will scarcely amount to $m^m .01$ as it lies in a region of rather low V filter transparency.

Since the continuum color, $(B-V)_c$ is affected by space reddening and the spectral type as determined from the absorption lines is not, one is afforded a means of determining the approximate magnitude of the space reddening for the program stars. Adopting $B-V = +0.67$, as the unreddened continuum color corresponding to Joy's (1960) classification and assuming the mean of all $(B-V)_c$ values to represent the space reddened colors, E_{B-V} is found to be 0.46 for T Tau and zero for RW Aur. This is in excellent agreement with previous determinations. The mean value $E_{B-V} = 0.30$ has been adopted in many investigations of the Taurus-Auriga dark cloud in the past (see Chapter I). The amount of space

reddening for RW Aur, however, has long been suspected of being small or nonexistent (Joy (1945)), particularly since no obscuring material is observed in the immediate vicinity. The usual surrounding nebulosity is notably absent in direct photographs of this star.

The T Tau continuum curves, before being corrected, resemble that of the K5V standard; this is especially true on the earlier plates. Significant changes appear to have taken place between the late 1963 and early 1965 observations. T Tauri appears bluer on plates 236 and 240. The continuum of RW Aur is much more difficult to match with those of the standards because it is even more erratic but the general indication is that the spectral type inferred from the shape of the continuum is earlier than that of T Tau in spite of space reddening. It would be informative to attempt to assign MK types to these stars on the basis of continuum color. Table 20 lists for each spectrum the MK type as determined from $(B-V)_C$, referred to as $Sp=f((B-V)_C)$, Arp's (1958) table has been employed for this purpose. The correction $E_{B-V} = 0.46$ has been applied to the T Tauri colors before the spectral type was determined. For T Tau the continuum color determinations give a range of spectral types between F7 and K0 with a mean of about G5; for RW Aur a range of F0-G8 in spectral types is observed with the mean at approximately F8. Assuming the variables to be main sequence stars and assuming changes in the continua as well as the continua themselves to be of a thermal nature, the corresponding effective surface temperature range is $6300-5100^{\circ}\text{K}$ for T Tau and $7600-5300^{\circ}\text{K}$ for RW Aur.

Table 20 Spectral Types of T Tauri Variables

<u>Object</u>	<u>Plate No.</u>	<u>Sp=f((B-V)_c)</u>
RW Aur	23	G5
	25	F7
	26	G0
	28	G8
	232	F5
	236	F0
	240	F5
	mean	F8
T Tau	25	G2
	28	K0
	232	G8
	236	G0
	237	G8
	240	F7
	242	G8
	mean	G5

Chapter VI Summary and Final Discussion

The principal aim of this work has been to interpret the effect of line emission upon the B-V colors of T Tauri objects. The program is intended to determine (a) the "emission-tracks", as contrasted to the reddening or blanketing tracks in the case of absorption effects, in the UBV diagram and (b) the energy distribution in the continuum after correction for the presence of emission. The spectral types of the T Tauri class are generally regarded to be of types GO-K5. One should therefore find that the corrected continua agree with the absolute energy distribution curves for main-sequence stars as published by Code (1960).

In preparation for this work, the author obtained an extensive series of plates from the Mount Wilson Observatory through the assistance of Dr. A. H. Joy. These included some of the objects for which he has published spectra (Joy (1945)). A preliminary study of these plates indicated that significant corrections to the measured colors for the presence of emission are found for nearly all objects. It must be admitted that the study of these older spectrograms in which the calibration is to some extent open to uncertainties must be accorded low weight even though the effect seems to be too large to explain in this manner. One possibility to explain the discrepancy is the presence of many faint and unresolved emission lines, especially in the region of $\lambda 4200\text{-}4400\text{\AA}$. Low dispersion spectra ($240\text{\AA}/\text{mm}$) of two bright T Tauri stars, T Tau and RW Aur, were obtained with the 36-inch telescope of the Steward Observatory. From microdensitometer tracings of these

spectra two B-V colors were computed:

- 1) The color $(B-V)_c$ of the continuum devoid of emission lines.
- 2) The color $(B-V)_{cl}$ of the continuum with the emission lines included.

The latter color was compared with the photometric B-V color observed at the time the spectra were taken.

The reduction program is a laborious one principally because of problems encountered in the photographic reductions.

A brief outline of the method employed to obtain true UBV magnitudes follows:

1. The basic format adopted involves the observations of
 - (1) the program star, for example T Tau; (2) an AOV standard star, for example α Lyr, which can be assumed as representative of the Code standard energy distribution for an AOV star; (3) a GOV star, for example HD157214;
 - (4) an F9V star, for example HD142373; and (5) a G1V star, for example HD160269, to represent standard stars whose continua presumably are close to that expected for T Tau;
 - (6) a wavelength comparison, Fe for the wide spectral sensitivity of the 103a-F plate (3500-6800Å with the Steward instruments); (7) a multi-step tungsten lamp comparison spectrum is normally placed on the plate at opposite sides of the above spectra. In this program, however, this problem is circumvented by taking the spectrum of a Code (1960) standard, whose intensity distribution is

already known, through the step wedge.

2. Simultaneous UBV measures and spectra of several T Tauri objects were required, the former with the Kitt Peak 16-inch telescope and the 21-inch telescope at the Catalina Station (Lunar and Planetary Laboratory), the latter with the 36-inch telescope at the Kitt Peak Observing Station.
3. The wavelength distribution of the flux emitted by the Code standard star at several intensity increments, is used to obtain the characteristic curve and the wavelength sensitivity for the plate.
4. This information yields a set of corrections to be applied to the observed stellar spectra to obtain absolute intensities for both the continuum and emission features.
5. Those portions of the area under the stellar curve which fall within the UBV passbands are numerically integrated using the known transmission functions for these passbands. Thus, one obtains "synthetic" UBV magnitudes for the stellar body after determination of the transformation equation through use of the AOV star.
6. The measured UBV magnitudes are then compared with those computed to determine the effect of emission lines in altering the positions of the objects in the color magnitude and two-color diagrams.
7. One can obtain an independent evaluation of the effect on the UBV magnitudes from the emission lines by reducing the observed

line intensities in the manner of step 5. If proper evaluation of each step in the reduction has occurred, the line plus continuum color and the observed photometric color will agree. This procedure, therefore, provides a valuable crosscheck.

A number of unexpected correction factors had to be considered in the reduction of the observations:

- 1) When the step wedge consisted of multiple layers of neutral density filters, considerable light loss was found to occur. This was remedied by employing single filter layers as much as possible.
- 2) The quoted Wratten neutral filter densities were found to be erroneous; there occurs an apparent wavelength dependence of filter transmission. This correction was determined instrumentally and applied in the program.
- 3) The characteristic curve of the 103a-F photographic plate varies considerably with wavelength. Characteristic curves were computed at 500\AA intervals over the range of the visible spectrum. For wavelength regions lying between two computed curves interpolation was used to obtain the intensity.
- 4) Employing a Code standard in place of a tungsten lamp vastly simplifies the reduction procedure because it effectively places the "laboratory reference source" outside the atmosphere. This entirely eliminates the atmospheric extinction correction if the Code standard and the T Tauri star are observed at the same air mass. When the air masses of the

two are not the same a small differential extinction correction is necessary.

The present method has the distinct advantage that it treats each emission feature separately. The flux emitted by every resolvable feature is numerically integrated into the B-V color. There is no question that the multitude of photographic corrections have been properly assessed. The method is accurate enough to predict the B-V colors of standard stars to within $\pm .016$ p.e. Simultaneous photometric colors of the T Tauri variables should agree with those computed from the spectra. This provides a second test of the validity of the spectroscopic method. Complications enter, however, because of the extremely rapid variations in light cycle and continuum color coupled with the long exposure times required to obtain a spectrum. During a single two hour exposure the B-V color determined photometrically was found to vary by up to $0^m.10$. The photographic process places severe limits on the technique. Since the number of low excitation Fe, Ti, and Cr lines common to these spectra increase toward the ultraviolet, the U-B color also needs to be corrected. The emission tracks in the two color diagram are not really lines of constant U-B but probably slope downward and to the right. The correction to the U magnitude simply cannot be done photographically.

The principal result of this work is that the computed emission line flux masks the true B-V color of T Tauri objects by up to $0^m.15$. The parameter δ , defined as the difference between the line free color and the color with line emission contributions included, varies

between $0^m.06$ and $0^m.15$ (mean = $0^m.11$) for RW Aur and between $0^m.07$ and $0^m.14$ (mean = $0^m.10$) for T Tau. If one were to include the unresolved emission lines in the B region the bluing effect would be even more pronounced. Redder continuum color seems to be associated with large values of δ . "Emission tracks" drawn in the color magnitude and two color diagrams vividly illustrate the magnitude of the line emission correction. The shift toward the right in the color magnitude diagram caused by removal of the emission lines doubles the distances of these stars from the main sequence; this can be interpreted to mean that these objects are as much as 20% younger than previously believed; the corresponding change $\Delta \log T_e$ is .047 for T Tau, .068 for RW Aur.

The most recent spectral type assigned to both program stars is G5Ve (Joy (1960)) but estimates have ranged from G2 to G8. Spectral classification is extremely difficult in this class of variables for two reasons:

- 1) The absorption lines are obscured by numerous emission lines showing complicated structure.
- 2) The absorption lines are wide and diffuse.

The wide band photometry included in this work shows $0.50 < B-V < 0.60$ for RW Aur, $1.00 < B-V < 1.17$ for T Tau. These correspond, respectively, to the spectral type ranges F7-G0 and K3-K5.

Space reddening affects the B-V continuum color but not the color determined from absorption spectra. This affords an approximate means of determining the space reddening in the vicinity of these stars. Adopting the B-V color corresponding to spectral type G5V one finds $E_{B-V} = 0.46$ for T Tau. The space reddening is essentially zero in the vicinity of RW Aur.

There is good agreement with previous work on this problem. RW Aur has no surrounding obscuring nebula as do most other T Tauri stars. Space reddening in its vicinity has long been suspected of being small. Previous estimates of $E_{B-V} = 0.30$ have been given by Herbig (1962) for the Taurus dark cloud. A "continuum classification type" can be obtained by comparing the wavelength distribution of the continuum of the T Tauri star with that of a Code standard provided the space reddening correction is applied. The continuum spectral type for T Tau redetermined after correction for space reddening falls in the range G0-K0. The effective surface temperatures corresponding to the range of types for each star are:

5300 - 7600°K for RW Aur (Spectral class mean at F8)

5100 - 6300°K for T Tau (Spectral class mean at G5)

Due to the detailed reduction procedure employed in this work, it is necessary to sacrifice large numbers of information elements for the sake of high accuracy. Smak (1964) made use of a filter which is transparent to a region containing relatively few emission lines ($4300 < \lambda < 5100\text{\AA}$). He is able to set up a relatively free color base, $B - V$ (the \mathcal{B} filter consists of 2mm. BG12 + 2mm. GG3 + 1mm. Corning 3387) Smak's photometric method is extremely useful for compiling vast amounts of data. The low dispersion Steward spectrograms, however, reveal that more than twenty strong emission features exist in the region of \mathcal{B} filter transparency. Substitution of the \mathcal{B} filter for the wide band B filter solves only part of the problem. For Steward Observatory Plate No. 28 of RW Aur, the ratio of emission line to continuum flux in the B passband is 26%. The same ratio in the \mathcal{B} passband is 21%. Indeed no filter exists which is completely blind to line emission in these stars. A glance at any of Joy's

early spectrograms or Fig. 1 of this text confirms this statement.

The problem of emission line identification is complicated by a number of effects:

- 1) Extreme crowding of lines occurs in all active T Tauri spectra.
- 2) The ultraviolet and blue regions of the spectra contain strong emission continua.
- 3) It has been necessary to use low dispersion equipment in order to limit exposure times on the 36-inch instrument to about three hours.

In spite of these complications 56 emission features are observed over the region of 103a-F plate transparency. Two thirds of these features lie between CaII H and K and H β and arise from low levels of excitation in the metals. Neutral and singly ionized iron contribute a majority. Some fluorescence is observed to occur in both stars. FeI λ 4063, 4132 (43) appear strengthened relative to the other members of (43). Population of the upper 3F level for these transitions probably occurs through the action of the wide CaII 3968.5 emission line upon λ 3969.3 (Herbig (1945)). FeI 4415.1 (41) and FeI 4271.8 (42) are also abnormally strong but there appears to be no chance coincidence of level separations which can act as a source of supply to the upper $^5G_3^o$ and $^3G_5^o$ levels where these transitions originate. It seems clear, for a number of reasons, that excitation conditions in the T Tauri atmosphere exceed those of the solar chromosphere:

- 1) The easily produced SrII resonance lines are strong in the

chromosphere, weak in T Tauri.

2) TiIII predominates over FeII in the chromosphere but not in T Tauri spectra.

3) CrI lines are weak in T Tauri, strong in the chromosphere.

Although the basic aim of this research has been to determine the true significance of the T Tauri emission line problem in a manner previously untried, the project is certain to open up new areas of investigation concerning these and related objects.

The same type of investigation might also be applied to Herbig-Haro objects, dense clots of nebulosity which could very well exemplify the stellar birth process itself. These objects have been closely associated with the T Tauri stars not only because of certain spectral similarities but also because of their proximity to them in space.

The method as employed here is accurate enough to be tried in Herbig's (1958) suggestion of a location study of T Tauri variables.

Since the parameter δ constitutes an operational definition of Herbig's degree of advancement of T Tauri line spectra, it can be particularly useful since the spectra of summer and winter Milky Way T Tauri objects are quite different. The variation of this parameter and of continuum color itself is not completely understood. Will the correlations observed for the paucity of stars in this study obtain in other regions of the Galaxy?

The blue continuum and the hypothesis that it is constituted of line emission must be further studied. The ultraviolet continuum and the effect of this and line emission upon U-B color has been completely

neglected. The author hopes to initiate a "location study" which will be conducted in the following succeeding steps:

1. Investigate, by means of low dispersion spectroscopy, stars in the neighborhood of previously observed T Tauri stars in order to determine whether this region is as populous as the Taurus dark cloud region. Selection of stars for observation on the basis of association with dark clouds can be decided with the aid of the Palomar Sky Atlas.
2. Select the brightest stars and examine them with a high dispersion Cassegrain spectrograph to determine whether the continua are the same as those in the Taurus region, and to determine whether the over-all emission line characteristics are the same as those in the Taurus region.
3. Correct the B-V color for effects due to emission lines by the same method used in the present T Tauri investigation. Determine the manner in which δ , $(B-V)_c$, and the intensity of the blue continuum vary.
4. Perform UBV photometry on the bright stars in order to determine the nature of the light curve as a function of position. The Bootes region is particularly interesting since we have here a high galactic latitude region containing stars with the low excitation spectrum that is so characteristic of T Tauri variables.

Observations of the Taurus region, though by no means exhausted, are relatively more abundant. A three or four week consecutive observing run on these objects is something which has never been initiated to the author's knowledge. However, it is quite necessary

considering the importance we attach to this class of variables.

Perhaps direct scanning spectrophotometry can be employed in future endeavors. This should lead to considerable improvements in the reduction program.

This research was supported in part by the National Science Foundation and the Colgate University Research Council. The author wishes to express his sincere gratitude to Dr. Aden Meinel for his guidance and encouragement in this work. I am indebted to Dr. Ray Weymann and Dr. Beverly Lynds for their instructive discussion and numerous suggestions, which removed many stumbling blocks from my path, to Messrs. Julian Schreur, Thomas Lee, and Dr. Philip Steffey for their assistance in helping me to acquire simultaneous spectroscopic and photometric data, and to my colleagues at Colgate University for their interest and concern. I wish to thank Drs. Walter Fitch and Harold L. Johnson for relinquishing pre-publication UBV observations of some of the standard stars used in the program. The author wishes to express his gratitude once again to the staff of the Kitt Peak Observatory for its cooperation and assistance in the attainment of the photometric observations. Most of all, I wish to express my appreciation to my wife who not only assisted greatly in the reduction of data and in the preparation of the format for this work, but also provided me with direction and purpose throughout its entirety. To her I affectionately dedicate this research.

APPENDIX

I. USEFUL TABLES

Table Al

Calibrated Density vs Wavelength of Wratten Filters

$\lambda(\text{\AA})$	T=2.5%	T=3.2%	T=5.3%	T=6.3%	T=10%	T=12.6%	T=25.1%	T=25.1%	T=50%
	d=1.0+0.6	d=5x0.3	d=2x0.5	d=4x0.3	d=1.0	d=3x0.3	d=0.6	d=2x0.3	d=0.3
3400	∞	∞	2.523	2.699	1.770	1.770	1.050	1.142	.562
3600	3.000	2.699	1.959	2.046	1.509	1.481	.943	.962	.480
3800	2.699	2.398	1.770	1.796	1.387	1.319	.857	.883	.429
4000	2.301	2.097	1.658	1.578	1.284	1.229	.799	.812	.396
4200	2.046	1.959	1.538	1.552	1.187	1.161	.750	.759	.371
4400	1.959	1.796	1.456	1.442	1.136	1.066	.719	.708	.352
4600	1.854	1.745	1.397	1.387	1.097	1.036	.688	.695	.336
4800	1.796	1.678	1.347	1.337	1.065	1.004	.657	.667	.328
5000	1.745	1.620	1.328	1.292	1.046	.970	.651	.644	.314
5200	1.721	1.602	1.310	1.284	1.031	.950	.644	.632	.305
5400	1.699	1.585	1.301	1.276	1.022	.950	.646	.632	.308
5600	1.699	1.585	1.301	1.268	1.017	.950	.648	.632	.310
5800	1.699	1.552	1.292	1.229	1.013	.928	.640	.620	.303
6000	1.678	1.523	1.260	1.215	1.000	.906	.622	.606	.298
6200	1.699	1.569	1.276	1.244	1.022	.932	.632	.622	.304
6400	1.721	1.620	1.319	1.234	1.046	.954	.641	.632	.312
6600	1.721	1.602	1.310	1.276	1.040	.954	.640	.632	.310
6800	1.721	1.585	1.310	1.260	1.036	.943	.640	.627	.307

Table A2

Extinction Curve for Kitt Peak (after Meinel (1962)).

<u>λ</u>	<u>Extinction in Mag's</u>
3600	.63
3800	.53
4000	.46
4200	.40
4400	.37
4600	.34
4800	.32
5000	.29
5200	.27
5400	.25
5600	.23
5800	.22
6000	.21
6200	.20
6400	.19
6600	.18
6800	.17

Table A3

The Kitt Peak Differential Atmospheric Extinction Correction

(log k'(λ))

<u>λ/Δsec z</u>	<u>0.1</u>	<u>0.2</u>	<u>0.3</u>	<u>0.4</u>	<u>0.5</u>	<u>0.6</u>	<u>0.7</u>	<u>0.8</u>	<u>0.9</u>	<u>1.0</u>	<u>1.1</u>	<u>1.2</u>	<u>1.3</u>	<u>1.4</u>	<u>1.5</u>
3600	025	050	075	100	125	150	175	200	225	250	275	300	325	350	375
3800	021	042	063	084	105	126	147	168	189	210	231	252	273	294	315
4000	019	036	054	072	090	108	126	144	162	180	198	216	234	252	270
4200	016	032	048	064	080	096	112	128	144	160	176	192	208	224	240
4400	015	029	044	059	074	089	103	118	133	148	163	178	192	207	222
4500	014	028	043	057	071	086	099	114	128	142	157	171	185	199	213
4600	013	027	041	054	068	082	095	109	122	136	150	163	177	190	204
4800	013	026	038	051	064	077	090	102	115	128	141	154	166	179	192
5000	012	023	031	046	058	070	081	095	104	116	128	139	151	162	174
5200	011	022	032	043	054	065	076	086	097	108	119	130	140	151	162
5400	010	020	030	040	050	060	070	080	090	100	110	120	130	140	150
5600	009	018	028	037	045	055	064	074	083	092	101	110	120	129	138
5800	009	018	025	035	044	053	062	070	079	088	097	106	114	123	132
6000	008	017	025	033	042	050	059	067	075	084	092	101	109	117	126

Table A3
The Kitt Peak Differential Atmospheric Extinction Correction

<u>$\lambda/\Delta\text{sec}$</u>	<u>0.1</u>	<u>0.2</u>	<u>0.3</u>	<u>0.4</u>	<u>0.5</u>	<u>0.6</u>	<u>0.7</u>	<u>0.8</u>	<u>0.9</u>	<u>1.0</u>	<u>1.1</u>	<u>1.2</u>	<u>1.3</u>	<u>1.4</u>	<u>1.5</u>
6200	008	016	024	032	040	048	056	064	072	080	088	096	104	112	120
6400	007	015	023	030	038	045	053	062	069	076	083	091	099	106	114
6600	007	014	022	029	036	043	050	058	065	072	079	086	094	101	108
6800	007	014	020	027	034	041	048	054	061	068	075	082	089	095	102

-1

Table A4Photometric Sensitivity Correction

<u>Wavelength(Å)</u>	<u>log Q_B</u>	<u>log Q_V</u>
3600	- ∞	
3800	- .854	
4000	- .027	
4200	- .004	
4400	- .046	
4600	- .134	
4800	- .268	- ∞
5000	- .444	- .444
5200	- .678	- .032
5400	-1.155	- .009
5600	- ∞	- .027
5800		- .229
6000		- .328
6200		- .620
6400		-1.000
6600		-1.523
6800		- ∞

II. The Reduction Procedure--Illustrative Examples

This section illustrates the use of Tables 8 - 10 for obtaining reduced relative intensities.

Example I. To determine the relative intensity of the continuum as viewed with the B filter at $\lambda 4000$ in RW Aur (Plate No. 25).

- A. From table 9 for Plate No. 28 the strip chart reading of the continuum is 45.5 at 4000\AA (Column 2).
- B. The corresponding density from Fig. 2 is .312 (Column 3).
- C. To obtain the unreduced relative intensity the density must be entered along the ordinate of Fig. 3b. These curves have been plotted from the measured intensity increments obtained with the step wedge and listed in Table 8 for Plate No. 25. The relative intensity corresponding to $d = .312$ is $\log I = -1.239$ (Column 4).
- D. In Table 9 $\Delta \sec z = .054$ for this star. This is the number of differential air masses, RW Aur minus Code Standard for the plate (4 Aur). Since $\Delta \sec z$ is negative the zenith distance of this star must be "effectively increased" in order to eliminate atmospheric extinction. This implies subtracting the correction given in Table A3 ($\log k'(\lambda) = .009$). The relative intensity corrected for differential atmospheric extinction is 1.248 (Column 5).
- E. The relative intensity is normalized to .000 at $\lambda 4500$ and reads -.134 (Column 6).

F. The instrumental sensitivity correction is now applied.

From Table 9 for the calibration star of Plate No. 25, $\log S'(\lambda) = -.004$ at $\lambda 4000$. Thus, $\log I$ is corrected to read $-.138$ (Column 7).

G. The logarithm of the transparency of the B filter at 4000\AA is found from Table A4 to be $-.027$. This is added to the figure in Column 7 to give $\log I (\text{B PHTM}) = -.165$ (Column 8).

H. The intensity corresponding to the logarithm $-.165$ is $.684$ (Column 10). This point is among those plotted vs wavelength. The relative area under the curves $\log I (\text{B PHTM})$ vs λ and $\log I (\text{V PHTM})$ vs λ is used to compute the "synthetic" $(\text{B-V})_c$ color.

Example II. To determine the contribution to the observed B, V fluxes of the CaII 3968 line in the spectrum of RW Aur Plate No. 25.

A. From Table 10 the chart recorder readings of the line center and adjacent continuum are 24.2 and 48.6 respectively (Columns 2 and 3, Table 10).

B. From Fig. 2 the corresponding densities are .591 and .281 (Columns 4 and 5).

C. From Fig. 3b the relative intensities are $-.933$ and $-.1284$ (Columns 6 and 7).

D. The difference between the relative intensities is $.351$ (Column 8).

E. Next the curves $\log I (\text{B PHTM})$ vs λ and $\log I (\text{V PHTM})$ vs λ for this star are consulted. The sum of the logarithms, continuum plus line, is $.162$ for the B filter (Column 9) and $-\infty$ for the

V filter, since the latter is completely opaque at $\lambda 3968$.

- F. The relative intensity at the line center is the antilogarithm of .162 or 1.452. This quantity is not recorded in the line analysis tables. The next quantity to be recorded is the difference of relative intensities, line center minus adjacent continuum. The intensity of the adjacent continuum from a plot of I (B PHM) vs λ (Table 9) is .647. The difference 1.452 minus .647 is .805 (Column 11).
- G. The measured width of the rectangular CaH profile on the microdensitometer tracing is 14\AA (Column 13).
- H. The product of line minus continuum intensity and line width is $.805 \times 14 = 10.8 \text{\AA} \times$ relative intensity units (Column 14). This quantity is added to the sum of all line contributions in the B passband. The final total is added to the area under the I (B PHM) vs λ curve for the continuum. From Table 11 it is seen that CaII H is one of 30 lines contributing to the B magnitude. These lines produce a total flux 13.8% as strong as the continuum and alter the B-V color from 1.11 to 0.99.

REFERENCES

- Adams, W.S. and Pease, F.C. 1915, Pub.A.S.P. 27, 132.
- Allen, C.W. 1960, N.N. 121, 299.
- Allen, C.W. 1963, Astrophysical Quantities. (London Athlone Press), 195.
- Aller, L.H. 1943, Ap.J. 97, 135.
- Ambartsumian, V. 1954, Comm. Buraikan Obs., No. 13.
- Arp, H.C. 1958, Hdbk. der Physik, 51 (Berlin: Springer Verlag), 75.
- Artyukhina, N.M. 1960, A.J.U.S.S.R. 37, No. 1.
- Beals, C.S. 1934, Obs. 57, 319.
- Bohm, K.K. 1953, Kom. Soc. Roy. Sci. Leige, 271.
- Bonsack, W.K. 1961, Ap.J. 133, 340.
- Bonsack, W.K. and Greenstein, J.L. 1960, Ap.J. 131, 83.
- Ceraski, A. 1906, A.N. 170, 339.
- Code, A.D. 1960, Stellar Atmospheres, G.F. Kuiper, and B.M. Middlehurst (ed.), (Chicago, Univ. of Chicago Press), 50.
- Corliss, C.H. and Rozman, W.R. 1962, Experimental Transition Probabilities for Spectral Lines of 70 Elements, NBS Monograph No. 53.
- Crosswhite, H.M. 1958, The Spectrum of FeI, Johns Hopkins Spectroscopic Report No. 13.
- Enebo, S. 1907, A.N. 175, 205.
- Greenstein, J.L. 1948, Centennial Symposia, (Cambridge: Harvard Obs.), 19.

- Greenstein, J.L. 1950, Pub. A.S.P. 62, 156.
- Haro, G. et al 1953, Bul Obs. Ton. y Tac. No. 8, 8.
- Hayashi, C., Hoshi, R. and Sugimoto, D. 1962, Prog. Theo. Phys., Supp. No. 22, 1.
- Heney, L., LeLevier, R. and Levee, R. 1955, Pub. A.S.P., 67, 396.
- Herbig, G. 1945, Pub. A.S.P. 57, 166.
- Herbig, G. 1948, Dissertation, Univ. of Calif.
- Herbig, G. 1957, IAU Sym. No. 3: Non-Stable Stars, G. Herbig (ed.), (London: Cambridge U. Press), 3.
- Herbig, G. 1958, Mem. Soc. Roy. Sci. Leige, 251.
- Herbig, G. 1962, Adv. Astron. Astrophys., 1, A. Kopal (ed.), (New York: Academic Press), 1.
- Hunger, K. 1957, A.J. 62, 294.
- Hunger, K. and Kron, G.E. 1958, Mem. Soc. Roy. Sci. Leige, 285.
- Johnson, H.L. and Harris III, D.L. 1954, Ap.J. 120, 196.
- Johnson, H.L. 1955, Ann. d'Ap. 18, 292.
- Johnson, H.L. 1963, (Private Communication).
- Joy, A.H. 1945, Ap.J. 102, 168.
- Joy, A.H. 1949, Ap.J. 110, 424.
- Joy, A.H. 1960, Stellar Atmospheres, G.P. Kuiper and B.M. Middlehurst (ed.), (Chicago: University of Chicago Press), 653.
- Joy, A.H. 1961, Ap.J. 133, 493.
- King, R.B. and King, A.S. 1938, Ap.J. 87, 24.
- Kuhi, L.V. 1964, Ap.J. 140, 1409.

- Meinel, A.B. 1962, Contr. Steward Obs., N 44.
- Meinel, A.B. 1963, Ap.J. 137, 834.
- Meinel, A.B., Aveni, A.F., and Lee, T.A. (Unpublished).
- Merrill, P.W. 1958, Lines of Chem. Elements in Astron. Spectra, Carnegie Inst. of Wash., Pub. No. 610.
- Moore, C.E. 1952, Atomic Energy Levels, 2, Dept. of Commerce, Circ. No. 467.
- Moore, C.E. 1959, A Multiplet Table of Astrophysical Interest. Washington: NBS).
- Sahade, J. 1958, Obs., 78, 79.
- Smak, J. 1964, Ap.J. 139, 1095.
- Struve, O. 1950, Stellar Evolution. (Princeton: Princeton U. Press), 108
- Struve, O. and Rudkjøbing, M. 1949, Ap.J. 109, 92.
- Swings, P. and Struve, O. 1940, Ap.J. 91, 573.
- Thackeray, A. and Merrill, P.W. 1936, Pub.A.S.P. 48, 331.
- Thomas, R.N. and Athay, R.G. 1961, Phys. Sol. Chromos., (New York: Interscience Pub.), 391.
- Tifft, W.G. and Greenstein, J.L. 1958, Ap.J. 127, 160.
- Underhill, A.B. 1960, Pub. Dom. Ap. Obs., 11, 209.
- Varsavsky, C. 1960, Ap.J. 130, 354.
- Wyse, A.B. 1942, Ap.J. 95, 356.
- Zinner, E. 1913, A.N. 195, 456.